IMPROVING NITROGEN USE AND YIELD WITH STAY-GREEN PHENOTYPES IN WHEAT

ADINDA PIETERDINA DERKX, BSc MSc

Thesis submitted to the University of Nottingham
for the degree of Doctor of Philosophy

JULY 2013

ABSTRACT

Wheat grain yield is strongly related to nitrogen (N) fertiliser input, a major cost factor and potential environmental pollutant. Much of the grain N requirement is met by N remobilisation from the canopy. Unfortunately, a consequence is canopy senescence and decreased photosynthetic capacity, reducing carbon available for grain-filling. One approach to achieve both higher N use efficiency and grain yield would be to extend the duration of photosynthesis using delayed leaf senescence “stay-green” phenotypes.

Three stay-green and two fast-senescing EMS mutants of wheat (cv. Paragon) were characterised. A fast-senescing line, a stay-green line and the wild-type were grown to characterise the interaction between senescence and N availability. Stay-green line SG3 was able to allocate similar proportions of N to the grain under N-limiting and N-sufficient conditions. The accelerated senescence of line FS2 reduced grain yield and N allocation to the grain.

Candidate regulatory genes of leaf senescence genes were characterised by correlating their expression with leaf senescence by screening wheat genotypes with varied senescence characteristics in the field. Among the genes were members of the WRKY and NAC transcription factor families that have been related to senescence. Overexpression of the NAC gene resulted in a stay-green phenotype and increased grain N concentrations, but had no effects on shoot biomass or grain yield. Expression of a WRKY-RNAi construct did not reduce WRKY mRNA levels, but led to accelerated leaf senescence and increases in plant height, the number of fertile tillers and grain yield.

These results show that the relationships between senescence, nitrogen remobilisation and grain yield are complex and not easily manipulated. The phenotypes and genes identified could contribute to wheat improvement.

ACKNOWLEDGEMENTS

First of all I would like to thank my supervisors. Especially many thanks to Malcolm Hawkesford for welcoming me into his group and for four years of advice and support. I would also like to thank John Foulkes for the many suggestions for my work, especially the thesis.

I would specially like to thank Peter Buchner, Saroj Parmar, Emmanuelle Cabannes and Fumie Shinmachi for all the practical advice when I arrived and helping me master the new techniques. But also many thanks to all the other past and present lab members; it would have been a lot more difficult and less fun without having all of you around in the lab and the field. I am also thankful to the glasshouse staff, who have always done their best to keep my plants alive and healthy, sometimes despite me.

I am grateful to the Lawes Agricultural Trust for funding my project.

I would like to thank all my friends at Rothamsted for making me feel so welcome. The last four years would have been a lot less enjoyable without you.

Finally, I would like to thank my parents. Even though you were encouraging me to go abroad, it must have been a shock when I actually did!

TABLE OF CONTENTS

LIST OF FIGURES

CHAPTER 1: INTRODUCTION

CHAPTER 2: MATERIALS & METHODS

CHAPTER 3: GENE EXPRESSION STUDIES

CHAPTER 4: STAY-GREEN MUTANTS

CHAPTER 5: NAC TRANSCIPTION FACTOR

CHAPTER 6: WRKY TRANSCRIPTION FACTOR

LIST OF TABLES

LIST OF ABBREVIATIONS

A	Anthesis or Actin-promoter
ABA	Abscisic acid
ABC	ATP-binding cassette
AC	Avalon x Cadenza
AlaAT	Alanine aminotransferase
ANOVA	Analysis of Variance
BAR	Bialaphos resistance
bp	Base pairs
C	Carbon (biomass) or Control
CAB	Chlorophyll *a/b* binding protein
cDNA	Complementary DNA
Ch	Chaff
ChIP	Chromatin immunoprecipitation
Chl	Chlorophyll
CK	Cytokinin
CVA	Canonical Variates Analysis
Defra	Department for Environment, Food and Rural Affairs
DEPC	Diethylpyrocarbonate
d.f.	Degrees of Freedom
DM	Dry matter
DNA	Deoxyribonucleic acid
DNase	Deoxyribonuclease
dNTP	Deoxyribonucleotide
dpa	days post-anthesis
DRTF	Database of Rice Transcription Factors
dT	Deoxythymidine
DTT	Dithiothreitol
DW	Dry weight
E	Ear
EDTA	Ethylenediaminetetraacetic acid
EIN	Ethylene-insensitive
EMS	Ethyl methanesulfonate
FAO	Food and Agriculture Organization
FCC	Fluorescent chlorophyll catabolite
FL	Flag leaf
F_M	Maximum fluorescence
FS	Fast-senescing
F_V	Variable fluorescence

G	Grain
gDNA	Genomic DNA
GLK	Golden-like
GM	Genetic modification
GMPase	GDP-D-mannose pyrophosphorylase
GPC	Grain protein content
Gr	Grain
GS	Glutamine synthetase or Growth stage
H	Harvest
HI	Harvest Index
IAA	Isoamyl alcohol
IPT	Adenosine phosphate-isopentenyltransferase
JA	Jasmonic acid
JIC	John Innes Centre
L	Leaves
LED	Light-emitting diode
LHCII	Light-harvesting complex II
LSD	Least significant difference
M	Maturity
MCS	Magnesium dechetalase
MeJA	Methyl jasmonate
mRNA	Messenger RNA
N	Nitrogen
NAC	NAM, ATAF1-2 and CUC2
NAM	No apical meristem
NCC	Non-fluorescent chlorophyll catabolite
NDVI	Normalised Difference Vegetation Index
NHI	Nitrogen Harvest Index
NIR	Near-infrared light
NO	Nitric oxide
NPT	Neomycin phosphotransferase
NUE	Nitrogen use efficiency
ORI	Origin of replication
pActin	Actin promoter
PAO	Pheophorbide *a* oxygenase
PCR	Polymerase chain reaction
pFCC	Primary fluorescent chlorophyll catabolite
P_i	Inorganic phosphorous
PPDK	Pyruvate orthophosphate dikinase
PPH	Pheophytinase
ρ_{NIR}	Reflectance of near-infrared light

pRTBV	RTBV promoter
pSAG12	SAG12 promoter
PSII	Photosystem complex II
PSMD	Potential soil moisture deficit
PTF	P_i starvation-induced transcription factor
ρ_{VIS}	Reflectance of visible light
PVP	Polyvinylpyrrolidone
QTL	Quantitative trait loci
QY	Quantum yield
R	RTBV-promoter
RBCS	Small subunit of Rubisco
RCCR	Red chlorophyll catabolite reductase
REML	Restricted Maximum Likelihood
RING	Really Interesting New Gene
RNA	Ribonucleic acid
RNAi	RNA interference
RNase	Ribonuclease
RIL	Recombinant Inbred Line
ROS	Reactive oxygen species
RTBV	Rice tungro bacilliform virus
RT-PCR	Reverse transcription PCR
Rubisco	Ribulose-1,5-biphosphate carboxylase / oxygenase
SA	Salicylic acid
SAG12	Senescence-associated gene 12
SDS	Sodium dodecyl sulphate
SE	Standard error
SG	Stay-green
Sh	Sheath
SPAD	Soil Plant Analysis Development
sq-PCR	Semi-quantitative PCR
St	Stem
T	Total
TAE	Tris acetate EDTA
T-DNA	Transfer DNA
TGW	Thousand grain weight
TIGR	The Institute for Genome Research
TILLING	Targeting Induced Local Lesions in Genomes
Tris	Tris (hydroxymethyl) aminomethane
UK	United Kingdom
UniProtKB	UniProt Knowledgebase
USA	United States of America

UV	Ultraviolet
VIS	Visible light
WGIN	Wheat Genetic Improvement Network
WS	Whole shoot
WT	Wild-type

1. INTRODUCTION

1.1 GENERAL INTRODUCTION

1.1.1 Wheat Production

Despite a doubling of the world population in the past half-century, the proportion of hungry people has actually fallen due to a substantial growth in food production (Godfray et al., 2010). Global production of the main grain crops such as wheat has increased nearly threefold since 1960 (FAO, 2010). Global wheat production was primarily raised by increasing the yield per area; the area on which wheat was grown only increased marginally (Figure 1.1).

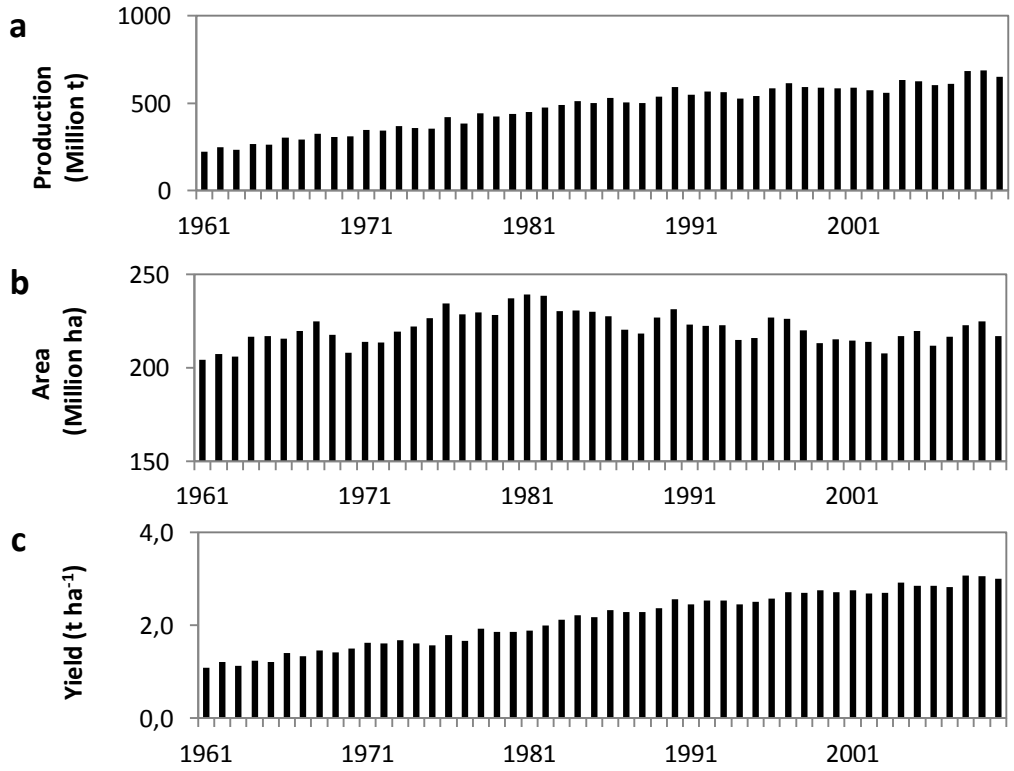

Figure 1.1: Global wheat production (a), area of wheat harvested (b), and average wheat yield (c) between 1961 and 2009. Data from FAO (2010).

It will be challenging to continue raising crop productivity to keep track with the growing population, and even more so to do this in a sustainable manner. In addition, the increasing demand for energy coupled with climate change is putting greater pressure on agriculture since one of the solutions is seen to be biofuel production. Biofuels ideally should not compete with food production and not result in the clearance of uncultivated lands (Tilman et al., 2009). Feedstock sources out of which sustainable biofuels can be obtained include industrial waste products, crops specifically grown for their biomass on land unsuitable for agriculture and straw residues of crops such as wheat (Tilman et al., 2009).

Since land available for agriculture is limited, the biggest rise in crop production will have to come from increasing yield per unit area. Crop yields are determined by local conditions such as soils and the climate, farming practises such as fertiliser use and pest management, and genetic properties of the crop itself.

Bread wheat (*Triticum aestivum* L.) is a hexaploid species, thus containing three complete genomes (termed A, B and D genomes). Two diploid grasses crossed to give rise to tetraploid wheat, which in farmer's fields later crossed to the diploid goat grass (*Triticum tauschii*) to produce hexaploid wheat (Hoisington et al., 1999). Because of its hexaploid nature, genes governing traits are difficult to identify in wheat, which makes breeding a time-consuming process. However, several traits have been successfully incorporated into wheat (Hoisington et al., 1999). The most well-known one is the dwarfing trait that makes wheat less vulnerable for lodging and improves its nutrient uptake and tillering capacity, allowing for higher N fertiliser applications. Breeding wheat with semi-dwarfing (*Rht*) genes led to a great increase in yield since the 1960s (Figure 1.1.c), which is now called the "Green Revolution". Wheat productivity has been raised further by increasing genetic yield potential, resistance to diseases, and adaptation to abiotic stresses, as well as by improved agronomic practices (Reynolds et al., 2009).

1.1.2 Nitrogen Fertiliser

One of the issues facing agriculture for both food and biofuels production is the dependency on nitrogen fertiliser, which is a major cost factor and a potential environmental pollutant (Good, Shrawat and Muench, 2004; Figure 1.2). Nitrogen (N) damages the environment by leaching, which leads to eutrophication and ecosystem damage (Carpenter et al., 1998), and by emissions of gaseous forms of nitrogen such as nitrous oxide (N_2O), which is a greenhouse gas 296 times more potent than carbon dioxide (Crutzen et al., 2008). Nitrous oxide can be produced in soils by bacteria from nitrate (NO_3^-) and ammonium (NH_4^+) in fertiliser through denitrification under anaerobic conditions ($NO_3^- \rightarrow NO_2^- \rightarrow NO + N_2O \rightarrow N_2$) and nitrification under aerobic conditions (oxidation of NH_4^+ to NO_3^-), and in tiny amounts by chemical processes in the soil (Bremner, 1997). The production of nitrous oxides in agricultural soils is estimated to be 4.3 - 5.8 Tg per year, which is between 3% and 5% of the anthropogenic nitrogen input by the Haber-Bosch process and fossil fuel production (Crutzen et al., 2008).

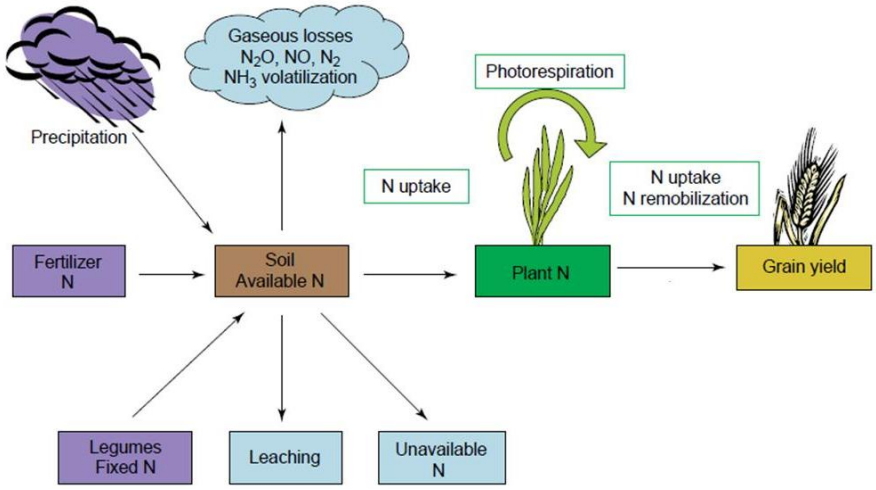

Figure 1.2: Nitrogen movements in and out of agricultural soils. Mechanisms of nitrogen input (purple) into agricultural soils can be both natural and anthropogenic. Nitrogen can be used for biomass production by the crop (green) or become unavailable for agriculture and move into the environment (blue). Adapted from Good et al. (2004).

Modern cereals require large amounts of fertilisers to reach maximum yield and protein content. Nitrogen use efficiency (NUE = grain dry mass per unit nitrogen available (from soil supply plus N fertiliser)) of modern cereals is not optimal, partly because they were selected in breeding programmes under non-limiting fertilisation conditions (Kichey et al., 2007). It is estimated that annually $1.1 billion could be saved by increasing NUE by just one per cent (Kant, Bi and Rothstein, 2011). Optimising carbon assimilation and minimising nitrogen inputs would therefore be highly beneficial, especially for the production of bioenergy crops for which a relatively high carbon content is required.

One approach to achieve this optimisation would be to prolong the duration of active carbon fixation during grain-filling. Extending the duration of photosynthesis is the easiest way to increase total photosynthesis, biomass and grain yield (Richards, 2000). A longer post-anthesis photosynthetic period could be achieved by bringing forward the anthesis date, but this would increase the chance of frost damage to the ear (Fuller et al., 2007). Therefore delaying the process of leaf senescence during grain-filling is probably the most promising option.

During leaf senescence chlorophyll and other macromolecules such as proteins, lipids and nucleic acids are broken down and the nutrients, most notably nitrogen, are remobilised to the developing grain. Unfortunately this results in a reduced photosynthetic capacity and consequently a decrease in the assimilation of carbon. Theoretically, a delay in leaf senescence would increase the amount of fixed carbon available for grain-filling whilst utilising the same amount of nitrogen. A better understanding of the relationship between nitrogen remobilisation and senescence is required so that both NUE and grain yield can be improved by manipulating leaf senescence.

1.2 NITROGEN REMOBILISATION AND SENESCENCE

During senescence nutrients present in vegetative organs are recycled to the grain to meet its demand for resources such as nitrogen (Gregersen, Holm and Krupinska, 2008). Illustrating the importance of this remobilisation, the proportion of nitrogen in wheat grain originating from remobilisation of pre-anthesis stored nitrogen is estimated to be over 70% (Kichey et al., 2007), and the amount of N contributed by the flag leaf was found to be about 18% in Canadian Red Spring wheat (Wang et al., 2008). N remobilization from leaves in winter wheat is estimated to be about 75% (Pask et al., 2012).

The amount of N taken up by the plant before anthesis mainly determines how much N will be remobilised at maturity (Bancal, 2009), and this N uptake is the main genetic factor determining nitrogen remobilisation in wheat (Barbottin et al., 2005). Generally, the amount of nitrogen remobilised to the grain is considered to be determined by the amount of N available in the canopy (source), not by the grain (sink) demand (Martre et al., 2003). However, another study suggested wheat grain-filling is not source-limited under optimal conditions (Borrás, Slafer and Otegui, 2004), and N remobilisation was halted when the developing ears were removed (Srivalli and Khanna-Chopra, 2004), indicating the presence of a sink organ is required. Furthermore, N availability may affect the size of the grain sink indirectly by influencing the size of the source canopy (Hirel et al., 2007).

Delayed onset of senescence in wheat also has been associated with maintaining post-anthesis N uptake (Bogard et al., 2011; Mi et al., 2000). If N remobilisation for grain-filling is sink-determined, delayed senescence and maintenance of N uptake would mean remobilisation would have to contribute less nitrogen for grain-filling, whilst under source-determination the result might be a higher grain N content.

There is still the possibility that grain-filling is source-limited under abiotic stress conditions such as nitrogen limitation. NUE appears to be a stable trait in *Arabidopsis thaliana* since relative NUE is the same under low and high N supply (Chardon et al., 2010). Yet a field study in wheat showed that at low N conditions onset of senescence was positively correlated with nitrogen utilisation efficiency (grain dry mass per unit of N taken up by the plant) and grain yield (Gaju et al., 2011).

It has been shown that plant nitrogen status has a major impact on the onset and progression of leaf senescence. In both barley (*Hordeum vulgare*) and Arabidopsis, nitrogen deprivation resulted in accelerated leaf senescence, and when additional nitrate was supplied at the start of senescence, the senescence-specific decrease of photosystem II (PSII) efficiency was halted and the decrease in chlorophyll content even reversed (Schildhauer, Wiedemuth and Humbeck, 2008). In sorghum (*Sorghum bicolor*), plant N status has been found to be an important determinant of genotypic differences in the rate of leaf senescence (van Oosterom et al., 2010). The Arabidopsis *nla* (nitrogen limitation adaptation) mutant displayed an early senescence phenotype under low nitrogen conditions, which was reversible by nitrogen application (Peng et al., 2007). The *nla* mutants could acquire nitrogen normally, but were impaired in adaptive responses such as nitrogen limitation-mediated senescence: senescence occurred very fast, N was less remobilised from senescing leaves, starch and soluble sugars accumulated less and anthocyanins did not accumulate at all. NLA is a RING-type ubiquitin E3 ligase, so it is probably involved in protein degradation, but of which proteins is not known.

Delayed senescence is also linked with higher grain yields, especially under nitrogen limitation. For instance, mutants in the senescence-associated gene *See2* of maize (*Zea mays*) stayed green longer and had a slight extension in photosynthetic activity, but the most dramatic effect was that unlike wild-type plants the mutant plants could maintain their cob weight under low N

conditions (Donnison et al., 2007). Tropical maize senesced immediately after flowering and therefore had lower biomass and grain yield than later senescing temperate maize (Osaki, 1995). However, it had a very high NUE at low N conditions since most N was rapidly remobilised from the leaves.

A few genes are known that regulate nitrogen use in plants. The early-nodulin gene *ENOD93-1* of rice *(Oryza sativa)* was identified as a nitrogen-responsive gene (Bi et al., 2009). *ENOD93-1* expression reacted to both N induction and N reduction. Overexpression resulted in 10-20% more spikes and spikelets, a higher grain yield under both limiting and high N conditions, and under N limiting conditions the shoot biomass was also higher. The transgenic plants had higher concentrations of amino acids in their xylem sap, especially under N stress, suggesting that the gene might have role in transporting amino acids from the roots to the shoot.

Two cases in which genetic modification was specifically used to improve nitrogen use were the maize Dof1 transcription factor and barley alanine aminotransferase *(AlaAT)*. Dof1 activates multiple organic acid metabolism genes. Expressing maize *ZmDof1* in Arabidopsis induced carbon metabolism genes and increased amino acid concentrations and total nitrogen content (Yanagisawa et al., 2004). Furthermore, under low-nitrogen conditions Dof1 plants had higher fresh weights and protein and chlorophyll contents. In rice overexpression of *ZmDof1* resulted in an induction of carbon metabolism genes and an increased carbon flow towards nitrogen assimilation, and increased root biomass and net photosynthesis rate under N deficient conditions (Kurai et al., 2011). Overexpression of the barley *AlaAT* gene under a root-specific promoter in rice and Brassica resulted in a higher biomass and grain yield (Good et al., 2007; Shrawat et al., 2008), in Brassica specifically under low-nitrogen conditions. It has been suggested amino acids such as alanine can act as a signal for whole-plant N status, so *AlaAT* overexpression may trick the plant into sensing low N status and it response might be to take up more nitrate (Good et al., 2007).

1.3 STAY-GREEN PHENOTYPES

1.3.1 Definition of Stay-Green

Stay-green phenotypes are a potential route to achieving a prolonged carbon fixation potential during grain-filling. Thomas and Howarth (2000) described five types of stay-green phenotypes:

- Type A: late initiation of senescence, but a normal senescence rate.
- Type B: normal initiation of senescence, but a slower rate of senescence.
- Type C: lesion in chlorophyll degradation, leaving the rest of the senescence process unaffected. The most well-known example of this is Mendel's *I* locus in pea *(Pisum sativa)* (Armstead et al., 2007).
- Type D: rapid death (freeze, boil, dry) ensures maintenance of leaf colour in dead leaf.
- Type E: enhanced greenness but unchanged initiation and rate of senescence. As a result the overall process of senescence will take longer to complete.

Types A, B, and possibly E are functionally stay-green: they maintain photosynthetic capacity in their green tissues. Therefore they may be a potential means to improve grain yield. For instance, for *Lolium temulentum* it was calculated that if the start of senescence in a leaf is delayed by two days, theoretically the leaf could contribute 11% more carbon to the plant over the lifetime of the leaf (Thomas and Howarth, 2000). Hence it is not surprising that stay-green mutants and varieties are a target for crop improvement for a number of agriculturally important species.

1.3.2 Stay-Green Phenotypes of Crops

Non-functional stay-green lines have been developed for crops for which colour is an important quality attribute, such as alfalfa *(Medicago sativa)* (Zhou et al., 2011a), soybean *(Glycine max)* (Kang et al., 2010), and tomato *(Solanum lycopersicum)* and pepper *(Capsicum annuum)* (Barry et al., 2008).

Functional stay-green phenotypes have been identified in many crop species. In sunflower (*Helianthus annuus*) stay-green was associated with higher post-anthesis biomass increase and leaf area index but not seed yield (de la Vega et al., 2011). In oil-seed rape (*Brassica napus*) delayed leaf senescence was positively correlated with NUE under low N supply (Erley et al., 2007). In soybean two mutations caused the maintenance of the photosynthetic machinery, but seed yield and stomatal conductance were lower and the plants were more susceptible to water stress (Luquez and Guiamét, 2001; Luquez and Guiamét, 2002).

Stay-green phenotypes have been described most extensively in monocotyledonous species. In rice a functional stay-green mutant has been described which had a number of positive effects on grain yield, especially for seed setting rate (Fu and Lee, 2008; Yoo et al., 2007). In sorghum a functional stay-green phenotype was found to be directly associated with grain yield (Borrell and Hammer, 2000). In addition, a relationship with nitrogen was found: at anthesis the stay-green phenotypes had more nitrogen per leaf area and they maintained this until maturity, extracting the majority of the nitrogen required for grain-filling from the soil (Borrell and Hammer, 2000) and stem (van Oosterom et al., 2010). In the biomass crop *Miscanthus* stay-green phenotypes were identified that might be useful for improving water use efficiency (Clifton-Brown et al., 2002).

Several studies in maize compared new stay-green hybrids with older non-stay-green hybrids to explain the new hybrids' better performance. Echarte, Rothstein and Tollenaar (2008) showed that a stay-green variety maintained photosynthesis for longer under both low and high N availability, accumulated more dry matter, took up more nitrogen, and had a higher grain yield, thus effectively showing a functional stay-green phenotype. Another study found that under nitrogen deficiency, newer (stay-green) varieties maintained photosynthesis for longer, which was associated with greater biomass and higher grain yield (Ding et al., 2005). In contrast, Martin et al. (2005) found

that a stay-green variety accumulated more biomass and took up more nitrogen, but its grain yield was not higher and its grain nitrogen concentration was lower as well. In another Canadian field study, increased leaf longevity was associated with a larger source-to-sink ratio, greater grain yield (Rajcan and Tollenaar, 1999a) and higher grain nitrogen, which was due to increased N uptake (Rajcan and Tollenaar, 1999b). In contrast, in another study both grain nitrogen concentration and nitrogen uptake did not differ at all (Subedi and Ma, 2005).

In durum wheat (*Triticum turgidum* ssp. *durum*) four ethyl methanesulfonate (EMS) mutants have been described which under glasshouse conditions remained green for longer, continued photosynthesizing, and had higher grain yields and seed weights (Spano et al., 2003). The stay-green characteristic was further validated by studying the expression of marker genes for senescence like the small subunit of Rubisco *(RBCS)* and the chlorophyll *a/b* binding protein *(CAB)*, providing further evidence that the photosynthesis machinery was still intact (Rampino et al., 2006). Grain N content was lower in some of the mutants though (Spano et al., 2003), again suggesting that the maintenance of nitrogen in the photosynthetic machinery might be limiting to nitrogen remobilisation to the grain.

Similarly, for hexaploid wheat stay-green phenotypes have been identified that improved grain yields. In China wheat lines with a wheat-rye chromosome translocation were developed which showed a functional stay-green phenotype combined with increased grain yield and total biomass of up to 25% when grown in the field (Chen et al., 2010; Luo et al., 2006). A study on Canadian Red Spring wheat found that grain yield was positively correlated with green flag leaf duration, total flag leaf photosynthesis and even grain N yield (Wang et al., 2008). Another variety also combined the maintenance of green leaf area with higher grain yield (Christopher et al., 2008), but whether the plants retained their photosynthetic capacity was not investigated.

However, the stay-green trait in wheat can also have negative effects. In a stay-green hybrid of winter wheat, chlorophyll content, photosynthesis, grain yield, final biomass and grain-filling rate were all higher, but the harvest index was lower, indicating that the hybrid was relatively inefficient in carbon remobilisation and that the extra photosynthesis products did not end up in the grain (Gong et al., 2005). Another line had a higher grain yield, probably caused by a higher biomass accumulation and a better harvest index, but the nitrogen concentration in straw remained higher, suggesting that more nitrogen is required to maintain a normal grain protein concentration (Chen et al., 2011a).

Studies on Red Spring wheat in the United States found that the effect of stay-green can depend on the environmental conditions. Blake et al. (2007) studied two sets of recombinant inbred lines (RILs). One population showed a positive correlation between the stay-green trait and grain yield, grain volume, and grain weight in both dry and wet conditions, while the other set only showed positive effects of stay-green on grain volume, grain weight and grain protein under drought. Another set of stay-green RILs of spring wheat had a lower grain yield under cool and well-watered conditions, but were able to maintain grain yield in a hot and dry environment (Naruoka et al., 2012). This seemed to be because even though the stay-green RILs always had a lower number of seeds per spike, their seed weight was higher under hot and dry conditions, neutralising the grain yield loss caused by the lower seed number.

Thus so far the studies on stay-green phenotypes in cereals show a mixed picture. In general a stay-green phenotype seems to increase carbon fixation and nitrogen uptake, but does not always have positive effects on the translocation of carbon and nitrogen to the grain.

1.4 THE SENESCENCE PROCESS

1.4.1 Chloroplast Degradation

The photosynthetic machinery is the main source of nitrogen remobilised out of senescing wheat leaves (Gregersen et al., 2008). Studies of cosmetic type C stay-green mutants (see Section 1.3) were crucial for the identification of genes and enzymes involved in the breakdown of both chlorophyll and other chloroplast proteins. Cell death mutants were found to be mutated in chlorophyll degradation enzymes; some of the intermediates in chlorophyll breakdown are toxic.

A summary of the chloroplast degradation pathways is shown in Figure 1.3. The degradation of chlorophyll (Chl) starts inside the intact senescing chloroplast, also called gerontoplast. First chlorophyll *a* is transformed into phein *a* through the removal of Mg^{2+} by Mg dechetalase (MCS). Phein *a* is then converted to pheide *a* by a pheophytinase (PPH). Pheophorbide *a* oxygenase (PAO) then converts pheide *a* to a red chlorophyll catabolite, which is reduced by red chlorophyll catabolite reductase (RCCR) to primary fluorescent chlorophyll catabolite pFCC, which is the first colourless catabolite of the pathway. pFCC is exported out of the gerontoplast, after which most FCCs are converted to non-fluorescent chlorophyll catabolites (NCCs). Only chlorophyll *a* can be broken down in this pathway; therefore chlorophyll *b* first has to be converted to chlorophyll *a* by a chlorophyll *b* reductase (Sato et al., 2009).

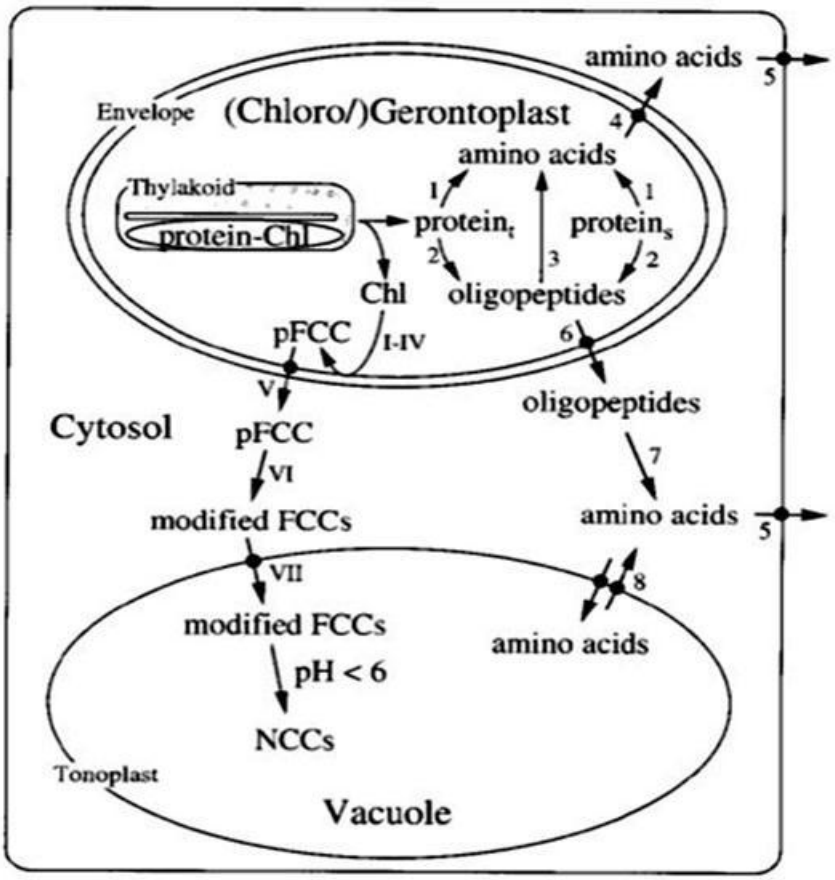

Chlorophyll degradation	
I.	Mg dechelatase (MCS)
II.	Pheophytinase (PPH)
III.	Pheide *a* oxygenase (PAO)
IV.	RCC reductase (RCCR)
V.	Chl catabolite trasnlocator
VI.	FCC-modifying enzymes
VII.	ABC transporter

Chlorophyll degradation	
1.	Exopeptidases
2.	Endopeptidases
3.	Exopeptidases
4.	Amino acid transporter (envelope)
5.	Amino acid exporter (plasma membrane)
6.	Oligopeptide transporter
7.	Cytosolic exopeptidases
8.	Amino acid transporter (tonoplast)

Figure 1.3: The degradation of the chloroplast. Pathways for the degradation of chlorophyll (Roman numbers) and proteins (Arabic numbers) of both the thylakoid (t) and stroma (s) are involved. Figure adapted from Hörtensteiner and Feller (2002).

A stay-green line grew slower under normal conditions but not under conditions where N cycling is normally low, indicating that chlorophyll is more than just a component of photosynthesis, but is also required for protein metabolism and nitrogen nutrition of the whole plant (Hauck et al., 1997). Even though the breakdown products of chlorophyll itself are not remobilised during senescence, NCCs usually are the end product of chlorophyll breakdown, chlorophyll degradation to colourless catabolites is probably necessary to prevent cell death since unbound chlorophyll results in the production of damaging reactive oxygen species (Hörtensteiner and Kräutler, 2011). As chlorophyll is detoxified the released chlorophyll-binding proteins, which form 20% of N in mesophyll cells, can be degraded to exportable N-forms such as amino acids. One of the genes that has been suggested to be involved in the destabilisation of chlorophyll and light-harvesting complex II (LHCII) proteins is the *STAY-GREEN (SGR)* gene (Barry, 2009), which has been identified in many species and is Mendel's *I* locus in pea. In Arabidopsis SGR binds to both LHCII and all five chlorophyll catabolic enzymes, so it appears that SGR directs chlorophyll degrading enzymes to the LHCII-bound chlorophyll (Sakuraba et al., 2012).

Approximately 80% of total leaf N is located in the chloroplasts, in C_3 species mostly in the form of ribulose-1,5-biphosphate carboxylase / oxygenase (Rubisco), while thylakoid membrane proteins such as photosynthesis reaction centres and antenna system account for the rest (Gregersen et al., 2008). Under sufficient N supply the amount of Rubisco can be more than halved before photosynthesis is affected (Quick et al., 1991) and photosynthesis in barley declines faster than Rubisco content (Humbeck, Quast and Krupinska, 1996), suggesting that Rubisco is not the factor limiting photosynthesis in senescing leaves. A more likely factor is the breakdown of less stable stromal proteins such as glutamine synthetase (GS), since this is an early event in senescence (Hörtensteiner and Feller, 2002).

Nearly all protease families appear to be involved in leaf senescence (Roberts et al., 2012). Several different proteases have been implicated in Rubisco degradation. In wheat flag leaves the expression of two subtilin-like proteases correlated with the degradation of the Rubisco small and large subunits (Roberts et al., 2011), inhibition of cysteine proteases in wheat resulted in reduced Rubisco breakdown (Thoenen, Herrmann and Feller, 2007) and the aspartic protease CND41 has been implicated in senescence in several species including Arabidopsis (Diaz et al., 2008), although the evidence relating it to Rubisco has been conflicting (Roberts et al., 2012).

Degradation of stromal proteins such as Rubisco and plastid GS also seems to take place (at least partially) in senescence-associated vacuoles (or Rubisco vescular bodies) (Martinez et al., 2008; Prins et al., 2008). One of these cysteine proteases is the senescence-associated gene *SAG12* (Otegui et al., 2005), which is often used as a marker gene of senescence.

The autophagy and vesicle-trafficking system have been shown to be involved in Rubisco (Ishida et al., 2008) and chloroplast (Wada et al., 2009) breakdown. Plants impaired in autophagy are impaired in nitrogen remobilisation to the seeds (Guiboileau et al., 2012).

The 26S proteasome has also been implicated in senescence (Lin and Wu, 2004; Yoshida et al., 2002a). Substrates have not been identified though and therefore it is not known whether the proteasome is just involved in the breakdown of regulatory proteins (a role suggested by Woo et al. (2001)) or has actually a role in mass protein breakdown for N remobilisation.

1.4.2 Nitrogen Trans-Location

Nitrogen mainly gets exported from leaves via the phloem in the form of amino acids. Glutamate is the main amino acid in phloem of barley and wheat, but glutamine and asparagine increase in late senescence (Gregersen et al., 2008). Since asparagine is synthesized out of glutamine, GS appears to be of major importance during nitrogen remobilisation; and then especially the cytosolic form GS1 since the chloroplast GS2 gets degraded during senescence (Gregersen et al., 2008). Expression of the two GS forms follows this pattern (Gregersen and Holm, 2007) and GS activity was found to be a good marker for nitrogen remobilisation (Kichey et al., 2007). However, expression patterns of different GS and other metabolic enzymes showed the process is complex and that many enzymes are involved (Gregersen and Holm, 2007; Masclaux-Daubresse, Reisdorf-Cren and Orsel, 2008). One of these enzymes is pyruvate orthophosphate dikinase (PPDK), which is expressed in senescing leaves and involved in the production of glutamine, and of which overexpression enhanced nitrogen remobilisation (Taylor et al., 2010).

For amino acids (or small peptides) to reach the growing seeds they have to be loaded onto the phloem. Several amino acid and small peptide transporters have been shown to be expressed in senescing leaves of Arabidopsis (Buchanan-Wollaston et al., 2005; Van der Graaff et al., 2006). Ay et al. (2008) recently claimed *senic4* of barley is the first identified amino acid transporter linked to leaf senescence in a monocotyledonous species. In addition, transporters are likely to be responsible for loading amino acids and / or small peptides from the phloem into the developing seeds (Masclaux-Daubresse et al., 2008).

1.5 GENETIC AND HORMONAL REGULATION OF LEAF SENESCENCE

1.5.1 General Overview

An alternative way to achieve a stay-green phenotype would be overexpression or knockout of genes regulating leaf senescence. A prerequisite for this is that key genes regulating the senescence process are identified. Many environmental factors as well as internal plant signals are thought to play a role in leaf senescence (Figure 1.4). Large-scale transcriptional studies in Arabidopsis (Breeze et al., 2011; Buchanan-Wollaston et al., 2005; Guo, Cai and Gan, 2004; Lin and Wu, 2004; Van der Graaff et al., 2006), barley (Ay et al., 2008), aspen (*Populus tremula)* (Andersson et al., 2004), rice (Liu et al., 2008), and wheat (Gregersen and Holm, 2007) have resulted in a long list of genes that are differentially expressed during developmental or dark-induced leaf senescence. When specifically focusing on transcription factors in Arabidopsis, Balazadeh, Riaño-Pachón and Mueller-Roeber (2008) found 185 differentially expressed transcription factors out of 1880 genes studied. For only a small number of such genes a role in senescence has been unequivocally demonstrated. However, many studies show that natural leaf senescence and senescence induced by abiotic stress or pathogens share many, but not all, of the signals and regulatory genes (Guo and Gan, 2012; Lim, Kim and Nam, 2007). The finding that many pathogen-defence genes are induced during leaf senescence under sterile conditions (Quirino et al., 2000) confirms this view.

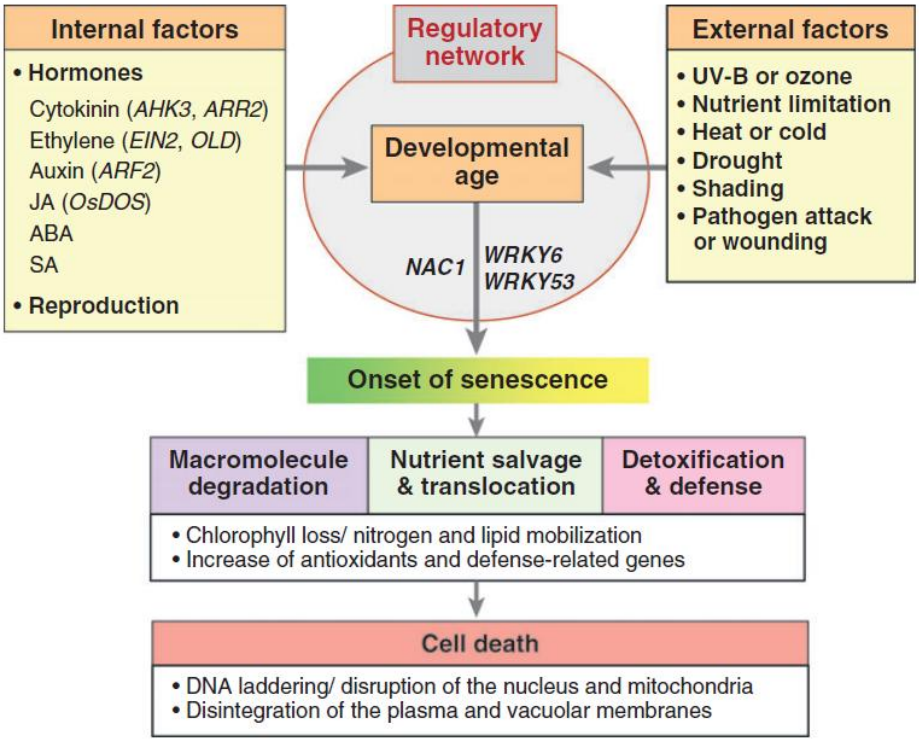

Figure 1.4: A model for the regulation of leaf senescence. Both internal signals, such as hormones and reproductive status, and environmental signals are thought to be integrated into the developmental age-dependent senescence pathway. With senescence different sets of senescence-associated genes responsible for the senescence process are activated, eventually resulting in cell death. Figure from Lim et al. (2007).

1.5.2 NAC Transcription Factors

The transcription factor family with relatively the most differentially expressed genes during leaf senescence is the NAC family (Guo et al., 2004). 117 putative NAC or NAC-like genes have been identified in Arabidopsis and 151 in rice (Nuruzzaman et al., 2010). Most NAC genes are transcriptional activators, although some have a transcriptional repressor domain as well (Hao et al., 2010). They may be involved in many processes such as embryo and shoot meristem development, lateral root formation, auxin signalling,

and defence and abiotic stress responses (Nuruzzaman et al., 2012; Olsen et al., 2005).

Various members of the NAC family have been implicated to have a positive regulatory role in leaf senescence in Arabidopsis. A transcriptome study showed that three NAC genes were up-regulated during senescence of leaves, siliques and petals (Wagstaff et al., 2009). In T-DNA knockout mutants of *AtNAP* leaf senescence was significantly delayed, while overexpression of the gene caused precocious senescence (Guo and Gan, 2006). NTL9 is a membrane-bound NAC protein that was initially linked to osmotic stress responses but was also found to show increased expression during leaf senescence, especially in the actual senescing parts of the leaf (Yoon et al., 2008). Overexpression of the NAC transcription factor *VNI2* resulted in delayed natural leaf senescence, while leaf ageing was accelerated in the *vni2* mutant (Yang et al., 2011). The same result was found for the H_2O_2-responsive NAC transcription factor ORS1 (Balazadeh et al., 2011). NTL4 mediates drought-induced senescence by promoting the production of reactive oxygen species (Lee et al., 2012). *NAC2/ORE1* also showed an increase in expression during senescence, while mutant plants displayed delayed loss of chlorophyll and photochemical efficiency (F_V/F_M), increased *CAB* and decreased *SAG12* expression, and a slower increase in membrane ion leakage (Kim et al., 2009). *NAC2* was age-dependently up-regulated by the ethylene-insensitive senescence-gene *EIN2* but negatively regulated by the microRNA *miR164* (Kim et al., 2009), showing that NAC2 itself is regulated within a regulatory pathway controlling senescence. NAC2 also controls other regulatory genes, as was shown when microarray analysis revealed that it is an upstream regulator of other NAC transcription factors in controlling leaf senescence (Balazadeh et al., 2010).

In the monocotyledonous species rice, bamboo *(Bambusa emeiensis)*, barley and wheat NAC genes have also been shown to have a role in senescence. In rice expression of the ABA-dependent NAC gene *Os*NAC5 gradually increased

during senescence and was higher in lines with high concentrations of seed protein, zinc and iron (Sperotto et al., 2009). Expression of the NAP-like transcription factor *BeNAC1* in bamboo was induced by natural senescence and dark-treatment (Chen et al., 2011b). Overexpression of *BeNAC1* in Arabidopsis resulted in senescence before flowering, and expression of *BeNAC1* in the *nap* mutant rescued its delayed-senescence phenotype. The wheat *Gpc-B1* locus, explained by the *NAM-B1* gene, is present in wild emmer wheat (*Triticum turgidum* ssp. *dicoccoides*) but not in modern durum and bread wheat, and is responsible for accelerated leaf senescence and increased nutrient remobilisation to the developing grain, resulting in higher grain protein, zinc and iron concentrations (Uauy, Brevis and Dubcovsky, 2006a; Uauy et al., 2006b). Flag leaves of plants containing the allele contained higher levels of amino acids (especially serine, alanine and threonine) at anthesis and these levels dropped to normal during grain-filling, possibly explaining the differences in nitrogen remobilisation and grain protein content, especially since nitrogen uptake did not differ (Kade et al., 2005). RNAi-mediated silencing of the four NAM homolog genes found in hexaploid wheat (*TaNAM-A1, D1, B2,* and *D2*) resulted in a delay in leaf senescence of 24 days, a delay in peduncle senescence of more than 30 days, and a reduction in grain protein content of more than 30% (Uauy et al., 2006b). Vegetative N decreased in wild-type, suggesting remobilisation, but increased in the *NAM* knockdown line (Waters et al., 2009a), again suggesting that remobilisation is the mechanism affected. Curiously, in barley containing the homologue locus the senescence and grain protein content phenotype was similar, but expression of the closest homologue to the wheat *NAM-B1* gene, *HvNAM1*, was not affected (Jukanti et al., 2008). Furthermore, expression of the closest rice homologue did not change during senescence (Sperotto et al., 2009).

Only recently a NAC gene has been described that negatively regulates senescence. Overexpression of the H_20_2-responsive NAC transcription factor *JUB1* in Arabidopsis resulted in delayed senescence and bolting, and also

resulted in enhanced abiotic stress tolerance (Wu et al., 2012). Apart from this example, only a wheat gene showing strong homology with rice *NAC2* was identified in a transcriptome study comparing *GPC*-RNAi with wild-type wheat during senescence (Cantu et al., 2011), but its function has not been determined.

1.5.3 WRKY Transcription Factors

A second family of transcription factors with many members differentially expressed during senescence is the WRKY family, which has 74 members in Arabidopsis and 104 in rice (Berri et al., 2009). WRKY gene function is conserved between monocotyledonous and dicotyledonous species; expression patterns of related Arabidopsis and barley genes were often similar (Mangelsen et al., 2008) and a wheat and an Arabidopsis WRKY gene were able to bind to each other's target promoters and drive gene transcription (Proietti et al., 2011).

The most investigated senescence-associated WRKY gene is *WRKY53* in Arabidopsis, which has been shown to be expressed at a very early stage of senescence, when photochemical efficiency (F_V/F_M) starts to decline but before senescence is visible (Hinderhofer and Zentgraf, 2001). The expression of the senescence marker genes *CAB* and *SAG12* (Noh and Amasino, 1999) indicated an early stage of senescence as well: when *WRKY53* was expressed *CAB* expression was already decreasing but *SAG12* was not expressed yet (Hinderhofer and Zentgraf, 2001). Furthermore, overexpression of *WRKY53* resulted in premature flowering and senescence, while a knock-out line was retarded in flowering and senescence (Miao et al., 2004). Although WRKY53 is seen as a key regulator of leaf senescence, the gene itself is under complex regulation as well. A mitogen-activated protein kinase kinase kinase (MEKK1), an activation domain protein, the GATA4 transcription factor, histone methylation, ubiquitin-mediated degradation by the proteasome, H_2O_2, the protein ESR/ESP, and the hormones jasmonic acid (JA), salicylic acid (SA) and abscisic acid (ABA) are all know to have a role in regulating *WRKY53*

expression (Ay et al., 2009; Miao and Zentgraf, 2007; Miao and Zentgraf, 2010; Raab et al., 2009; Zentgraf, Laun and Miao, 2010).

Another Arabidopsis gene, *WRKY70*, was expressed during leaf senescence and *wrky70* loss-of-function mutants show markedly earlier senescence, indicating that this gene functions as a negative regulator of senescence (Ülker, Mukhtar and Somssich, 2007). WRKY70 is at least partially functionally redundant with WRKY54, since the *wrky70/wrky54* double mutant showed a stronger premature senescence phenotype than the *wrky70* mutant (Besseau, Li and Palva, 2012). *WRKY6* was also shown to be strongly up-regulated during the progression of leaf senescence, although *wrky6* null mutants did not display a mutant phenotype (Robatzek and Somssich, 2001). The expression patterns of these three WRKY genes showed a relation with at least one of the phytohormones SA, JA, and ethylene as well as with pathogen infection (Miao and Zentgraf, 2007; Robatzek and Somssich, 2001; Ülker et al., 2007), suggesting that WRKY genes might function in mediating hormone responses in both senescence and pathogen defence. WRKY22 is another positive regulator of senescence (Zhou, Jiang and Yu, 2011b). It was induced by H_2O_2 and darkness, also in the normal light-dark cycle. The *wrky22* mutant showed delayed senescence in darkness, while overexpression resulted in accelerated senescence during dark-treatment. This study also provided evidence that WRKY genes do not act by themselves but interact with other WRKY genes. *WRKY22* overexpression resulted in higher expression of *WRKY6* while *WRKY53* expression was increased in darkness and *WRKY70* expression decreased in light. In both the *wrky6* and *wrky70* mutants *WRKY22* expression was reduced. Yeast-two-hybrid studies also showed direct interactions between WRKY30, WRKY53, WRKY54 and WRKY70 (Besseau et al., 2012). That WRKY transcription factors are often part of networks is further illustrated by the discovery that 70% of the Arabidopsis WRKY genes analysed were co-regulated with other WRKY genes under biotic and/or abiotic stress (Berri et al., 2009).

Several senescence-related WRKY genes were identified in monocotyledonous species, primarily rice. Rice *WRKY23* was only expressed in roots and senescing leaves, and *p35S-OsWRKY23* Arabidopsis plants senesced faster after darkness-treatment than wild-type plants (Jing et al., 2009). *OsWRKY80* (or *OsWRKY13*) was up-regulated by iron-excess, drought-stress and dark-induced senescence, and this increase was accelerated by ABA (Ricachenevsky et al., 2010). Yet since the up-regulation of *WRKY80* is relatively late, it could be an effect of senescence (possibly of Fe release during chloroplast breakdown) rather than a cause. In wheat four isolated WRKY clones were up-regulated in senescing leaves (Wu et al., 2008a), but no functional study was performed.

1.5.4 Signalling Factors

Other than NAC and WRKY genes a wide range of other examples of genes regulating leaf senescence are known. Among these genes are transcription factors of the MYB (Zhang et al., 2011) and AP2/ERF (Xu, Wang and Chen, 2010) families, as well as signalling genes. A mutation in the Arabidopsis mitogen-activated kinase kinase *MKK9* gene resulted in delayed senescence, while overexpression had the opposite effect (Zhou et al., 2009). MKK9 has been shown to play a part in ethylene-signalling, so it is possible that its function in leaf senescence is ethylene-related as well. The senescence-induced receptor-kinase SIRK is a target of WRKY6 and solely expressed during leaf senescence (Robatzek and Somssich, 2002), and the SARK receptor-kinase of bean showed up-regulation during senescence (Hajouj, Michelis and Gepstein, 2000). A screen in barley for senescence-associated genes resulted in the isolation of a lectin receptor-kinase (Ay et al., 2008).

The G-box binding protein GBF1 regulates senescence by reducing catalase expression (Smykowski, Zimmermann and Zentgraf, 2010). The reduction in catalase activity resulted in higher levels of H_2O_2, which acts as a senescence signal. *gbf1* mutants displayed a lack of the H_2O_2 signal and a delay in leaf senescence. Comparison of gene expression between mutant and wild-type

showed that GBF1 directly negatively regulates RBCS1a while expression of *WRKY53*, which is normally expressed before visible senescence, is not induced. So GBF1 clearly has an early regulatory function in senescence. The role of H_2O_2 in senescence was confirmed by the delayed-senescence phenotype of GMPase-overexpressing tomato plants (Lin et al., 2011). These plants have a higher level of L-ascorbic acid (vitamin C) that protects them against oxidative stress caused by reactive oxygen species (ROS) such as H_2O_2. Furthermore, senescence was also delayed when the release of reactive oxygen species was halted by knockout of the chloroplast *NdhF* gene (Zapata et al., 2005). Interestingly, in wheat the removal of all the spikelets delayed and reduced the release of O_2^- and H_2O_2 respectively while N remobilisation was halted (Srivalli and Khanna-Chopra, 2004), indicating a role for the seed sink in initiating N remobilisation through ROS signalling.

Several studies indicate that hexose sugars act as a senescence-signal. Sugars in combination with low N cause senescence-like symptoms in Arabidopsis (Wingler, Marès and Pourtau, 2004). In sunflower the hexose/sucrose ratio increases at the start of senescence, even more so in low N (Agüera, Cabello and de la Haba, 2010), hexose-sugars accumulate in senescing Arabidopsis leaves (Pourtau et al., 2006), and a stay-green banana *(Musa acuminate)* has been shown to accumulate sugars (Yang et al., 2009). The *hyypersenescence1* (*hys1)* mutant of Arabidopsis showed early developmental leaf senescence and hypersensitivity to sugars (Yoshida et al., 2002b). Gene expression analysis of *hys1* showed a hexokinase sugar-signalling pathway was affected. Senescence in the Arabidopsis *gin2-1* mutant (*sugar sensor hexokinase1*) was delayed is because of decreased sugar accumulation and decreased sugar sensitivity (Pourtau et al., 2006). However, *gin2-1* also flowered late, which is consistent with the suggestion sugars might act as a developmental switch regulating ageing (Lim et al., 2007).

In contrast to the signalling factors described above, nitric oxide (NO) is a senescence-inhibiting signal. In Arabidopsis, NO-deficient mutants and plants

expressing a NO-degrading enzyme showed premature senescence (Mishina, Lamb and Zeier, 2007; Niu and Guo, 2012). In turn, NO-signalling is reliant on *EIN2* and Ca^{2+}-signalling (Ma et al., 2010; Niu and Guo, 2012).

1.5.5 Co-Regulation of Flowering and Senescence

Since monocarpic senescence results in remobilisation of nutrients to the seed, and it even seems to be a major function of this process, an obvious assumption would be that the regulation of flowering and senescence are linked. This is definitely true for tropical maize, of which senescence always starts directly after flowering, no matter the nitrogen status, indicating that in tropical maize senescence is probably exclusively regulated by developmental age (Osaki, 1995). Even though flowering is not required to initiate senescence in Arabidopsis (Hensel et al., 1993) and there is evidence for flowering-independent senescence pathways (Wingler et al., 2010), in several species senescence-associated mutants also show changes in flowering time (for example Donnison et al., 2007; Lacerenza, Parrott and Fischer, 2010; Miao et al., 2004; Wu et al., 2008b), supporting the existence of genetic links between the regulation of flowering and senescence. In Arabidopsis two quantitative trait loci (QTL) for senescence co-localise with the flowering genes *FLC* and *FRI*, and expression of other flowering genes was correlated with senescence (Wingler et al., 2010), showing coupling of reproduction to whole-plant senescence. This is not unique for Arabidopsis; also in wheat anthesis date and the total duration of leaf senescence are negatively correlated (Bogard et al., 2011).

1.5.6 Hormonal Regulation

Apart from the aforementioned *WRKY53* and *MKK9*, many other genes indicate the role of phytohormones in senescence regulation. ORE9 in Arabidopsis and its rice ortholog DWARF3 are F-box proteins (Woo et al., 2001; Yan et al., 2007), and their mutants show increased leaf longevity. Since the function of F-box proteins is to target specific proteins for degradation by the 26S proteasome, it is likely that ORE9 and DWARF3 are responsible for

degradation of a key negative regulator of leaf senescence. Since *ore9-1* mutants showed a delay in the response to MeJA, ethylene, and ABA modulated senescence, ORE9 might function in a pathway common to senescence induced by these three hormones (downstream of their signalling) as well as age-dependent senescence (Woo et al., 2001).

A mutation in the ABA-dependent receptor kinase RPK1 resulted in delayed senescence while overexpression resulted in early senescence, showing that the gene is a positive regulator of senescence (Lee et al., 2011). Only ABA-dependent senescence was affected, dark-induced senescence for instance was not, indicating that the gene is ABA specific and also that ABA has a role in the regulation of senescence. The effect of ABA on senescence is age-dependent: ABA makes leaves that have started to senesce do so faster but cannot induce senescence in immature plants (Lee et al., 2011; Weaver et al., 1998). However, in cucumber *(Cucumis sativus)* ABA seemed to promote biosynthesis and inhibit degradation of chlorophyll under low N conditions (Oka et al., 2012), indicating that under some conditions ABA can also inhibit senescence.

Most JA-biosynthesis genes are up-regulated during developmental but not dark-induced senescence, suggesting developmental stimuli activate their expression (Van der Graaff et al., 2006). The rice CCCH-type transcription factor OsDOS is a JA-related negative regulator of leaf senescence, which is confirmed by its expression pattern in natural leaf senescence as well as the phenotypes of RNAi and overexpression transgenic lines that show accelerates and delayed leaf senescence respectively (Kong et al., 2006). Similarly, Rubisco activase was found to be a JA-dependent negative regulator of senescence in Arabidopsis (Shan et al., 2011). Mutants in the histone deacetylase gene *HDA6*, which is needed for expression of JA-response genes, displayed a delayed senescence phenotype (Wu et al., 2008b), further confirming a role of JA in senescence.

SA-deficient mutants and RNAi lines lose chlorophyll at a normal rate but maintain PSII functionality for longer (Abreu and Munné-Bosch, 2009), thus being able to maintain photosynthesis. Interestingly, the genes induced by SA and senescence appear to be specific for natural senescence and are not regulated in dark-induced senescence (Buchanan-Wollaston et al., 2005; Van der Graaff et al., 2006).

The delayed senescence phenotype of the *auxin response factor 2* mutant (*arf2*) indicates a possible role for auxin in leaf senescence (Ellis et al., 2005). A mutant of the E3 ubiquitin ligase SAUL1 showed premature senescence under low light conditions. Under senescence-inducing conditions (low light) *saul1* had increased levels of ABA, indicating ABA biosynthesis was switched on (Raab et al., 2009). This was due to higher expression of the ABA biosynthesis gene *AAO3*, indicating that SAUL1 normally prevents premature low-light-induced senescence by lowering ABA levels through targeting AAO3 for degradation. Overexpression of another auxin biosynthesis gene, *YUCCA6*, resulted in delayed natural and dark-induced senescence and a prolonged lifespan in general (Kim et al., 2011). Overexpression of a mutated YUCCA6 that is not able to reduce auxin did not result in delayed (dark-induced) leaf senescence, indicating that auxin mediates its phenotype.

Many ethylene-biosynthesis genes are synchronically up-regulated during senescence (Van der Graaff et al., 2006). Even though ethylene is neither necessary nor sufficient for the occurrence of leaf senescence, the *onset of leaf death (old)* mutants show early senescence, most of them especially after ethylene treatment (Jing et al., 2002). The MKK9-MPK3/MPK6 signalling cascade has been shown to have a role in ethylene signalling, so it is possible it mediates ethylene-regulated leaf senescence (Zhou et al., 2009).

Mutations in specific cytokinin (CK) receptors, especially AHK3, caused a reduction in the leaf chlorophyll content, indicating CK mediates chlorophyll retention (Riefler et al., 2006). CK prevents senescence of pre-senescent

leaves, but it is not very effective in halting senescence after initiation (Weaver et al., 1998). Modification of CK levels by manipulating gene expression has been applied to delay leaf senescence. By expressing the *Agrobacterium* CK biosynthesis gene *IPT* under control of the senescence-specific *SAG12* promoter, tobacco plants were produced that were delayed in leaf senescence (Gan and Amasino, 1995). However, N was preferentially allocated to the old leaves, possibly even driving young leaves into early senescence when N was limiting (Jordi et al., 2000). In wheat, *pSAG12-IPT* expression delayed chlorophyll breakdown but did not lead to the desired higher grain yields, probably because translocation of nutrients from leaves to the grain was delayed (Sýkorová et al., 2008). When *IPT* was expressed under the control of the SARK-promoter in tobacco, increasing CKs in all leaves so N remobilisation would not be affected, there was no effect on the phenotype under normal conditions, but under drought stress leaf senescence was prevented and grain yields were dramatically increased (Rivero et al., 2007).

That many potential regulatory genes of senescence respond to several hormone treatments indicates that hormones influence each other, so genes responding to different hormones and influencing others could be involved in the integration of hormone signals. For example, the senescence-associated receptor-like kinase SARK is dependent on both ethylene and auxin signalling pathways while it seems to reduce cytokinin function (Xu et al., 2011).

1.6 PROJECT OUTLINE

1.6.1 Central Hypothesis

The maintenance of a photosynthetically active canopy in the post-anthesis period will positively influence grain yield, and control of its senescence will produce a product rich in carbon with optimum efficiency of nitrogen input.

1.6.2 Aims of the Project

1. To identify genes correlating with leaf senescence in wheat by screening genotypes with varied senescence characteristics.
    a. *To compare senescence phenotypes of wheat genotypes grown under different nitrogen regimes in the field.*
    b. *To assess effects of differential senescence on grain yield, harvest index and grain nitrogen concentration and content.*
    c. *To examine patterns of expression of candidate regulatory genes of leaf senescence leaf samples from these field experiments.*

2. To identify wheat genotypes with fast-senescing and delayed leaf senescence “stay-green” phenotypes and study the effects of nitrogen nutrition on their phenotypes.
    a. *To identify stay-green and fast-senescing mutant lines of wheat.*
    b. *To assess senescence, yield characteristics and biomass and nitrogen distribution of these differential senescing lines.*
    c. *To assess the effects of nitrogen supply on the senescence phenotypes by studying the performance of fast-senescing and stay-green wheat lines.*
    d. *To assess patterns of expression of candidate regulatory genes of leaf senescence.*

3. To study the function of a NAC transcription factor in leaf senescence of wheat.
   a. *To establish the possible identity of the NAC gene by analysing its sequence and phylogeny.*
   b. *To determine in which plant tissues the NAC gene is expressed.*
   c. *To analyse the effects of overexpression of the NAC gene on morphology, development, senescence, biomass, grain yield and grain nitrogen content of wheat.*

4. To study the function of a WRKY transcription factor in leaf senescence of wheat.
   a. *To establish the possible identity of the WRKY gene by analysing its sequence and phylogeny.*
   b. *To analyse the effects of RNAi knockdown of the WRKY gene on morphology, development, senescence and grain yield of wheat.*
   c. *To determine in which plant tissues the WRKY gene is expressed.*

These aims were addressed through three experimental approaches, as outlined below.

1.6.3 Experimental Approaches

1. Gene expression studies of field-grown wheat

As a screening for genes correlating with leaf senescence, the expression of candidate genes was quantified in time courses of leaf tissues of the wheat cultivar Hereward, which was grown at standard and low nitrogen fertilisation regimes and therefore differed in their rates of senescence. A second set of field materials consisted of two doubled haploid lines of an Avalon x Cadenza mapping population differing in their rate of senescence grown at low and high nitrogen fertilisation in two consecutive seasons. Candidate gene expression was quantified in these materials to further corroborate the found expression patterns of selected genes.

2. Stay-green mutants

In a field trial at the John Innes Centre (JIC) a number of mutant wheat lines (cv. Paragon) had been identified that were visually stay-green. These were grown in the glasshouse to confirm their stay-green phenotypes and to test their photosynthetic capacity to find out which of these lines have functional stay-green phenotypes. A small number of lines was selected and grown in the glasshouse to characterise further. Stay-green and fast-senescing lines were identified. A fast-senescing, a stay-green and a wild-type line were then grown under high and low nitrogen nutrition to assess the interaction between different senescence phenotypes and nitrogen nutrition.

3. Transgenics

Transgenic plants with modified expression levels of two genes identified in the gene expression studies were created with the aim to delay leaf senescence. A NAC gene which expression normally declines during senescence was overexpressed, while the expression of a WRKY gene of which the expression normally increases during senescence was reduced using RNAi.

2. MATERIALS AND METHODS

2.1 EXPERIMENTAL DESIGNS

2.1.1 Field Experiments (Chapter 3)

2.1.1.1 Hereward Field Experiment

Six varieties of wheat (*Triticum aestivum* L.), including cultivar Hereward, were grown in the Stackyard field at Rothamsted Research (Harpenden, UK) in 2006/7 at two nitrogen fertilisation regimes (50 kg N ha^{-1} and 200 kg N ha^{-1}) in a randomised block design with four replicate blocks. Between anthesis and seven weeks post-anthesis four replicate leaf 2 samples were sampled weekly (by Dr Jonathan Howarth, Rothamsted Research) and stored at -80°C to allow subsequent RNA extraction and semi-quantitative RT-PCR analysis (Sections 2.2.1 – 2.2.3). At the same time the relative chlorophyll content (SPAD) was determined (Section 2.3.1) to follow the progress of leaf senescence. Measurements were performed on the second leaf because it senesces earlier and at a slower rate than the flag leaf (Wittenbach, 1979) and is therefore more likely to show differences in senescence.

2.1.1.2 Avalon x Cadenza Doubled Haploid Lines Field Experiment

The Diversity Trial 2008/9, which was part of the Defra-funded Wheat Genetic Improvement Network (WGIN) project, consisted of eighteen commercial varieties and six doubled haploid Avalon x Cadenza mapping population lines of winter wheat, which had been selected for high and low values of certain traits. The Avalon x Cadenza come from a doubled haploid population developed from F1 progeny of a cross between cultivars Avalon and Cadenza at the JIC as part of the WGIN project. Two of the double haploid lines with high and low rate of early export of nitrogen from the leaf, AC127 and AC82, were chosen for measurements since it was hypothesised the differences in nitrogen export should equate to differences in leaf senescence. The

experiment was grown at the Summerdells I and II fields at Rothamsted Research (Harpenden, UK) on four nitrogen levels (0, 100, 200 and 350 kg N ha^{-1}) in three completely randomised replicate blocks. The plots were split in a 3.0 m x 3.5 m section for any measurements during the growing season, including destructive sampling, and a 3.0 m x 10.0 m section for yield measurements at final harvest. SPAD measurements (Section 2.3.1) were taken at anthesis, 21 days post-anthesis (dpa) and 35 dpa. All field plots were screened for senescence by monitoring canopy reflectance (NDVI) with a Crop Canopy Sensor (Section 2.3.4) on a weekly basis. For gene expression analyses (Sections 2.2.1 – 2.2.3) and nitrogen analysis (Section 2.2.6) weekly leaf 2 samples were taken of the selected lines, starting at anthesis.

The Diversity Trial 2009/10 contained nineteen commercial varieties and six Avalon x Cadenza mapping population lines. The field experiment was grown at the Black Horse and Bylands fields at Rothamsted Research (Harpenden, UK). The lines were fully randomised in three replicate blocks with the four nitrogen levels (0, 100, 200, 350 kg N ha^{-1}) arranged in sub-blocks within them. All field plots were scanned weekly with a crop canopy sensor (Section 2.3.4) to follow the process of senescence. For gene expression analyses (Sections 2.2.1 – 2.2.3) and nitrogen analysis (Section 2.2.6) weekly leaf 2 samples (starting at anthesis) were taken of the six mapping population lines and stored at -80°C. The relative chlorophyll content of the six doubled haploid lines was determined weekly from anthesis with a SPAD meter (Section 2.3.1) until the SPAD values had reached zero. Of lines AC127 and AC82 grown at 100, 200 and 350 kg N ha^{-1} the maximum efficiency of photosystem II (quantum yield; Section 2.3.3) was determined weekly from anthesis until it had reached zero.

2.1.2 Stay-Green Mutants (Chapter 4)

2.1.2.1 Screening of Mutant Collection

A collection of 54 ethyl methanesulfonate (EMS) mutant lines of spring wheat (*Triticum aestivum* L. cv. Paragon) and two replicates of Paragon wild-type (seed supplied by Dr Simon Griffiths, JIC) were grown in the glasshouse (18°C day / 14°C night temperature with a minimum photoperiod of 16 hours as controlled by supplementary lighting when natural light levels came below 200 µmol m^{-2} s^{-1}) in a temporal staggered randomised block design consisting of four blocks and five plants per pot (Ø 20 cm, 4 l). Plants were grown in "Rothamsted Prescription Mix" compost: 75% medium grade peat, 12% screened sterilised loam, 3% medium grade vermiculite, 10% grit (5mm screened, lime free), 3.5 kg m^{-3} Osmocote Exact, 0.5 kg m^{-3} PG mix, lime to pH 5.5-6.0, and 200 ml m^{-3} Vitax Ultrawet wetting agent. The total N supply was approximately 2.5 g N per pot. The plants were kept well watered. The relative chlorophyll content (Section 2.3.1) and photosynthetic rate (Section 2.3.2) of flag leaves were measured at two fixed moments that were roughly at anthesis (totally green leaves) and six weeks after anthesis (senescing leaves). Measurements were done on the flag leaf because it is the biggest leaf, at least for cultivar Paragon, and at the top of the canopy, so it should contribute most carbon and nitrogen for grain-filling. Saroj Parmar and Silvia Celletti (Rothamsted Research) assisted with the measurements. Relative levels of SPAD and photosynthesis at the second time point were calculated: $\frac{Value_{6weeks}}{Value_{Anthesis}} \times 100\%$.

2.1.2.2 Characterisation of Selected Lines

Seven lines were selected for more detailed analysis: three stay-green lines, three fast-senescing lines and a wild-type line (Table 2.1). They were grown in the glasshouse in a randomised complete block design (Figure 2.1) with four replicate blocks and five plants per pot (Ø 20 cm, 4 l) (seed supplied by Dr Simon Griffiths, JIC) at the same growing conditions as the mutant screening

(see above). Each block contained seven pots per line: six for the different time points and one for dissection at maturity. An eighth pot of each line was located at the end of the block for dissection at anthesis: the end location prevented the existence of gaps in the "field" during the experiment.

The anthesis date was determined separately per pot. Anthesis was defined as "three or more plants (main shoots) per pot had visible anthers" (GS61; Zadoks, Chang and Konzak, 1974). Each pot had already been allocated randomly to a certain time point before the start of the experiment, and chlorophyll fluorescence (Section 2.3.3) and SPAD (Section 2.3.1) measurements were performed at anthesis, 14 days post-anthesis (dpa), 21 dpa, 28 dpa, 35 dpa or 42 dpa, or when the ears (three or more) of the main shoots had reached maturity. All senescence measurements were performed on the flag leaves of main shoots (see Section 2.3 for details) and averaged per pot. Line 1439 (A) was not measured because in this experiment its anthesis date was about four weeks later than that of the other lines and was therefore incomparable.

The total number of tillers (including the main shoots) was determined per pot (five plants). At maturity the ears of all tillers were harvested per pot to determine the grain yield. Thousand grain weights (Section 2.2.7) were determined on three replicate samples of the pooled grain per line, since there was not enough seed per pot. Total straw mass was determined to calculate the Harvest Index (HI) according to the formula: $HI = Grain\ DW/(Grain\ DW + Straw\ DW)$.

To determine dry matter distribution at anthesis and maturity, the five main shoots per pot were pooled and partitioned into flag leaf lamina, leaf lamina of the other leaves, leaf sheaths, stem, and ear fractions and the dry weights were determined after drying 1-2 days at 80°C. The fractions were milled and nitrogen concentration and contents determined (Section 2.2.6).

Table 2.1: Selected mutant lines used for further studies.

Line	Code	Name	Supposed phenotype
1439m5	A	-	Fast-senescing
862a	B	FS1	Fast-senescing
2514a	C	FS2	Fast-senescing
2056a	D	SG1	Stay-green
1389a	E	SG2	Stay-green
555a	F	SG3	Stay-green
Paragon wild-type	G	WT	Wild-type (intermediate)

I																	
Fa	Ca	Aa	D2	G4	B5	F4	F1	E2	F2	A4	D1	D4	G2	Dh	C1	F5	A3	C4
Ba	Da	B2	F3	D6	Bh	Gh	Ch	D5	A6	Ah	B6	G6	B3	F6	E4	Fh	C5	A5
Ga	Ea	G1	E6	E1	E3	A2	B4	C2	B1	C6	A1	C3	Eh	G5	E5	G3	D3	
II																		
	E4	B6	B2	Ch	G3	B4	F6	B5	F2	D4	A4	C3	B1	E1	Dh	G6	Ba	Ga
D3	G2	C2	G4	Fh	A2	D2	F1	G5	E2	A5	C4	E6	F3	F5	Eh	Ah	Fa	Ea
B3	D6	A6	E5	Gh	C1	E3	G1	F4	A1	D5	A3	D1	Bh	C5	C6	Ca	Aa	Da
III																		
Ba	Aa	C2	C3	D5	Dh	A2	E1	F1	B4	B2	D4	A1	F3	D6	G2	Eh	C6	
Ga	Ca	F6	D3	C4	Ah	E2	F4	A3	E5	D1	G4	G1	G3	E6	D2	G5	F2	C5
Fa	Ea	Da	C1	A4	A6	B6	B5	F5	G6	Fh	B1	E4	Bh	Gh	B3	E3	A5	Ch
IV																		
	Gh	B6	A2	D5	G3	F3	G2	C2	A6	E6	E4	D2	D6	Fh	Bh	Ah	Ea	Ga
F5	C6	B3	D4	B1	B4	E1	A1	Dh	E3	D1	C1	B5	C3	B2	A4	F6	Ba	Da
Eh	D3	F4	F1	C5	E5	F2	G1	Ch	C4	E2	G5	A3	G4	A5	G6	Ca	Fa	Aa

Figure 2.1: Experimental design for characterization of selected mutant lines. A randomised block design with 4 blocks (I-IV) containing a complete 7 by 6 factorial treatment set for 7 genotypes by 6 time points for leaf measures on plants, and 1 pot of each genotype at anthesis and harvest for whole plant destructive measurements. Codes: A-G = lines (Table 2.1), a = anthesis, h = harvest, and 1-6 = the leaf sampling time points.

2.1.2.3 Nitrogen Nutrition Experiment

For the nitrogen nutrition experiment one fast-senescing line (FS2), one stay-green line (SG3) and a wild-type line (WT) were grown at two nitrogen levels; the low N treatment containing 10% nitrogen of the high N treatment. The six genotype x nitrogen combinations were grown in the glasshouse at the same temperature and lighting conditions as the previous two experiments in a randomised complete block design (Figure 2.2) with four blocks (replicates) and five plants per pot (Ø 20 cm; 4 l). Each block contained five pots per genotype x nitrogen combination to allow for destructive sampling at five time points, and each pot had already been allocated randomly to a certain time point before the start of the experiment

Plants were grown in the nutrient poor soil "Rothamsted Nematode mix" (80% sterilised loam, 15% 2EW sand, 5% grit (5mm)). Nitrogen was applied in the form of nutrient solution (Table 2.2). 0.5 l of solution was applied twelve times between planting and anthesis, amounting to a total of 67.2 and 672 mg N for low and high N treatments respectively. The pots were placed on saucers to keep the supplied nutrients in the pots. Additional demineralised water was supplied when required.

The anthesis date was determined separately per pot. Anthesis was defined as "three or more plants (main shoots) per pot had visible anthers" (GS61).. For the low N treatment SPAD (Section 2.3.1) and chlorophyll fluorescence (Section 2.3.3) measurements were taken at anthesis, 12 dpa (WT started to senesce), 17 dpa (rapid senescence) and 21 dpa (WT completely senesced). For the high N treatment the equivalent time points were anthesis, 21 dpa (last time point low N), 25 dpa (WT started to senesce) and 35 dpa (WT completely senesced). All senescence measurements were performed on the flag leaves of main shoots and values were averaged per pot.

Table 2.2: Nutrient solutions used for the nitrogen nutrition experiment. The low N solution contained 10% $Ca(NO_3)_2.4H_2O$ of the high N solution. The deficient calcium was supplied in the form of extra $CaCl_2$. N concentrations were 0.8 mM and 8.0 mM in the low and high N solutions, respectively.

Solution	Ingredient	Concentration
		mM
	KH_2PO_4	0.25
	KOH	0.50
	$MgSO_4.7H_2O$	0.75
	$CaCl_2$	0.03
	FeNaEDTA	0.10
High N	$Ca(NO_3)_2.4H_2O$	4.00
Low N	$Ca(NO_3)_2.4H_2O$	0.40
Low N	$CaCl_2$	3.60
		µM
	H_3BO_3	30.0
	$MnSO_4.4H_2O$	10.0
	$ZnSO_4.7H_2O$	1.0
	$CuSO_4.5H_2O$	3.0
	$Na_2MoO_4.2H_2O$	0.5

Destructive sampling was performed at the same time points and final harvest (complete senescence of the whole pot). Two main shoot flag leaves were collected and frozen in liquid nitrogen and stored at -80°C for gene expression analysis (Sections 2.2.1 – 2.2.3). Two other main shoots were taken and partitioned into flag leaf lamina, lamina of other leaves, leaf sheaths, stem, and ear fractions and all dry weights were determined after drying 1-2 days at 80°C. At maturity the ears were split into grain and chaff. The samples taken at anthesis and maturity were milled for nitrogen analysis with a combustion N-analyser (Section 2.2.6). As flag leaf samples were too small, the total sample was used but the result must be considered less reliable.

	3 FS2 N1	3 WT N1	2 SG3 N1	1 FS2 N2	1 FS2 N1	4 SG3 N1	5 WT N1	5 SG3 N2	3 WT N2	2 WT N1
Block I	1 WT N2	5 WT N2	4 SG3 N2	1 SG3 N1	2 WT N2	4 WT N1	3 FS2 N2	5 FS2 N2	1 SG3 N2	5 FS2 N1
	2 FS2 N2	2 FS2 N1	2 SG3 N2	4 WT N2	1 WT N1	5 SG3 N1	3 SG3 N2	3 SG3 N1	4 FS2 N2	4 FS2 N1
	5 SG3 N2	4 SG3 N1	2 WT N2	2 FS2 N1	1 WT N2	4 SG3 N2	3 FS2 N2	3 SG3 N1	5 WT N2	1 SG3 N1
Block II	4 WT N2	3 SG3 N2	3 WT N1	4 FS2 N2	5 FS2 N2	4 WT N1	5 WT N1	1 WT N1	1 FS2 N1	2 SG3 N2
	5 SG3 N1	1 FS2 N2	2 SG3 N1	4 FS2 N1	2 WT N1	1 SG3 N2	3 FS2 N1	3 WT N2	5 FS2 N1	2 FS2 N2
	1 SG3 N2	3 WT N2	4 WT N2	3 SG3 N1	5 SG3 N2	2 WT N1	2 SG3 N1	2 FS2 N2	2 SG3 N2	2 WT N2
Block III	4 SG3 N1	4 FS2 N2	4 WT N1	1 WT N1	5 WT N2	4 FS2 N1	3 SG3 N2	2 FS2 N1	4 SG3 N2	1 WT N2
	1 FS2 N1	3 FS2 N2	5 FS2 N1	3 WT N1	1 SG3 N1	5 SG3 N1	5 FS2 N2	1 FS2 N2	5 WT N1	3 FS2 N1
	2 WT N2	3 SG3 N1	5 WT N2	5 FS2 N2	4 WT N2	3 WT N1	1 SG3 N2	4 FS2 N1	1 FS2 N2	1 WT N2
Block IV	3 FS2 N2	3 FS2 N1	5 SG3 N1	5 SG3 N2	1 SG3 N1	4 FS2 N2	4 WT N1	2 SG3 N1	4 SG3 N1	2 WT N1
	4 SG3 N2	3 SG3 N2	5 WT N1	3 WT N2	1 FS2 N1	2 SG3 N2	2 FS2 N2	5 FS2 N1	2 FS2 N1	1 WT N1

Figure 2.2: Experimental design for the nitrogen nutrition experiment. A randomised block design with 4 blocks (I-IV) containing a complete factorial set of three lines x two nitrogen nutrition levels x five time points. N1 (pink) = low N; N2 (green) = high N; 1-5 = time points; FS2 (red), SG3 (black) and WT (blue) = lines.

The total number of tillers (including the main shoots) was determined per pot (five plants). Plant heights were determined for the tallest tiller or main shoot per plant, after which this was averaged per pot. At maturity all the ears per plant were harvested per pot to determine the grain yield. Total straw mass was determined to calculate the Harvest Index: $HI = Grain\ DW/(Grain\ DW + Straw\ DW)$. Thousand grain weights (Section 2.2.7) and the grain numbers were determined on the pooled grain per genotype x N group per block, since there was not enough seed per pot.

2.1.3 Analysis of NAC-Overexpressing Wheat (Chapter 5)

2.1.3.1 Creating and Screening of NAC-Overexpressing Wheat

A wheat NAC transcription factor (TA65763_4565) was overexpressed in wheat cultivar Cadenza with the aim to delay leaf senescence. Two constructs (Figure 5.5) were made (by Dr Peter Buchner, Rothamsted Research): one with the rice tungro bacilliform virus (RTBV) promoter and one with the rice *actin1* promoter. The RTBV promoter has good expression in wheat leaves, immature floral tissues and endosperm but no expression in roots, pollen or the axis of immature embryos (Rothamsted Cereal Transformation Group, unpublished). In rice the expression of the RTBV promoter in leaves was mainly localised in the phloem, although there also was low expression in the mesophyll parenchyma (Bhattacharyya-Pakrasi et al., 1993). The *actin1* promoter is considered to be constitutively expressed in all tissues (Zhang, McElroy and Wu, 1991). Transformations of wheat were performed by the Rothamsted Cereal Transformation Group using the particle bombardment technique (Sanford, 1988) as described by Sparks and Jones (2009).

Two pActin-NAC lines and eight pRTBV-NAC lines were generated (Table 2.3). Second generation (T2) plants were grown in the glasshouse to determine whether there was a resulting phenotype. 10-12 seeds were germinated and the seedlings were screened for presence of the transgene by PCR on genomic DNA (Sections 2.2.4 and 2.2.5). The transgenic lines were compared

with a transformation control line (which went through the transformation process but no construct was inserted) and wild-type (cv. Cadenza) wheat.

2.1.3.2 Analysis of NAC-Overexpressing Wheat

Four positive plants per line were grown in the glasshouse (20°C day / 15°C night temperature with a minimum photoperiod of 16 hours as controlled by supplementary 400 watt SON-T lighting) in a complete randomised block design with four replicate blocks (Figure 2.3) with one plant per pot (Ø 13 cm, 0.8 l). Plants were grown in "Rothamsted Prescription Mix" compost: 75% medium grade peat, 12% screened sterilised loam, 3% medium grade vermiculite, 10% grit (5mm screened, lime free), 3.5 kg m^{-3} Osmocote Exact, 0.5 kg m^{-3} PG mix, lime to pH 5.5-6.0, and 200 ml m^{-3} Vitax Ultrawet wetting agent. The total N supply was approximately 0.5 g N per pot. Development was followed by determining when key developmental stages were reached by the main shoot: Growth Stage 39 (flag leaf totally emerged), GS49 (booting complete, start heading), GS61 (start anthesis) and GS89 (physiological maturity) of the Zadoks classification (Zadoks et al., 1974). The anthesis date was not only determined for the main shoot but also for the first three tillers. Morphological features determined were: height of main shoot and first two tillers, length and width of top three leaves of the main shoot, the number of leaves on the stem of the main shoot, and the number of tillers (including the main shoot). Senescence was followed by measuring SPAD (Section 2.3.1) and quantum yield (Section 2.3.3) of the top three leaves of the main shoot weekly from anthesis until seven weeks post-anthesis. Grain was collected and weighed to determine the grain yield.

2.1.3.3 Gene Expression, Biomass and Grain Nitrogen Analysis

An experiment was set up with a selection of the lines to analyse gene expression, biomass distribution and grain nitrogen concentration and content of selected lines. The experiment consisted of three replicate blocks with five lines and four time points (Figure 2.4). Plants were grown at the

same conditions as in the previous characterisation experiment. The lines included were R5 (greenest), R8 (longest green duration), R4 (average stay-green), A1 (actin promoter line) and C (control line). There were four sample points at which SPAD (Section 2.3.1) of the top three leaves of the main shoot was measured and the second leaf of the main shoot was harvested for gene expression analysis (Sections 2.2.1 - 2.3.3). The first two sample points were anthesis (0 dpa) and 10 dpa (no visible senescence control line) Senescence differed dramatically between the blocks depending on position: an unusual warm and sunny march week induced senescence and the effects were stronger for blocks B and C which were located at the south-facing window of the glasshouse. Therefore the last two sample points were different per block: 20 dpa (start visible senescence control line) and 25 dpa (strong senescence control line) for block A and 15 (start visible senescence control line) and 20 dpa (strong senescence control line) for blocks B and C. At anthesis, after the leaf had been collected, the whole shoot was harvested, oven-dried at 80°C and weighed to determine the biomass. At maturity the biomass of ears, grain, and the rest of the aboveground tissues of the remaining plants was determined. Total grain per plant was milled and the nitrogen concentration and content determined (Section 2.2.6).

Table 2.3: Lines used for characterisation of NAC-overexpressing wheat. The transgenic plants used were from the T2 generation.

Line	Description	Bombardment	Replicate	Plant T0	Plant T1
A1	pActin-NAC	2806	6	1	16
A2	pActin-NAC	2806	11	1	11
R1	pRTBV-NAC	2789	7	3a	10
R2	pRTBV-NAC	2789	7	5	14
R3	pRTBV-NAC	2802	4	1a	4
R4	pRTBV-NAC	2802	8	1	8
R5	pRTBV-NAC	2802	9	1	16
R6	pRTBV-NAC	2802	13	1	8
R7	pRTBV-NAC	2802	13	2	12
R8	pRTBV-NAC	2802	14	1	14
C	Transformation control	2802	3	1	1
WT	Cadenza wild-type	x	x	x	x

1

R3	R5	R4
R6	R8	R1
A1	R2	WT
R7	A2	C

2

R2	R7	R5
A1	R8	A2
R1	WT	R4
C	R6	R3

3

R2	A2	R4
R1	WT	R6
C	R5	R7
R8	R3	A1

4

R3	R7	R1
A1	R2	A2
R6	R4	WT
R8	R5	C

Figure 2.3: Experimental design for characterisation of NAC-overexpressing wheat. A randomised block design with four blocks (1-4). A1 + A2 = pActin-NAC 1 + 2, R1-R8 = pRTBV-NAC 1 – 8, C = transformation control, WT = wild-type Cadenza.

A

A1-1	R4-4	R5-2	R4-1	R5-3
C-3	A1-3	R8-3	R4-3	R8-4
R5-4	R4-2	R5-1	A1-4	A1-2
R8-2	C-1	R8-1	C-2	C-4

B

R4-4	R4-3	C-4	R8-3	R8-2
R8-1	C-2	A1-2	C-1	A1-3
R4-2	R4-1	R5-1	R5-4	R5-2
A1-4	R8-4	C-3	A1-1	R5-3

C

R8-1	A1-4	A1-3	C-2	C-3
C-4	R5-4	R4-1	R8-2	R8-3
R4-4	R5-1	R5-3	A1-2	R8-4
C-1	R4-3	R4-2	R5-2	A1-1

Figure 2.4: Experimental design for the second NAC transgenics experiment. A randomised block design with three blocks (A-C), four time points (1-4) and five lines. A1 = pActin-NAC 1; R4, 5 and 8 = pRTBV-NAC 4, 5 and 8; C = transformation control.

2.1.4 Analysis of WRKY-RNAi-Knockdown Wheat (Chapter 6)

In an attempt to delay leaf senescence in wheat, an RNAi-construct was made to silence a wheat WRKY transcription factor (accession numbers TC271537 and BE406842) in wheat cultivar Cadenza. As for NAC-overexpression, a construct with the RTBV promoter and one with the *actin1* promoter were made (see Section 2.1.3.a and Figure 6.3 for more details).

Six pActin-WRKY-RNAi and eleven pRTBV-WRKY-RNAi lines generated (Table 2.4). Second generation (T2) plants were grown to determine whether there was a resulting phenotype. 10-12 seeds were germinated and the seedlings were screened for presence of the transgene by PCR on genomic DNA (Sections 2.3.4 and 2.3.5). Four positive plants per line were selected and grown in the glasshouse (20°C day / 15°C night temperature with a minimum photoperiod of 16 hours as controlled by supplementary 400 watt SON-T lighting) in a complete randomised block design with four replicate blocks (Figure 2.5) with one plant per pot (Ø 13 cm, 0.8 l). Plants were grown in "Rothamsted Prescription Mix" compost: 75% medium grade peat, 12% screened sterilised loam, 3% medium grade vermiculite, 10% grit (5mm screened, lime free), 3.5 kg m^{-3} Osmocote Exact, 0.5 kg m^{-3} PG mix, lime to pH 5.5-6.0, and 200 ml m^{-3} Vitax Ultrawet wetting agent.

Development was followed by determining when key developmental stages were reached by the main shoot: Growth Stage 39 (flag leaf totally emerged), GS49 (booting complete, start heading), GS61 (start anthesis) and GS89 (physiological maturity) of the Zadoks classification (Zadoks et al., 1974). GS89 was also determined for the whole plant. The anthesis date (GS61) was also determined for the first three tillers. Morphological features determined were height of main shoot and first three tillers, length and width of top three leaves of the main shoot, the number of leaves on the stem of the main shoot, and the number of tillers (including the main shoot). Senescence was followed by measuring SPAD (Section 2.3.1) and quantum yield (Section 2.3.3) of the top three leaves of the main shoot weekly from anthesis until 7 weeks

post-anthesis. A second leaf was sampled at 7 days post-anthesis (tiller 1), 21 dpa (tiller 3) and 28 dpa (tiller 2) for gene expression analysis (Sections 2.2.1 – 2.3.3). Grain was collected and weighed per plant to determine the yield.

Table 2.4: Lines used for characterisation of WRKY-RNAi wheat. The transgenic plants used were from the T2 generation.

Line	Description	Bombardment	Replicate	Plant T0	Plant T1
A1	pActin-WRKY-RNAi 1	2849	3	1a	2
A2	pActin-WRKY-RNAi 2	2849	5	3a	2
A3	pActin-WRKY-RNAi 3	2849	5	4b	3
A5	pActin-WRKY-RNAi 5	2853	3	3a	1
A6	pActin-WRKY-RNAi 6	2853	3	4	6
A7	pActin-WRKY-RNAi 7	2853	3	5b	7
R1	pRTBV-WRKY-RNAi 1	2848	3	1a	3
R2	pRTBV-WRKY-RNAi 2	2848	3	9b	6
R3	pRTBV-WRKY-RNAi 3	2848	4	1	1
R4	pRTBV-WRKY-RNAi 4	2848	6	7b	4
R5	pRTBV-WRKY-RNAi 5	2848	7	2a	1
R6	pRTBV-WRKY-RNAi 6	2852	5	2	2
R7	pRTBV-WRKY-RNAi 7	2852	6	1	7
R8	pRTBV-WRKY-RNAi 8	2852	6	2	8
R9	pRTBV-WRKY-RNAi 9	2852	6	3	8
R10	pRTBV-WRKY-RNAi 10	2852	6	4	8
R11	pRTBV-WRKY-RNAi 11	2852	6	7a	4
C	Transformation control	2853	1	2	1
WT	Cadenza wild-type	x	x	x	x

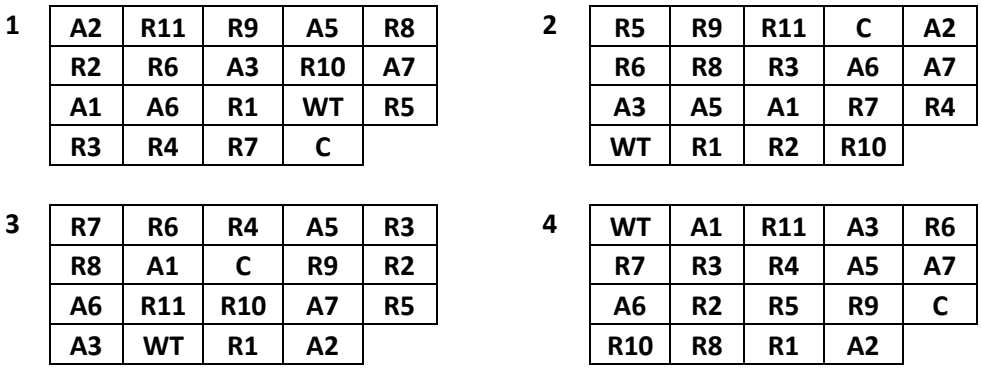

Figure 2.5: Experimental design for characterisation of WRKY-RNAi wheat. A randomised block design with four blocks (1-4). A1 - A7 = pActin-WRKY-RNAi 1-7 (4 does not exist), R1-R11 = pRTBV-WRKY-RNAi 1 – 11, C = transformation control, WT = wild-type (cv. Cadenza).

2.1.5 NAC and WRKY Expression in Different Tissues (Chapters 5 & 6)

To be able to determine the expression (Sections 2.2.1 – 2.2.3) of the NAC and WRKY transcription factors in different plant tissues, the plant parts were harvested from wheat plants grown in the glasshouse (Table 2.5) and stored at -80°C. Most tissues were harvested at anthesis. Exceptions were grain and other flower parts, since grain has not yet developed at anthesis. In this experiment the roots were not harvested; root tissues from a field experiment were used instead.

Table 2.5: Tissues used for expression analysis. Three biological replicates of each were used. RNA samples provided by Dr Peter Buchner (Rothamsted Research).

Tissue	Growing conditions	Variety	Sampling stage
Roots	Field	Hereward	Booting
Flag leaf (First Leaf)	Glasshouse	Paragon	Anthesis
Second Leaf	Glasshouse	Paragon	Anthesis
Third Leaf	Glasshouse	Paragon	Anthesis
Sheath	Glasshouse	Paragon	Anthesis
Stem	Glasshouse	Paragon	Anthesis
Rachis	Glasshouse	Paragon	Anthesis
Glume + Lemna	Glasshouse	Paragon	7 days post-anthesis
Grain	Glasshouse	Paragon	7 days post-anthesis

2.2 LABORATORY PROCEDURES

2.2.1 RNA Extraction

RNA was extracted from ground frozen (-80°C) leaf material using a modified version of the hot phenol extraction method of Verwoerd et al. (1989). A first extraction was performed with hot (80°C) 1:1 phenol/extraction buffer (0.1M Tris/HCl, 0.1M LiCl, 1% SDS, 10mM EDTA, pH 8.0) and chloroform / isoamyl alcohol (IAA) (24:1). A second extraction of the aqueous phase was performed with chloroform/IAA. The aqueous phase was than mixed with 1 volume 4M LiCl to let the RNA precipitate overnight at 4°C. The RNA was then collected

by centrifugation and the pellet washed with 70% ethanol. After a DNase treatment with 5.0 units of RNase-free DNase (Promega), another chloroform/IAA extraction was performed. The RNA was then precipitated by adding 1/10 volume 3M sodium acetate and 2.75 volume ethanol to the aqueous phase and incubation at -20°C. After collecting the RNAs by centrifugation the pellet was washed with 70% ethanol and solved in 50 µl DEPC-treated water. Quality and quantity of the RNAs were checked by measuring the concentration with a Nano Drop™ ND-1000 photo-spectrometer (Thermo Scientific, USA) and by TAE-agarose electrophoresis (1% gel).

2.2.2 cDNA Synthesis

cDNA was synthesised using Superscript III reverse transcriptase (Invitrogen). 2.0 µg RNA, 1.0 µl 10 mM dT-adapter primers and H_2O_{Depc} to a total volume of 13.0 µl were mixed and incubated at 70 °C for 10 minutes. After chilling on ice 4.0 µL 5x buffer, 1.0 µl 0.1M DTT, 1.0 µl 10mM dNTPs and 1.0 µl Superscript III enzyme were added and the solution was first incubated for 5 minutes at room temperature, then 90 minutes at 50°C, and finally 15 minutes at 70°C. In some cases 5.0 µl H_2O_{DEPC} was then added to a total volume of 25.0 µl.

2.2.3 Semi-Quantitative PCR

1.0 µl of cDNA was used for semi-quantitative PCR (sq-PCR) in a reaction volume of 15.0 µl containing 0.3 µl of both sense and antisense primer, 7.5 µl RedTaq mix (Sigma) and 5.9 µl H_2O. The PCR regime consisted of an initial 2 minutes at 94°C, then an *x* number of cycles with 30 seconds at 94°C, 20 seconds at 57 °C (except for total NAC expression at 60°C**)** and 40 seconds at 72 °C, and finally 5 minutes at 72 °C. The primers and the number of PCR cycles (during the linear phase of amplification) depended on the gene analysed (Table 2.6). All primers were designed to give PCR products of approximately 500bp.

Table 2.6: Primers used for semi-quantitative PCR. * are TIGR plant transcript assemblies. † annealing temperature of 60°C instead of 57°C.

Gene	Accession number	Sense primer	Antisense primer	Number of cycles
Actin2	TC234027	CCTTCAATGTTCCAGCCATGTA	ATAGTTGAGCCACCACTGAGCA	25
CCT	TC266579	CGAGCTCTACAACCCCATGC	CGGTAAGTCCAGCCAGGAATC	32
DNA-binding	TC240748	GTTGAAGCGAGTCATCCACTTG	CGAAGATCGTCCAGAGTATCAGC	32
F-box	TC257395	GGTTCCGTTCGGTTGCTTATC	GCACACGACGGAGGAAGTAAG	30
GLK1	TA110567_4565*	GCATGCCGGTGTAAGTTCAGC	GTGGTATCATCGGCGTGGATAA	38
MYB*a*	TC275306	GCTCATACAGCTGCAACAGACA	CTGTGTATTAAGGTGGTGGCTGA	33
MYB*b*	TC263812	CTAACCTCACCATTTCAGGAAGC	CATGGCTGAGAAGATAGGACGAG	23
MYC	TA70705_4565*	ACGCCATCTCCTACATCAACG	CGGTGGTGAGTAATAGGATCACG	32
NAC endogenous	TA67563_4565*	CAAGGAAGACTGGGTGCTATGC	GGAACAGACACTGCATCAACCA	33
NAC total†	TA67563_4565*	GGCAGGGAGTGGTACTTCTTCAG	CACTTGCTCGATGGTGTTCATC	31
NAC transgenic	TA67563_4565*	CAAGGAAGACTGGGTGCTATGC (= same as endogenous NAC)	GAGAGAGACTGGTGATTTCAGCG (35S terminator primer)	40
PTF1	TC253044	CTAATGGAAACAGTGCCAGTGC	GTGCCTTTCTGGTTGGATATGG	31
RBCS	TC263601	AAGCCAGAGTGCCTCCTCCTA	GTACGCGTCAGGGTACTCCTTC	17
RING	TC268503	CAACATTTGGCTGAGAATGACC	GATCAACTATGCCCTGCATTTG	33
SAG12	TC63758	AGAGAACGGCAAGGACTACTGG	GTCGTGATGCAAATGTTTACGCG	27
WRKY total	TC271537 BE406842	CTTCGTCCAAGAACAGCAAGAAC	CTCATAAACCCATGTCCCCTTG	33
WRKY transgenic	TC271537 BE406842	GACGTCGGCGCCCAGTCCATCATGAATA	GAGAGAGACTGGTGATTTCAGCG (35S terminator primer)	40
ZFP-TF	TC235744	CTTGGTGGTGACTACGCCAAC	TGATGATGTCGACTGCRGGAC	33

All PCR samples were run on a 1.2% TAE-agarose gel with ethidium-bromide staining (3.0 µl per 100 ml gel), keeping replicates together in the cases all samples did not fit on one gel. An example gel is shown in Figure 2.6. In the case of the Hereward samples 11.0 µl of PCR product was run on a gel with medium-sized wells (comb of 20 on 100 ml gel). The band intensities were analysed using GeneSnap (6.00.21) and GeneTools (3.02.00) Analysis Software (Syngene, Cambridge). For the Avalon x Cadenza and the transgenic wheat samples, 5.0 µl of the PCR product was loaded into small wells (comb of 30 on 100 ml gel). The band intensities were analysed using GeneSnap (7.8.1.0) and GeneTools (4.1.2.0) Analysis Software (Syngene, Cambridge).

Expression of the *actin2* reference gene was measured first for all samples to assess differences in cDNA concentrations between the samples. a*ctin2* expression of all samples was related to the sample with the highest expression to get "conversion factors" for normalisation of other genes:

($conversion\ factor\ sample_x = actin_x / actin_{highest}$). These factors were multiplied with expression values of all other genes to normalise for differences in cDNA concentrations. For all experiments except the Hereward samples, an extra normalisation step was introduced: the relative expression of each sample was related to the 500bp band of 1.0 µl of the GeneRuler 100bp DNA ladder (Fermentas) to get comparable numbers for all the genes. However, since the number of PCR cycles differed between genes (Table 2.6), expression of different genes cannot be compared. Therefore the expression measured was relative rather than absolute, and only indicative of relative differences in expression of a single gene between different samples.

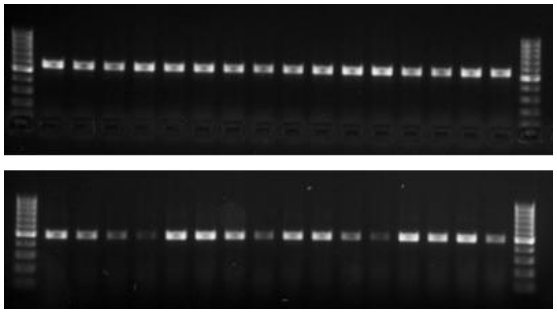

Figure 2.6: Example of a gel of semi-quantitative PCR. Expression of the *actin2* reference gene (top) was similar in all samples while expression of the *RBCS* marker gene (bottom) in the same samples differed depending on senescence status of the leaves. The ladder is the GeneRuler 100bp DNA ladder (Fermentas).

2.2.4 Genomic DNA Extraction

Genomic DNA (gDNA) was extracted from ground frozen leaf material (1-2 cm section) according to a protocol modified from Lin et al. (2001). 600 µl DNA extraction buffer (0.1M Tris-HCl pH 8.0, 10mM EDTA pH 8.0, 1.0M KCl, 0.75% PVP-40, 3.6 g/L $NaHSO_4$) was added and the samples were incubated at 65°C while shaking. 200 µl of 5M KAc (pH 5.2) was added and the samples were mixed and then centrifuged for 5 min at maximum speed. 0.6 volume

isopropanol was added to the supernatant and the samples were precipitated for 10 minutes at -20°C. After 10 minutes centrifugation the pellet was washed with 70% ethanol. The pellet was than dried and solved in 200 µl 10mM Tris-HCl buffer (pH 8.0) containing 200 µg RNase A.

2.2.5 PCR Screening for Transgenic Plants

The primers used for the screening of plants containing a NAC-overexpression construct were a primer on the NAC gene (NAC-CK208366for = 5'- CAA GGA AGA CTG GGT GCT ATG C- 3') and a primer on the 35S-terminator (35S-TermRev = 5'- CCC GGG ATC TGG ATT TTA GTA CTG GAT -3'), so that the endogenous NAC would not be detected. For the WRKY-RNAi plants the same 35S reverse primer was used together with a primer based on the border of spacer and WRKY sequence (WRKY-RNAi-Rev = 5'- GAC GTC GGC GCC CAG TCC ATC ATG AAT A -3'). 0.2 µl of gDNA (or 1 µl 10x diluted gDNA) was used for PCR in a reaction volume of 15 µl (0.3 µl of both the sense and antisense primers, 7.5 µl RedTaq mix (Sigma), rest H_2O). The PCR regime is an initial 2 minutes at 94°C, then 40 cycles with 30 seconds at 94°C, 20 seconds at 57 °C and 40 seconds at 72 °C, and finally 5 minutes at 72 °C. The product was run on a 1%-TAE-gel with ethidium-bromide staining. The product sizes were 653 and 485 bp for NAC and WRKY respectively.

2.2.6 Nitrogen

The nitrogen concentration of dried plant material was analysed using either a CNS 2000 or a TruSpec Combustion Analyser (both from LECO Corporation, USA) via the Dumas combustion method (Dumas, 1831). The samples were first milled and then oven-dried overnight at 80°C, after which either 300 mg (CNS 2000) or 150 mg (TruSpec) samples were weighed out for analysis. Total nitrogen contents were calculated according to the formula: $Total\ N\ content = \%N \times DW$. The nitrogen harvest index was calculated according to the formula: $NHI = \frac{Total\ N_{Grain}}{Total\ N_{Whole\ shoot}}$.

2.2.7 Thousand Grain Weight

Thousand grain weights (TGW) were determined by counting out two sets of 500 seeds, drying them overnight at 105°C and then weighing them. Two sets of 500 were used instead of one of 1000 to be able to check whether there was variation within the sample (so if a representative subsample was taken).

2.3 SENESCENCE MEASUREMENTS

2.3.1 Relative Chlorophyll Content

Relative chlorophyll content was assessed using a Soil Plant Analysis Development (SPAD) meter (SPAD-502, Minolta, Japan). SPAD meters measure absorbance at two wavelengths: red light (650 nm) which is absorbed by chlorophyll and near-infrared light (940 nm) as a reference wavelength to adjust for differences in leaf thickness (Richardson, Duigan and Berlyn, 2002). For the stay-green mutant screening and the transgenics experiments two measurements were taken approximately in the middle of each leaf at one (transgenics) or both (stay-green screening) sides of the midvein, hallway between midvein and leaf edge. For the further experiments on the stay-green mutants two readings were taken of each individual flag leaf: one at one-third and a second at two-third down the leaf.

2.3.2 Photosynthesis

Photosynthetic rate was determined by measuring changes in CO_2 levels using the Li-6400 Portable Photosynthesis System (LI-COR Inc, Lincoln, NE, USA). Conditions for all measurements were kept as constant as possible: the LED light source set to 1000 µmol m^{-2} s^{-1}, the relative humidity in the sample chamber at 65%, a 385 µmol mol^{-1} sample CO_2 concentration, and the leaf temperature set to be between 23.8°C and 24.2°C by adjusting the block temperature. The reading was taken when photosynthesis had stabilised. Measurements were done of one flag leaf per pot with the light on the adaxial side of the leaf.

2.3.3 Chlorophyll Fluorescence

Quantum yield is a measure of the photosystem II (PSII) maximum efficiency of a leaf and can be determined by measuring the ratio between variable (F_V) and maximum (F_M) chlorophyll fluorescence (Maxwell and Johnson, 2000). Chlorophyll fluorescence measurements were taken halfway between the midvein and the edge of the adaxial side of light-adapted leaf blades, in which case quantum yield is equivalent to F_V'/F_M'. Measurements were performed with a FluorPen FP100s handheld chlorophyll fluorometer (Qubit Systems Inc, Canada). For the stay-green mutant experiments two readings were taken of each individual flag leaf: one at one-third and a second at two-third down the leaf. For the Avalon x Cadenza field experiment and analysis of transgenic plants one measurement per leaf was taken in the middle of the leaf.

2.3.4 Canopy Reflectance

The Normalised Difference Vegetation Index (NDVI) was determined by using a Crop Circle ACS-210 crop canopy sensor (Holland Scientific, USA). When the canopy is fully closed the NDVI is proportional to senescence, while under partial canopy closure the NDVI is directly proportional to plant biomass. The Crop Canopy Circle emits visible light (VIS) at 590nm and near-infrared light (NIR) at 880nm and computes the NDVI from the reflectances (ρ) of both forms of light according to the formula: $NDVI = \frac{\rho_{NIR} - \rho_{VIS}}{\rho_{NIR} + \rho_{VIS}}$.

In the field the Crop Circle was used according to the manufacturer's instructions to take one measurement per plot per time point in the middle of the canopy. Care was taken that the distance to the canopy was the same at all times so that a similar area was measured.

In the glasshouse the sensor was placed in a hole on top of a closed box that was black on the inside, so that the sensor could only pick up reflections originating from the plants (Figure 2.7). Single measurements were

performed weekly from just before anthesis until the week NDVI did not decrease further.

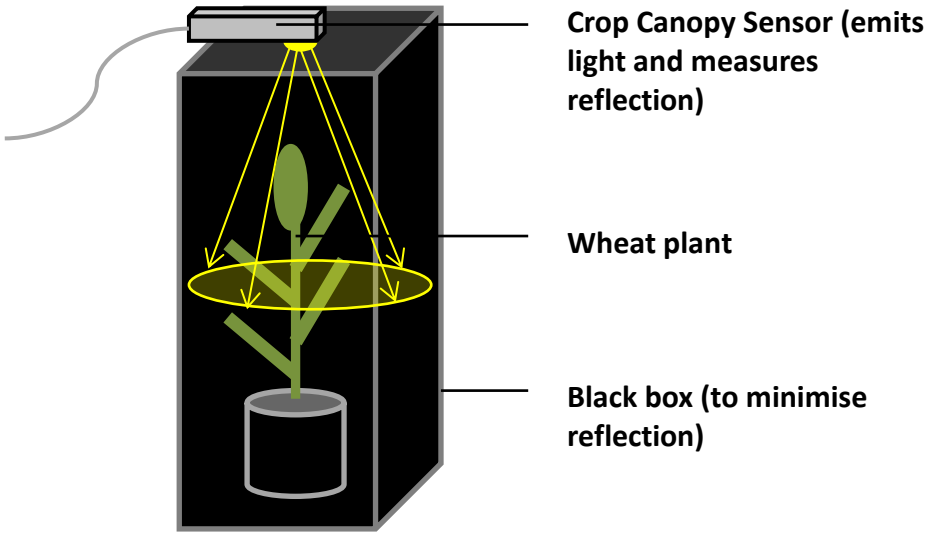

Figure 2.7: Setup of the Crop Canopy Sensor on a black box to measure whole-plant senescence (not on scale). Measurements: height 100 cm x length 50 cm x width 50 cm.

2.4 PHYLOGENETIC ANALYSIS

To infer the phylogenetic relationship of the WRKY and NAC genes, they were compared to all rice family members, known wheat genes and senescence-related genes from all other plant species. Protein sequences of all known rice NAC and WRKY genes were downloaded from the Database of Rice Transcription Factors (DRTF). Only sequences of the *Japonica* rice cultivar were used. All other protein sequences were collected from the UniProtKB database.

The total protein sequences were aligned using the MEGA5 software with the built-in ClustalW algorithm (Larkin et al., 2007). Next the sequences were cropped to only include the WRKY or NAC domain. Duplicate sequences (usually splicing variations of the rice loci) and genes that did not contain (most of) the domain were deleted. The sequences were then aligned again.

Phylogenetic trees were constructed using the Neighbor-Joining method in MEGA5 (Tamura et al., 2011). The stability of the nodes was tested using bootstrap analysis with 1000 replicates as implemented in MEGA5.

2.5 STATISTICAL ANALYSES

In principle all results were analysed by Analysis of Variance (ANOVA) using GenStat® software (Payne et al., 2009). The Least Significant Difference (LSD) at 5% level was used to assess whether two individual values were statistically different. If data were not normally distributed, they were log-transformed or square-root-transformed.

Restricted Maximum Likelihood (REML) analysis was used in two cases where ANOVA analysis was not appropriate: in (a) the Paragon nitrogen nutrition experiment because the time points of the two nitrogen treatments were not the same, resulting in an unbalanced experimental design unsuitable for ANOVA; and (b) the Hereward expression data because the field samples were randomised again for laboratory testing. As for ANOVA, for REML analysis differences were assessed using the (estimated) 5% LSD and data were transformed when required. For time course a test for autocorrelation was performed.

Canonical Variates Analysis (CVA) was used to analyse the data from the initial screening of the Paragon mutant collection (by Dr Stephen Powers, Rothamsted Research).

Regression analysis and Pearson's correlation coefficients calculations were performed using Microsoft Office Excel. In all cases except the screening of the Paragon mutant collection, single data points (so not the means) of each replicate were used. The correlation coefficients (R) with the appropriate Degrees of Freedom (sample size minus two) were used to assess whether a correlation was significant at the 5% level.

Standard Errors (SE) were calculated and plotted in the graphs when appropriate (three or more replicates). They were not used for assessing significant differences, but are displayed for clarity only.

3. GENE EXPRESSION ANALYSIS OF CANDIDATE REGULATORY GENES OF LEAF SENESCENCE IN DIFFERENTIAL SENESCING FIELD-GROWN WHEAT

3.1 INTRODUCTION

Theoretically, a delay in leaf senescence should result in an extended carbon fixation period during grain-filling, thereby enhancing biomass and grain yield potential (Richards, 2000). This model assumes that the additional produced carbohydrates are trans-located from the source leaves to the developing grain and that the remobilisation of nitrogen is unaffected.

One approach to investigate the relationship between canopy senescence and nitrogen remobilisation and grain yield is to compare wheat genotypes with different senescence patterns. As grain yield is best assessed in the field, field-grown wheat with different canopy senescence patterns would be of specific importance.

As plant nitrogen status has been shown to have a major impact on the onset and progression of leaf senescence in wheat, barley and Arabidopsis (Peng et al., 2007; Schildhauer et al., 2008), manipulation of nitrogen availability is another route to generate wheat with different patterns of senescence.

To facilitate manipulation of leaf senescence in plant breeding programmes, and therefore indirectly nitrogen remobilisation and possibly even grain yield, it would be advantageous to know how leaf senescence is regulated at the molecular level. Regulatory genes of leaf senescence, most likely transcription factors, will need to be identified. One approach to do this is screening

candidate genes by comparing their expression in wheat genotypes displaying different patterns of senescence.

The aims of the experiments reported in this chapter were:

1. To compare senescence patterns of wheat genotypes grown under different nitrogen regimes in the field.
2. To assess the effects of differential senescence on grain yield, harvest index and grain nitrogen concentration and content.
3. To examine patterns of expression of candidate regulatory genes of leaf senescence in leaf samples from these field experiments.

3.2 GENE EXPRESSION UNDER DIFFERENT NITROGEN REGIMES

To identify genes involved in the regulation of leaf senescence, gene expression studies were performed on leaf tissues of the wheat cultivar Hereward grown under two nitrogen fertilisation regimes in the field. The leaf greenness data, as measured with a SPAD meter, demonstrated that a low nitrogen supply of 50 kg N ha^{-1} advanced the onset of senescence of the second leaf of wheat compared to senescence occurring at a standard nitrogen supply of 200 kg N ha^{-1} ($P<0.001$; Figure 3.1). At low N, SPAD values at 21 days post-anthesis (dpa) were already significantly lower than at anthesis ($P<0.001$), and at 28 dpa values were significantly lower than at 14 dpa. After 28 dpa senescence progressed rapidly with significant decreases in greenness each week. In contrast, at high N relative chlorophyll content did not change between anthesis and 35 dpa; the first significant decrease occurred between 35 and 42 dpa ($P<0.001$).

The small subunit of Rubisco *(RBCS)* and senescence-associated gene 12 *(SAG12)* genes are commonly used markers for leaf senescence (for instance Noh and Amasino, 1999; Rampino et al., 2006). Expression of these genes was analysed to validate the suitability of the leaf material collected. Gene expression was analysed by two-phase semi-quantitative RT-PCR as described in Sections 2.3.1 - 2.3.3. *RBCS* expression was higher under high N availability ($P<0.01$) and decreased as senescence progressed ($P<0.001$; Figure 3.2.a). *SAG12* expression increased with senescence ($P<0.001$); as greenness decreased under low N, between 28 and 35 dpa, SAG12 expression increased (Figure 3.2.b). So the expression of the marker genes was in agreement with the course of senescence.

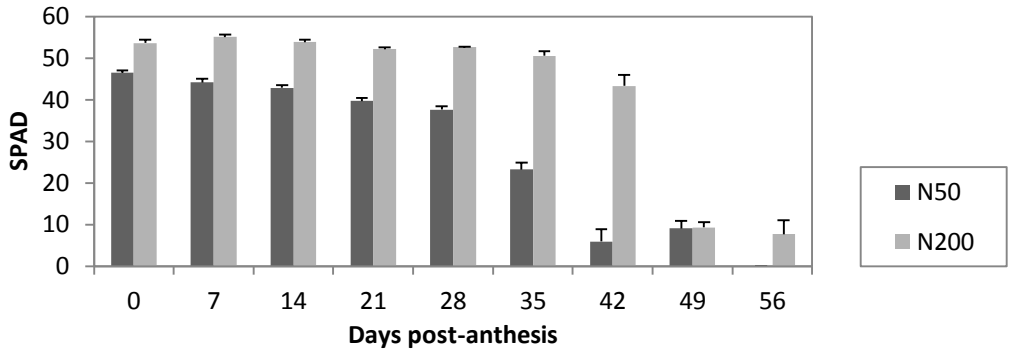

Figure 3.1: The progression of leaf 2 senescence of field-grown wheat (cv. Hereward) at two nitrogen regimes. Relative chlorophyll content was determined with a SPAD meter. N was supplied at 50 kg N ha^{-1} and 200 kg N ha^{-1}. LSD = 4.20. Data are means + SE of four replicates. Data were collected by Dr Jonathan Howarth (Rothamsted Research) in 2007.

A transcriptomics study of six wheat varieties grown at two nitrogen levels (50 and 200 kg N ha^{-1}) resulted in a list of candidate genes that may be involved in nitrogen remobilisation and / or leaf senescence during grain-filling (Hawkesford and Howarth, 2010). This list included several potential regulatory genes, such as transcription factors (Howarth, Barraclough and Hawkesford, unpublished). The expression of twelve of these genes was evaluated by two-phase semi-quantitative RT-PCR (Sections 2.2.1 – 2.2.3) in the Hereward leaf 2 tissues collected in 2007 (stored at -80°C). The analysed genes were a CCT-motif-containing protein, a DNA-binding protein, a F-box protein, a gene resembling Golden-like protein 1 *(GLK1)*, two MYB transcription factors (designated MYB*a* and MYB*b*), a MYC transcription factor, a NAC transcription factor, a gene similar to P_i starvation-induced transcription factor 1 *(PTF1*), a RING-domain-containing protein, a WRKY transcription factor, and a zinc-finger protein transcription factor (Figure 3.2.c - 3.2.n).

The gene showing an expression pattern most obviously related to the observed senescence pattern was the WRKY transcription factor (Figure

3.2.m). At low N, the expression increased slowly between anthesis and 28 dpa. Between 28 and 35 dpa, when the wheat started to senesce rapidly, expression of the WRKY gene increased more than three-fold. At high N, the expression was initially constant; the expression was only significantly higher at 42 dpa when the first fall in greenness had occurred. So expression was influenced both by senescence ($P<0.001$) and nitrogen availability ($P<0.01$).

Three other genes showed a significant increase in expression when senescence was occurring most rapidly, at low N between 28 and 35 dpa: the F-box protein (Figure 3.2.e), MYB transcription factor *a* (Figure 3.2.g), and the PTF1-like gene (Figure 3.2.k). Expression of the MYC transcription factor also seemed to gradually increase with time; but there were large fluctuations in expression and the increase did not relate well with senescence (Figure 3.2.i).

Expression of two genes decreased with time: the NAC and MYB *b* transcription factors. Expression of the NAC gene was similar at anthesis at both N regimes. NAC expression decreased gradually at low N, while at high N expression remained high between anthesis and 35 dpa after which it decreased. This resulted in significant differences in expression at 14, 28 and 35 dpa ($P<0.001$; Figure 3.2.j). The expression of MYB*b* decreased gradually at low N, while at high N it was unchanged (Figure 3.2.h). The DNA-binding protein showed a decrease in expression between 35 and 42 dpa under high N conditions only (3.2.d), so there was little relation with senescence.

The CCT-motif-containing protein and the GLK1-like gene were significantly more highly expressed under high N conditions ($P<0.05$) but no consistent changes with time were observed (Figures 3.2.c and 3.2.f), correlating with the response to nitrogen availability but with leaf senescence.

Expression of the RING-domain-containing protein and the zinc-finger protein transcription factor did not show any response to the different nitrogen regimes and did not change with time (Figures 3.2.l and 3.2.n).

(a) RBCS

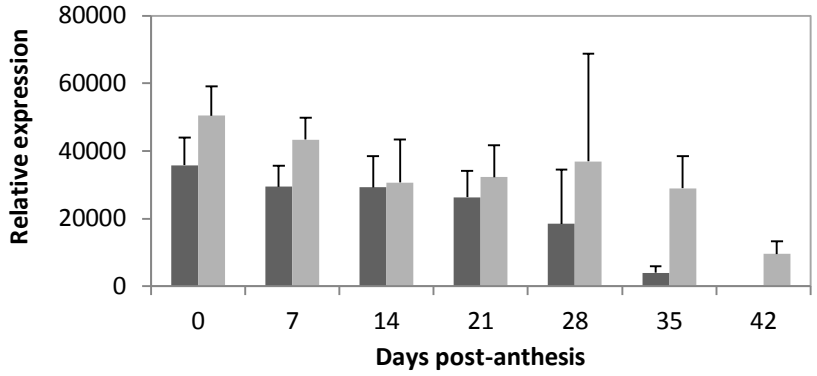

(b) SAG12

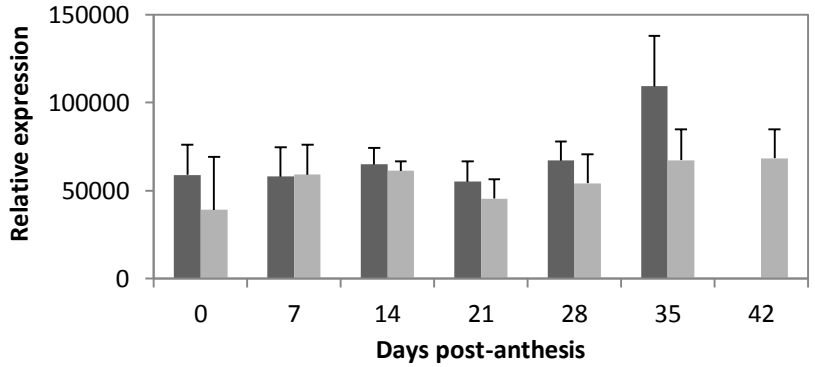

(c) CCT

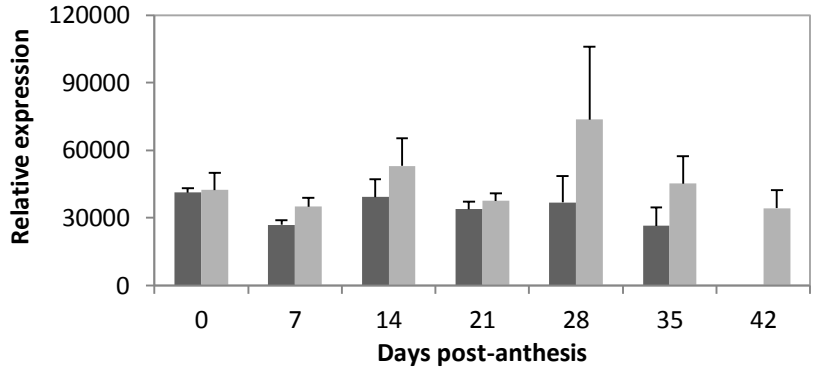

(d) DNA-binding

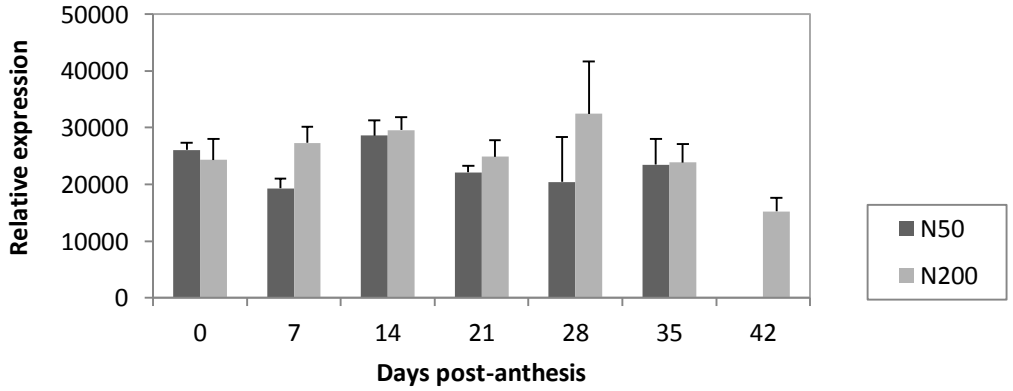

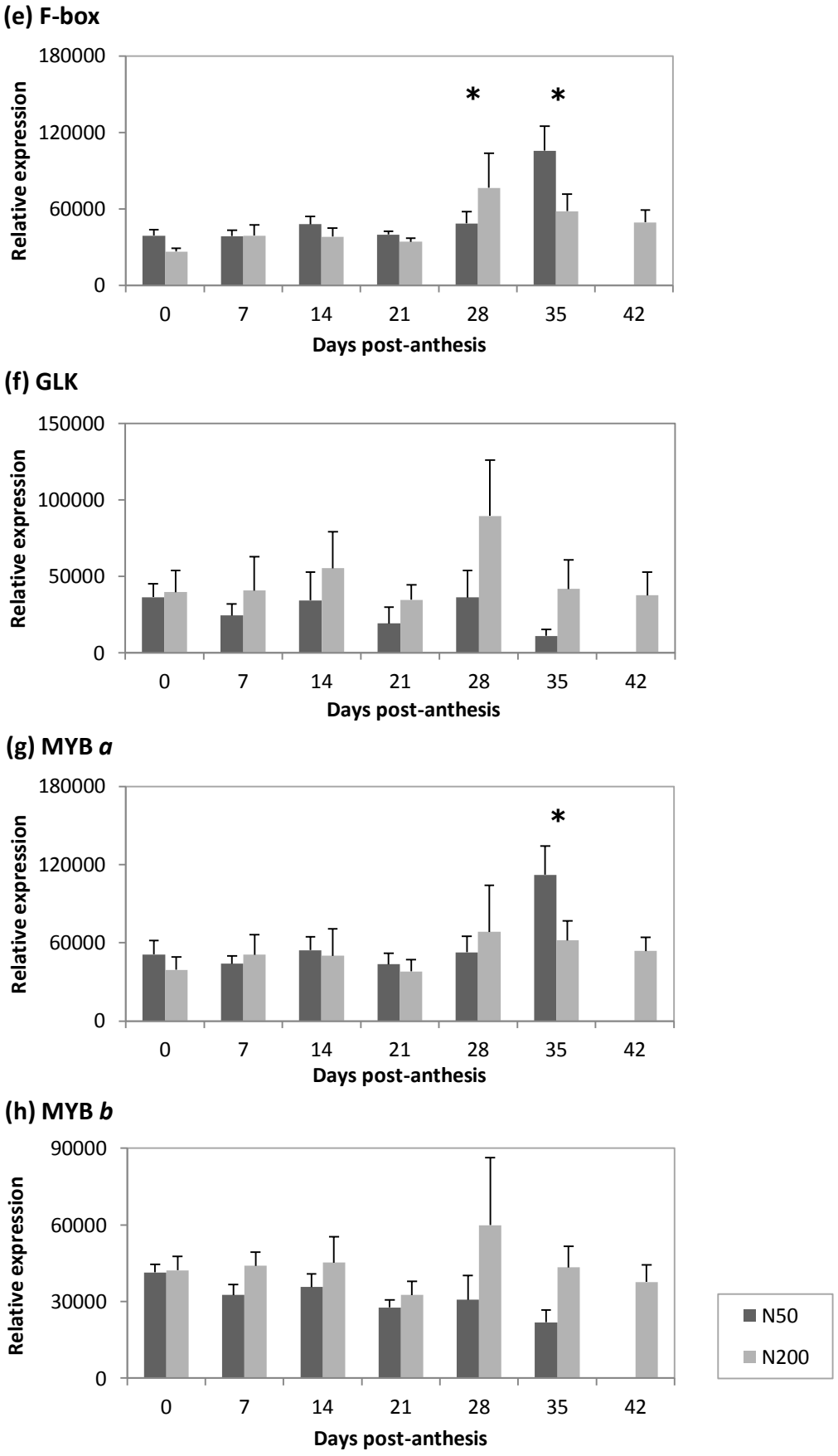
(e) F-box
180000
120000
60000
0
Relative expression
*
*
0
7
14
21
28
35
42
Days post-anthesis
(f) GLK
150000
100000
50000
0
Relative expression
0
7
14
21
28
35
42
Days post-anthesis
(g) MYB a
180000
120000
60000
0
Relative expression
*
0
7
14
21
28
35
42
Days post-anthesis
(h) MYB b
90000
60000
30000
0
Relative expression
0
7
14
21
28
35
42
Days post-anthesis
N50
N200

(i) MYC

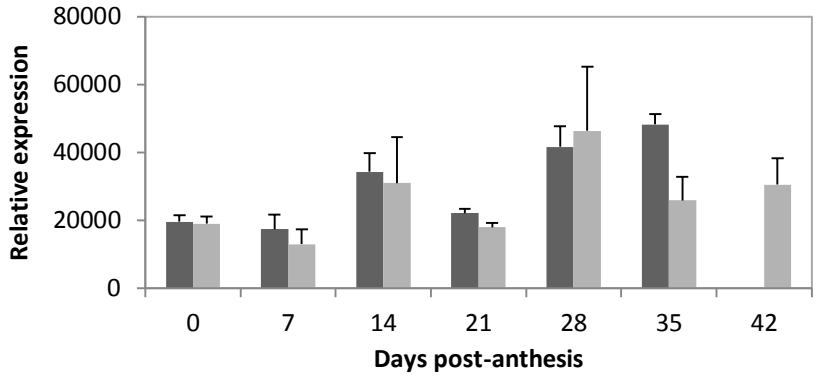

(j) NAC

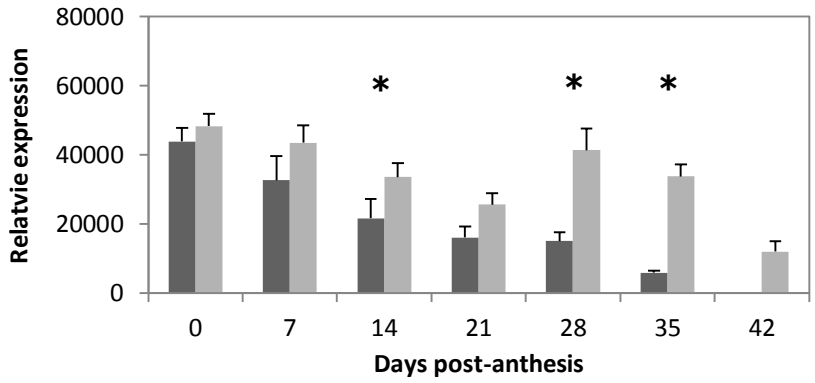

(k) PTF †

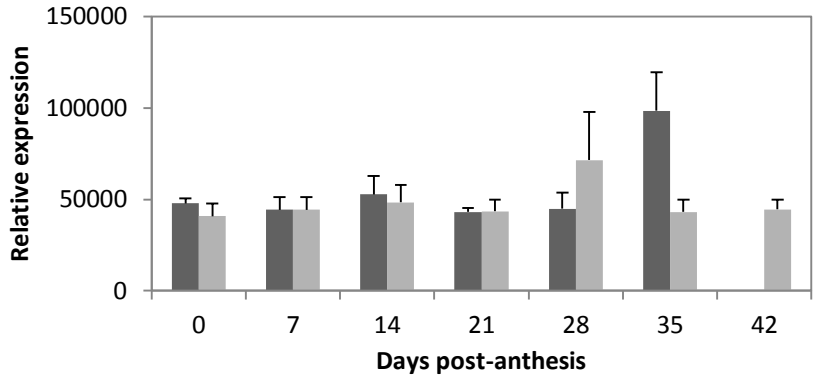

(l) RING

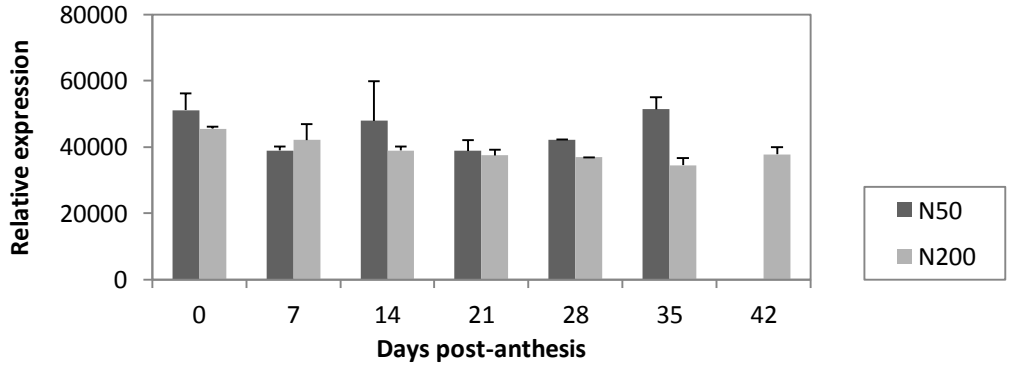

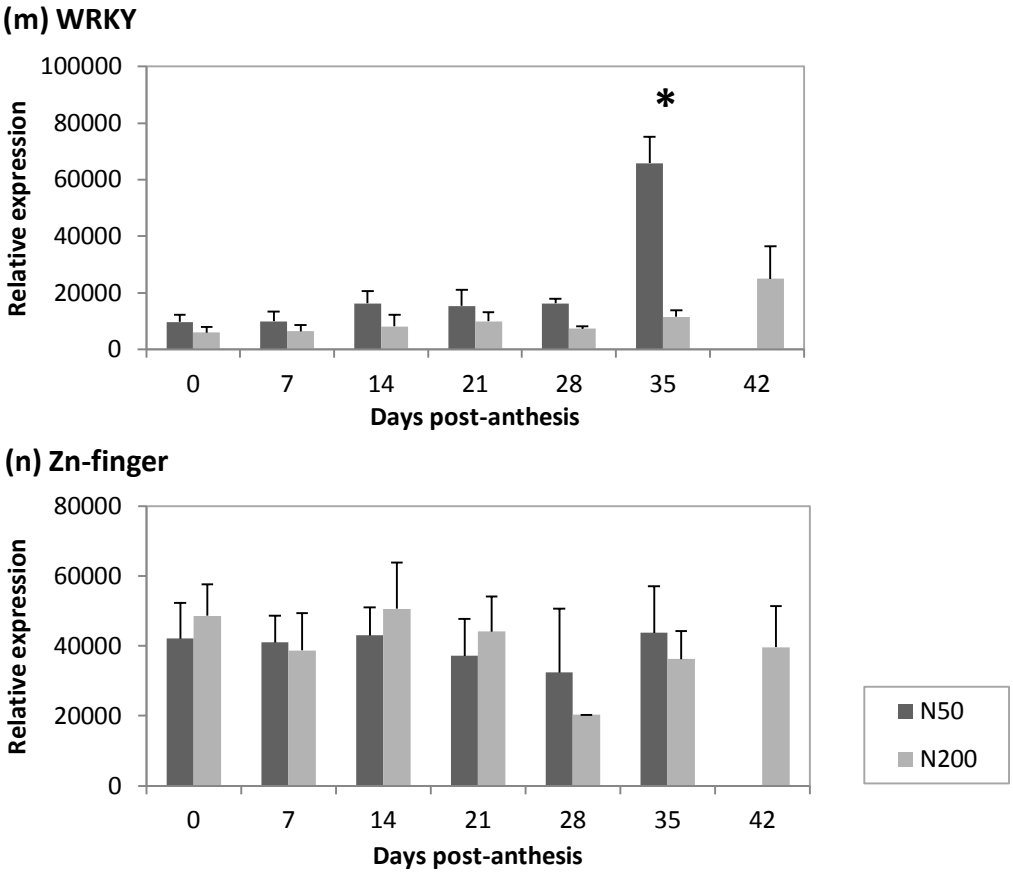

Figure 3.2: Relative gene expression in the second leaf of field-grown wheat (cv. Hereward) at two nitrogen regimes. (a) *RBCS*, **(b)** *SAG12*, **(c)** CCT-motif-containing protein, **(d)** DNA-binding protein, **(e)** F-box protein, **(f)** GLK1-like gene, **(g)** MYB transcription factor *a*, **(h)** MYB transcription factor *b*, **(i)** MYC transcription factor, **(j)** NAC transcription factor, **(k)** PTF1-like gene, **(l)** RING-domain-containing protein, **(m)** WRKY transcription factor, **(n)** zinc-finger protein transcription factor. Nitrogen was supplied at 50 kg N ha^{-1} and 200 kg N ha^{-1}. At 42 days after anthesis low N samples did not contain sufficient quantities of RNA for gene expression analysis. Data are means + SE of four replicates, except for 28 days after anthesis for which only two replicates were available. Leaf samples were collected by Dr Jonathan Howarth at Rothamsted Research in 2007. ***** = significant difference ($P<0.05$). **†** model did not fit; therefore no LSD available for ad-hoc significance testing.

3.3 PHENOTYPE OF AVALON X CADENZA DOUBLED HAPLOID LINES

3.3.1 Senescence

As described above, gene expression studies of a single wheat cultivar grown under two nitrogen regimes revealed several candidate genes showing differential expression which may be involved in the regulation of leaf senescence. To be able to separate the effects of senescence from the effects of nitrogen availability, wheat lines differing in senescence patterns at different nitrogen levels have to be compared.

To identify wheat lines with different senescence patterns under different nitrogen levels, several lines of an Avalon x Cadenza doubled haploid population were grown in the field in 2008/9 at four different nitrogen fertilisation regimes to compare the onset and rate of senescence (see also Derkx, Foulkes and Hawkesford, 2010). Two lines, AC127 and AC82, were selected based on the change in relative chlorophyll content of the second leaf when grown under low (100 kg N ha^{-1}) and high (350 kg N ha^{-1}) nitrogen fertilisation. SPAD data showed that under low nitrogen conditions AC82 had not senesced 21 days post-anthesis unlike AC127, while when supplied with high nitrogen the two lines senesced similarly (Figure 3.3.a). Nitrogen remobilisation from the second leaf, as measured by leaf nitrogen concentration, followed a similar pattern (Figure 3.3.b).

The field experiment with the Avalon x Cadenza lines was repeated in 2009/10. In this year there was a post-anthesis drought: just 55 mm of precipitation in June and July produced a potential soil moisture deficit (PSMD) of 271 mm at the end of July, compared to 141 mm rain and a PSMD of 177 mm in 2008/9 (Rothamsted Research Weather Station). This resulted in faster senescence than in 2008/9 (compare the x-axes of Figures 3.3 and 3.4), but also in enhanced differences in senescence. Both SPAD and leaf nitrogen concentration data showed that plants grown under low N senesced significantly earlier than plants grown under high N, and in both high and low

nitrogen conditions, AC127 senesced significantly faster than AC82 (all P<0.001; Figures 3.4.a and 3.4.b). Chlorophyll fluorescence, as measured with a FluorPen handheld fluorescence meter, showed that photosynthetic capacity of all lines and nitrogen conditions started to decrease simultaneously (Figure 3.4.c). But the decrease at low N was significantly faster than at high N (P<0.001), and AC127 lost photosystem II efficiency significantly faster than AC82 (P<0.01).

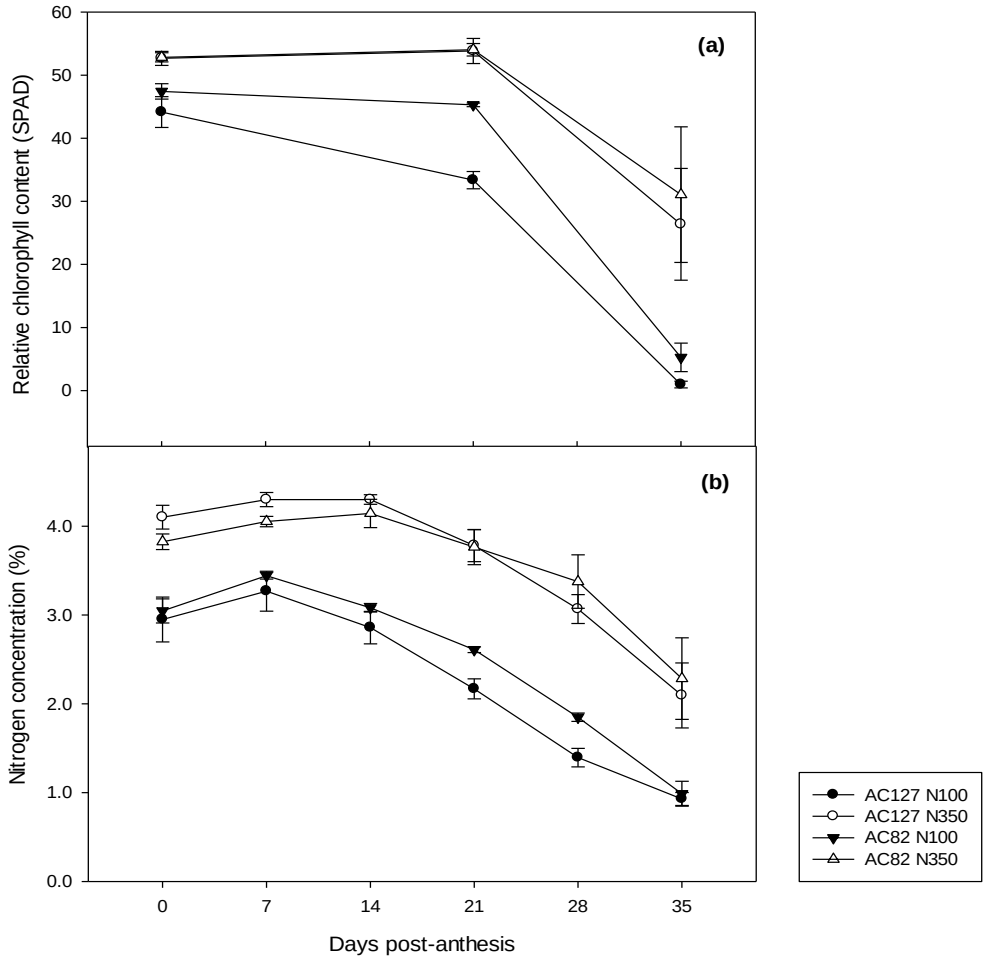

Figure 3.3: The progression of leaf 2 senescence of two Avalon x Cadenza doubled haploid lines grown in the field at two nitrogen regimes in 2008/9. **(a)** Relative chlorophyll content as determined with a SPAD meter. LSD = 9.76. **(b)** Nitrogen concentration (% DM). LSD = 0.167 (square root transformed data). Nitrogen was supplied at 100 kg N ha^{-1} and 350 kg N ha^{-1}. Data are means ± SE of three replicate field plots. Figure adapted from Derkx et al. (2010).

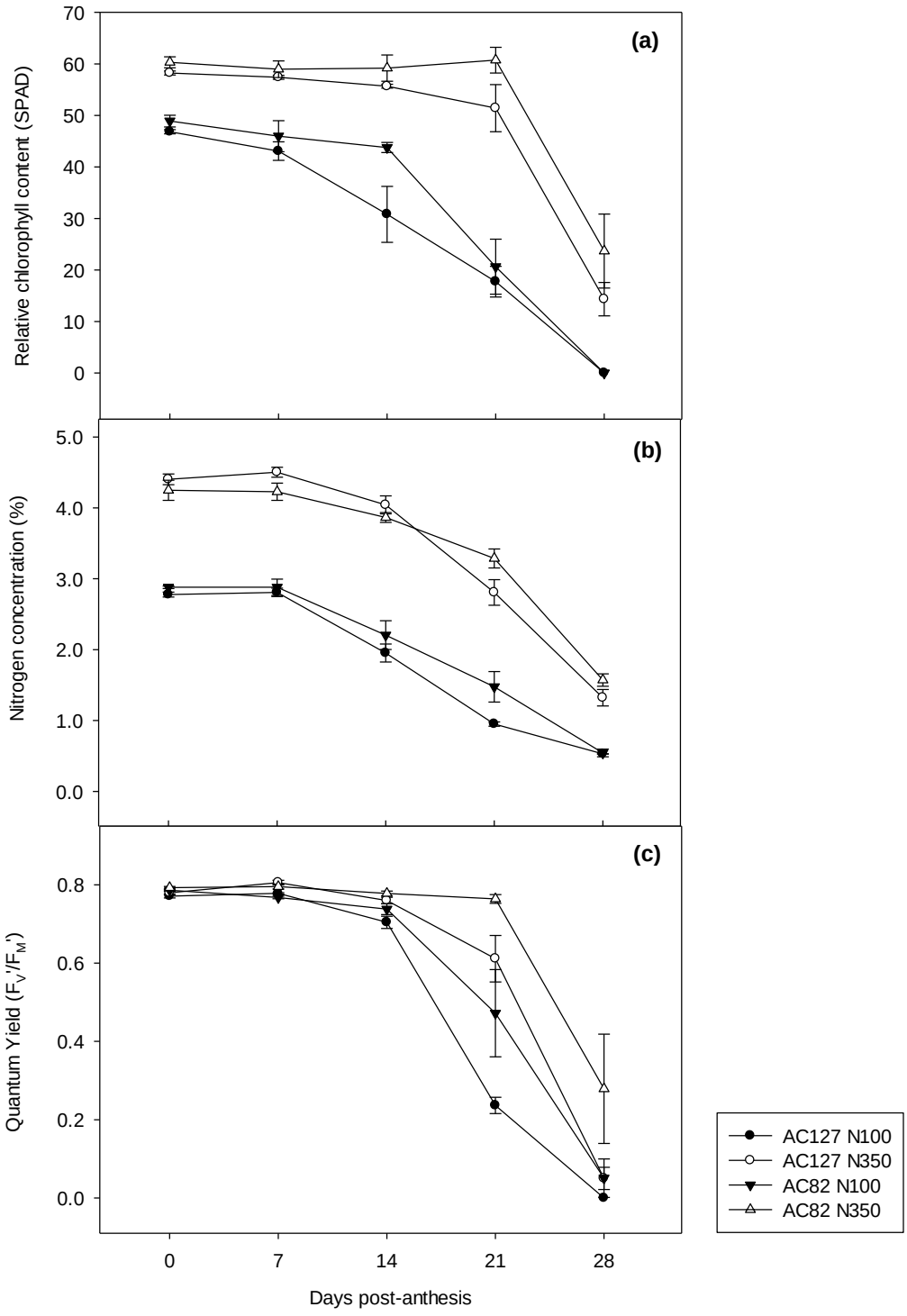

Figure 3.4: The progression of leaf 2 senescence of two Avalon x Cadenza doubled haploid lines grown in the field at two nitrogen regimes in 2009/10. **(a)** Relative chlorophyll content as determined with a SPAD meter. LSD = 7.38. **(b)** Nitrogen concentration (% DM). LSD = 0.263. **(c)** Quantum yield (F_V'/F_M') as determined with a FluorPen. LSD = 0.1253. Nitrogen was supplied at 100 kg N ha^{-1} and 350 kg N ha^{-1}. Data are means ± SE of three replicate field plots.

In both years canopy senescence was studied at the plot level by determining the Normalised Difference Vegetation Index (NDVI), a measure of total green canopy area, with a Crop Canopy Sensor. In 2008/9 plots supplied with high N were greener at anthesis (Figure 3.5). The onset of whole-plot senescence was comparable to that of the second leaf, but in contrast, the difference in onset of senescence between the lines at plot-level was greater at high than at low nitrogen fertilisation (Figure 3.5).

In 2009/10 the NDVI of all plots was lower than in 2008/9, and the difference between the two nitrogen treatments was greater (Figure 3.6). The earlier onset of senescence caused by the drought was apparent as well. In 2009/10, line AC127 started to senesce earlier than line AC82, but the difference in onset of senescence between the two lines was equal in both N treatments (Figure 3.6). The rates of senescence were comparable.

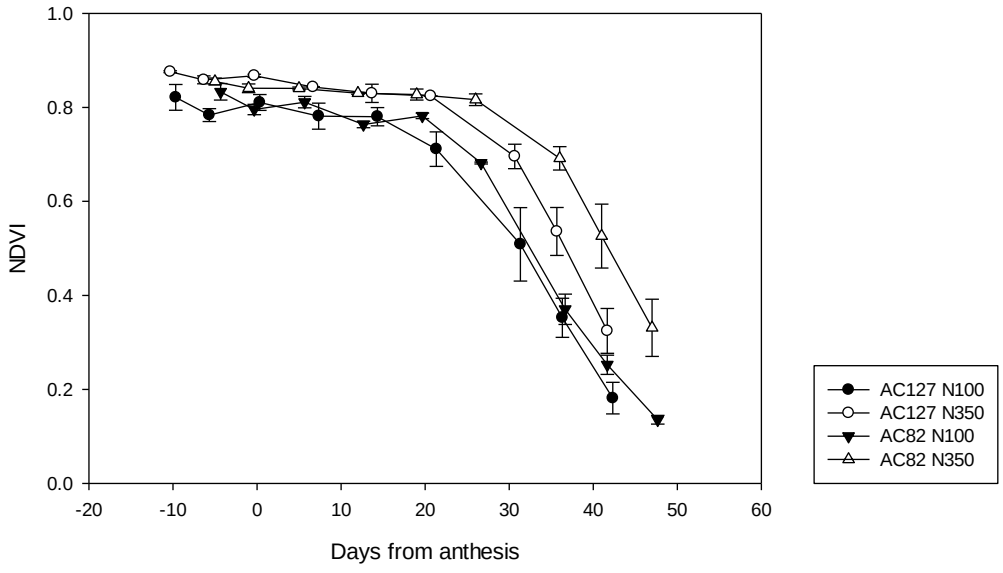

Figure 3.5: The progression of senescence of whole field plots of two Avalon x Cadenza doubled haploid lines grown at two nitrogen regimes in 2008/9. Nitrogen was supplied at 100 kg N ha^{-1} and 350 kg N ha^{-1}. The Normalised Difference Vegetation Index (NDVI) was measured with a Crop Canopy Sensor. Data are means ± SE of three replicate field plots.

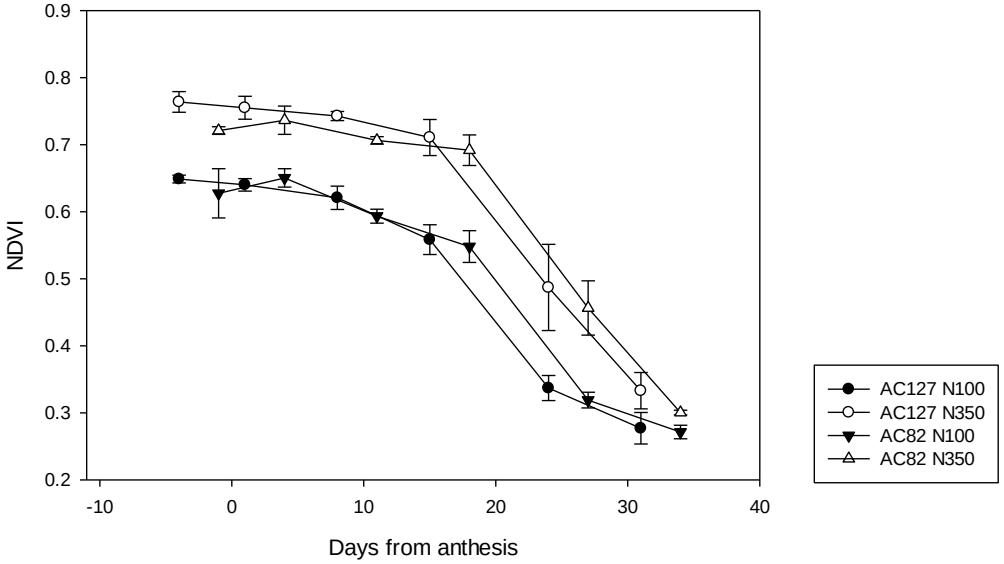

Figure 3.6: The progression of senescence of whole field plots of two Avalon x Cadenza doubled haploid lines grown at two nitrogen regimes in 2009/10. Nitrogen was supplied at 100 kg N ha^{-1} and 350 kg N ha^{-1}. The Normalised Difference Vegetation Index (NDVI) was measured with a Crop Canopy Sensor. Data are means ± SE of three replicate field plots.

3.3.2 Yield Characteristics

Grain yield differed between N levels, but not significantly between the lines at any N rate in any year (Figure 3.7.e and 3.7.f). However, the two lines showed highly significant differences in straw yield ($P<0.001$): the straw dry weight of AC127 was higher than that of AC82, independent of the N rate (Figure 3.7.c and 3.7.d). This resulted in a significantly lower harvest index for AC127 ($P<0.001$; Figure 3.7.e and 3.7.f). In both years both the grain N concentration and total N content did not differ at any N level (Figure 3.7.g – 3.7.j). This suggests that onset and rate of senescence did not influence the final amount of nitrogen remobilised to the grain. Taking together the results from both lines, total grain N content at different nitrogen regimes followed the same pattern as grain yield and grain N concentration (Figure 3.7) and correlated significantly with both features (R^2 of 0.92 and 0.92 in 2008/9, and 0.82 and 0.91 in 2009/10 respectively), indicating grain dry matter and grain nitrogen concentration change concomitantly in response to N availability.

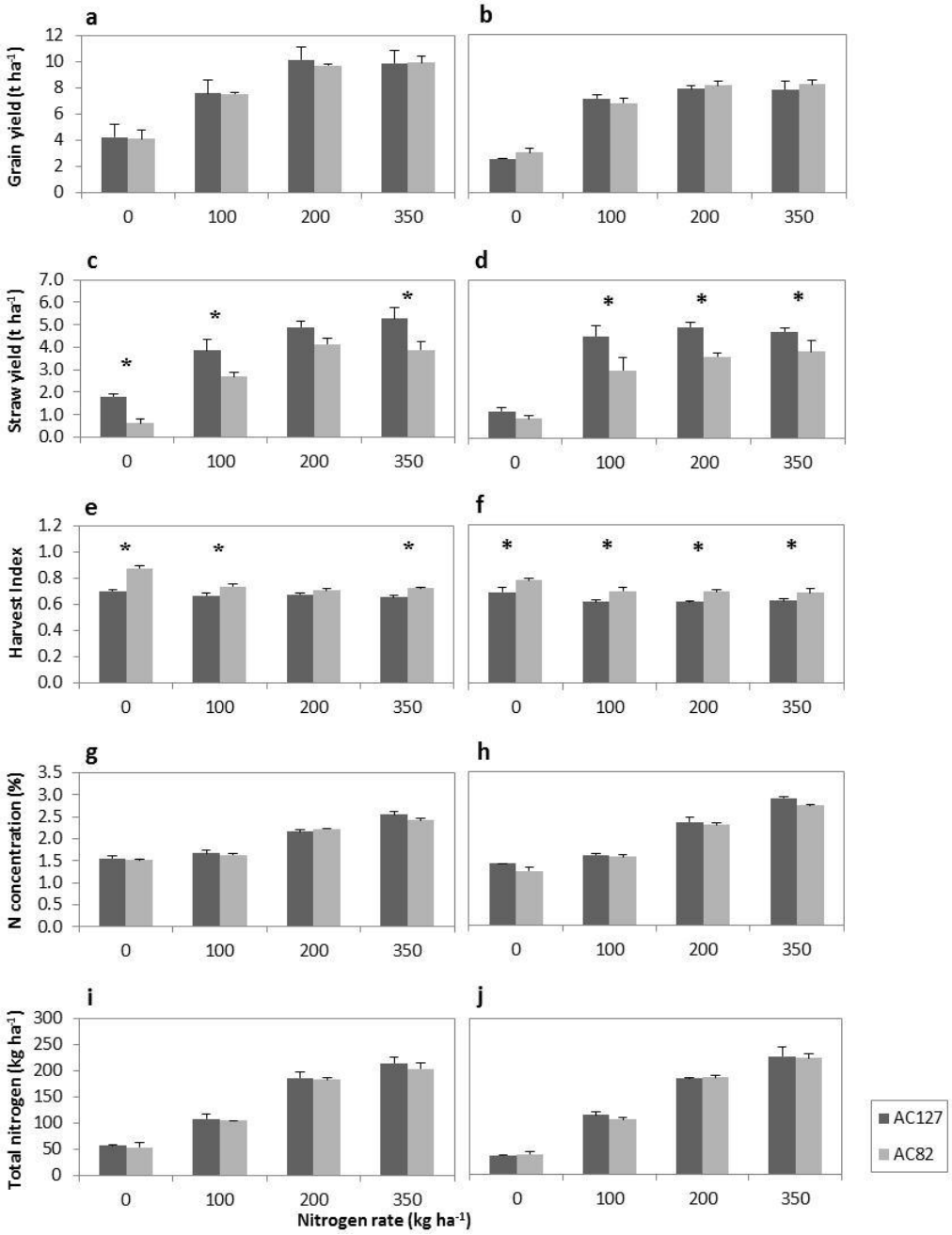

Figure 3.7: Yield characteristics of two Avalon x Cadenza doubled haploid lines grown in the field at four nitrogen regimes in 2008/9 and 2009/10. Grain yield (t ha^{-1} at 85% dry matter) in 2008/9 **(a)** and 2009/10 **(b)**. Straw yield (t ha^{-1} 85% DM) in 2008/9 **(c)** and 2009/10 **(d)**. Harvest Index in 2008/9 **(e)** and 2009/10 **(f)**. Grain nitrogen concentration (% DM) in 2008/9 **(g)** and 2009/10 **(h)**. Total grain nitrogen content (kg N ha^{-1}) in 2008/9 **(i)** and 2009/10 **(j)**. Data are means + SE of three replicate field plots. ***** = significant difference ($P<0.05$). Panels for 2008/9 data were adapted from Derkx et al. (2010).

3.4 GENE EXPRESSION IN AVALON X CADENZA DOUBLED HAPLOID LINES

Gene expression was analysed by semi-quantitative PCR as described in Section 2.3.3. The senescence patterns of the leaf 2 tissues of the Avalon x Cadenza lines were first validated with the *RBCS* and *SAG12* marker genes. *RBCS* expression in 2008/9 decreased with time and followed the same pattern as leaf nitrogen concentration: N level influenced the onset and rate of senescence ($P<0.05$) but there was no significant difference between the lines (Figure 3.8.a). In 2009/10, *RBCS* expression was lower under low N conditions and also lower in AC127 than in AC82 (both $P<0.05$), but the onset and rate of decrease in expression were not different (Figure 3.8.b).

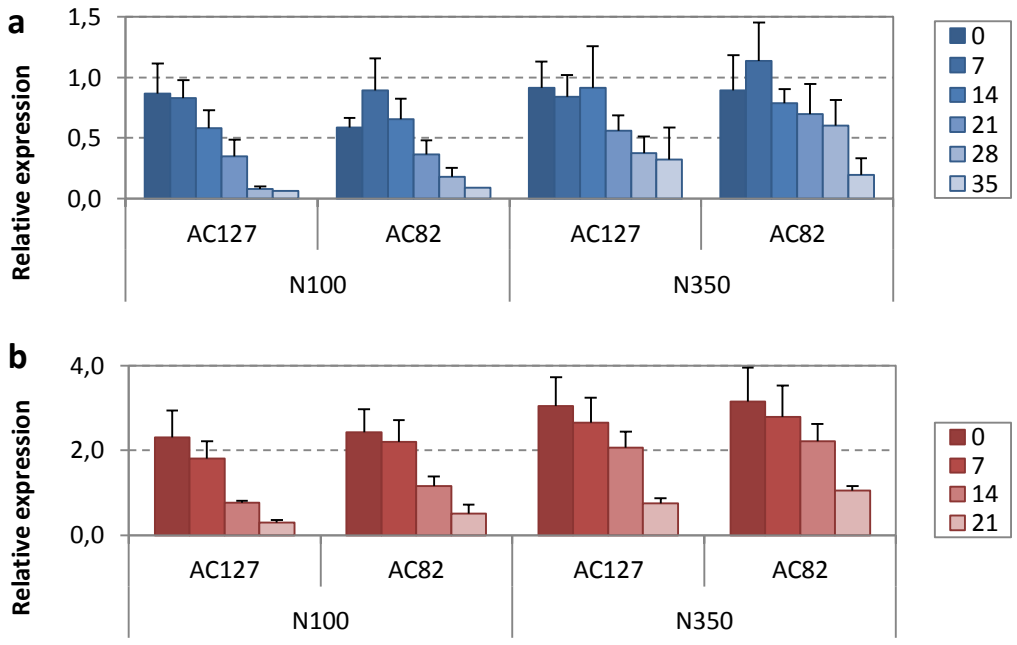

Figure 3.8: Expression of *RBCS* in the second leaf of two Avalon x Cadenza doubled haploid lines grown in the field at two nitrogen regimes in 2008/9 (a) and 2009/10 (b). LSDs are 0.196 and 0.826 respectively. Nitrogen was supplied at 100 kg N ha^{-1} and 350 kg N ha^{-1}. Expression was determined at weekly intervals from anthesis (0) to 35 and 21 dpa respectively. Data are means + SE of three replicate field plots.

In 2008/9, *SAG12* expression was significantly higher in the faster-senescing line AC127 than in AC82 ($P<0.05$), and started to increase earlier at low N ($P<0.01$; Figure 3.9.a). In 2009/10, line AC127 showed a significantly earlier and stronger increase in expression ($P<0.001$; Figure 3.9.b). At low N the increase in expression was significantly stronger between 7 and 14 days post-anthesis, while at high N the increase was later between 14 and 21 dpa ($P=0.001$).

The findings that *RBCS* expression matched senescence patterns and *SAG12* showed a contrasting pattern confirmed *RBCS* and *SAG12* are good molecular markers for leaf senescence.

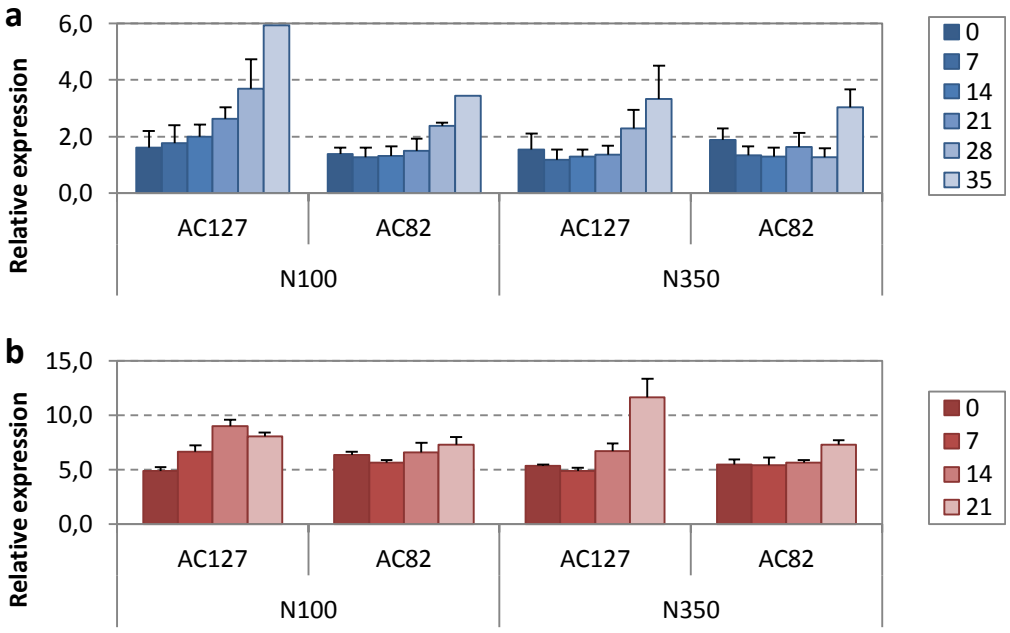

Figure 3.9: Expression of *SAG12* in the second leaf of two Avalon x Cadenza doubled haploid lines grown in the field at two nitrogen regimes in 2008/9 (a) and 2009/10 (b). 2008/9 data were square-root-transformed and 2009/10 date were log-transformed. LSDs are 0.2987 and 0.1035 respectively. Nitrogen was supplied at 100 kg N ha^{-1} and 350 kg N ha^{-1}. Expression was determined at weekly intervals from anthesis (0) to 35 and 21 dpa respectively. Data are means + SE of three replicate field plots.

One of the genes which showed a decreasing expression during senescence under different nitrogen regimes was the NAC transcription factor (Figure 3.10). Similarly, in the Avalon x Cadenza lines grown under different nitrogen levels, NAC expression decreased significantly in both years ($P<0.001$). In 2008/9 there was no significant difference between the N levels and the lines. In 2009/10 expression was significantly higher under high nitrogen, matching slower senescence ($P<0.01$; Figure 3.10.b). Unexpectedly, fast-senescing line AC127 had an overall higher expression of NAC than AC82, but this was mainly caused by the higher expression at anthesis.

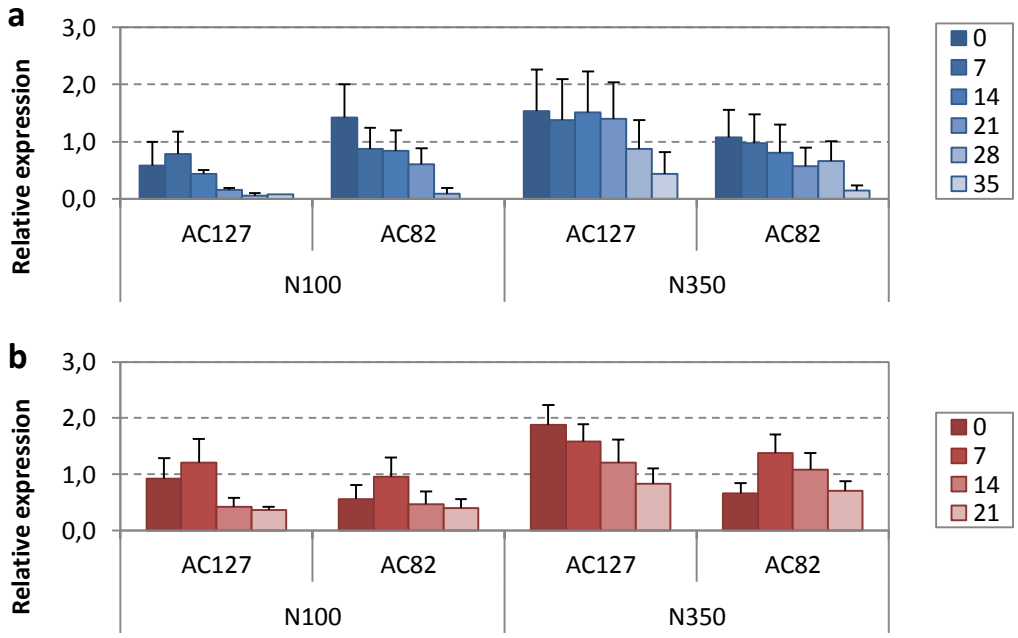

Figure 3.10: Expression of the NAC transcription factor in the second leaf of two Avalon x Cadenza doubled haploid lines grown in the field at two nitrogen regimes in 2008/9 (a) and 2009/10 (b). LSDs are 0.953 and 0.494 respectively. Nitrogen was supplied at 100 kg N ha^{-1} and 350 kg N ha^{-1}. Expression was determined at weekly intervals from anthesis (0) to 35 and 21 dpa respectively. Data are means + SE of three replicate field plots.

Another gene that previously showed decreasing expression during senescence was MYB transcription factor *b*. A decrease was apparent also in the two Avalon x Cadenza lines (Figure 3.11). In 2008/9 MYB*b* expression was significantly lower under low N conditions ($P<0.05$). The onset of the decrease was determined by the line ($P<0.05$): in AC127 MYB*b* expression already started to decline at 28 dpa, while expression only decreased at 35 dpa in AC82 (Figure 3.11.a). In 2009/10 there was no difference between lines; MYB*b* expression decreased only under low nitrogen conditions ($P<0.01$; Figure 3.11.b).

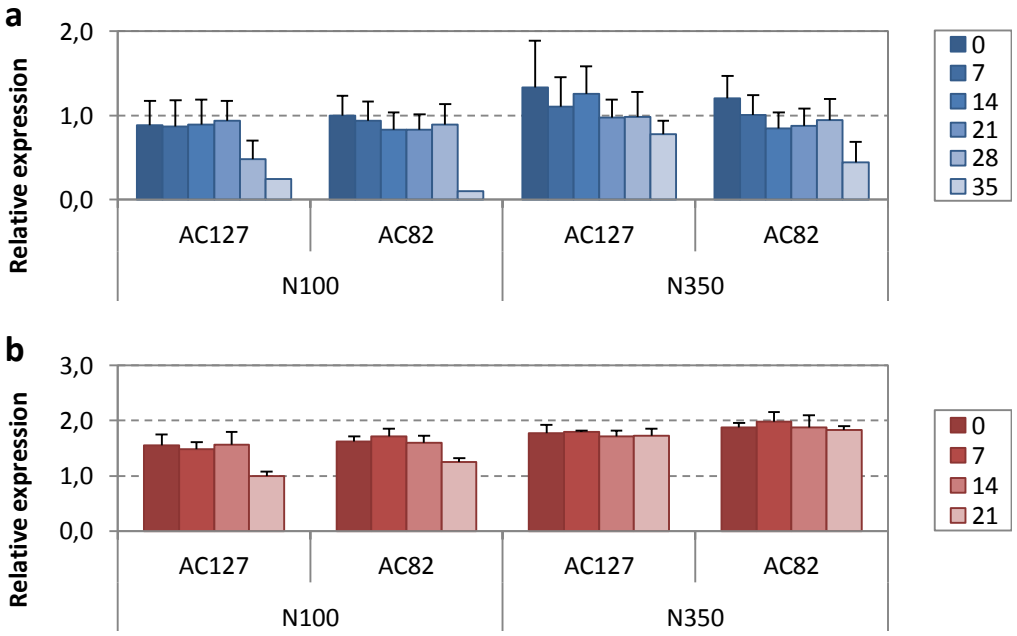

Figure 3.11: Expression of MYB transcription factor *b* in the second leaf of two Avalon x Cadenza doubled haploid lines grown in the field at two nitrogen regimes in 2008/9 (a) and 2009/10 (b). LSDs are 0.369 and 0.315 respectively. Nitrogen was supplied at 100 kg N ha^{-1} and 350 kg N ha^{-1}. Expression was determined at weekly intervals from anthesis (0) to 35 and 21 dpa respectively. Data are means + SE of three replicate field plots.

The GLK1-like gene previously showed a higher expression under high N conditions, but no significant change in expression (Figure 3.2.f). However, in the Avalon x Cadenza lines expression significantly decreased during senescence ($P<0.001$; Figure 3.12.a). In 2008/9 the expression pattern was significantly dependent on N level ($P<0.05$): under low nitrogen expression of the GLK1-like gene showed a continuous decrease, while at high N expression increased until 14 dpa, after which expression decreased. In 2009/10 such a pattern was not observed (Figure 3.12.b), possibly because the small number of time points did not allow such a detailed analysis.

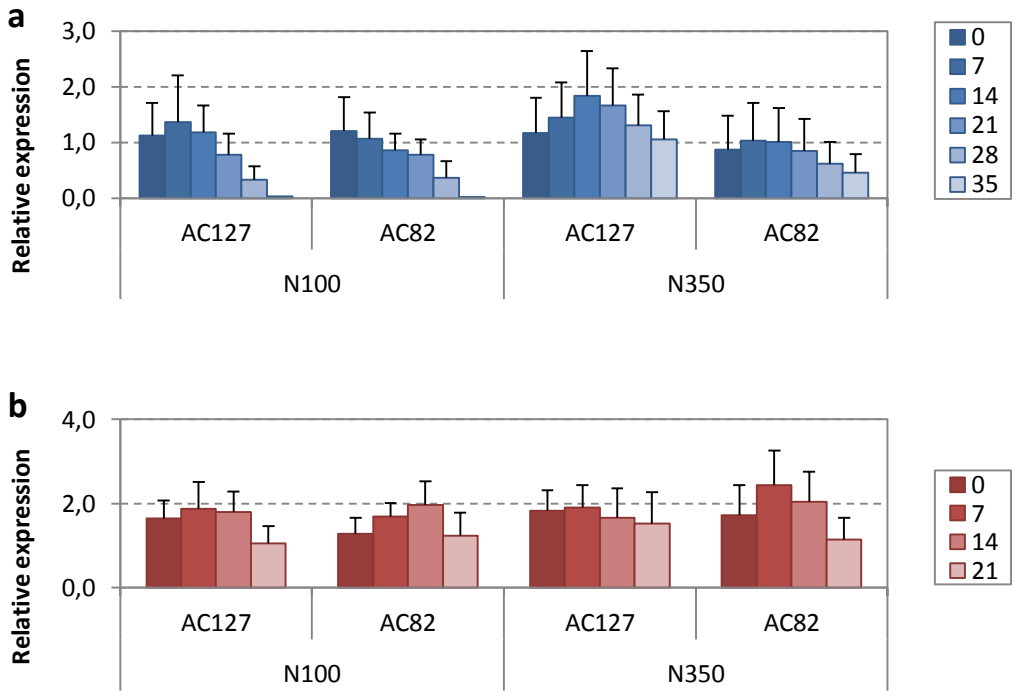

Figure 3.12: Expression of the GLK1-like gene in the second leaf of two Avalon x Cadenza doubled haploid lines grown in the field at two nitrogen regimes in 2008/9 (a) and 2009/10 (b). 2009/10 data were square-root-transformed. LSDs are 0.788 and 0.464 respectively. Nitrogen was supplied at 100 kg N ha^{-1} and 350 kg N ha^{-1}. Expression was determined at weekly intervals from anthesis (0) to 35 and 21 dpa respectively. Data are means + SE of three replicate field plots.

The gene that showed the biggest increase in expression in the two N-levels Hereward experiment was the WRKY transcription factor. In the Avalon x Cadenza lines WRKY expression increased with senescence as well (P<0.001; Figure 3.13). In 2008/9 expression was higher in AC127 than in AC82, and higher under a low than a high nitrogen regime (both P<0.05; Figure 3.13.a). In 2009/10, WRKY expression increased only significantly under low N conditions (P<0.001; Figure 3.13.b). There were no differences between the lines.

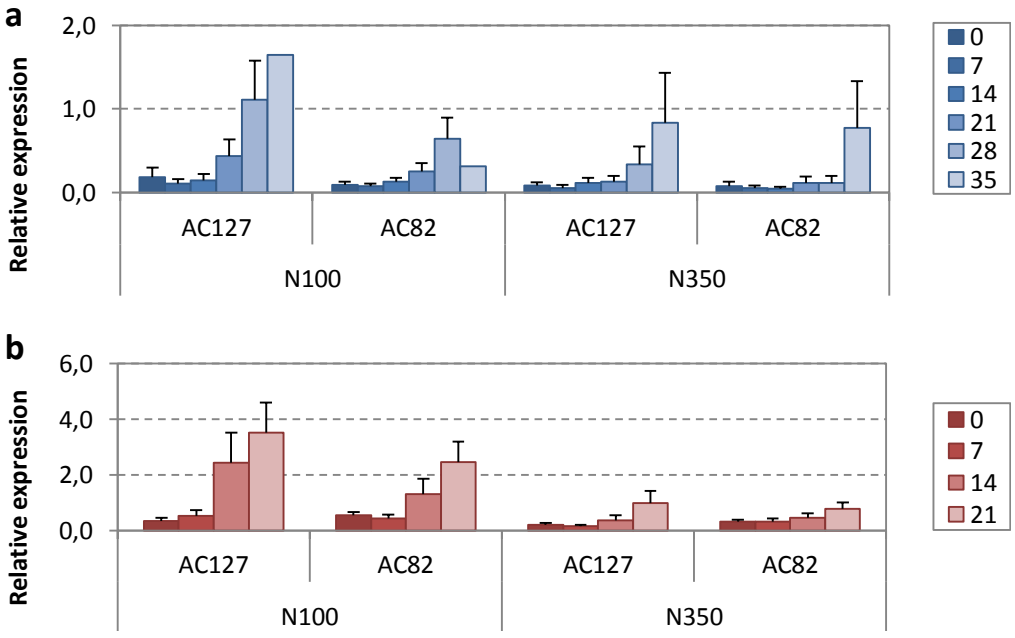

Figure 3.13: Expression of the WRKY transcription factor in the second leaf of two Avalon x Cadenza doubled haploid lines grown in the field at two nitrogen regimes in 2008/9 (a) and 2009/10 (b). LSDs are 0.534 and 1.203 respectively. Nitrogen was supplied at 100 kg N ha^{-1} and 350 kg N ha^{-1}. Expression was determined at weekly intervals from anthesis (0) to 35 and 21 dpa respectively. Data are means + SE of three replicate field plots.

Another gene that showed an increase with senescence in the previous experiment was the MYB transcription factor *a*. An increase was also found in the Avalon x Cadenza lines in both years ($P<0.001$; Figure 3.14). In both years the overall expression was higher at low nitrogen fertilisation ($P<0.05$). The expression was also higher in fast-senescing line AC127 (only significant in 2008/9, $P<0.05$). The onset of the increase did not seem to be affected by either genotype or nitrogen availability.

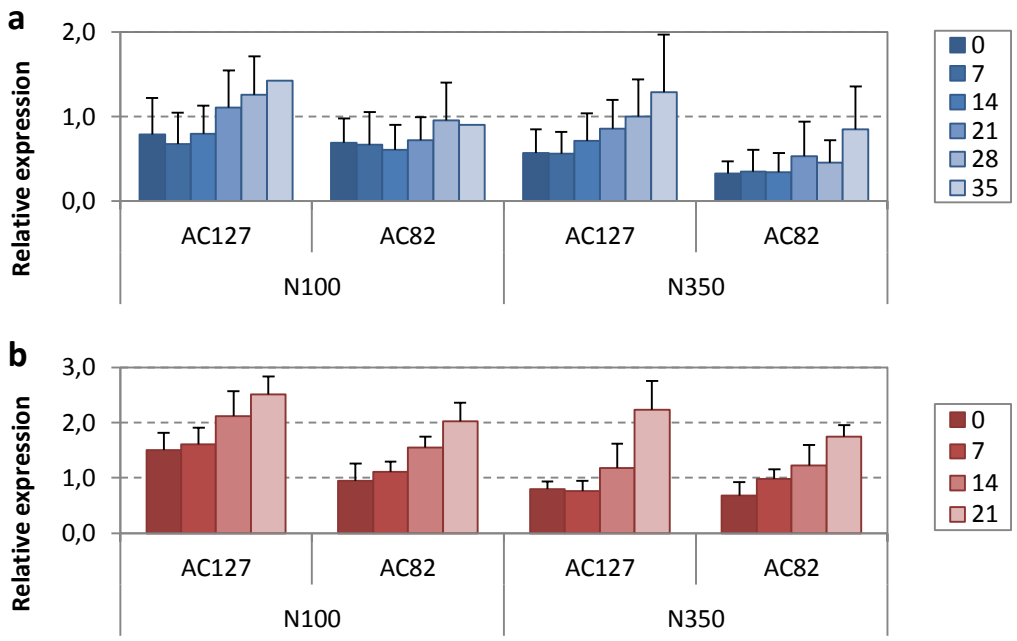

Figure 3.14: Expression of MYB transcription factor *a* in the second leaf of two Avalon x Cadenza doubled haploid lines grown in the field at two nitrogen regimes in 2008/9 (a) and 2009/10 (b). LSDs are 0.490 and 0.744 respectively. Nitrogen was supplied at 1100 kg N ha^{-1} and 350 kg N ha^{-1}. Expression was determined at weekly intervals from anthesis (0) to 35 and 21 dpa respectively. Data are means + SE of three replicate field plots.

Expression of the F-box gene increased with time (Figure 3.15). In 2008/9 expression was higher at low N ($P<0.05$; Figure 3.15.a). In 2009/10 F-box expression was significantly higher at low N as well ($P<0.05$; Figure 3.15.b), but now the onset of the increase was influenced by genotype ($P<0.05$; AC127 earlier than AC82).

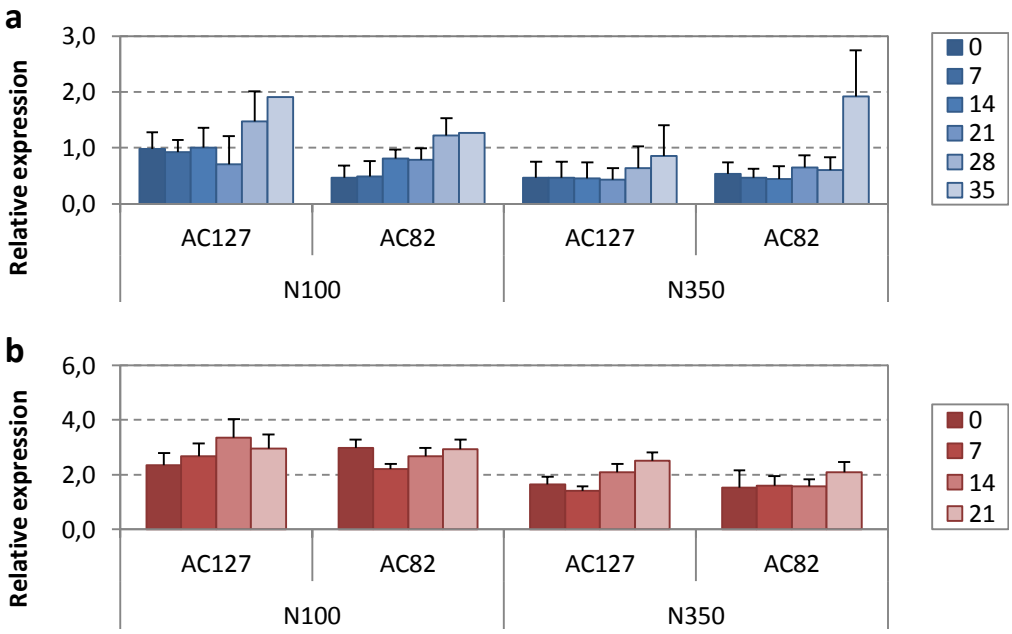

Figure 3.15: Expression of the F-box gene in the second leaf of two Avalon x Cadenza doubled haploid lines grown in the field at two nitrogen regimes in 2008/9 (a) and 2009/10 (b). LSDs are 0.731 and 0.687 respectively. Nitrogen was supplied at 100 kg N ha^{-1} and 350 kg N ha^{-1}. Expression was determined at weekly intervals from anthesis (0) to 35 and 21 dpa respectively. Data are means + SE of three replicate field plots.

The final gene analysed that showed an increase in expression in Hereward during senescence was the PTF1-like gene. In 2008/9, expression of the PTF1-like gene increased nearly threefold in AC127 at low N between 21 and 35 dpa ($P<0.01$; Figure 3.16.a). In 2009/10, AC127 showed a complex interaction between nitrogen availability and line ($P<0.001$; Figure 3.16.b). Expression of the PTF1-like gene increased at both nitrogen levels between 7 and 21 dpa; however, the increase was stronger under a low nitrogen regime. In contrast, AC82 showed an increase between 14 and 21 dpa at low N only. However, the increases and decreases in AC82 were significant too, thus showing a pattern not clearly related to senescence.

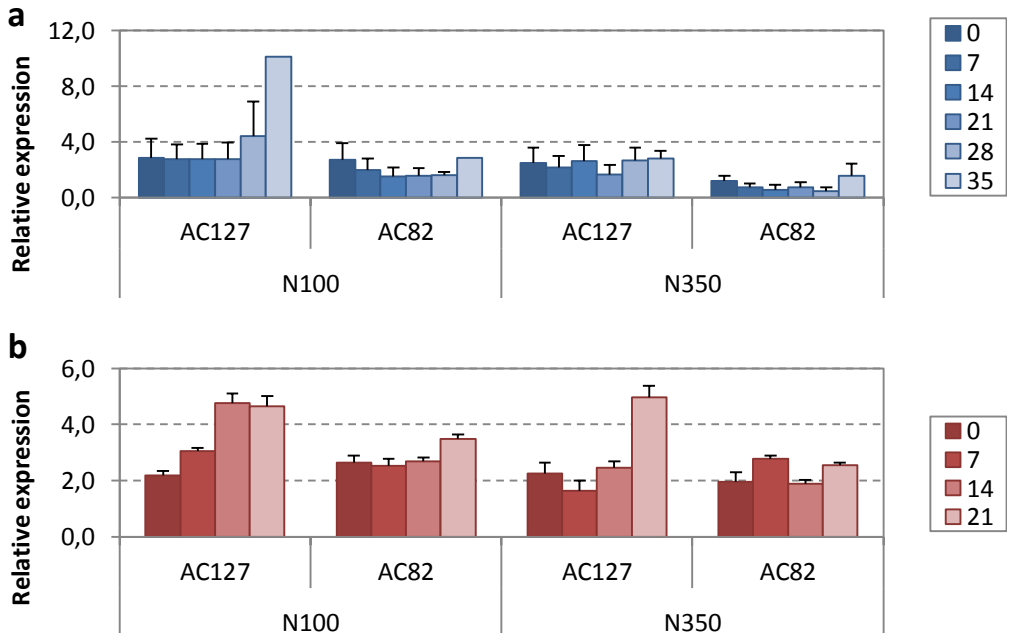

Figure 3.16: Expression of the PTF1-like gene in the second leaf of two Avalon x Cadenza doubled haploid lines grown in the field at two nitrogen regimes in 2008/9 (a) and 2009/10 (b). LSDs are 2.172 and 0.656 respectively. Nitrogen was supplied at 100 kg N ha^{-1} and 350 kg N ha^{-1}. Expression was determined at weekly intervals from anthesis (0) to 35 and 21 dpa respectively. Data are means + SE of three replicate field plots.

The other five tested genes; the CCT-motif-containing protein, the DNA-binding protein, the MYC transcription factor, the RING-domain-containing protein and the zinc-finger protein transcription factor; did not show consistent expression patterns related to senescence (data not shown).

Correlations between leaf nitrogen concentration and gene expression were calculated to validate the visual gene expression patterns. Leaf N concentration data were used instead of SPAD values because more data points were available (SPAD had only been determined at two time points in 2008/9). The expression of all genes except the GLK1-like gene showed a significant correlation with leaf N concentration (Table 3.1). The correlations were especially strong for the WRKY transcription factor. *SAG12* expression was not correlated with leaf N concentration at high N, suggesting the gene was only expressed when senescence was really under way (at low leaf N concentrations). Since expression of the GLK1-like gene increased first before decreasing (Figure 3.12) while leaf N concentration only decreased in time (Figures 3.3.b and 3.4.b), it is not surprising these traits did not correlate.

Table 3.1: Correlations between nitrogen concentration (% DM) and relative gene expression in the second leaf of two Avalon x Cadenza doubled haploid lines grown in the field at two nitrogen regimes in 2008/9 and 2009/10. N100 = 100 kg N ha^{-1} and N350 = 350 kg N ha^{-1}. Correlation coefficients (R) were calculated on the combined data from the two growing seasons. A negative correlation with leaf %N indicates a positive correlation with leaf senescence, while a positive correlation indicates expression decreased during senescence. Correlations highlighted in green are significant (P<0.05) at the indicated appropriate degrees of freedom (d.f.).

	All	N100	N350	AC127	AC82	AC127		AC82	
						N100	N350	N100	N350
RBCS	0.472	0.415	0.508	0.523	0.420	0.519	0.542	0.297	0.483
SAG12	-0.316	-0.531	-0.196	-0.362	-0.235	-0.549	-0.298	-0.482	-0.016
WRKY	-0.640	-0.704	-0.642	-0.654	-0.619	-0.703	-0.690	-0.702	-0.573
NAC	0.482	0.469	0.345	0.566	0.372	0.419	0.397	0.510	0.280
MYB *a*	-0.516	-0.541	-0.463	-0.558	-0.453	-0.535	-0.566	-0.503	-0.340
MYB *b*	0.340	0.209	0.339	0.366	0.311	0.243	0.256	0.132	0.440
F-box	-0.431	-0.380	-0.271	-0.444	-0.411	-0.354	-0.245	-0.389	-0.306
PTF1	-0.470	-0.504	-0.249	-0.540	-0.381	-0.610	-0.386	-0.211	-0.111
GLK1	0.167	0.173	0.079	0.225	0.113	0.252	0.042	0.092	0.118
d.f.	114	54	58	56	56	26	28	26	28

3.5 DISCUSSION AND CONCLUSIONS

Wheat (cv. Hereward) grown in the field under a low nitrogen regime started to senesce about two weeks earlier than wheat grown under higher nitrogen conditions (Figure 3.1). Two Avalon x Cadenza doubled haploid lines, AC127 and AC82, were identified that displayed different senescence patterns under high and low nitrogen fertilisation (Figures 3.3 – 3.6).

Although grain nitrogen concentration and content differed significantly between N levels, AC127 and AC82 did not differ in grain N concentration or content at any nitrogen level (Figure 3.7.g – j). Differences in grain and straw yields and therefore harvest index were consistent across all nitrogen levels (Figure 3.7.a – f), indicating that both lines responded similarly to changes in nitrogen availability. Furthermore, grain N content correlated significantly with both grain N concentration and grain yield over all lines and N levels, indicating grain N concentration and yield responded concomitantly to N availability. This suggests that, at least under these conditions, grain yield of both AC127 and AC82 was limited by N availability and not by photosynthetic production.

Gene expression studies on both the Hereward and Avalon x Cadenza field experiments provided evidence for a set of seven genes that showed expression patterns correlating with leaf senescence: a WRKY transcription factor, a NAC transcription factor, two MYB transcription factors (MYB*a* and MYB*b*), a gene resembling P_i starvation-induced transcription factor 1 *(PTF1)*, a gene similar to Golden-like 1 *(GLK1)*, and an F-box protein. These correlations may be indicative of functional roles in leaf senescence, but they could also be direct or indirect consequences of senescence processes.

The WRKY gene showed the most consistent strong increase in expression during leaf senescence (Figures 3.2.m and 3.13). Since various WRKY transcription factors have been shown to have a role in leaf senescence in

several plant species, or were at least up-regulated in expression (Hinderhofer and Zentgraf, 2001; Jing et al., 2009; Miao et al., 2004; Ricachenevsky et al., 2010; Robatzek and Somssich, 2001; Ülker et al., 2007; Wu et al., 2008a; Zhou et al., 2011b), it is plausible the WRKY gene is involved in the regulation of leaf senescence in wheat.

Another transcription factor family for which there is a significant body of evidence indicating a role in leaf senescence of both monocotyledonous and dicotyledonous plant species is the NAC family (Balazadeh et al., 2011; Chen et al., 2011b; Guo and Gan, 2006; Kim et al., 2009; Sperotto et al., 2009; Uauy et al., 2006b; Wu et al., 2012; Yang et al., 2011; Yoon et al., 2008). In all except one of these cases, expression of the NAC genes increased during senescence. In contrast, the expression of the NAC gene identified in the Hereward and Avalon x Cadenza field experiments decreased consistently during senescence (Figures 3.2.j and 3.10). This suggests that if this NAC gene is involved in senescence it would be as a negative regulator (inhibitor) of senescence, while nearly all the senescence-associated NAC genes described so far are positive regulators of senescence. It is therefore almost certainly a NAC gene that has not been described before, at least not in relation to senescence.

The same is the case for at least one of the two MYB transcription factors. Only one MYB gene with a role in senescence has been identified so far: Arabidopsis *MYBL* is involved in promoting leaf senescence (Zhang et al., 2011). The Avalon x Cadenza and Hereward gene expression studies revealed both a possible positive regulator of senescence (MYB*a*; Figures 3.2.g and 3.14) and a negative regulator of senescence (MYB*b*; Figures 3.2.h and 3.11).

The F-box protein showed an increase in expression during senescence in all tissues tested (Figures 3.2.e and 3.15). Interestingly, in the 2009/10 Avalon x Cadenza experiment its expression was also influenced by the genotype. F-box proteins are part of the molecular machinery that targets specific

proteins for degradation by the 35S proteasome. It is attractive to think the F-box gene is involved in breaking down an inhibitor of senescence, thereby promoting its progression. Examples of protein degradation genes involved in leaf senescence have been described before. ORE9 is an F-box protein that positively regulates leaf senescence in Arabidopsis (Woo et al., 2001). The DLS1 protein functions in the N-end rule pathway of protein degradation (Yoshida et al., 2002a). And the *nla* mutant, which is impaired in nitrogen-limitation-mediated senescence, lacks the RING domain of a RING-type ubiquitin E3 ligase (Peng et al., 2007).

The P_i starvation-induced transcription factor 1 (PTF1) like gene showed an increase in expression during senescence (Figures 3.2.k and 3.16). Expression of this gene also showed a relation to nitrogen availability, which is surprising since *PTF1* so far has only been described in relation to phosphate limitation in wheat, maize and rice (Espindula, Minella and Delatorre, 2009; Li et al., 2011; Yi et al., 2005). The mechanism seems to be alterations in sugar signalling and root morphology (Li et al., 2011). It is not immediately apparent why this gene would be up-regulated during leaf senescence.

The Golden-like 1 (GLK1) like gene showed a decreasing expression in the Avalon x Cadenza experiment, and in both the Hereward and Avalon x Cadenza experiments 2008/9 expression was also higher at high nitrogen (Figures 3.2.f and 3.12). This is not unexpected since *GLK1* and *GLK2* are genes involved in regulation of photosynthesis and chloroplast development in maize, rice and Arabidopsis. *glk1/glk2* double mutants have a pale green phenotype with smaller and rudimentary chloroplasts (Fitter et al., 2002), and constitutive expression of *GLK1* and *GLK2* enhances expression of light-harvesting and chlorophyll biosynthesis genes (Waters et al., 2009b). Interestingly, GLK1 was found to be also a central component of the organic nitrogen signalling network (Gutiérrez et al., 2008).

Of the two Avalon x Cadenza field experiments, the 2009/10 experiment showed the biggest differences in leaf senescence. However, because senescence was so rapid, there were less time points available for gene expression analysis. This made it more difficult to assess expression patterns. The best example is probably the GLK1-like gene (Figure 3.12). This gene showed a complex expression pattern in Avalon x Cadenza 2008/9; first an increase in expression, and only after that a stronger decrease in expression. It is difficult to capture such an intricate expression pattern with only four time points, such as was available in the 2009/10 Avalon x Cadenza experiment.

In summary, seven genes with a possible function in leaf senescence have been identified by screening field-grown wheat with differential leaf senescence patterns. Since grain nitrogen concentration and total nitrogen content did not differ between the two Avalon x Cadenza lines, it is questionable whether any of the identified genes are directly involved in nitrogen remobilisation. However, gene expression studies merely associate a gene with a process; they cannot distinguish between whether a gene has a functional role in leaf senescence or if its expression is an indirect consequence of senescence. To actually demonstrate the function of a gene it is necessary to study mutants or transgenic plants. With this objective the expression of the NAC and WRKY transcription factors was manipulated through a transgenics approach. This work is described in Chapters 5 and 6.

4. COMPARISON OF FAST-SENESCING AND STAY-GREEN MUTANTS OF WHEAT

4.1 INTRODUCTION

Extending the duration of photosynthesis is a possible means to increase total photosynthesis, biomass and grain yield in wheat (Richards, 2000). Total flag leaf photosynthesis, chlorophyll content, the onset of senescence (at low nitrogen availability) and green leaf duration have all been found to be positively correlated with wheat grain yield (Gaju et al., 2011; Kichey et al., 2007; Wang et al., 2008). Although under optimal conditions wheat crops may not be limited by assimilate supply during grain-filling (Borrás et al., 2004), under abiotic stress grain yields may be limited by photosynthetic capacity, so extending the duration of photosynthesis may in these cases increase grain yield. One approach to achieve a longer photosynthetic period is the use of functional stay-green phenotypes, which show either delayed onset and / or a slower rate of senescence whilst maintaining photosynthetic activity (Thomas and Howarth, 2000).

Stay-green phenotypes and broader genetic variation in leaf senescence have been described in wheat (Blake et al., 2007; Bogard et al., 2011; Chen et al., 2011a; Chen et al., 2010; Christopher et al., 2008; Gong et al., 2005; Joshi et al., 2007; Li et al., 2012; Luo et al., 2006; Naruoka et al., 2012; Silva et al., 2000; Spano et al., 2003; Verma et al., 2004; Vijayalakshmi et al., 2010). The stay-green trait has been reported to increase grain yields (Chen et al., 2010; Christopher et al., 2008; Gong et al., 2005; Luo et al., 2006; Spano et al., 2003), and there were positive correlations with nitrogen use efficiency (Gaju et al., 2011), water use efficiency (Christopher et al., 2008; Górny and Garczyński, 2002), spot blotch resistance (Joshi et al., 2007) and grain yields under heat and drought (Naruoka et al., 2012). However, less favourable

effects also have been observed, such as a decreased harvest index (Gong et al., 2005), more nitrogen remaining in the straw (Chen et al., 2011a), and a reduced grain number per ear (Naruoka et al., 2012). These inconsistent phenotypes indicate the interaction of the stay-green trait with the environment is likely to be strong.

The aims of the experiments reported in this chapter were:

1. To identify stay-green and fast-senescing mutant lines of wheat.
2. To assess senescence, yield characteristics and biomass and nitrogen distribution of these differential senescing lines.
3. To assess the effects of nitrogen supply on the senescence phenotypes by studying the performance of fast-senescing and stay-green wheat lines.
4. To assess patterns of expression of candidate regulatory genes of leaf senescence.

4.2 SCREENING OF A MUTANT POPULATION

A field screening at the John Innes Centre identified EMS mutant lines of wheat cultivar Paragon that displayed a visual stay-green phenotype. In this project, 54 of these lines and the wild-type were screened in the glasshouse and the relative chlorophyll content and photosynthetic rate of the flag leaf were measured at two time points, independently of the developmental status of individual plants. The first time point was when the first plants were at anthesis, so all plants were fully green, and the second time point was six weeks later during the senescence phase. Highly significant differences in retention of photosynthesis and greenness were found (Figure 4.1.a and 4.1.b; $P<0.001$), and maintenance of greenness and photosynthesis were correlated significantly with one another (Figure 4.1.c; $P<0.001$).

The selection of candidate lines was focused on the photosynthetic rate, since only lines that maintain photosynthesis longer than others can be considered functionally stay-green. Lines with similar anthesis dates were chosen since they would have been in a similar developmental stage and will have experienced similar environmental conditions. For further detailed studies of senescence six lines were selected (Figure 4.1.a): wild-type (WT), three lines that maintained over 60% of their photosynthesis (stay-green 1-3) and two fast-senescing lines (fast-senescing 1 and 2) that had less than 25% of their original capacity left after a senescence period of six weeks. The selected lines showed similar differences in greenness (Figure 4.1.b).

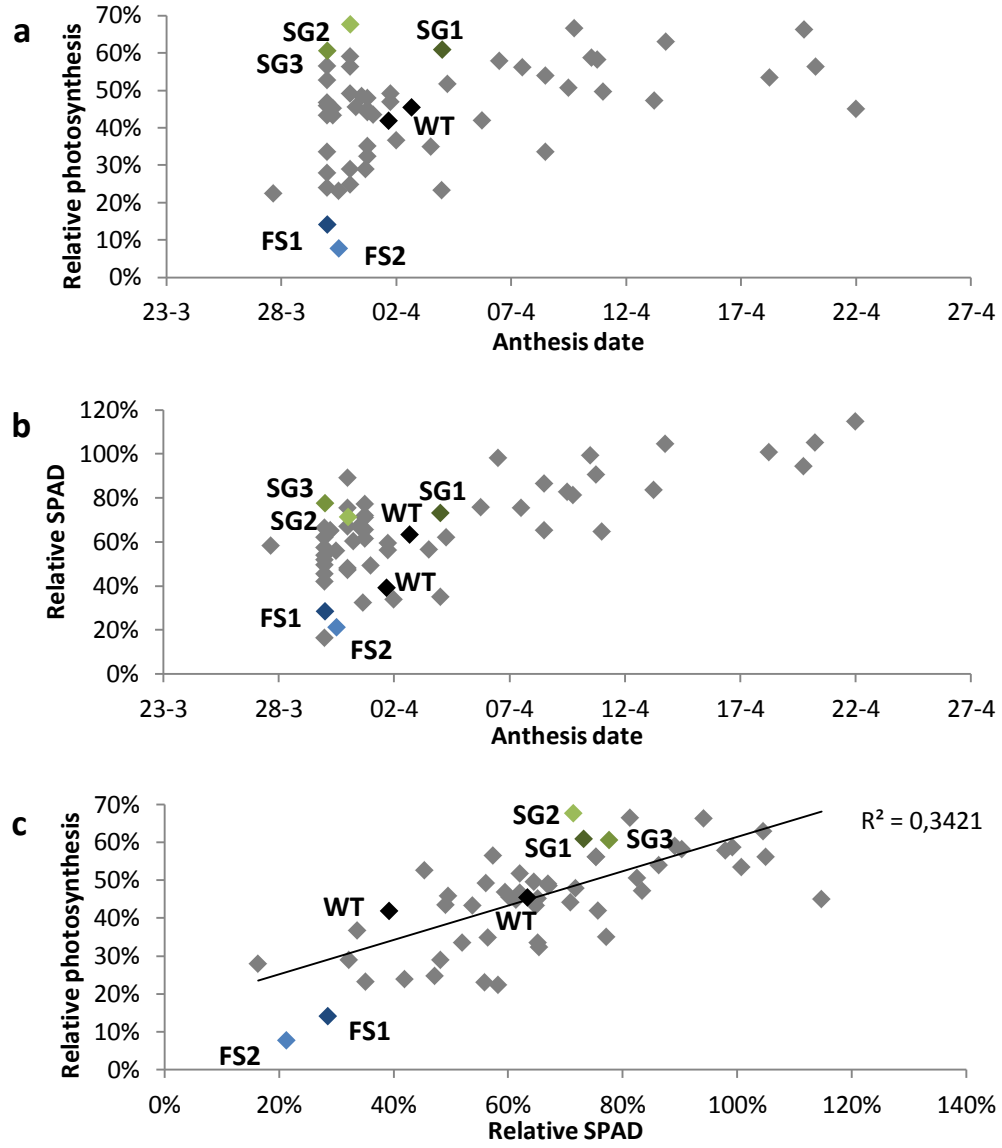

Figure 4.1: Relative maintenance of photosynthesis (a) and relative chlorophyll content (b) of the flag leaf as a function of anthesis date, and relationship between relative maintenance of relative chlorophyll content and photosynthesis (c) of a population of mutant wheat lines after a six-week senescence period. The first measurement was done between heading and anthesis, when the plants were green (same date for all plants irrespectively of developmental stage), and the second measurement six weeks later during senescence. Relative performance values were plotted against anthesis date to correct for differences in developmental stage. The lines used for further experiments are marked: three stay-green lines (green, SG1-3), two fast-senescing lines (blue, FS1-2) and wild-type (black, WT). Data points are the means of four replicate pots (five plants/pot). (c) $y = 0.7567x + 0.3086$; $R^2 = 0.3421$; $P<0.001$. Figure adapted from Derkx et al. (2012).

4.3 CHARACTERISATION OF STAY-GREEN AND FAST-SENESCING LINES

4.3.1 Flag Leaf Senescence

The post-anthesis senescence process of the six selected lines was studied in further detail. Relative chlorophyll content (SPAD) and chlorophyll fluorescence (quantum yield = F_V'/F_M') of flag leaves of main shoots were measured at anthesis (Zadoks growth stage 61; (Zadoks et al., 1974)), weekly from 14 days post-anthesis (dpa) until 42 dpa, and at physiological maturity (GS89). At 42 dpa the flag leaves were photographed to visualise differences in senescence (Figure 4.2.a).

Relative chlorophyll content declined slower in the stay-green lines (Figure 4.2.b). ANOVA analysis revealed a significant interaction between line and time ($P<0.01$) as well as a significant effect of line ($P<0.01$), the latter mainly driven by SG3. At 42 dpa lines SG1 and SG3 differed significantly from FS2. At physiological maturity lines SG2 and SG3 retained significantly more chlorophyll than the other lines, while SG1 lost its chlorophyll in a fast rate between 42 dpa and maturity.

Comparison of quantum yield data revealed similar differences (Figure 4.2.c): both an effect of line ($P<0.001$) and an interaction between line and time ($P<0.001$) was found. Lines SG1 and SG3 had significantly higher F_V'/F_M' values than lines FS2 and WT over the entire senescence period. At 42 dpa the three stay-green lines SG1, SG2 and SG3 had lost less of their photochemical capacity, a difference that remained until physiological maturity (except for an unexpectedly high value of FS1 when considering its chlorophyll loss).

Overall, these results show that lines SG1, SG2 and SG3 are functional stay-green mutants and FS1 and FS2 fast-senescing mutants.

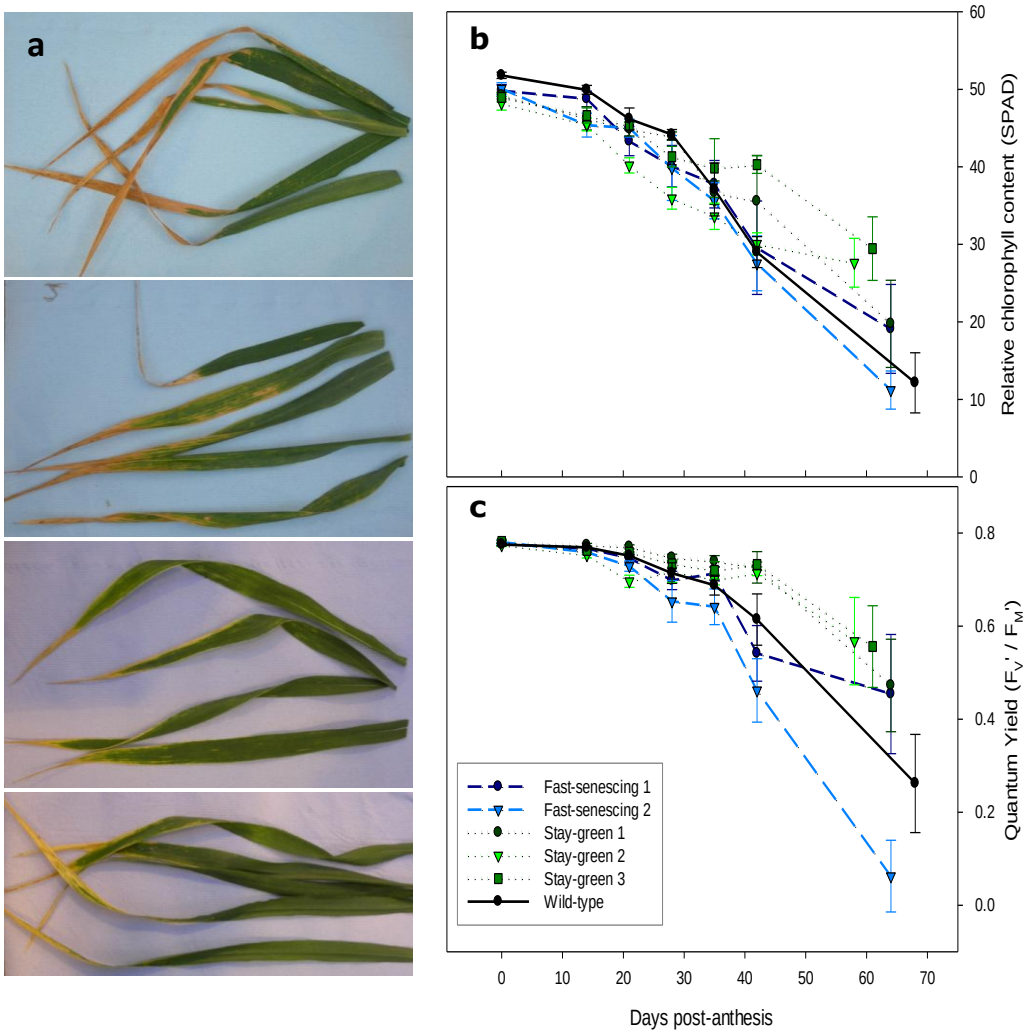

Figure 4.2: The progression of flag leaf senescence in selected mutant wheat lines. (a) Flag leaves 42 days post-anthesis of FS2 (fast senescing), WT (wild-type), and SG1 and SG3 (stay-green) respectively. **(b)** Relative chlorophyll content as determined with a SPAD meter. LSD = 7.16. **(c)** Quantum yield (QY = F_V'/F_M'), which is a measurement of Photosystem II maximum efficiency, as determined with a handheld chlorophyll fluorescence meter. LSD = 0.120. Data are means ± SE of four replicate pots (five plants/pot). Figure from Derkx et al. (2012).

4.3.2 Yield Characteristics

Grain yield differed significantly between lines (P<0.001). Wild-type had a significantly higher grain yield than all the other lines, and lines SG2 and SG3 had in turn a higher grain yield than lines FS1 and FS2 (Figure 4.3.a). The lines with the highest grain yield had the lowest thousand grain weights (P<0.001; Figure 4.3.b). The number of shoots differed significantly between the lines (P<0.001; Figure 4.3.c), but there was no relationship with grain yield; so the differences in grain yield must have been due to differences in grain number.

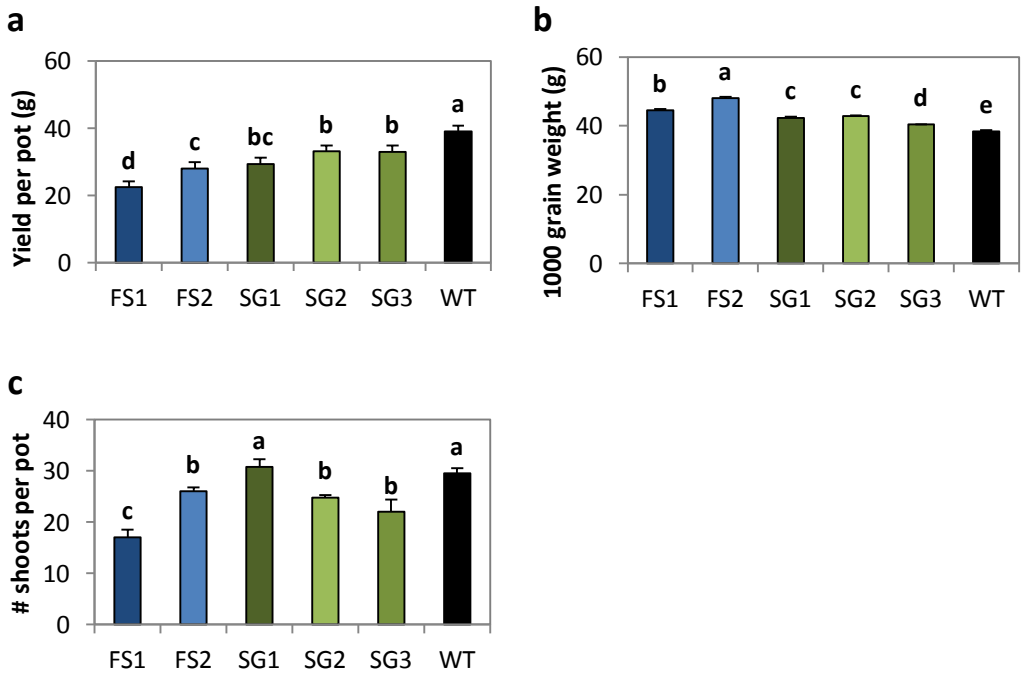

Figure 4.3: Yield characteristics of selected mutant wheat lines. (a) Grain yield per pot (28 replicates + SE), corrected for number of plants/pot. **(b)** Thousand grain weight (three replicates of pooled grain + SE). **(c)** Average number of shoots per pot (four replicates + SE). FS1 has a low tiller number due to a higher death rate, which resulted in less plants/pot. Letters indicate significant differences at the 0.05 level as determined by using the LSD.

4.3.3 Biomass Accumulation and Allocation

A functional stay-green phenotype should result in prolonged photosynthetic production and consequently a higher accumulation of biomass. To test this hypothesis, main shoots were partitioned into different tissues (flag leaf, rest of the leaves, stem, sheath, and ear), and their dry weights were compared at anthesis and at physiological maturity (Figures 4.4 and 4.5; Table 4.1).

The grain yields of the main shoots gave roughly the same pattern as grain yields of whole plants (4.3.a and 4.4.b): the fast-senescing lines FS1 and FS2 had the lowest grain yields; the stay-green lines SG1, SG2 and SG3 had higher yields; whilst wild-type had a significantly higher grain yield than all other lines ($P<0.01$). The only exception was SG2, which had a higher grain yield than SG3 for the main shoot, while at the whole plant level their grain yields were very similar.

The total biomass of the three stay-green lines was different. SG3 had a significantly lower total biomass than any other line both at anthesis and maturity, SG1 had the highest biomass of all lines, while SG2 was of average weight (Figure 4.4; $P<0.001$). While plants of SG1 were the largest at anthesis and still at maturity (Figure 4.4), the total increase in biomass was only 33%, compared to around 50% for the other two stay-green lines, FS1 and wild-type (Table 4.1; differences not significant; LSD = 29.4%). The relative allocation of dry matter to the grain was very low in SG1 compared to all the other lines (Figure 4.5.b; Table 4.1). On the other hand, SG3 had a low biomass at maturity, yet it had a high relative grain mass and was overall higher yielding than all other lines except WT (Figures 4.3.a and 4.5).

Post-anthesis stem dry mass decreases ranged from 15% to 39% and sheath mass from 1% to 16% (Table 4.1), without any clear pattern relating to the senescence phenotypes of the lines. Dry weights of the flag leaf and other leaves differed according to the senescence phenotype. Fast-senescing lines FS1 and FS2 showed a relatively bigger post-anthesis decrease in flag leaf

mass but a limited decrease in dry matter of the other leaves, while the stay-green lines SG1, SG2 and SG3 showed the opposite pattern (Table 4.1). There was a large decrease in dry mass in all leaves of wild-type.

In summary, there was no direct relationship between the rate of senescence and total biomass accumulation and its allocation to different plant tissues. There appeared to be a relationship between post-anthesis decrease in leaf dry matter and increase in grain yield, but this had no direct association with the leaf senescence phenotype.

Table 4.1: Relative changes (%) in dry weight of different plant tissues of main shoots of selected mutant wheat lines between anthesis and maturity. The "rest leaves" fraction does not include the flag leaf and is incomplete at maturity; the ear fraction includes the grain. Data are based on the means of four replicate pots (five plants/pot) at anthesis and physiological maturity.

Line	Flag Leaf	Rest Leaves	Sheath	Stem	Ear	Whole Shoot
FS1	-10%	-16%	-1%	37%	243%	45%
FS2	-25%	-24%	-14%	15%	207%	31%
SG1	-5%	-52%	-12%	33%	151%	33%
SG2	-5%	-36%	-3%	39%	294%	56%
SG3	-9%	-33%	-10%	32%	291%	54%
WT	-20%	-58%	-16%	29%	319%	53%

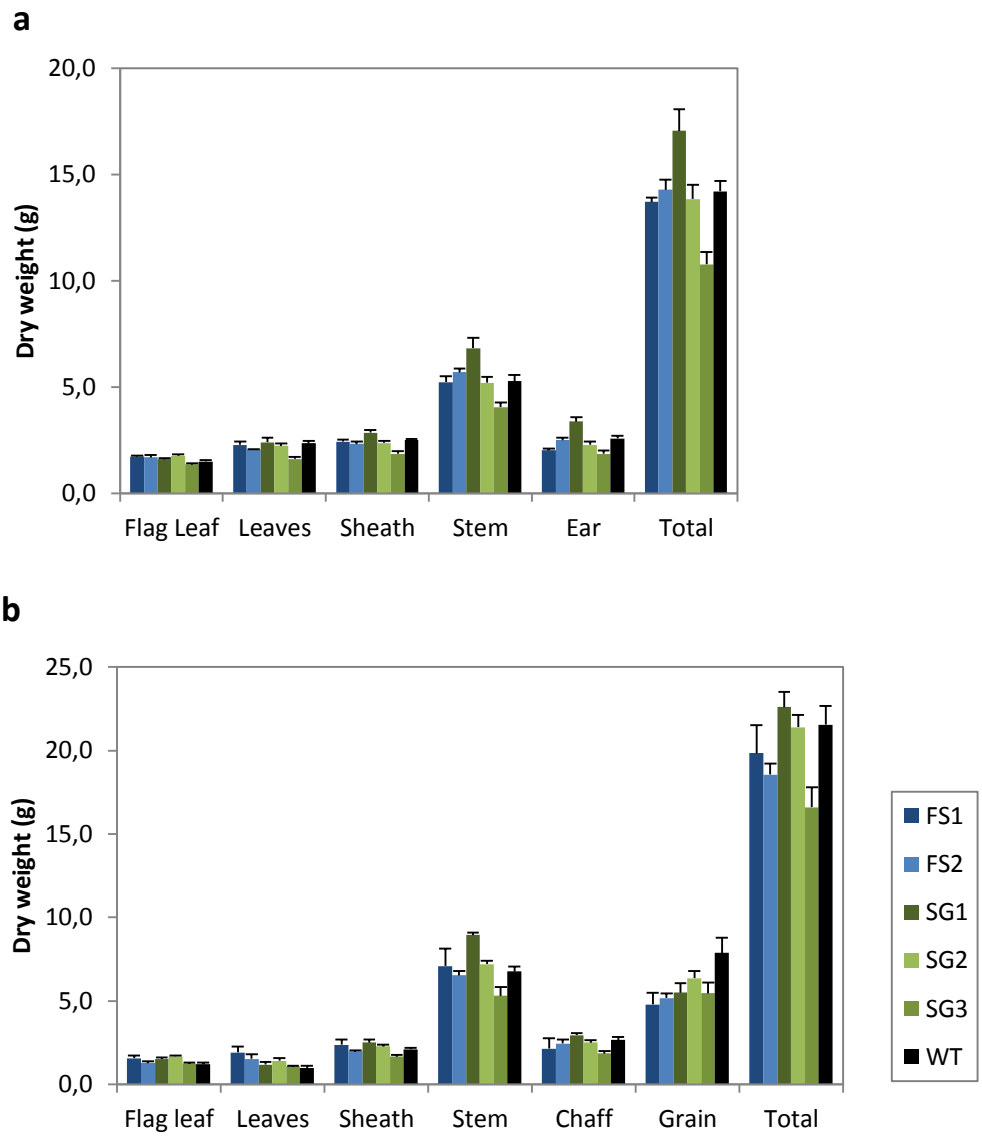

Figure 4.4: Biomass accumulation (g) of tissues of the main shoot of selected mutant wheat lines at anthesis (a) and physiological maturity (b). The leaves fraction does not include the flag leaf and is incomplete at maturity. LSDs: FL=0.25, L=0.44, Sh=0.36, St=1.08, E/Ch=0.63, Gr=1.33, T=2.35. Data are means + SE of four replicate pots (five plants/pot). Statistical analysis was performed per tissue but encompassing both time points.

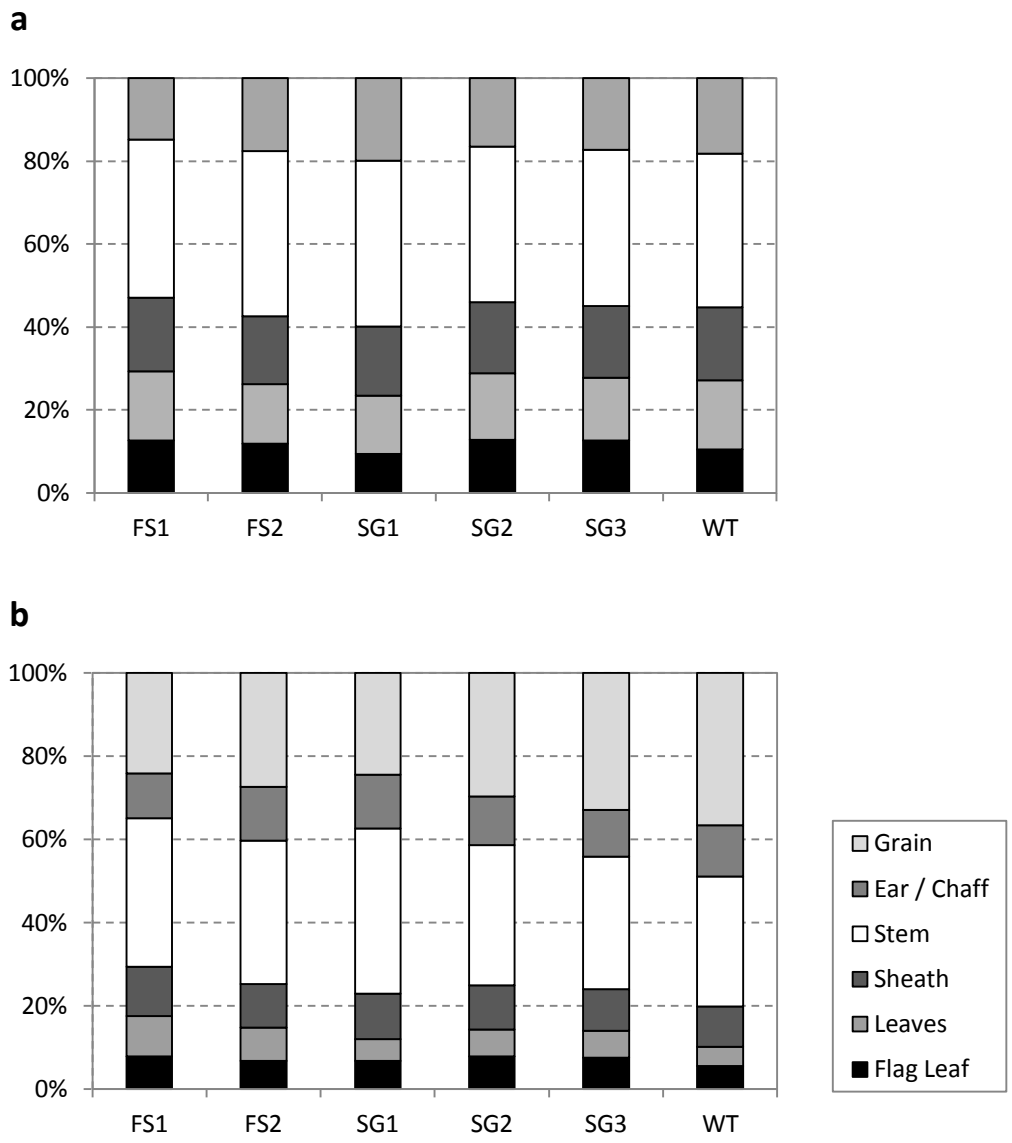

Figure 4.5: Biomass partitioning between tissues of the main shoot of selected mutant wheat lines at anthesis (a) and physiological maturity (b). The leaves fraction does not include the flag leaf and is incomplete at maturity. LSDs: FL=0.25, L=0.44, Sh=0.36, St=1.08, E/Ch=0.63, Gr=1.33, T=2.35. Data are means of four replicate pots (five plants/pot). Statistical analysis was performed per tissue but encompassing both time points.

4.3.4 Nitrogen Accumulation and Allocation

A key process during grain-filling is nitrogen remobilisation from the canopy to the grain. Therefore the nitrogen concentrations of different plant parts of the main shoot were compared at anthesis and at physiological maturity. Since the dry weights were known already (Figure 4.4) the total nitrogen content could be calculated and therefore the net amount of nitrogen remobilised from and to these tissues could be determined.

There were significant differences in grain nitrogen concentration between the lines ($P<0.01$): the nitrogen concentration was the highest in the fast-senescing low-yielding lines FS1 and FS2 and the lowest in WT (Figure 4.6.b). The differences in total nitrogen contents of the grain were highly significant ($P<0.001$; Figure 4.7.b), but there was no association with either senescence phenotype or grain yield.

Total nitrogen contents of the flag leaves were significantly different between anthesis and maturity ($P<0.001$) but not between lines, while that of the lower leaves differed between times and lines ($P<0.01$). N content was reduced more in WT than all three stay-green lines, both in absolute and relative sense (Figure 4.8; not significant). This was because the final nitrogen concentration of wild-type flag leaves was lowest (Figure 4.6.b). The total nitrogen content of the lower leaves varied at anthesis but showed a trend at maturity: the fast-senescing lines FS1 and FS2 retained most nitrogen in the leaves, the stay-green lines SG1, SG2 and SG3 retained less, whilst WT had the lowest leaf total N content at maturity (Figure 4.7.b). So total N content of the lower leaves at maturity showed a negative association with grain yield.

There were some significant differences between lines in leaf sheath, stem and ear nitrogen concentrations. The N content mostly followed the pattern of the differences in biomass (Figures 4.4 and 4.7) and differences and changes in biomass seemed mostly driven by plant-size, not senescence characteristics.

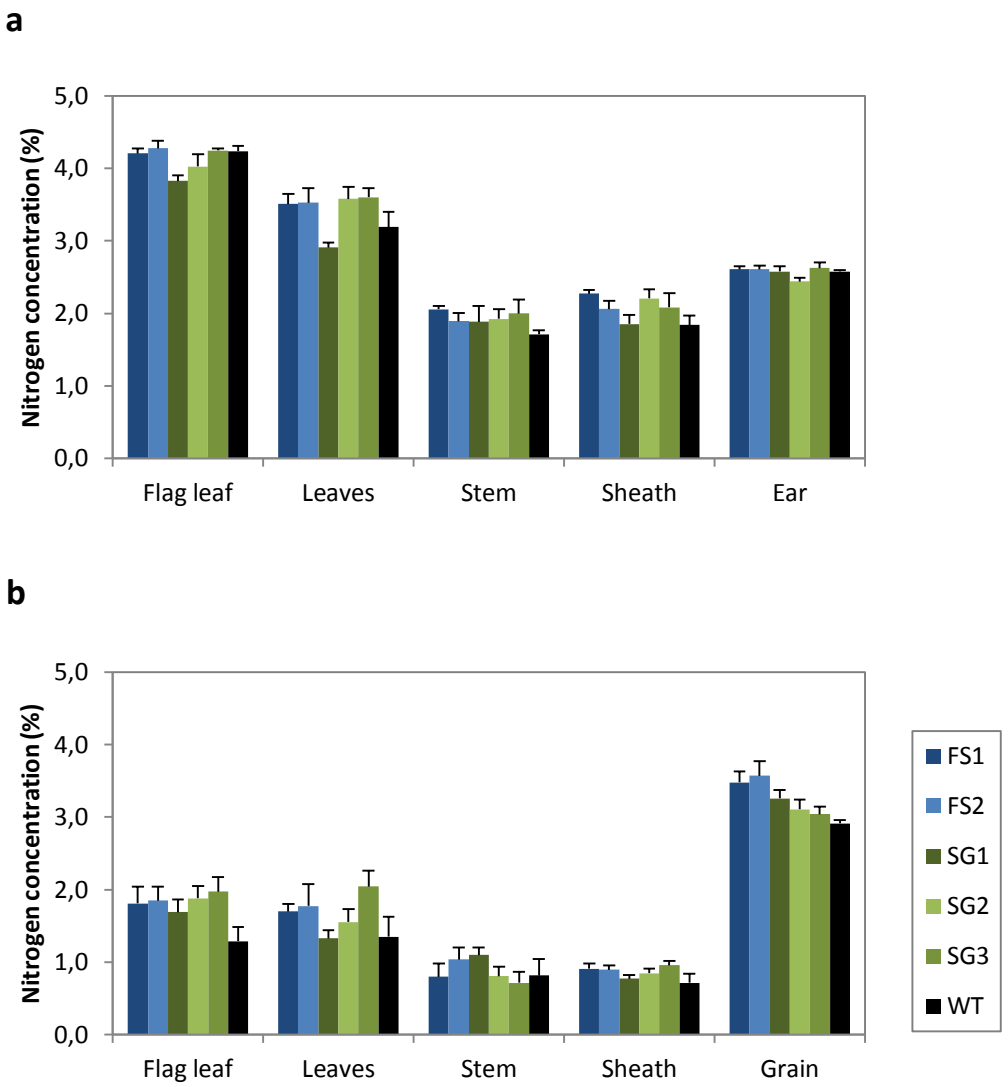

Figure 4.6: Nitrogen concentration (% dry matter) of different tissues of the main shoot of selected mutant wheat lines at anthesis (a) and physiological maturity (b). The leaves fraction does not include the flag leaf and is incomplete at maturity; the ear fraction (chaff) at maturity is missing. LSDs: FL=0.440, L=0.507, St=0.425, Sh=0.296, E=0.112, Gr=0.305. Data are means + SE of four replicate pots (five plants/pot). Statistical analysis was performed per tissue but encompassing both time points.

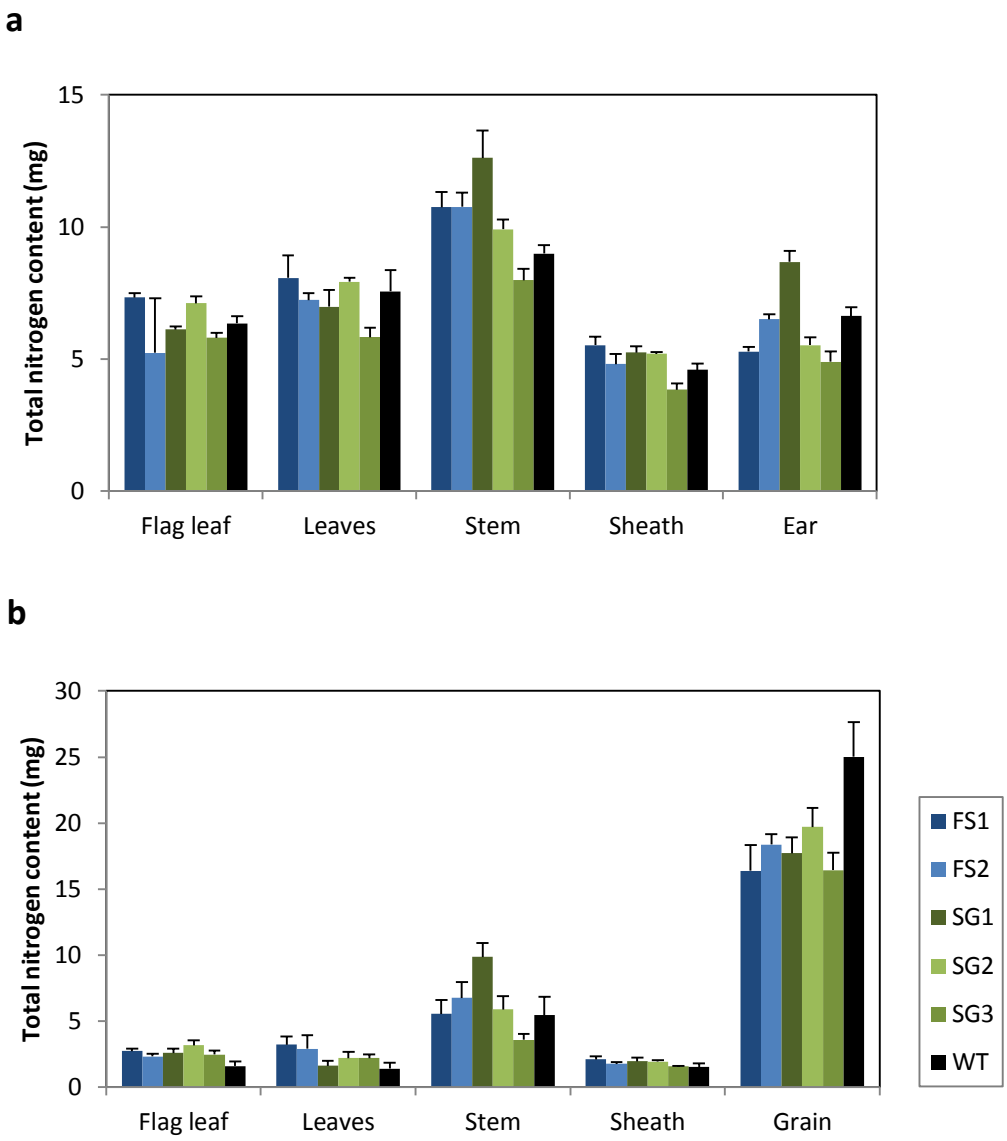

Figure 4.7: Total nitrogen content (mg) of different tissues of the main shoot of selected mutant wheat lines at anthesis (a) and physiological maturity (b). Total N content = %N x dry weight. LSDs: FL=1.629, L=1.698, St= 2.454, Sh=0.676, E=0.553, Gr=3.045. The leaves fraction does not include the flag leaf and is incomplete at maturity; the ear fraction (chaff) at maturity is missing. Data are means + SE of four replicate pots (five plants/pot). Statistical analysis was performed per tissue but encompassing both time points.

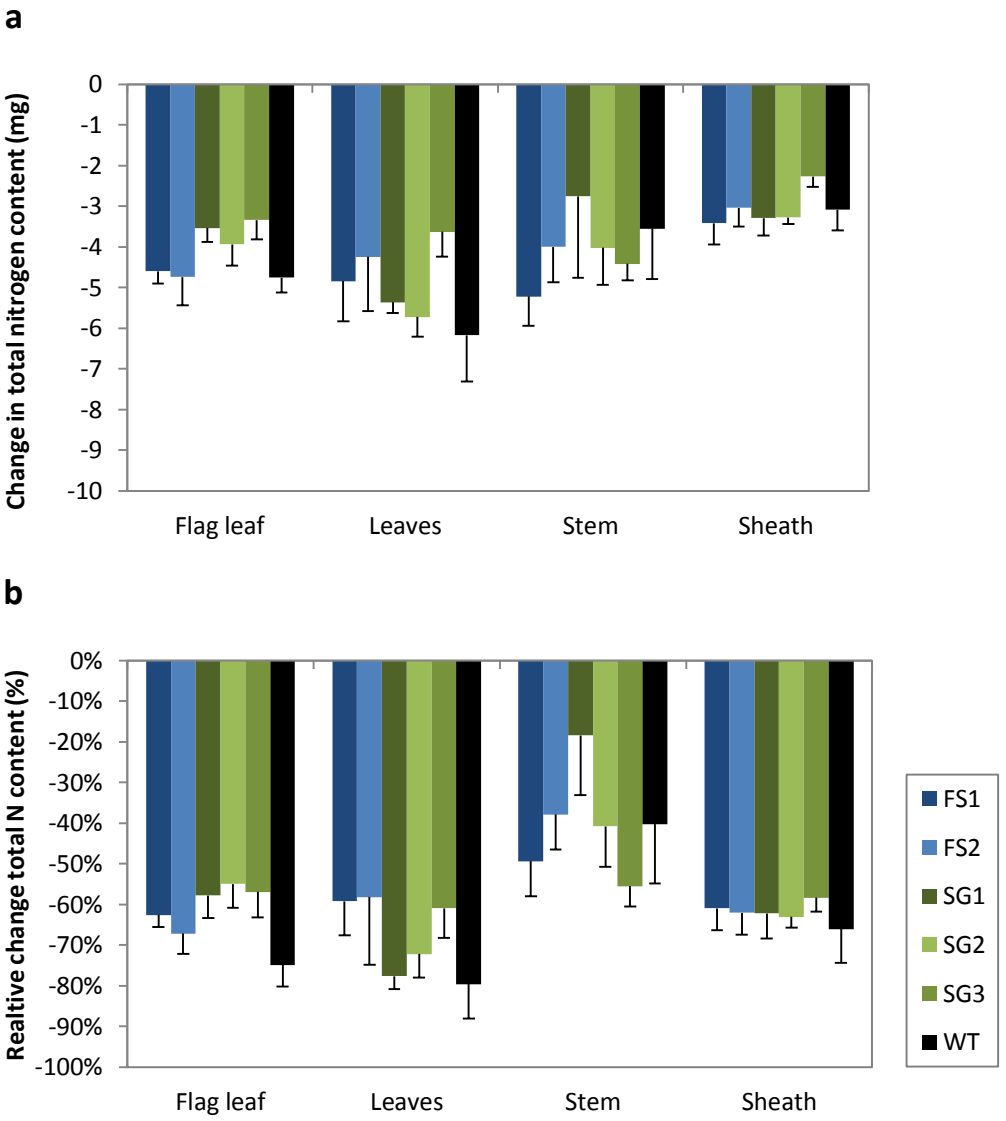

Figure 4.8: Absolute (a) and relative (b) change in total nitrogen content of different tissues of the main shoot of selected mutant wheat lines between anthesis and physiological maturity. Total N content = %N x dry weight. The leaves fraction does not include the flag leaf and is incomplete at maturity. The ear fraction (chaff) at maturity is missing, so therefore the change in total N content could not be calculated. LSDs (a and b respectively): FL=0.014 and 0.162, L=0.680 and 0.214, St=0.030 and 0.284, Sh=0.354 and 0.112. Data are means + SE of four replicate pots per time point (five plants/pot). Statistical analysis was performed per tissue but encompassing both time points.

4.4 NITROGEN NUTRITION EXPERIMENT

4.4.1 Experimental Design

In the experiment described above, mutant lines SG1, SG2 and SG3 displayed a stay-green phenotype. Yet these stay-green lines were not able to accumulate more biomass or realise higher grain yields, at least under the optimal growth conditions used. To examine this further the lines were compared under different nitrogen conditions. Two N levels were used: a "high" N treatment, which was about five times lower than used in the previous experiment but was sufficient to grow green tillering plants; and a "low" N treatment which contained 10% of the nitrogen of the high N treatment and resulted in lighter green coloured plants that scarcely tillered (Figure 4.9). Three lines were compared: fast-senescing line FS2, stay-green line SG3, and WT.

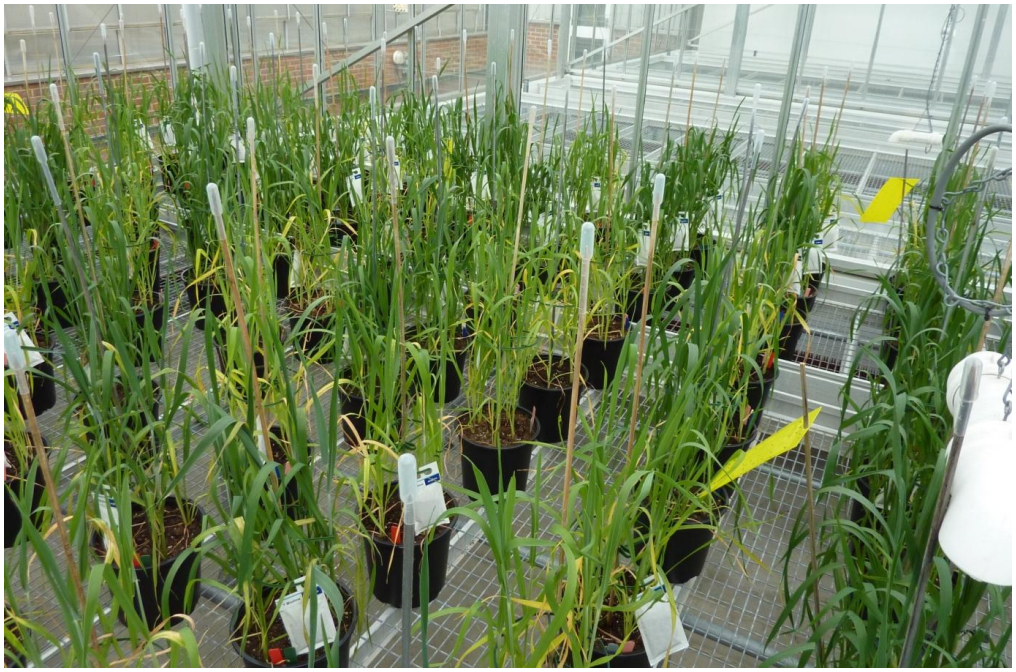

Figure 4.9: The nitrogen nutrition experiment, in which three mutant lines of wheat with different senescence patterns were grown under high and low nitrogen nutrition. The plants grown under high N (dark green) are easily distinguishable from those grown under low N (light green). The picture was taken six weeks after sowing.

4.4.2 Senescence

4.4.2.1 Flag Leaf Senescence

The post-anthesis senescence process of the flag leaves of the three lines under two nitrogen levels was studied by measuring the relative chlorophyll content (SPAD) and maximum photosystem II efficiency (quantum yield = F_V'/F_M') of flag leaves of main shoots (Figure 4.10). The flag leaves of the plants grown under low nitrogen started senescing about two weeks earlier than those grown under high nitrogen. At 21 dpa the flag leaves of the low N treatment already had lost most chlorophyll and the photosystem II efficiency had gone down significantly ($P<0.001$), while flag leaves of the high N treatment had barely started senescing. FS2, which had senesced the fastest in the first experiment, senesced significantly earlier under both low and high N conditions ($P<0.001$). SG3 and WT senesced at the same rate at high N, while at low N SG3 started senescing before the wild-type.

4.4.4.2 Canopy Senescence

To determine if the senescence of the flag leaf is representative of senescence of the whole plant, the senescence of the whole pot (five plants/pot) was evaluated by measuring NDVI with a crop canopy sensor (Section 2.3.4). Results showed that SG3 was greener under high N conditions roughly between one and two weeks post-anthesis (Figure 4.11). SG3 was also the greenest under low N conditions, but this difference was much smaller. A higher NDVI may be the result of greener leaves or more leaves, depending whether there was a full or partial canopy cover. SG3 had more tillers (Figure 4.12.a) and therefore possibly more leaves. However, this was not necessarily the case since SG3 was shorter in height (Figure 4.12.b). If this was caused by a lower number of internodes, the number of leaves should be equal and the leaves of SG3 therefore greener than those of the other lines. The limited perceived differences in senescence at low N might be caused by insufficient canopy cover, caused by lack of tillers (Figure 4.12.a), to make useful measurements and not by actual differences in canopy senescence.

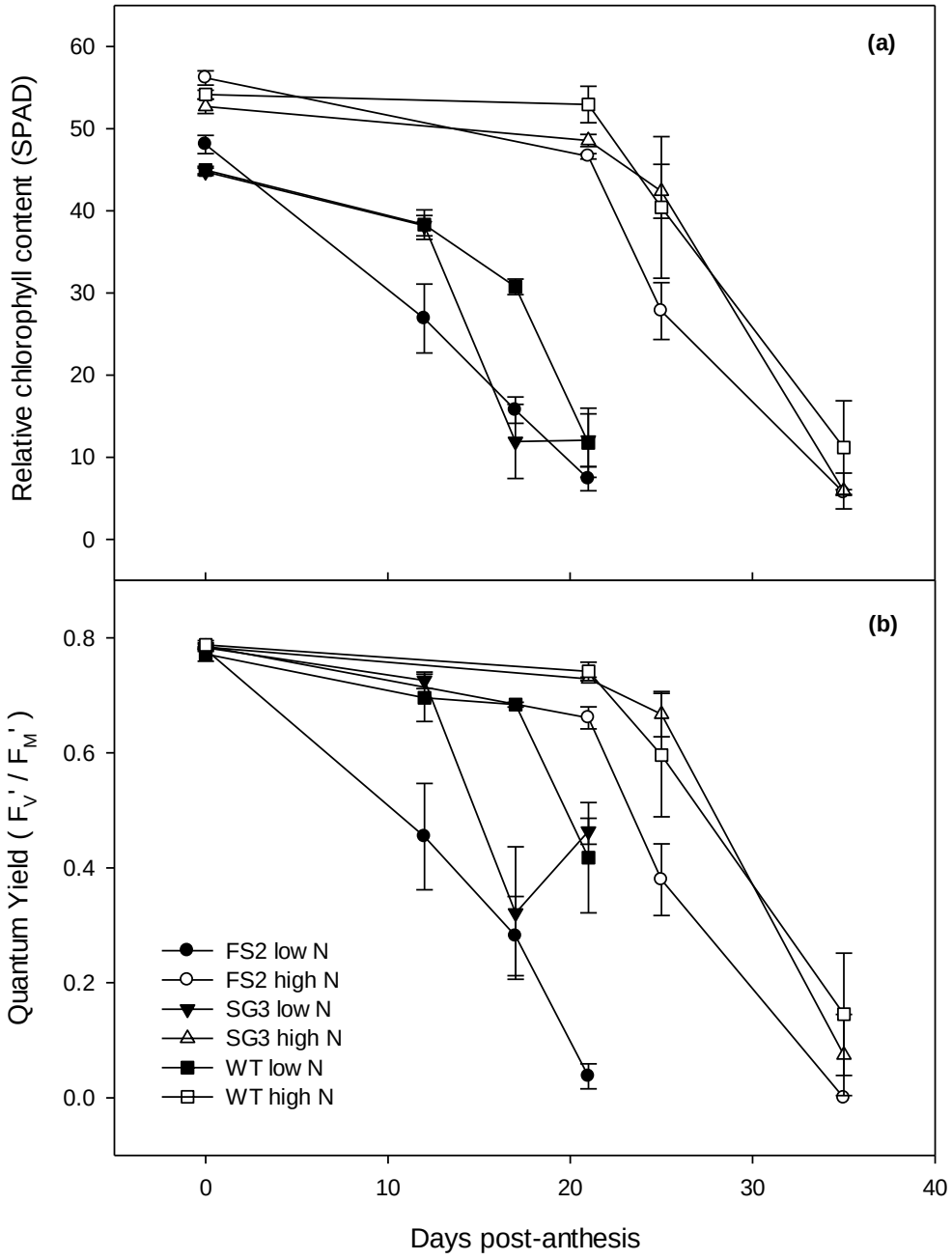

Figure 4.10: The progression of flag leaf senescence in selected mutant wheat lines grown under high and low nitrogen nutrition (open and closed symbols respectively). **(a)** Relative chlorophyll content as determined with a SPAD meter. LSD = 8.457. **(b)** Quantum yield (F_V'/F_M'), as determined by a handheld chlorophyll fluorescence meter, which is a measurement of photosystem II maximum efficiency. LSD = 0.1560. Data are means ± SE of four replicate pots (five plants/pot).

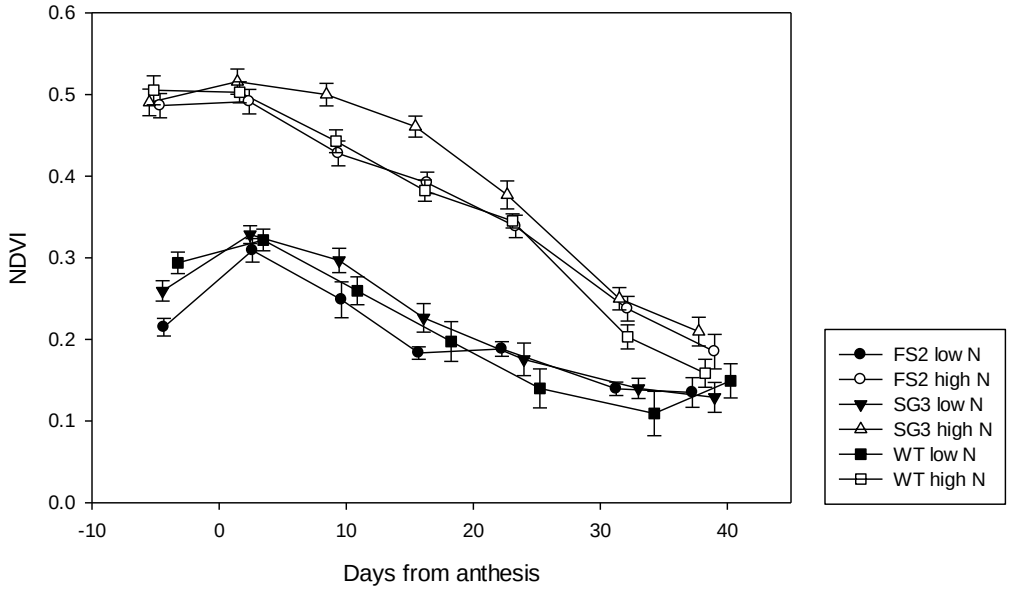

Figure 4.11: Progression of senescence of whole pots of selected mutant wheat lines grown under high and low nitrogen nutrition (open and closed symbols respectively). Measurements were done with a Crop Canopy Sensor. Measurements were done once a week; the graph is corrected for the different anthesis dates of the pots. NDVI = Normalised Difference Vegetation Index. LSD = 0.0714. Data are means ± SE of four replicate pots (five plants/pot). Figure from Derkx et al. (2012).

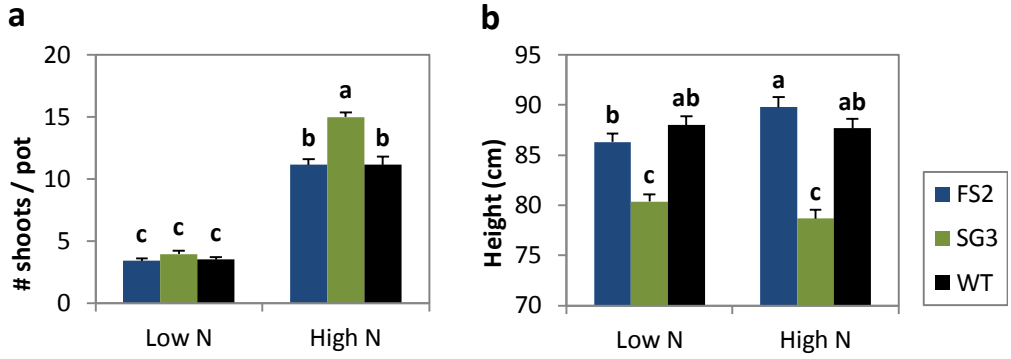

Figure 4.12: The number of shoots per pot (a) and the height in cm (b) of selected mutant wheat lines grown under low and high nitrogen nutrition. Data are means + SE of four replicate pots (five plants/pot). Letters indicate significant differences at the 0.05 level as determined by the LSD. Panel (a) was adapted from Derkx et al. (2012).

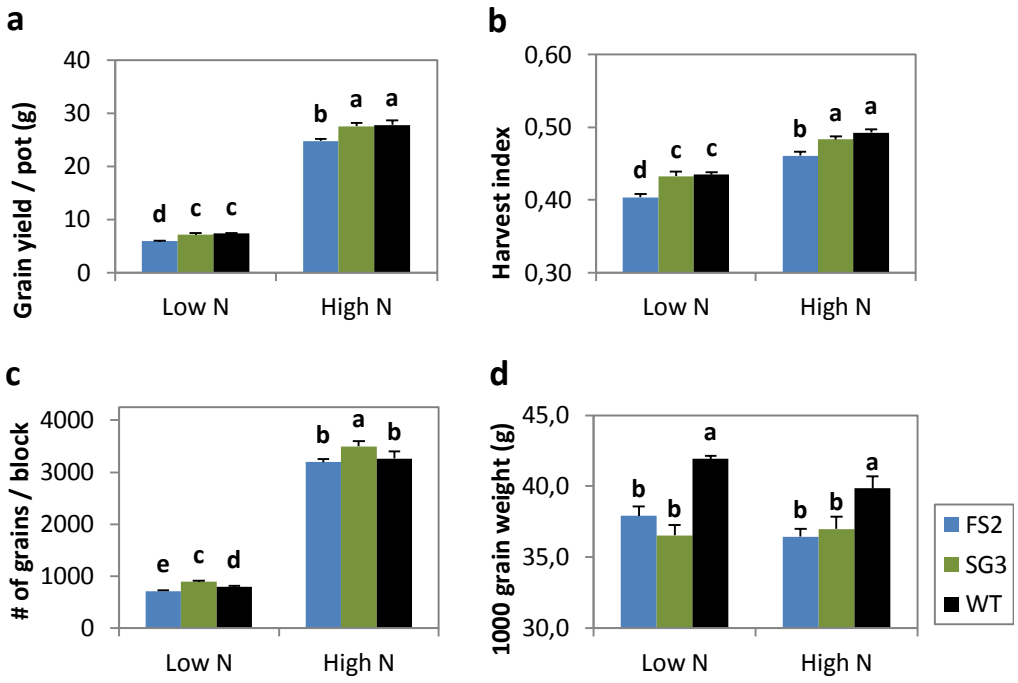

Figure 4.13: Yield parameters of selected mutant wheat lines grown under low and high nitrogen nutrition. (a) Grain yield (g) per pot (five plants/pot). Data are means + SE of 20 replicate pots (five plants/pot). **(b)** Harvest Index. Data are means + SE of 20 replicate pots (five plants/pot). **(c)** Number of grains per 25 plants. Data are means + SE of four replicate blocks. **(d)** Thousand Grain Weight (g). Data are means + SE of four replicate blocks. Letters indicate significant differences at the 0.05 level as determined by using the LSD. Figure adapted from Derkx et al. (2012).

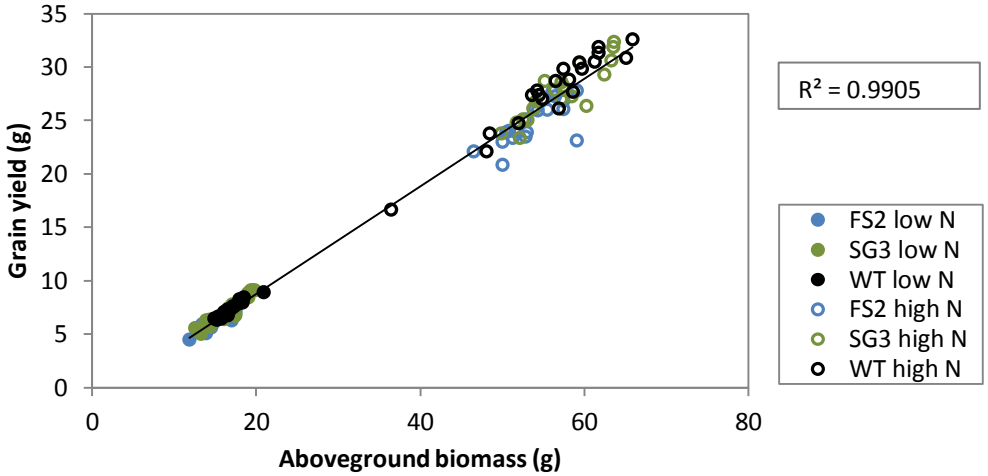

Figure 4.14: Relationship between aboveground biomass with grain yield of selected mutant wheat lines grown under low and high nitrogen nutrition. Data points correspond to the biomass and grain yield of all 120 pots (five plants/pot). $y = 0.5033x - 1.2802$; $R^2 = 0.9905$, $P<0.001$.

4.4.3 Yield Characteristics

Grain yield was significantly different between lines and nitrogen levels (both $P<0.001$) but there was no interaction. Yield under low N nutrition was about a fifth of that under high N. FS2 had a significantly lower grain yield than SG3 and WT under both N conditions (Figure 4.13.a), suggesting early senescence resulted in lower grain yields. The harvest index showed a similar pattern (Figure 4.13.b).

Under optimal conditions WT had the lowest thousand grain weight (TGW) (Figure 4.3.b). Yet in this experiment wild-type had a significantly higher TGW under both N levels ($P<0.001$; Figure 4.13.d). The grain number of SG3 was significantly higher than that of WT, whilst the grain number of FS2 was significantly lower than that of WT (Figure 4.13.c; $P<0.001$). So in this experiment lines SG3 and WT had similar grain yields, but their grain yields were driven by different yield components: grain number and TGW respectively. Another important factor appeared to be total biomass, which was strongly correlated with grain yield (Figure 4.14; $P<0.001$).

4.4.4 Biomass Accumulation and Allocation

Plants grown under low N accumulated significantly less biomass than plants grown under high N conditions (Figure 4.15; $P<0.001$). Not only had plants already a lower biomass at anthesis under low N supply, but because all the leaves of these plants were almost completely senesced at 21 dpa (Figure 4.10), there was little photosynthetic production to sustain plant growth. Therefore the post-anthesis biomass gain of low N plants was significantly smaller than that of high N plants (Figure 4.21.a; $P<0.05$).

Under low N nutrition there were no significant differences in biomass of the main shoot between the lines. WT shoots gained more biomass in the first two weeks post-anthesis, but lines FS2 and SG3 made up this difference later. Under high N, WT shoots accumulated significantly more biomass than lines FS2 and SG3 (Figure 4.15). FS2 probably had a lower biomass because of its

accelerated senescence, whilst in the case of SG3 its lower biomass could be explained by its limited height (Figure 4.12.b). There were no significant differences between the lines in absolute and relative post-anthesis biomass gains; although FS2 added the least biomass under both N levels (Figure 4.21).

Any increase in total biomass between anthesis and maturity is generally attributable to grain-filling since other plant tissues generally lose biomass. Indeed the patterns of ear and total biomass development were very similar (Figures 4.15, 4.16.a and 4.21.a). However, when looking at the relative size of the ear, hence correcting for differences in size, SG3 had the biggest ears under both nitrogen levels (Figure 4.16.b; $P<0.001$), and the post-anthesis biomass gain of the ears was similar to that of WT (Figure 4.21). For its size FS2 had proportionally small ears, especially under high N when it did not outperform plants grown under a low nitrogen regime (Figure 4.16.b). The post-anthesis biomass gain of the ear of FS2 was low as well (Figure 4.21.b).

The flag leaf biomass of plants grown at high N was significantly higher than that of plants grown at low N (Figure 4.17.a; $P<0.001$), but there were no significant differences between the lines. The change in flag leaf biomass also only differed between N levels ($P<0.01$) and not between lines (Figure 4.21). However, there were significant differences in relative flag leaf biomass between the lines and also significant interactions with both nitrogen and time (all $P<0.001$). At high N, SG3 had allocated about twice as much of its biomass to the flag leaf as WT at anthesis, and although the proportion dropped, it stayed the highest throughout development (Figure 4.17.b). At low N, all lines started with equal dry mass allocations to the flag leaf, but at maturity FS2 retained more dry mass in the flag leaf than the other lines, both in absolute and relative terms (Figures 4.17 and 4.21).

The situation was quite different for the other leaves (Figure 4.18). There were highly significant differences ($P<0.001$) between lines and N levels and these factors interacted (also with time). At anthesis, the plants grown under

high N had significantly higher leaf biomass, while at maturity the relative leaf biomass was determined by line and not N level (Figure 4.18.b). Lower leaves of SG3 had a significantly lower dry weight than FS2 and WT under both nitrogen levels, both in absolute and relative terms (Figure 4.18), which is in contrast to the findings for the flag leaf, especially at high N (Figure 4.17). However, the relative change in leaf biomass of SG3 was similar to that of WT (Figure 4.21.b). FS2 had significantly higher leaf dry mass at maturity at both high and low N (Figure 4.18), losing relatively little leaf biomass post-anthesis (Figure 4.21.b; $P<0.05$), which indicates that fast senescence was not related to leaf biomass. Under high N nutrition WT had a high leaf biomass at anthesis, but this was already reduced to average by 21 dpa (Figure 4.18.a). Its post-anthesis biomass change was therefore significantly greater (Figure 4.21.a; $P<0.05$)

The stem was the only vegetative tissue that first increased in biomass before decreasing again to get back to roughly the original biomass levels at maturity, and this process was clearly related to the developmental stage, as the stem biomass of fast-senescing low N plants was already going down as that of high N plants was still increasing (Figure 4.19). This indicates the stem functioned as a temporary storage tissue. WT had significantly higher stem biomass than SG3 throughout development (Figure 4.19.a). Low N plants had relatively more biomass allocated to stems than plants grown under high N (Figure 4.19.b; $P<0.001$).

At high N, the sheath biomass of SG3 was significantly lower than that of FS2 and wild-type throughout development (Figure 4.20.a). Yet for relative sheath dry weight the main difference was found at maturity between N levels: the low N plants retained significantly more sheath dry weight than plants grown under high N conditions (Figure 4.20.b). The sheath biomass of WT at high N was high at anthesis but average at maturity (Figure 20.a) and therefore showed the largest decrease (Figure 4.21.a; $P<0.05$).

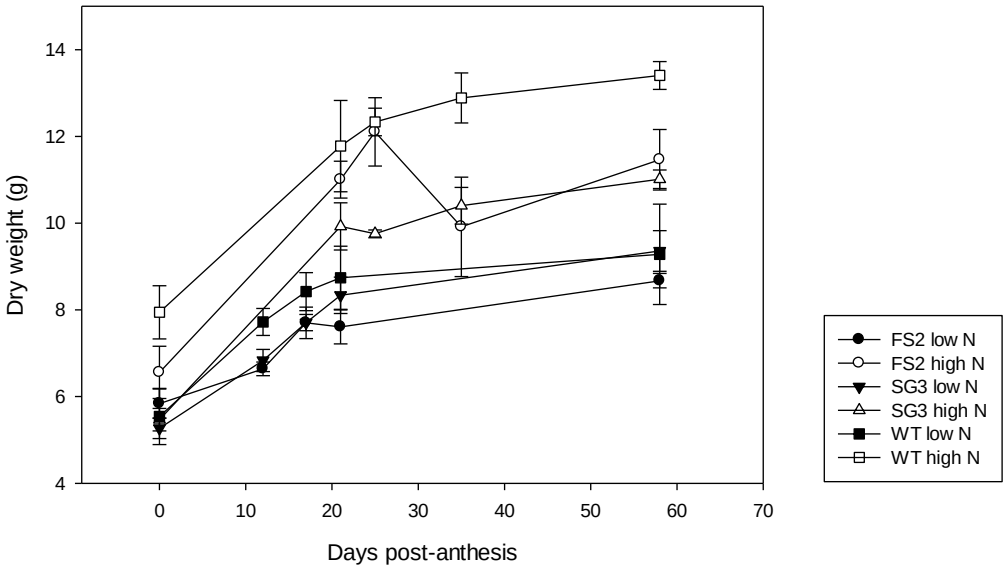

Figure 4.15: Post-anthesis dry weight (g) development of two main shoots of selected mutant wheat lines grown under high and low nitrogen nutrition (open and closed symbols respectively). LSD = 1.522. Data are means ± SE of four replicate pots (five plants/pot) of which two main shoots were harvested.

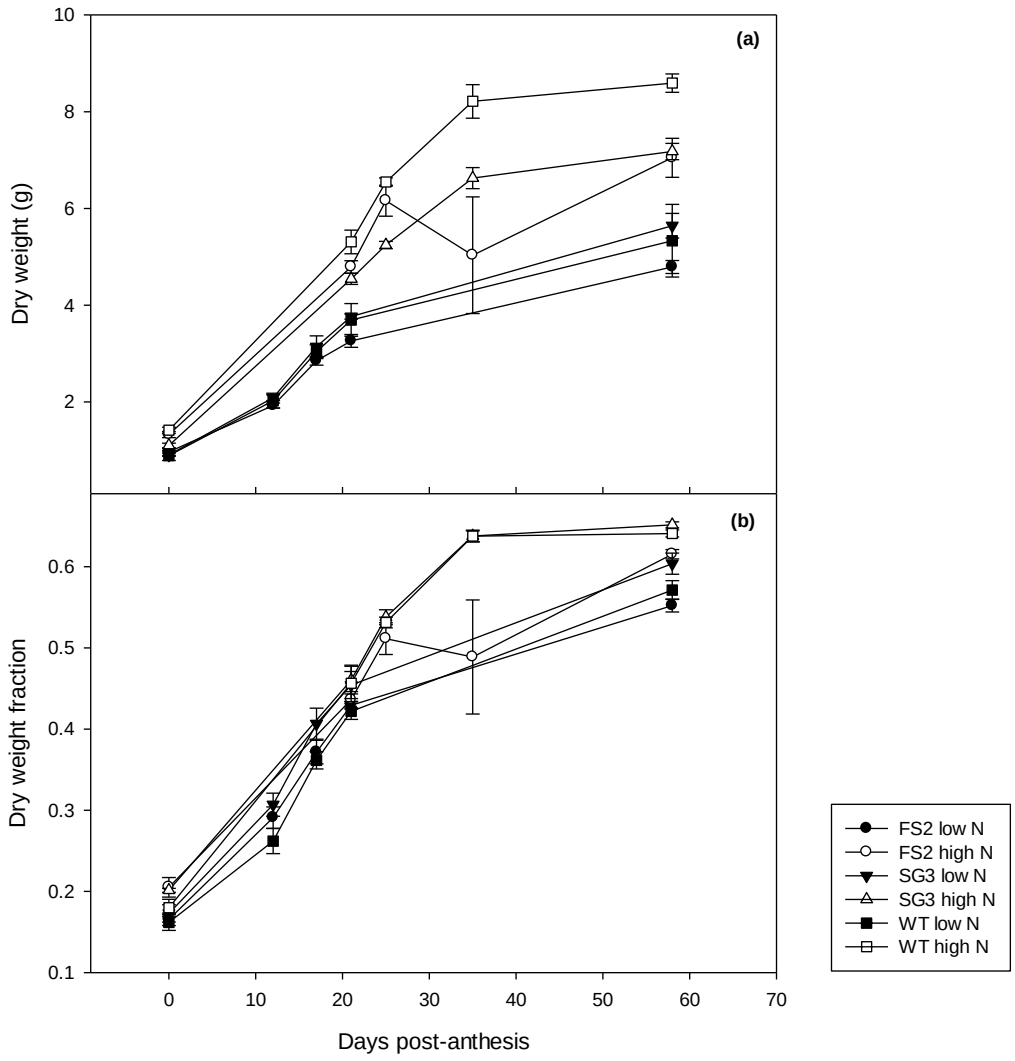

Figure 4.16: Post-anthesis ear dry weight development of main shoots of selected mutant wheat lines grown under high and low nitrogen nutrition (open and closed symbols respectively). **(a)** Absolute dry weight (g). LSD = 0.8837. **(b**) Dry weight as fraction of total shoot dry weight. LSD = 0.04586. The ear consists of the developing grain and surrounding tissues (chaff). Data are means ± SE of four replicate pots (five plants/pot) of which two main shoots were harvested.

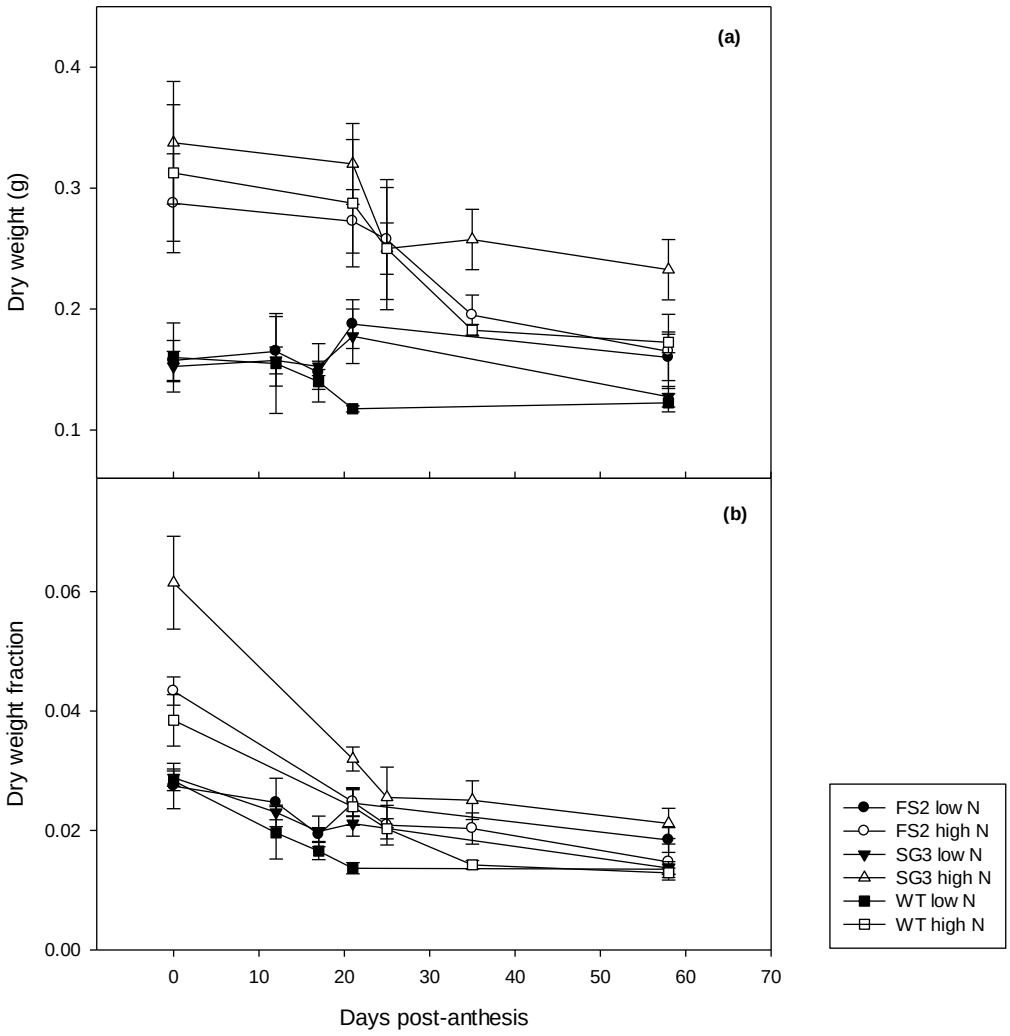

Figure 4.17: Post-anthesis flag leaf dry weight development of main shoots of selected mutant wheat lines grown under high and low nitrogen nutrition (open and closed symbols respectively). **(a)** Absolute dry weight (g). LSD = 0.07824. **(b**) Dry weight as fraction of total shoot dry weight. LSD = 0.007937. Data are means ± SE of four replicate pots (five plants/pot) of which two main shoots were harvested.

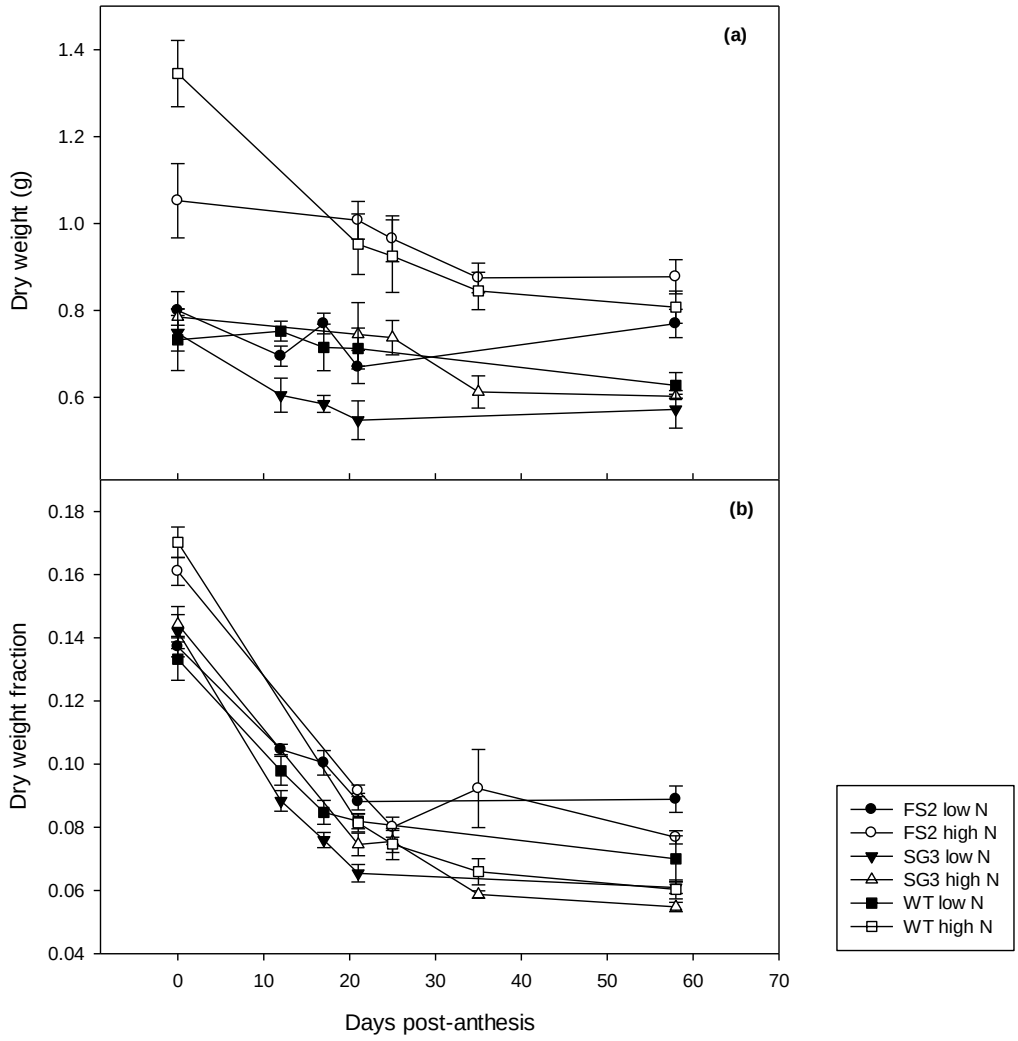

Figure 4.18: Post-anthesis dry weight development of the lower leaves of main shoots of selected mutant wheat lines grown under high and low nitrogen nutrition (open and closed symbols respectively). **(a)** Absolute dry weight (g). LSD = 0.1291. **(b**) Dry weight as fraction of total shoot dry weight. LSD = 0.01237. Fraction includes all leaves except the flag leaf. Data are means ± SE of four replicate pots (five plants/pot) of which two main shoots were harvested.

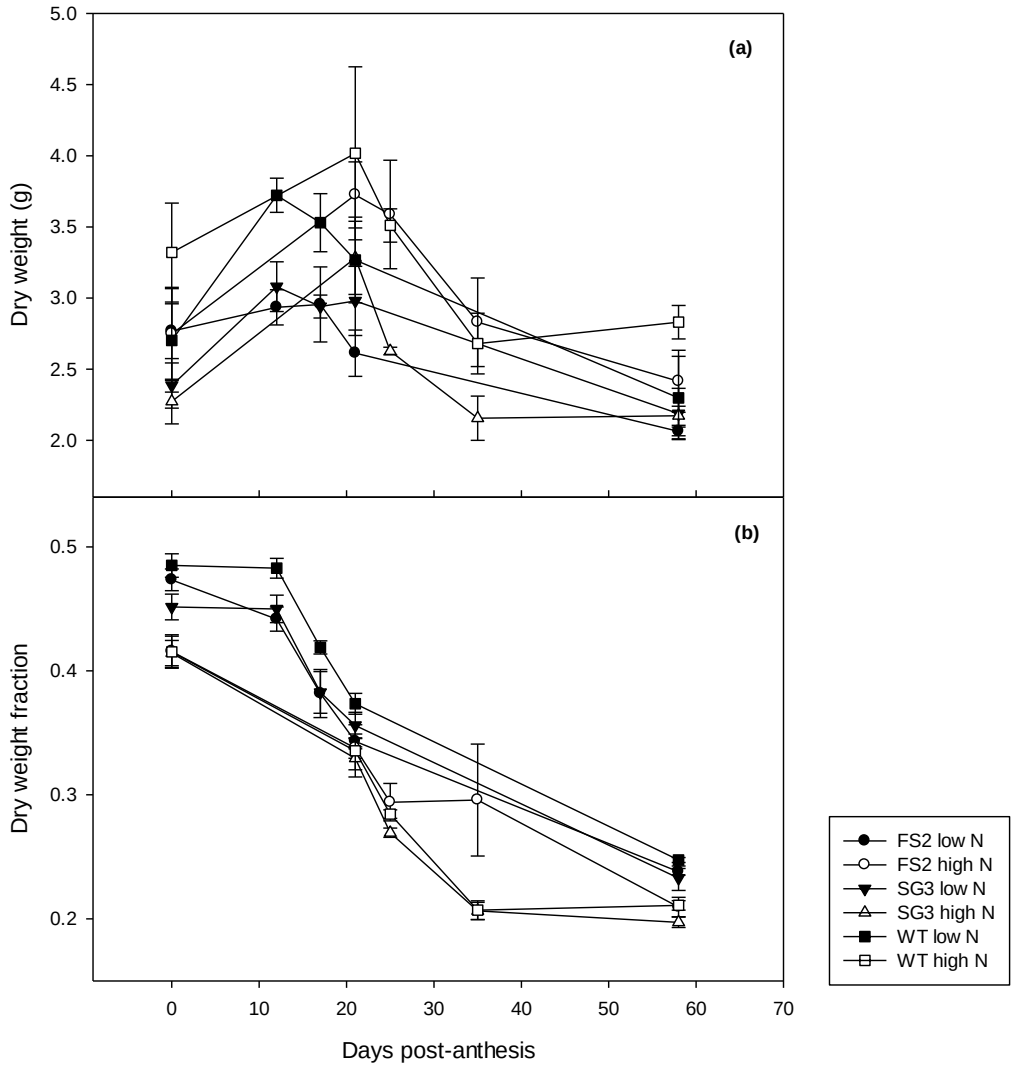

Figure 4.19: Post-anthesis stem dry weight development of main shoots of selected mutant wheat lines grown under high and low nitrogen nutrition (open and closed symbols respectively). **(a)** Absolute dry weight (g). LSD = 0.6372. **(b**) Dry weight as fraction of total shoot dry weight. LSD = 0.03337. Data are means ± SE of four replicate pots (five plants/pot) of which two main shoots were harvested.

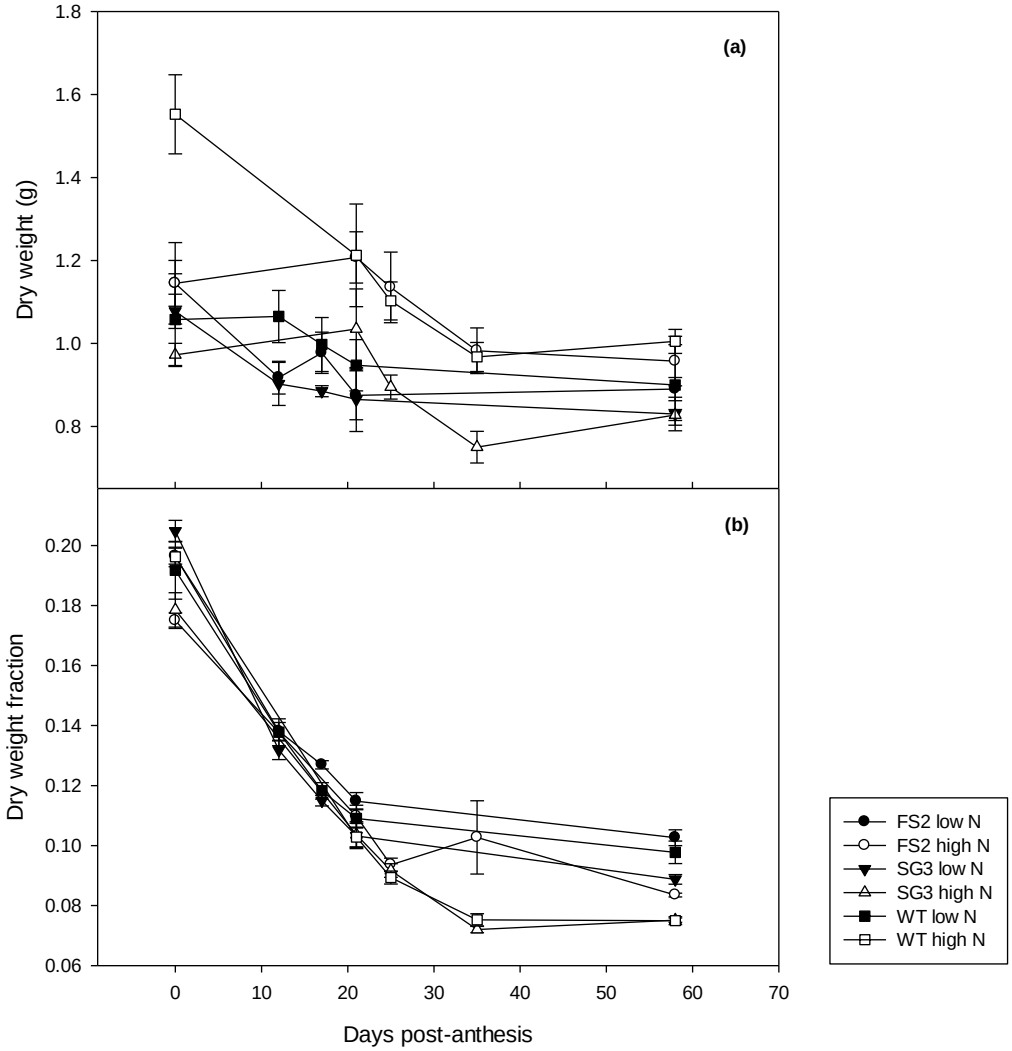

Figure 4.20: Post-anthesis sheath dry weight development of main shoots of selected mutant wheat lines grown under high and low nitrogen nutrition (open and closed symbols respectively). **(a)** Absolute dry weight (g). LSD = 0.1724. **(b**) Dry weight as fraction of total shoot dry weight. LSD = 0.01133. Data are means ± SE of four replicate pots (five plants/pot) of which two main shoots were harvested.

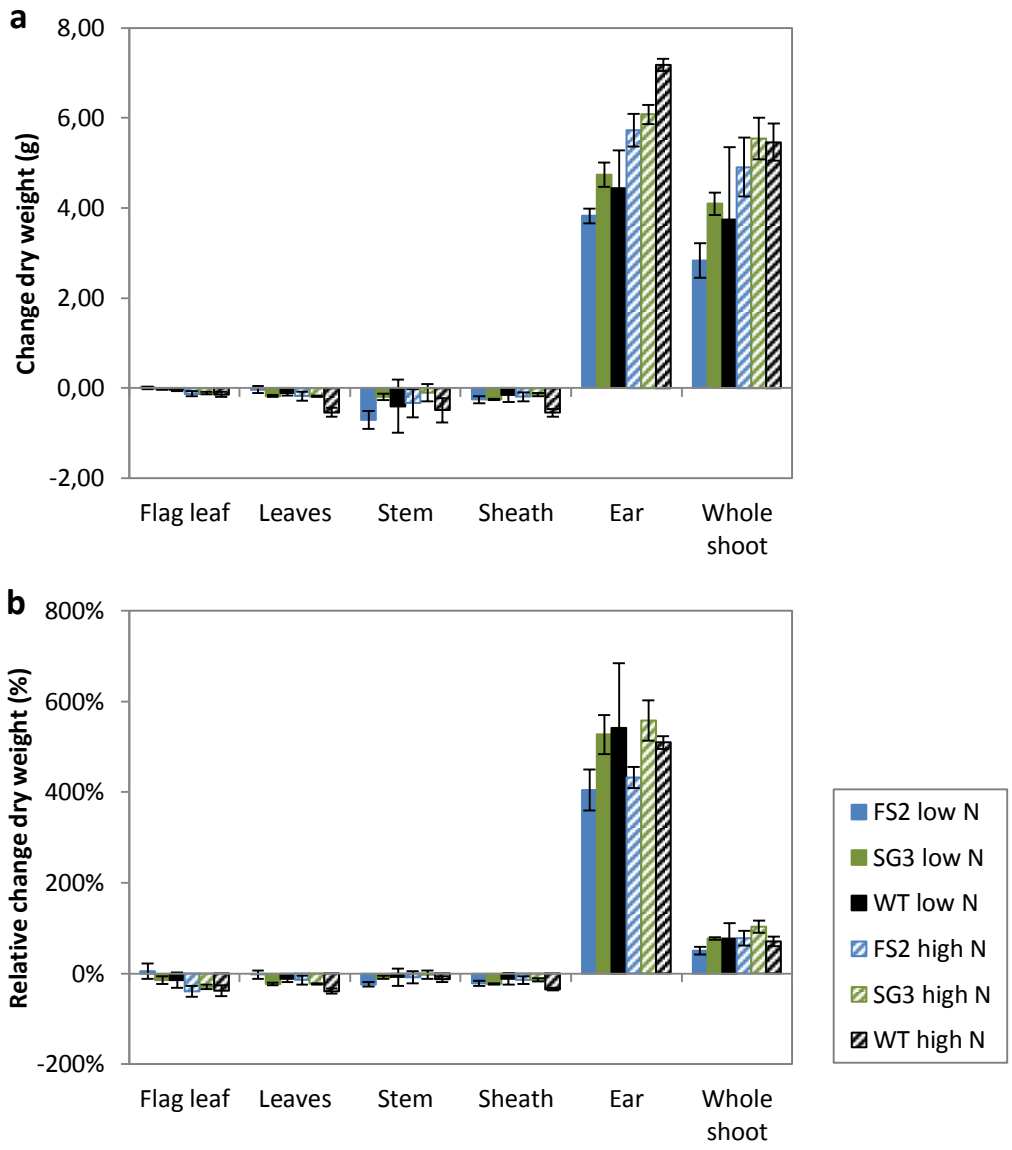

Figure 4.21: Absolute (a) and relative (b) post-anthesis change in dry weight of tissues of main shoots of selected mutant wheat lines grown under high and low nitrogen nutrition. LSDs (a and b respectively): FL = 0.121 and 40.24%, L = 0.201 and 18.98%, St = 0.911 and 32.93%, Sh = 0.260 and 21.16%, E = 1.232 and 198.55%, WS = 2.387 and 51.77%. The ear consists of the developing grain and surrounding tissues (chaff). Data are means ± SE of four replicate pots per time point (five plants/pot) of which two main shoots were harvested.

4.4.5 Nitrogen Accumulation and Allocation

The nitrogen concentration of the total grain differed significantly between lines and between N levels ($P<0.001$). The N concentration in grain of WT was significantly lower than that of the other two lines, while as one would expect the N concentration was higher in the plants supplied with more nitrogen (Figure 4.22.a). For grain total nitrogen content there was a significant interaction between N level and line ($P<0.05$). While there was no difference in grain N content between the lines grown at low N, SG3 had a higher grain nitrogen content at high N nutrition (Figure 4.22.b). The difference between N levels was 4- to 5-fold and highly significant ($P<0.001$).

Grain N concentration did not correlate significantly with grain yield at either N level (Figure 4.23) However, for similar grain yields SG3 reached higher and WT lower grain N concentrations than average at both N levels (Figure 4.23).

The results for grain N were somewhat different for the grain from just the main shoots. As expected, the high N plants had a significantly higher grain N concentration ($P<0.001$; Figure 4.24.b). However, grain total N content of SG3 at high N was significantly lower for the main shoots ($P<0.05$; Figure 4.25.b) compared to a higher total N content in total grain (Figure 4.22.b). This discrepancy can be explained by the fact that SG3 had relatively small ears (Figure 4.16.a), so individual ears will have a lower N content because the dry weight was lower, but the larger number of ears resulted in a high total grain yield (Figures 4.12.a and 4.13.a) and therefore a high grain total N content.

On the other hand, because SG3 had shorter shoots (Figure 4.12.b), its nitrogen harvest index (NHI) was not lower than that of WT, while the NHI of FS2 was significantly lower at both N levels (Figure 4.26; $P<0.01$). SG3 was the only line maintaining its NHI at low N, while the NHI of FS2 and WT were significantly lower at low N (Figure 4.26; $P<0.01$).

All other tissues showed highly significant differences in nitrogen concentration and total N content between N levels (low N < high N) and between anthesis and maturity, as well as a highly significant interaction between the two (all P<0.001; Figures 4.24.a, 4.24.b and 4.25). The absolute change between plants grown at high and low N was also significantly different (Figures 4.24.c and 4.27.a). So plants grown at high nitrogen remobilised more N from all vegetative tissues, presumably to the grain.

The flag leaves and sheaths of FS2 had a significantly higher N concentration than those of SG3 and wild-type (Figures 4.24.a and 4.24.b; P<0.001). The lower leaves and stem showed a similar trend but the difference between lines was not significant. The decrease in nitrogen concentration of these four tissues only differed significantly between N levels (P<0.001) but not lines (Figure 4.24.c), suggesting that the post-anthesis decrease in N concentration was 'set' and that the differences in N concentration between lines at maturity were determined by the starting nitrogen concentration at anthesis.

For the lower leaves there was a clear difference in total nitrogen content between the lines at different N levels and times (P=0.018). At low N the lines showed no difference at anthesis, but at maturity the total N content of FS2 was significantly higher. At anthesis under high N conditions SG3 had a significantly lower total N content than FS2, which had a significantly lower N content than wild-type, while at maturity there was no difference. In fact there were no differences between the plants grown at different N levels at maturity, and this was also the case for the flag leaf total N content (Figure 4.25; P<0.001). Consequently, plants grown at high nitrogen remobilised more N from all leaves (Figure 4.27.a). This was also the case for the relative decrease, but FS2 remobilised significantly less N from all leaves than SG3 and wild-type (Figure 4.27.b; P<0.001).

The total N contents in stems and sheath of SG3 were significantly lower than that of FS2 and WT at anthesis but not at maturity (Figure 4.25; P<0.01),

meaning that the total remobilisation of N from these tissues was significantly lower too (Figure 4.27.a; P<0.01). However, this must have been influenced by the small size of SG3 since the relative change in total N content was not different between the lines (Figure 4.27.b). The relative change in total N content was significantly different between plants grown at different N levels in sheaths but not in stems (Figure 4.27.b).

At anthesis at high N FS2 had a significantly higher ear nitrogen concentration than wild-type, which in turn had a higher N concentration than SG3 (Figure 4.24.a; P=0.035). There was no difference between the lines grown at low N. At maturity there were significant differences, but not within a line or N level (Figure 4.24.b). The decrease in N concentration of SG3 at high N was lower than the decrease in FS2 and wild-type, while the change in plants grown at low N was even smaller but there was no difference between the lines (Figure 4.24.c; P=0.017)). The total N content of SG3 at high N was lower at anthesis, while at high N there was no difference (Figure 4.25). The results for total N content (change) were comparable and significant (Figures 4.25 and 4.27.a). There were no significant differences in the relative change in N content (Figure 4.27.b).

The total N content of the whole shoot (sum of all tissues) increased between anthesis and maturity (Figure 4.27.c; P<0.001). At low N there were no differences between the lines, while at high N SG3 had a lower total N content than FS2 and wild-type (Figure 4.25; P<0.001). There was no significant difference in either the absolute or relative change between either lines or N levels (Figure 4.27.c and d), suggesting that post-anthesis N uptake was comparable as well. However, it must be noted that no nitrogen was applied post-anthesis, so at this stage the high N plants might not have had access to more N than the low N plants.

Most nitrogen, between 77.7 and 88.0%, ended up in the grain (Figure 4.28.b). FS2 was less able to use the nitrogen available in the shoot for grain-

filling at both N levels (P<0.001). At low N SG3 and WT allocated the same proportion of nitrogen to the grain, while at high N wild-type allocated more to the grain than SG3 (P<0.01). SG3 was the only line in which the proportion of N allocated to the grain was not significantly lower at low N compared to high N supply (P<0.01).

As a result of grain growth, all other tissues showed a highly significant decrease in proportion of N allocated to them (Figure 4.28; P<0.001). Flag leaf, other leaves, stem and ear all showed a significant interaction between N level and time (P<0.01): plants grown at high N supply had allocated significantly more N to leaves and flag leaf and less to stem and ear at anthesis than plants grown at low N, while there was no difference at maturity. The N allocated to sheaths only differed between lines: SG3 invested relatively less N in sheaths than FS2 (P<0.001).

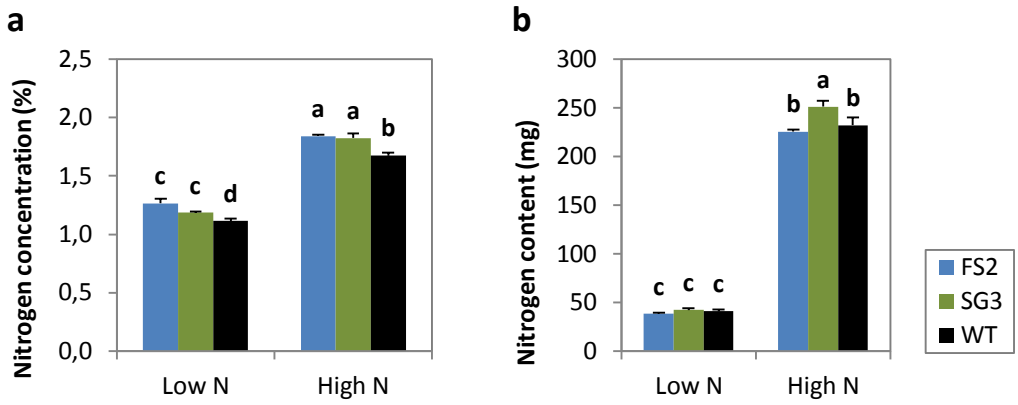

Figure 4.22: Total grain nitrogen concentration (a) and total grain nitrogen content (b) of selected mutant wheat lines grown under high and low nitrogen nutrition. Letters indicate significant differences at the 0.05 level as determined using the LSD. Data are means + SE of four replicate blocks (five pots, each containing five plants). Figure adapted from Derkx et al. (2012).

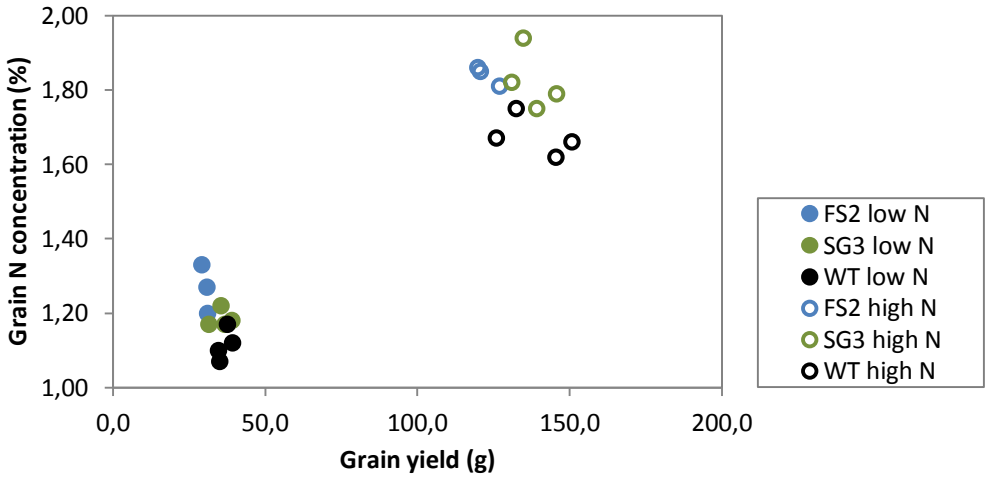

Figure 4.23: Relationship between grain yield and grain nitrogen concentration of selected mutant wheat lines grown under high (dashed line) and low (solid line) nitrogen nutrition. Data points are means per replicate block (five pots, each containing five plants).

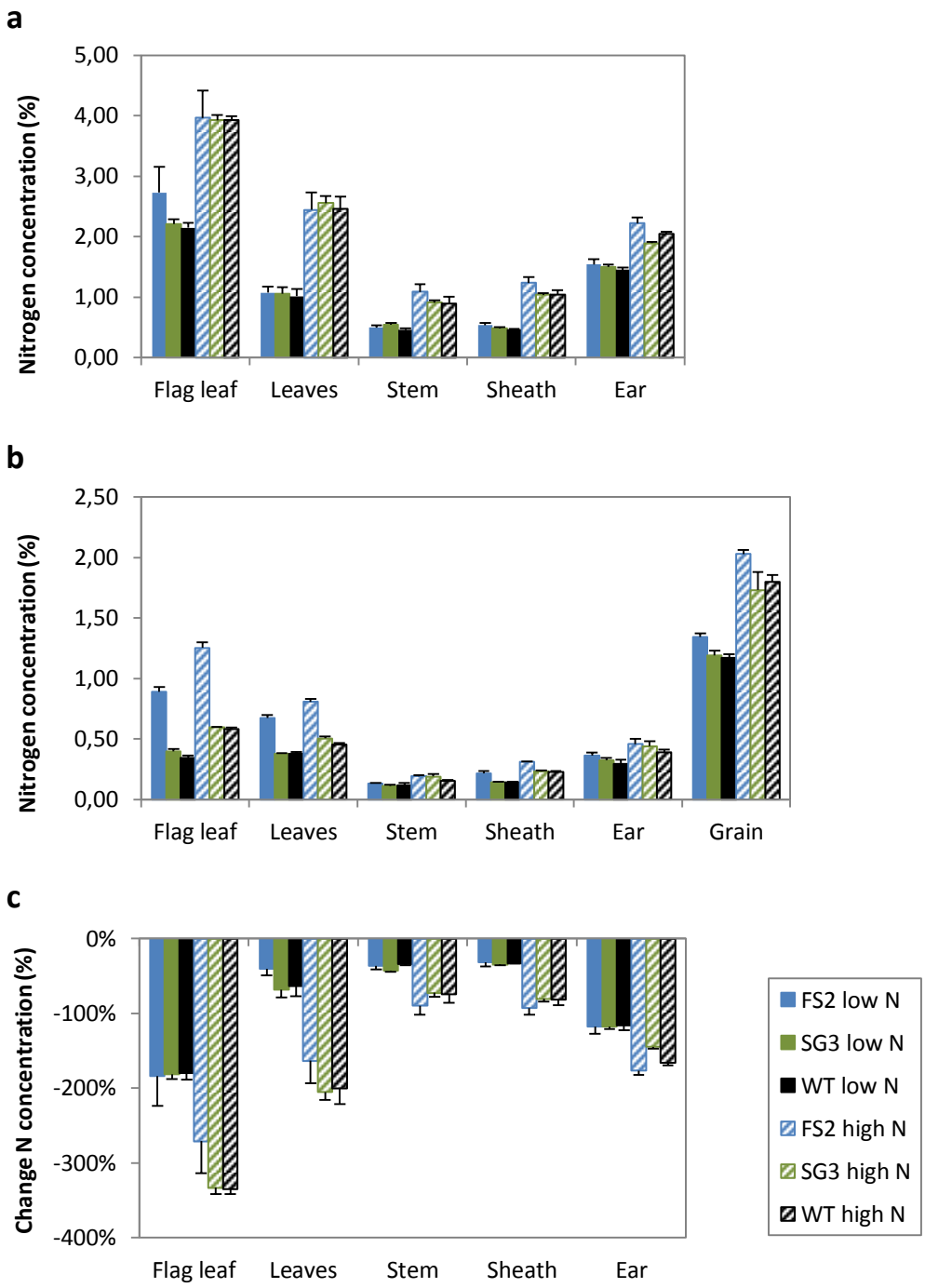

Figure 4.24: Nitrogen concentration (% DM) of tissues of main shoots at anthesis (a) and physiological maturity (b) and the difference in nitrogen concentration between anthesis and maturity (c) of selected mutant wheat lines grown under high and low nitrogen nutrition. LSDs (a/b and c): FL = 0.5010 and 0.6759, L = 0.3345 and 0.4865, St = 0.1417 and 0.2154, Sh = 0.1068 and 0.1691, E = 0.1233 and 0.1515, Gr = 0.1538. Data are means + or - SE of four replicate pots per time point (five plants/pot) of which two main shoots were harvested. Statistical analysis for (a) and (b) was performed per tissue but encompassing both time points.

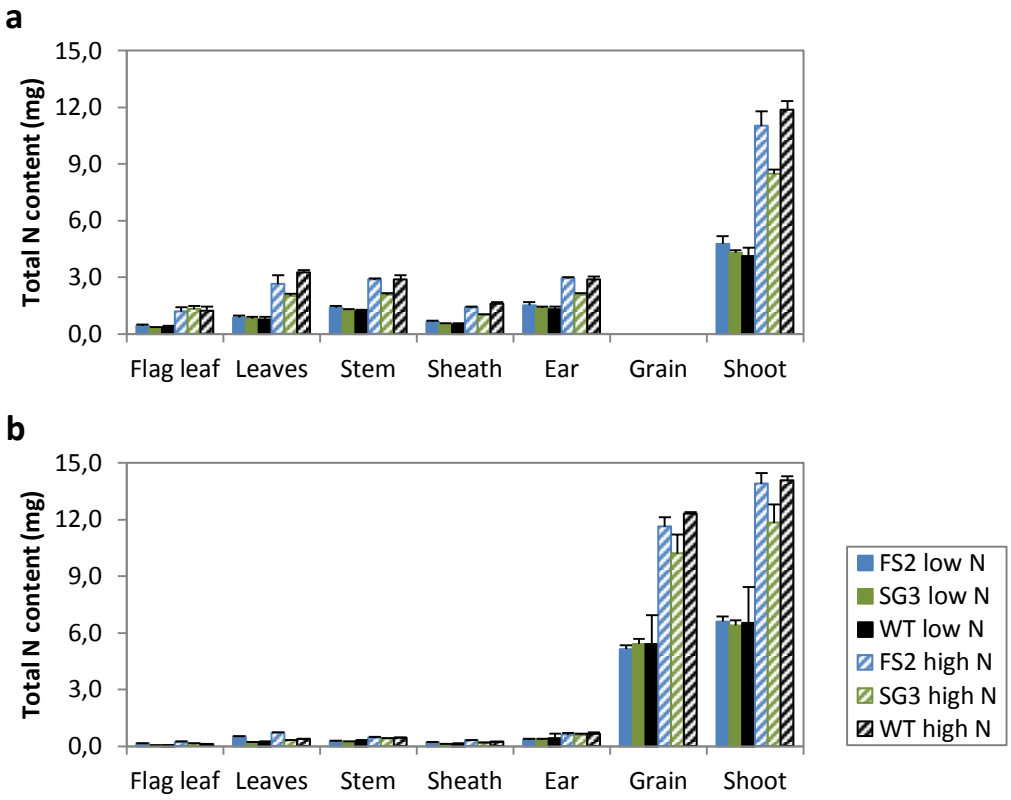

Figure 4.25: Total nitrogen content (mg) of tissues of main shoots at anthesis (a) and physiological maturity (b) of selected mutant wheat lines grown under high and low nitrogen nutrition. Dark colours = low N, light colours = high N. Total N content = dry weight x %N. LSDs: FL = 0.3091, L = 0.4274, St = 0.2474, Sh = 0.1007, E = 0.2967, Gr = 1.3018, whole shoot = 1.4736. Data are means + SE of four replicate pots (five plants/pot) of which two main shoots were harvested. Statistical analysis was performed per tissue but encompassing both time points.

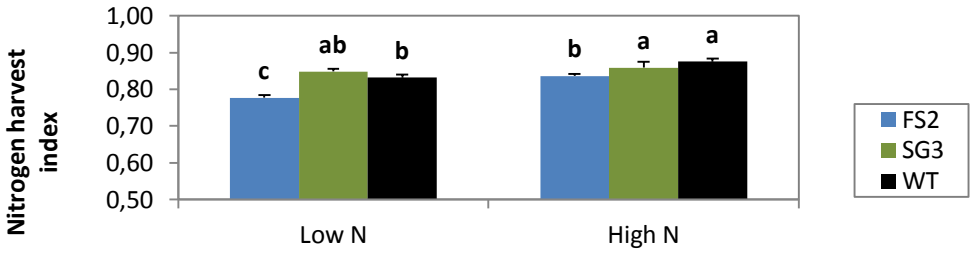

Figure 4.26: Nitrogen Harvest Index (NHI) of main shoots of selected mutant wheat lines grown under high and low nitrogen nutrition. Data are means + SE of four replicate pots (five plants/pot) of which two main shoots were harvested. Letters indicate significant differences at the 0.05 level as determined by using the LSD. Figure adapted from Derkx et al. (2012).

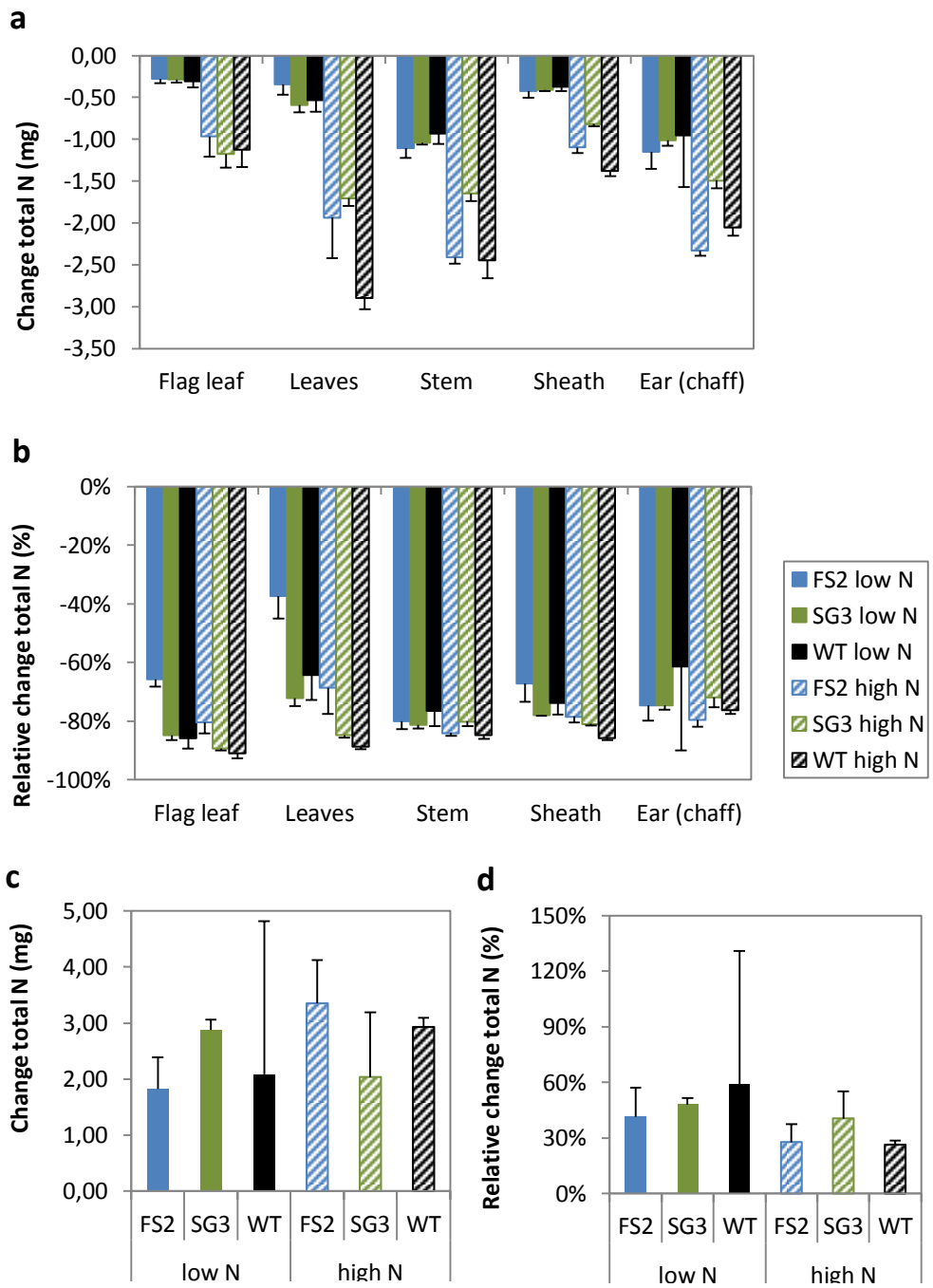

Figure 4.27: Absolute and relative differences in total nitrogen content of tissues (a and b) and the main shoot as a whole (c and d) between anthesis and physiological maturity of selected mutant wheat lines grown under high and low nitrogen nutrition. Total N content = dry weight x %N. LSDs: FL = 0.4285 and 0.0680, L = 0.6200 and 0.1435, St = 0.3728 and 0.0724, Sh = 0.1661 and 0.0910, E = 0.4895 and 0.2053, whole shoot = 2.8041 and 0.5266. Data are means + or - SE of four replicate pots per time point (five plants/pot) of which two main shoots were harvested.

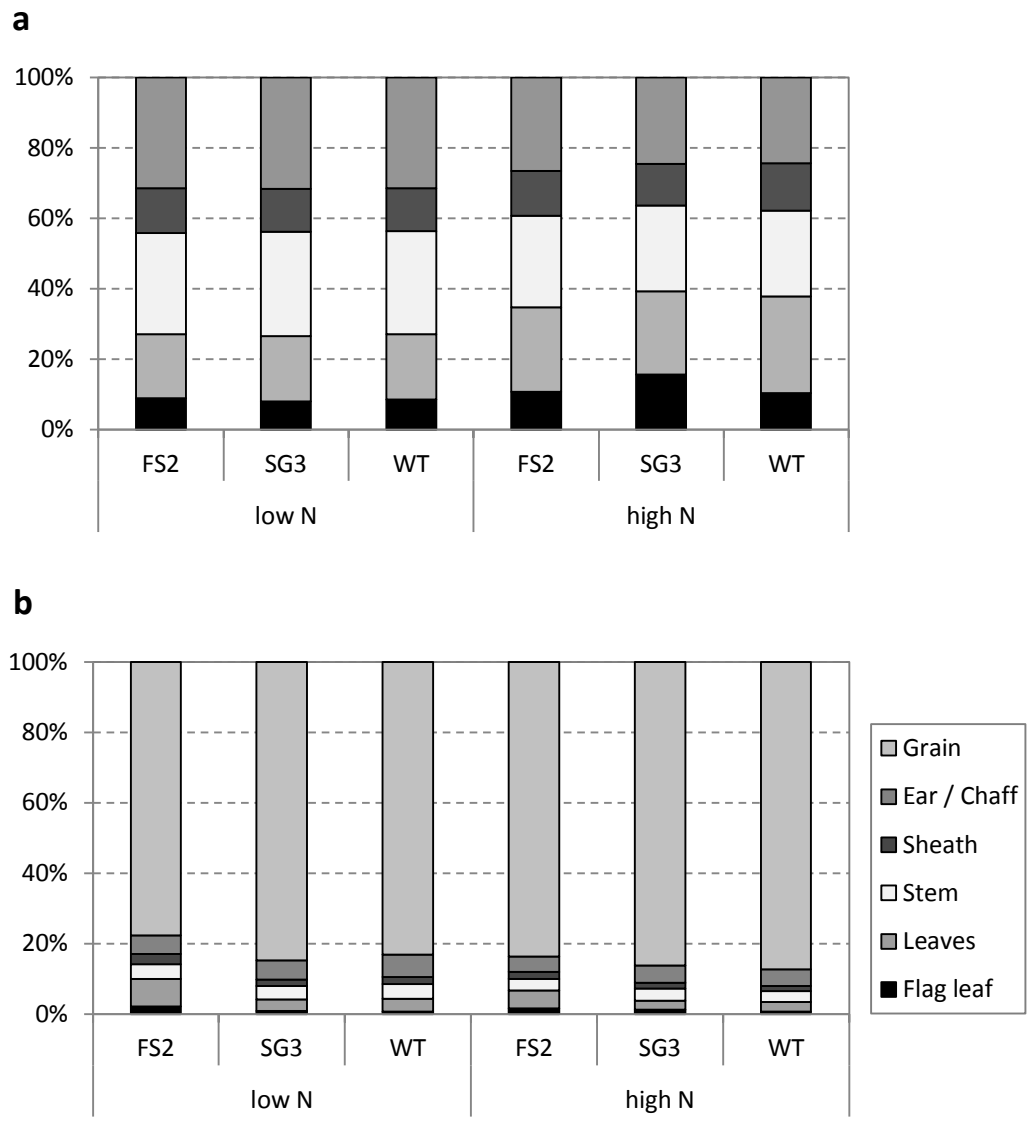

Figure 4.28: Nitrogen distribution between tissues of main shoots at anthesis (a) and maturity (b) of selected mutant wheat lines grown under high and low nitrogen nutrition. LSDs: FL = 2.94%, L = 4.29%, St = 2.24%, Sh = 1.12%, E = 3.65%, Gr = 2.17%. Data are means of four replicate pots (five plants/pot) of which two main shoots were harvested. Statistical analysis was performed per tissue but encompassing both time points. Figure adapted from Derkx et al. (2012).

4.4.6 Biomass and Nitrogen Uptake and Remobilisation

The post-anthesis changes in biomass (C) and N allocation for the main shoot of each line x N level combination are summarised in Table 4.2. SG3 had the greatest post-anthesis biomass gain (uptake) at both N levels and hardly remobilised C, which matched its stay-green phenotype, while FS2 showed the opposite pattern. WT maintained a high C uptake whilst also having a relatively high remobilisation, especially at high N.

WT had the highest post-anthesis N uptake and lowest N remobilisation at low N conditions, while at high N supply the pattern was reversed. SG3 had the highest N uptake and lowest remobilisation at high N, while at low N it had high remobilisation and average uptake. Post-anthesis N uptake of FS2 was low at the low N regime.

When comparing the interactions between shoot biomass (C) and nitrogen content at anthesis, post-anthesis C and N remobilisation and uptake and grain yield and N content, differences between the N levels were observed (Figures 4.29 and 4.30).

At both N levels the amount of nitrogen already accumulated at anthesis was positively correlated with post-anthesis N remobilisation (Figure 4.29.a; $P<0.001$). At low N, N uptake was negatively correlated with N accumulated at anthesis (Figure 4.29.b; $P<0.01$), while there was only a weak relationship at high N. The patterns for biomass were similar (Figure 4.29.c and 4.29.d). So when more C and N had accumulated in the plant at anthesis, more C and N could be remobilised and less would be taken up post-anthesis.

At low N conditions, the grain N content decreased with greater N remobilisation (Figure 4.30.a; n.s.), but was significantly positively correlated with post-anthesis N uptake (Figure 4.30.b; $P<0.001$). Results were similar for biomass: remobilisation showed a significant negative relationship with grain yield (Figure 4.30.c; $P<0.05$) and uptake a significant positive relationship with

grain yield (Figure 4.30.d; P<0.001). These results suggest that at low N supply the plants had not accumulated enough C and N at anthesis to rely on remobilisation for grain-filling and therefore depended on post-anthesis uptake, but concurrently the remobilisation of C and N from the shoot inhibited the post-anthesis uptake of more C and N for grain-filling.

At high N conditions, both greater post-anthesis N remobilisation and N uptake were only weakly associated with higher grain N content (Figure 4.30a and 4.30.b; n.s.). There were also no significant associations between grain yield and either C uptake (photosynthetic production of biomass) or remobilisation (Figure 4.30.c and 4.30.d). Plants with sufficient N available were thus able to use and remobilise C and N from their shoots for grain-filling without critically reducing their N uptake and photosynthetic abilities.

None of the lines strongly deviated from the found relationships and there was a lot of variation within N level x genotype combinations, indicating the relationships were robust and not dependent on plant genotype.

Table 4.2: Biomass and nitrogen content of the main shoot at anthesis and physiological maturity and post-anthesis uptake and remobilisation of selected mutant wheat lines grown under high and low nitrogen nutrition. Data are means of four replicate pots (five plants/pot) of which two main shoots were harvested. A, anthesis; M, physiological maturity; G, grain. Standard errors (SE) of the means of the measured parameters are indicated in parentheses. Since uptake and remobilisation could not be measured because of destructive sampling, but were derived from anthesis and maturity values, SE cannot be given. Table from Derkx et al. (2012).

		Biomass (g)					Nitrogen (mg)				
		Total		Uptake	Grain	Remobilisation	Total		Uptake	Grain	Remobilisation
		A	M	M-A	G	G-(M-A)	A	M	M-A	G	G-(M-A)
Low N	FS2	5.84 *(0.33)*	8.67 *(0.17)*	2.84	3.82 *(0.11)*	0.98	4.78 *(0.39)*	6.60 *(0.26)*	1.82	5.13 *(0.22)*	3.31
	SG3	5.27 *(0.23)*	9.36 *(0.47)*	4.09	4.57 *(0.25)*	0.47	4.31 *(0.11)*	6.39 *(0.28)*	2.08	5.42 *(0.27)*	3.34
	WT	5.54 *(0.65)*	9.28 *(1.16)*	3.74	4.46 *(1.26)*	0.72	4.11 *(0.46)*	6.53 *(1.89)*	2.42	5.41 *(1.51)*	3.00
High N	FS2	6.56 *(0.60)*	11.46 *(0.70)*	4.91	5.74 *(0.34)*	0.83	11.01 *(0.77)*	13.89 *(0.58)*	2.88	11.62 *(0.51)*	8.74
	SG3	5.47 *(0.26)*	11.01 *(0.21)*	5.55	5.87 *(0.12)*	0.32	8.47 *(0.22)*	11.82 *(0.97)*	3.35	10.19 *(1.00)*	6.84
	WT	7.94 *(0.61)*	13.41 *(0.32)*	5.46	6.78 *(0.14)*	1.32	11.86 *(0.45)*	14.06 *(0.22)*	2.20	12.30 *(0.08)*	10.10

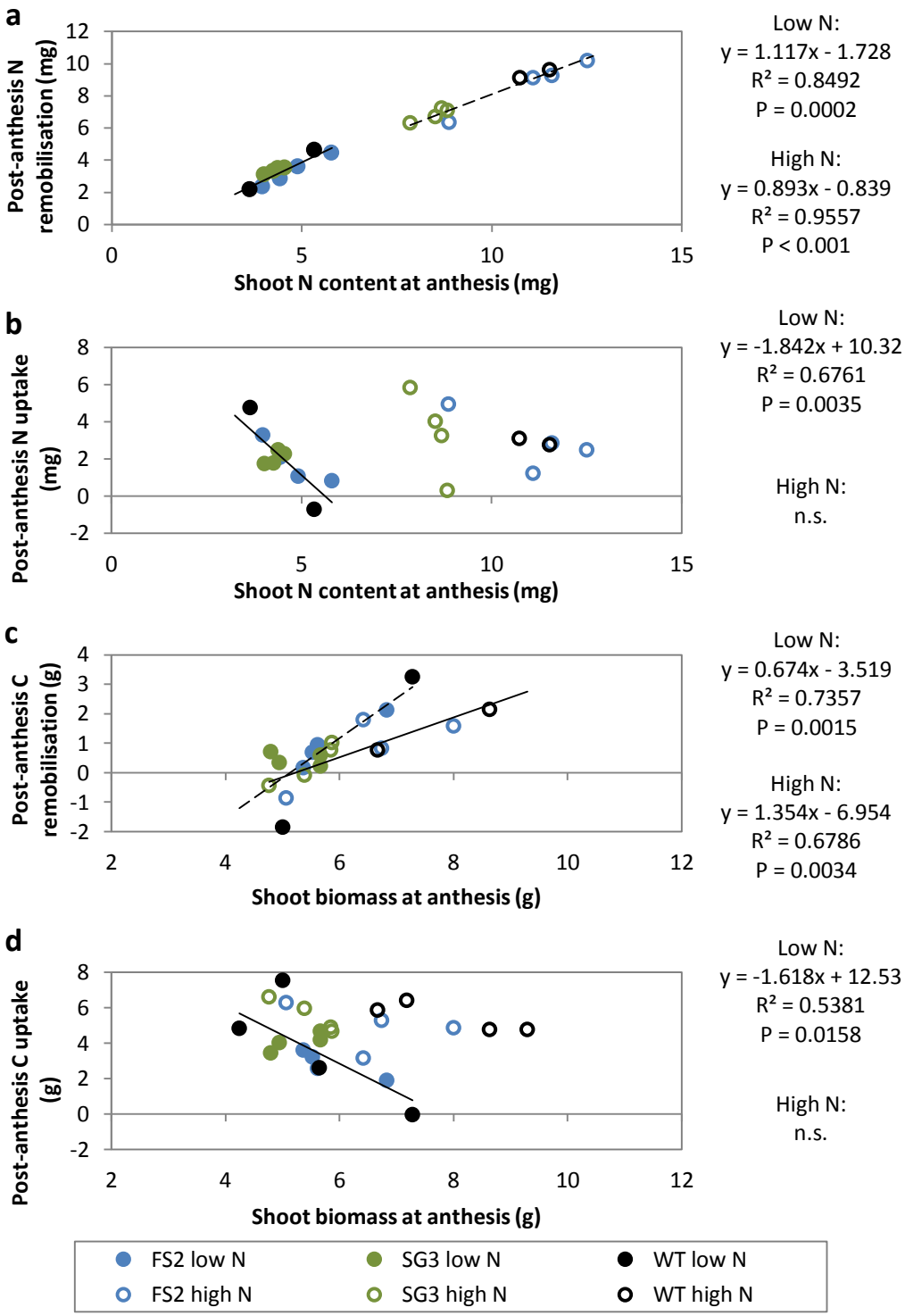

Figure 4.29: Relationships between shoot nitrogen (N) content at anthesis and post-anthesis N remobilisation (a) and N uptake (b), and between shoot biomass (C) at anthesis and post-anthesis C remobilisation (c) and C uptake (d) of selected mutant wheat lines grown under high (dashed line) and low (solid line) nitrogen nutrition. Data points are means per replicate block.

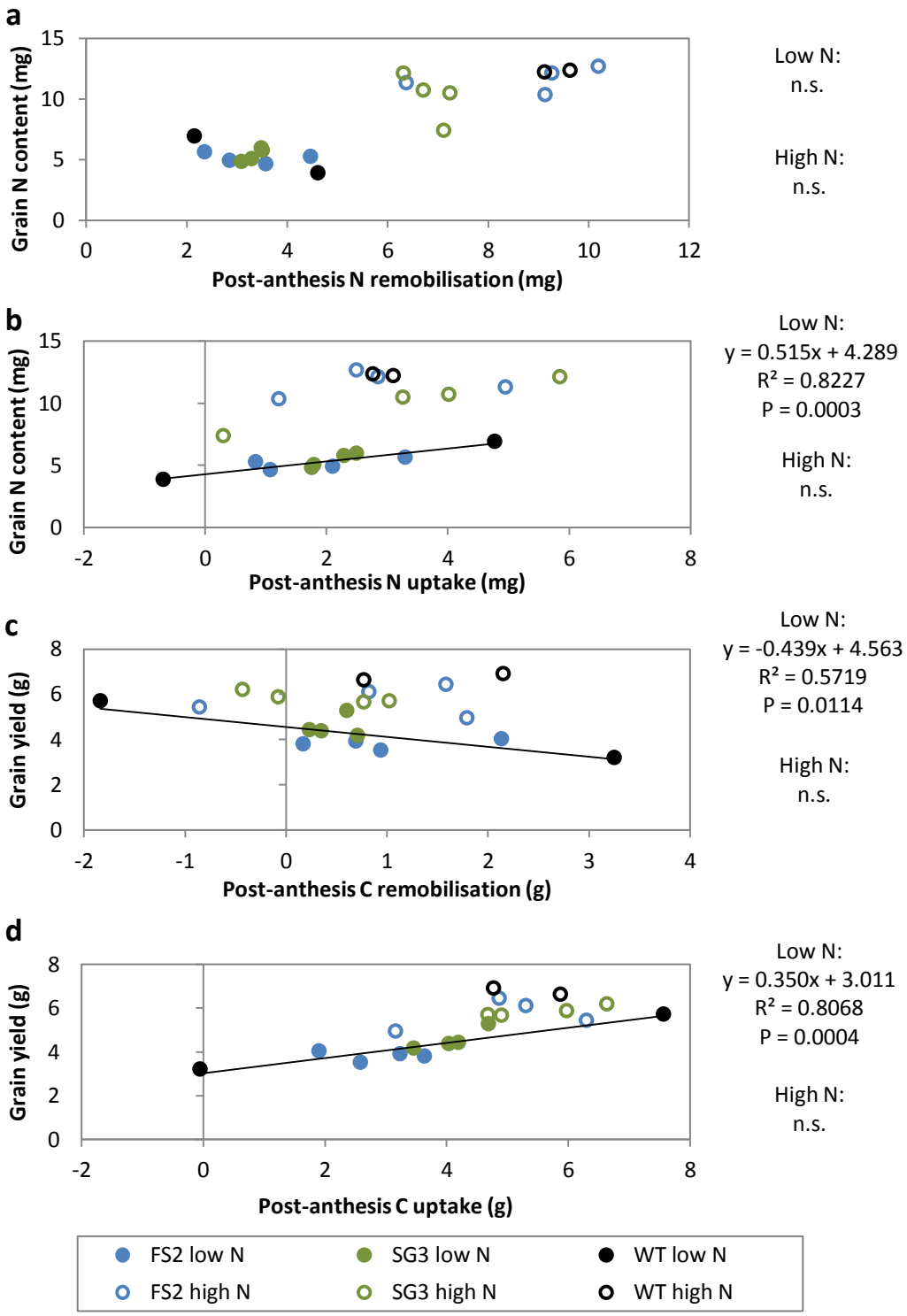

Figure 4.30: Relationships between grain nitrogen (N) content and post-anthesis N remobilisation (a) and N uptake (b) and between grain yield and biomass (C) remobilisation (c) and C uptake (d) of selected mutant wheat lines grown under high (dashed line) and low (solid line) nitrogen nutrition. Data points are means per replicate block.

4.4.7 Gene Expression

Genes for which the expression correlated with leaf senescence were identified in Chapter 3. The expression of a number of these genes was analysed in lines FS2 and WT at both N levels to assess whether the differential senescence phenotypes of these lines were reflected at the molecular level. Line SG3 was not included since it showed very similar flag leaf senescence to WT in this experiment, especially at high N (Figure 4.10). Flag leaves were collected at the same time points as senescence was measured (Figure 4.10), so the early and late senescence time points of plants grown at low N were at 12 and 17 days post-anthesis, while the similar time points for the high N plants were at 21 and 25 dpa. To be able to compare these data fairly, gene expression was not only shown against time (Figure 4.31) but also plotted against greenness (Figure 4.32).

RBCS expression decreased in time for all four line x N level combinations (Figure 4.31.a) and correlated significantly with greenness (Figure 4.32.a; $P<0.001$). *RBCS* expression was significantly higher at anthesis in WT at high N ($P<0.001$), but at early and late senescence *RBCS* expression was the same in both lines at both N levels.

SAG12 expression was already high at anthesis and increased significantly only under low N conditions, and earlier in FS2 than in WT (Figure 4.31.b). Overall there was a significant relationship between *SAG12* expression and greenness (Figure 4.32.b; $P<0.001$).

Expression of the NAC transcription factor was barely detectable. The little expression that was there even seemed to disappear in time (Figure 4.31.c), but there was no significant relationship with senescence (Figure 4.32.c) since most leaves did not show any expression at all.

Expression of the WRKY transcription factor increased significantly in time (Figure 4.31.d; $P<0.001$) and correlated well with senescence (Figure 4.32.d).

The increase was earlier and stronger at low N compared to high N. There were no significant differences between the lines.

Expression of the MYB*a* transcription factor showed great variation and was therefore not correlated with senescence (Figure 4.32.e). However, MYB*a* expression in WT increased significantly between early and late senescence (Figure 4.31.e). MYB*a* expression increased in early senescence for FS2 at low N, but was not significantly higher than that of plants grown under high N plants during late senescence.

Expression of MYB transcription factor *b* in flag leaves decreased in time for both lines at both N levels (Figure 4.31.f). Expression was significantly higher in plants grown at high N nutrition throughout senescence ($P<0.001$), and correlated with greenness (Figure 4.32.f; $P<0.001$). There was no difference between the lines.

Expression of the F-box protein gene increased significantly during senescence in low N supplied plants only (Figure 4.31.g), but still overall correlating with greenness (Figure 4.32.g; $P<0.01$). Compared with high N supplied plants with similar greenness, the expression of the F-box gene was higher in low N plants than one would expect (Figure 4.32.g). This indicates that this gene mainly responded to the N level and not the senescence status of the plants.

Expression of the PTF1-like gene correlated well with greenness (Figure 4.32.h; $P<0.001$), but expression only increased in plants grown at low N (Figure 4.31.h). In FS2, expression increased first and then decreased again, although it stayed higher than it was at anthesis, while in WT expression increased only later in time.

(a) RBCS

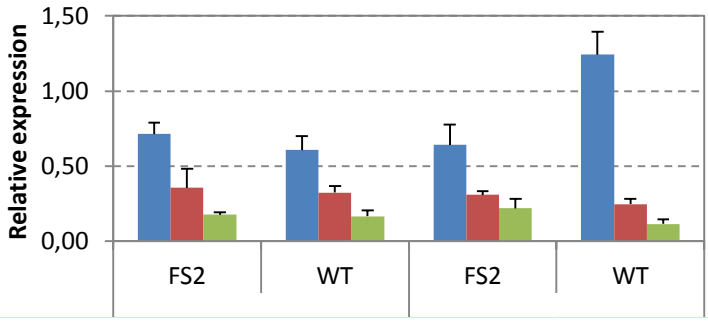

(b) SAG12

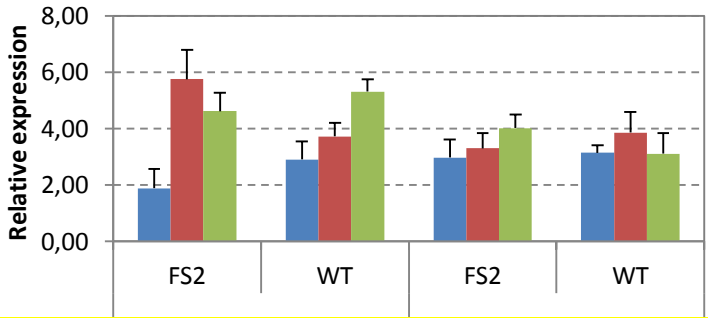

(c) NAC

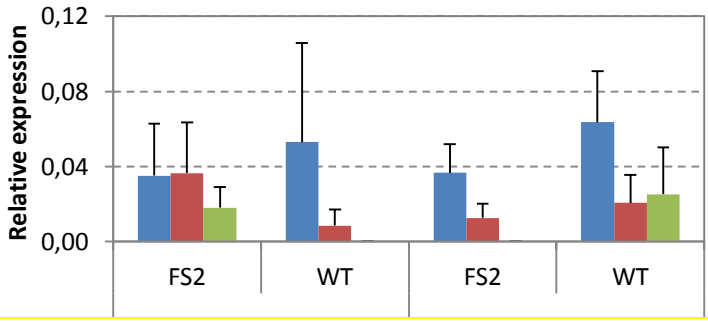

(d) WRKY

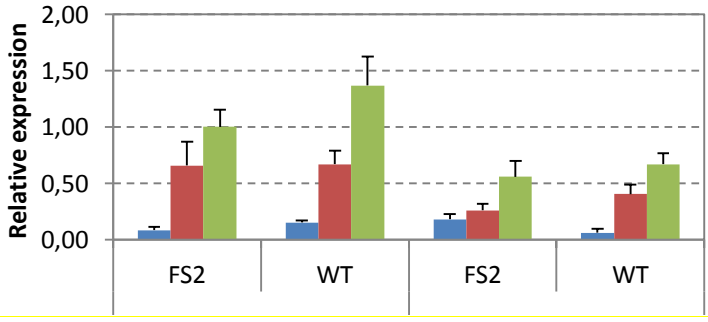

(e) MYB *a*

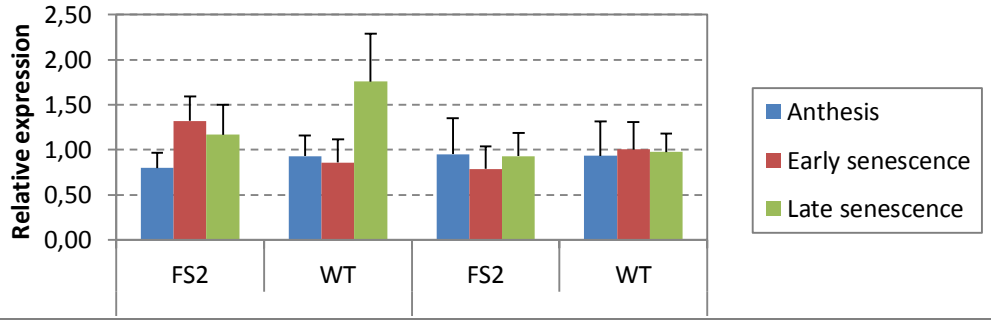

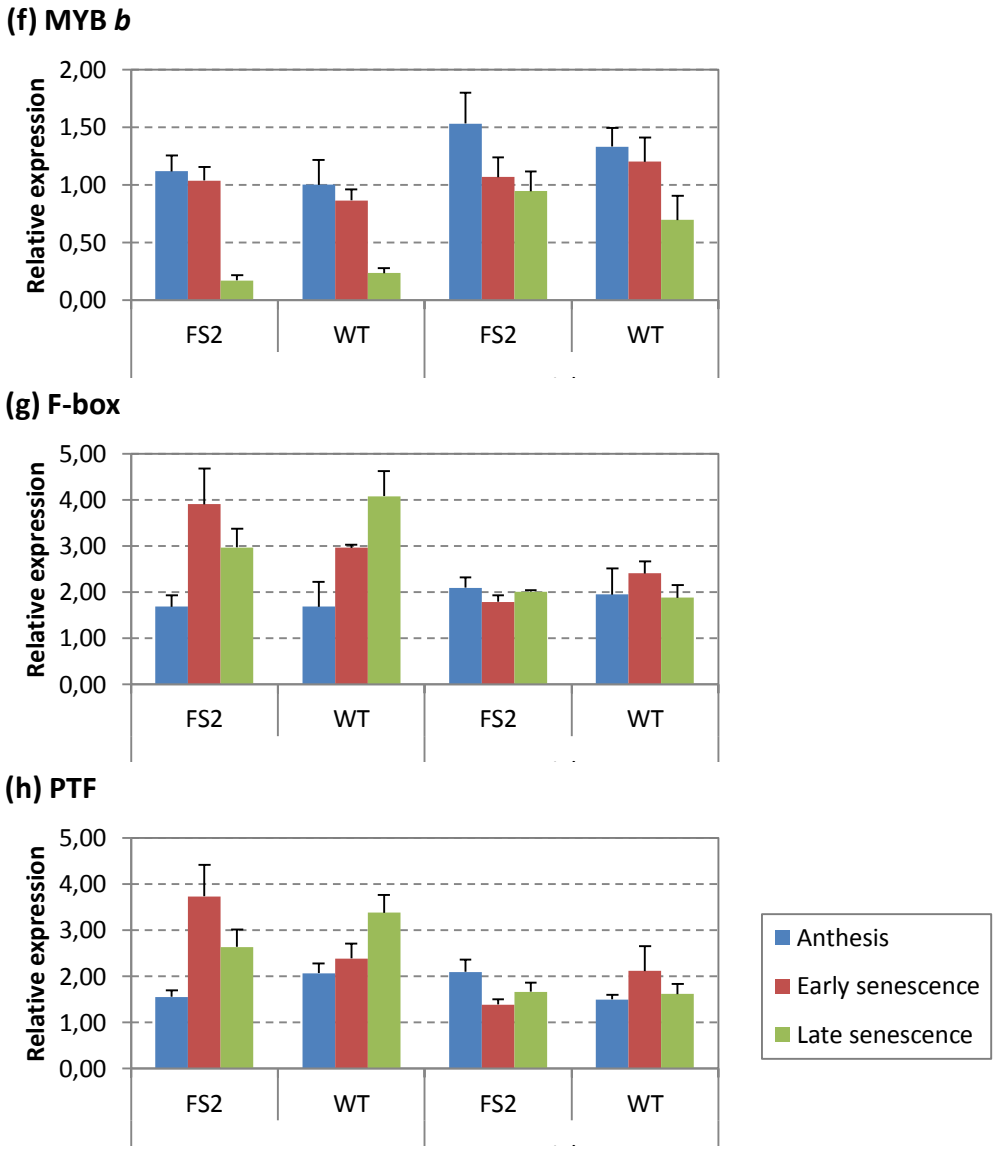

Figure 4.31: Relative gene expression in flag leaves of selected mutant wheat lines grown under high and low nitrogen nutrition. (a) *RBCS*, **(b)** *SAG12*, **(c)** NAC transcription factor, **(d)** WRKY transcription factor, **(e)** MYB transcription factor *a*, **(f)** MYB transcription factor *b*, **(g)** F-box protein, **(h)** PTF1-like gene. Data are means + SE of four replicate pots (five plants/pot) of which the flag leaves of two main shoots were harvested.

(a) RBCS

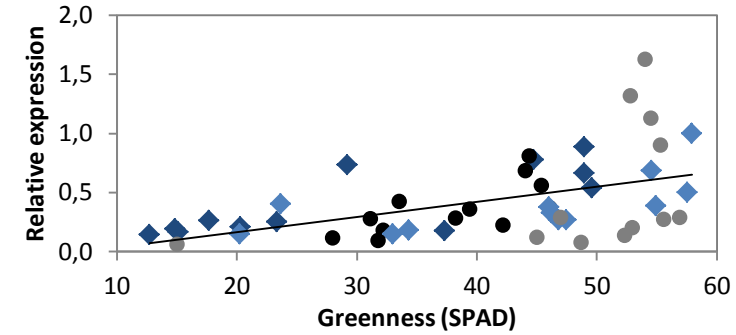

y = 0.0128x - 0.0903
R^2 = 0.2483
P = 0.0003

(b) SAG12

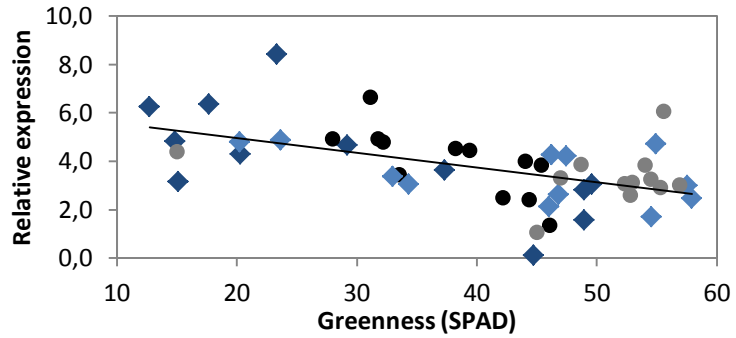

y = -0.0613x + 6.1879
R^2 = 0.2875
P < 0.001

(c) NAC

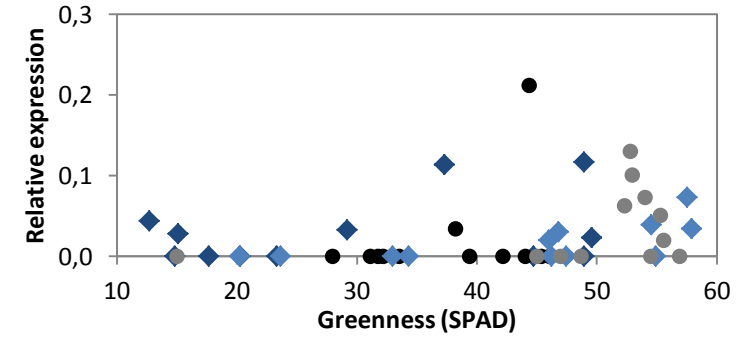

(d) WRKY

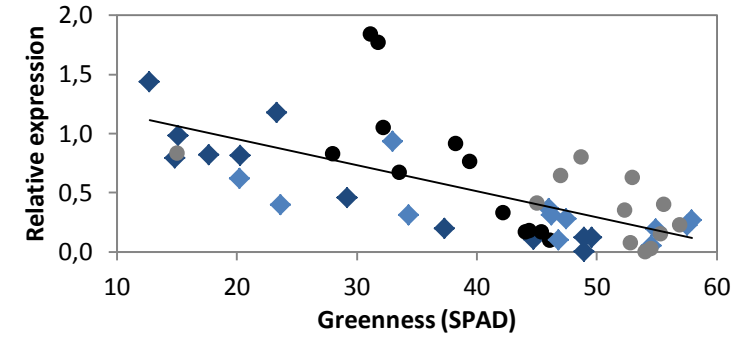

y = -0.022x + 1.3936
R^2 = 0.4419
P < 0.001

FS2 low N
WT low N
FS2 high N
WT high N

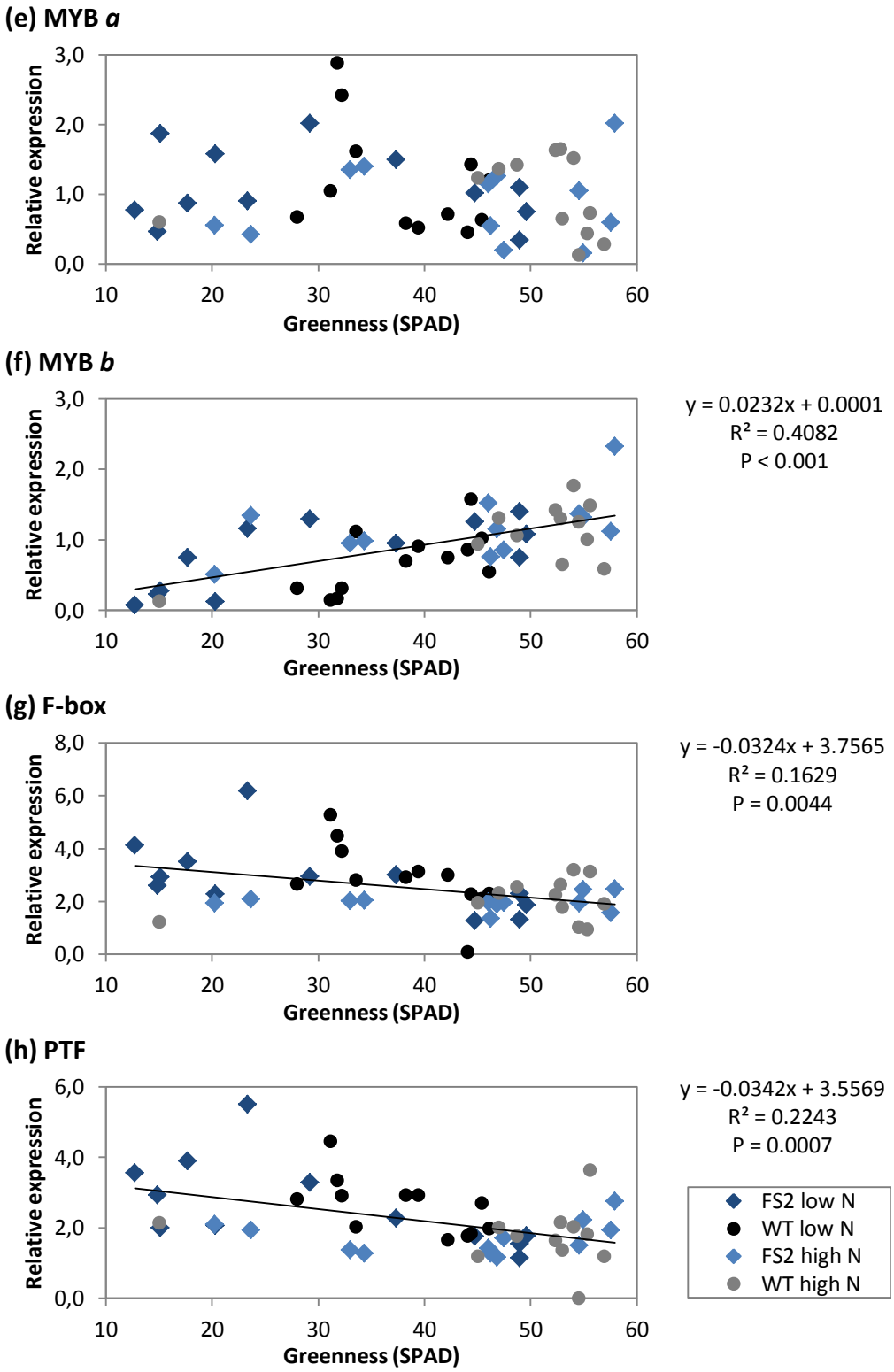

Figure 4.32: Relationships between greenness (SPAD) and relative gene expression in flag leaves of selected mutant wheat lines grown under high and low N nutrition. (a) *RBCS*, **(b)** *SAG12*, **(c)** NAC transcription factor, **(d)** WRKY transcription factor, **(e)** MYB transcription factor *a*, **(f)** MYB transcription factor *b*, **(g)** F-box protein, **(h)** PTF1-like gene.

4.5 DISCUSSION AND CONCLUSIONS

Three mutant wheat lines showed a stay-green phenotype and two lines a fast-senescing phenotype in three separate experiments: the field study at the John Innes Centre in which they were selected originally, the screening of 54 mutant lines, and the follow-up experiment in which they were studied in more detail. The senescence phenotypes were confirmed by relative chlorophyll content (greenness), continuation of photosynthesis, and maintenance of photosystem II efficiency (Figures 4.1 and 4.2).

When one of the stay-green lines (SG3) was grown again, this time under high and low nitrogen, it showed flag leaf senescence similar to wild-type at high N while at low N it seemed to senesce faster than wild-type (Figure 4.10). However, the faster senescence at low N seemed to occur just in the individual plants selected randomly for this particular time point; other plants seemed to be similar to wild-type. When examining the senescence of the whole plant, SG3 showed a stay-green phenotype, especially at high N (Figure 4.11). FS2 was fast-senescing at all nitrogen regimes. In the field SG3 showed a stay-green and FS2 a fast-senescing phenotype, and at low N SG3 did not senesce faster while FS2 and WT did (Derkx et al., 2012).

SG3 had the highest N uptake and lowest remobilisation at high N, while at low N it had high remobilisation and average uptake (Table 4.2). SG3 also reached higher grain N concentrations than FS2 and WT for similar grain yields (Figure 4.23). However, N remobilisation per mg shoot N available at anthesis of SG3 was similar to that of WT and FS2 at both N levels (Figure 4.29.a), suggesting the differences in remobilisation were determined by N status and not by differences in leaf senescence. SG3 had a similar NHI as WT at both N levels (Figure 4.26), indicating the stay-green trait had no negative effects on final grain nitrogen content.

The three stay-green mutant lines were not able to accumulate more biomass or increase their grain yield as was reported for other stay-green wheat genotypes (Chen et al., 2011a; Chen et al., 2010; Christopher et al., 2008; Gong et al., 2005; Luo et al., 2006; Spano et al., 2003); in fact, they were even less effective in this than wild-type (Figures 4.3.a and 4.4). This was also the case when a selection of lines was grown at high and low N supply, although accelerated senescence was even more detrimental (Figures 4.13.a and 4.15). However, in the field SG3 had a higher grain yield than WT at low N, while FS2 had strongly reduced yields at both low and high N (Derkx et al., 2012).

The EMS mutagenesis procedure could have resulted in multiple mutations that diminished fitness of the mutants, both stay-green and fast-senescing plants, adversely affecting grain yield. However, since wheat is a hexaploid species it is unlikely background mutations occurred in all copies of a gene simultaneously. Visible mutants are most likely to be affected by gain-of-function mutations or mutations in genes that are already knocked out on the other genomes. So the background mutation load of the EMS procedure is unlikely to be high in a hexaploid species such as wheat.

None of the lines deviated from the found relationships between shoot C and N at anthesis, uptake and remobilisation of C and N, and grain yield and grain N content (Figures 4.29 and 4.30), suggesting that leaf senescence was induced by plant C and / or N status irrespective of the plant's senescence phenotype. This raises the possibility that the mutations of the stay-green and fast-senescing mutants affected C and / or N status, and that differences in leaf senescence were indirect consequences. In support of this, plant N status has been found to be an important determinant of genotypic differences in the rate of leaf senescence in sorghum (van Oosterom et al., 2010).

Considering the extended photosynthesis period of the stay-green lines, it was surprising that they did not have a higher photosynthetic production (biomass). Lack of remobilisation of photo-assimilates and nitrogen to the

grain might not be so unusual though. One study showed that wheat seed weight hardly responds to photosynthesis levels during seed filling, indicating that wheat seeds experience no source limitation for seed growth (Borrás et al., 2004). This was also found for a wheat stay-green variety: even though the grain-filling period of a stay-green hybrid was extended by 6-7 days the harvest index was lower, indicating that the hybrid was relatively inefficient in remobilisation of carbon and that most of the extra photosynthesis products remained in the vegetative parts instead of being trans-located to the grain (Gong et al., 2005). It can be speculated that a reduced grain N sink size for the stay-green lines may have been associated with a low potential grain weight, since grain number was slightly higher. So it is plausible that under the conditions used in the experiments reported in this thesis wheat grains do not have a sufficient demand for extra carbon-products, and that their remobilisation therefore did not take place. The extra post-anthesis photosynthetic capacity of SG3 may have been resulted in additional allocation of assimilates to other plant parts such as the roots. Consequently, enhancing photosynthetic production would not have an effect on grain yield.

It is conceivable that the stay-green trait has different effects under different environmental conditions. Results from the nitrogen nutrition experiment suggested that nitrogen nutrition was not of influence. However, there are other environmental conditions, notably drought, which could achieve an effect. Alternatively, the conditions used in the nitrogen nutrition experiment conducted here might not have been optimal to create differences between the lines. It is possible that plants grown in pots in the glasshouse are more likely to be sink-limited than plants grown under standard plant population densities in field conditions. The plants would then be insensitive to a change in supply (source) of carbon and nitrogen. Another possible issue is that that the EMS mutagenesis procedure could have resulted in multiple mutations that diminished the fitness of the mutants (as discussed above), both stay-green and fast-senescing, so that they have an inherent disadvantage in development compared to wild-type plants.

It has been suggested that a supplemental investment of nitrogen in the photosynthetic machinery may be detrimental to the transfer of nitrogen to the grain and thus to final grain yield, at least if N uptake does not increase as well (Sinclair, Purcell and Sneller, 2004). In support of this, it has been found that the nitrogen concentration in straw of a stay-green line of wheat remained higher, making it likely more N uptake is required to achieve a grain protein content comparable to wild-type (Chen et al., 2011a). Even though SG3 had the lowest remobilisation at high N (Table 4.2), there were no differences between FS2, SG3 and WT in N remobilisation or N uptake per mg shoot N available at anthesis (Figure 4.29.a). Furthermore, SG1, SG2 and SG3 reached a grain N concentration similar or higher than wild-type in all experiments under all levels of nitrogen nutrition (Figures 4.6.b, 4.22.a, 4.23 and 4.24.b), indicating nitrogen was not limiting at maturity. This would suggest carbon was the factor limiting grain yield and total grain nitrogen content. Such a coupling between carbon economy and grain nitrogen concentration was found by Sandaña, Harcha and Calderini (2009), while the other theory would assume grain nitrogen content was source-limited, as found by Martre et al. (2003). Since grain concentration in the stay-green lines was always equal or higher than wild-type (Figures 4.6.b and 4.22.a), one would assume there is scope for a reduction in nitrogen concentration accompanied with an increase in grain yield. Furthermore, it seems that accelerated senescence resulted in reduced remobilisation of nitrogen from the leaves (Figure 4.27), especially at low N supply. In addition, the results suggest that the accumulation and allocation of carbon (biomass) was affected by the stay-green phenotype (see above). So grain yield and therefore grain total nitrogen content of the stay-green lines appears to have been limited by carbon remobilisation, not by a shortage of nitrogen available for grain-filling. This is in contradiction to findings in wheat (Gaju et al., 2011) and sorghum (Borrell and Hammer, 2000), which showed that faster senescence was accompanied with higher nitrogen remobilisation and less nitrogen uptake.

In FS2 and WT grown under high and low N supply, *SAG12* and the WRKY transcription factor showed a significant positive relationship with senescence and transcription factor MYB*b* a significant negative relationship (Figure 4.32.a, 4.32.d and 4.32.f). Transcription factor MYB*a*, the PTF1-like gene and the F-box gene showed a change in expression under low N conditions only (Figure 4.31.e, 4.31.g and 4.31.h), suggesting their expression is modulated more directly by nitrogen status than by senescence.

Unexpectedly, even though expression of the marker gene Rubisco decreased in time (Figure 4.31.a) it did not show an overall significant relationship with greenness (Figure 4.32.a). In less green senescing leaves *RBCS* levels associated well with the SPAD readings. In contrast, in green leaves (high SPAD) of plants grown with high N supply there was considerable variation in *RBCS* levels, which corresponds with the suggestion that Rubisco can function as a storage protein (Breeze et al., 2011). In summary, senescence is generally accompanied by a decrease in *RBCS* expression, but *RBCS* expression in green leaves is not determined by senescence status but by nitrogen availability.

Expression of the NAC transcription factor was not or barely detected. This result does not match the expression studies on the Avalon x Cadenza doubled haploid lines in which expression of the NAC gene was clearly present and correlated with senescence (Figure 3.10). However, in the few samples expression was found, the pattern showed a decrease in senescence as had been found before (Figure 4.31.c).

In summary, stay-green and fast-senescing mutant lines of wheat were identified and characterised. Stay-green line SG3 had higher grain N concentrations than WT and was able to allocate similar proportions of nitrogen to the grain under N-limiting and N-sufficient conditions. In contrast, the accelerated senescence of line FS2 resulted in lower grain yield and reduced nitrogen allocation to the grain.

5. FUNCTIONAL STUDY OF A SENESCENCE-ASSOCIATED NAC TRANSCRIPTION FACTOR IN WHEAT

5.1 INTRODUCTION

Members of the NAC transcription factor family (named after the petunia *NAM* and Arabidopsis *ATAF1-2* and *CUC2* genes) have been shown to be involved in developmental and physiological processes such as embryo and shoot meristem development, lateral root formation, auxin signalling, defence, abiotic stress responses and senescence (Nuruzzaman et al., 2012; Olsen et al., 2005). Senescence-associated NAC transcription factors have been described in Arabidopsis (Balazadeh et al., 2011; Guo and Gan, 2006; Kim et al., 2009; Lee et al., 2012; Wu et al., 2012; Yang et al., 2011; Yoon et al., 2008), rice (Sperotto et al., 2009), bamboo (Chen et al., 2011b) and wheat (Uauy et al., 2006b). The majority of these genes showed increased expression during senescence and are therefore positive regulators of senescence. As yet only one NAC gene that is a potential negative regulator of leaf senescence has been described in detail (Wu et al., 2012).

A transcriptomics study of six wheat varieties grown at multiple levels of nitrogen fertiliser (Hawkesford and Howarth, 2010) resulted in a list of candidate genes that may be involved in leaf senescence and nitrogen remobilisation during grain-filling (Howarth et al, unpublished). To corroborate the expression patterns of several of these genes, expression was evaluated during senescence of wheat cultivar Hereward and two Avalon x Cadenza doubled haploid lines grown under different nitrogen levels in the field in multiple years (Chapter 3) and in wild-type and a fast-senescing mutant line of wheat cultivar Paragon grown at two N levels (Section 4.4.7). The decreasing expression of the NAC transcription factor during senescence in all tested leaf materials suggested this gene could be a negative regulator

of senescence in wheat. Therefore the role of this NAC gene in senescence was studied further.

The aims of the experiments reported in this chapter were:

1. To establish the possible identity of the NAC gene by analysing its sequence and phylogeny.
2. To determine in which plant tissues the NAC gene is expressed.
3. To analyse the effects of overexpression of the NAC gene on morphology, development, senescence, grain yield and grain nitrogen content of wheat.

5.2 SEQUENCE AND PHYLOGENETIC ANALYSES

The NAC family of transcription factors is large, with 151 members in rice split into two groups with 16 subgroups (Nuruzzaman et al., 2010). To classify the wheat NAC gene, the sequence was analysed in detail (Figure 5.1). Ooka et al. (2003) identified five subdomains common to all NAC domains in rice and Arabidopsis, and 13 motifs unique to different subgroups. The wheat NAC gene contains all five subdomains, as well as a motif unique to the NAC1-type and NAM-type NAC transcription factors (Figure 5.1).

To determine the relationship with previously described NAC genes, a phylogenetic tree of NAC protein sequences was constructed (Figure 5.2). This tree encompasses all senescence-related NAC genes in all other plant species (Arabidopsis, bamboo, rice, tomato, and wheat), all rice (cv. Japonica) NAC proteins, and all described wheat NAC proteins so far. The wheat NAC gene closely resembled another wheat NAC protein, ADG85703, in the UniProtKB database. The two genes had identical NAC domains, but differed in three residues outside the domain. A biological function of ADG85703 has not been described to date.

The closest rice NAC gene was found to be Os08g10080, named ONAC104 by Fang et al. (2008). In agreement with the domains found in the wheat sequence, Os08g10080 is a NAC1-type gene (Nuruzzaman et al., 2010). Os08g10080 has not been functionally analysed.

In summary, the sequence and phylogenetic analyses suggest the wheat NAC gene is a NAC transcription factor of the NAC1-type that so far has not been described in detail.

a. Coding DNA sequence of the wheat NAC gene

ATGAGCTCTATTGGCATGATGGAGGCGAGGATGCCGCCGGGGTTCCGGTTCCACCCACGGG
ACGAGGAGCTGGTCCTCGACTACCTCCTCCACAAGCTCACCGGCCGGCGCGCATACGGTGG
CGTCGACATCGTGGACGTCGACCTCAACAAGTGCGAGCCATGGGACCTTCCAGAGGCGGCG
TGCGTGGGCGGCAGGGAGTGGTACTTCTTCAGCCTGCGCGACCGCAAGTACGCCACCGGCC
AGCGCACCAACCGCGCCACGCGCTCCGGCTACTGGAAGGCCACCGGCAAGGACCGCGCCAT
CCTCGCGCACGGCGAGGCGTTGGTGGGGATGCGCAAGACGCTCGTCTTCTACCAGGGGAGG
GCCCCCAAGGGGACGAGAACGGAGTGGGTCATGCACGAGTTCCGCCTCGAGGAGGAGCGAC
ACCGCCACCACCACCAGCAGAAGGGCGGCGCCGCCGCCGCCGAGGCGAGGTGCCAGCTCAA
GGAAGACTGGGTGCTATGCAGGGTGTTCTACAAGAGCAGAACAAGCAGCCCAAGGCCACCA
TCTGAAGAAGTCTGCACATTTTTTAGCGAGCTGGACCTTCCGACTATGCCACCGCTCGCGC
CCCTCATCGACGCGTGCATCGCCTTCGACAGCGGCACCGCGATGAACACCATCGAGCAAGT
GTCCTGCTTCTCCGGCCTGCCAGCACTACCCCTCAGGGGATCGATGAGCTTCGGGGACCTG
CTGGGCTGGGACAACCCTGAGAAGAAGGCCATCAGGACAGCTCTGAGCAACATGTCAAGTA
ACAGCAATTCCAAGTTGGAGTTGACCCCAAACTGGAGCCAGGAGAACGGCTTGTCACAAAT
GTGGACACCCCTCTGA

b. Protein sequence of the wheat NAC gene

MSSIGMMEARMPPGFRFHPRDEELVLDYLLHKLTGRRAYGGVDIVDVDLNKCEPWDLPEAA
CVGGREWYFFSLRDRKYATGQRTNRATRSGYWKATGKDRAILAHGEALVGMRKTLVFYQGR
APKGTRTEWVMHEFRLEEERHRHHHQQKGGAAAAEARCQLKEDWVLCRVFYKSRTSSPRPP
SEEVCTFFSELDLPTMPPLAPLIDACIAFDSGTAMNTIEQVSCFSGLPALPLRGSMSFGDL
LGWDNPEKKAIRTALSNMSSNSNSKLELTPNWSQENGLSQMWTPL

c. Predicted NAC domain (Interpro) of the wheat NAC gene

MPPGFRFHPRDEELVLDYLLHKLTGRRAYGGVDIVDVDLNKCEPWDLPEAACVGGREWYFF
SLRDRKYATGQRTNRATRSGYWKATGKDRAILAHGEALVGMRKTLVFYQGRAPKGTRTEWV
MHEFRLEEERHRHHHQQKGGAAAAEARCQLKEDWVLCRVFYK

Figure 5.1: Sequence analysis of the wheat NAC gene. (a) The coding DNA sequence and **(b)** the translated protein sequence with the NAC domain highlighted in yellow and the NAC1/NAM-group-specific motif in green. **(c)** The five subdomains of the NAC domain (highlighted). Indicated in **red** are amino acids that are 100% conserved between all NAC domains in rice and Arabidopsis, in **bold** amino acids that are >50% conserved (according to Ooka et al., 2003).

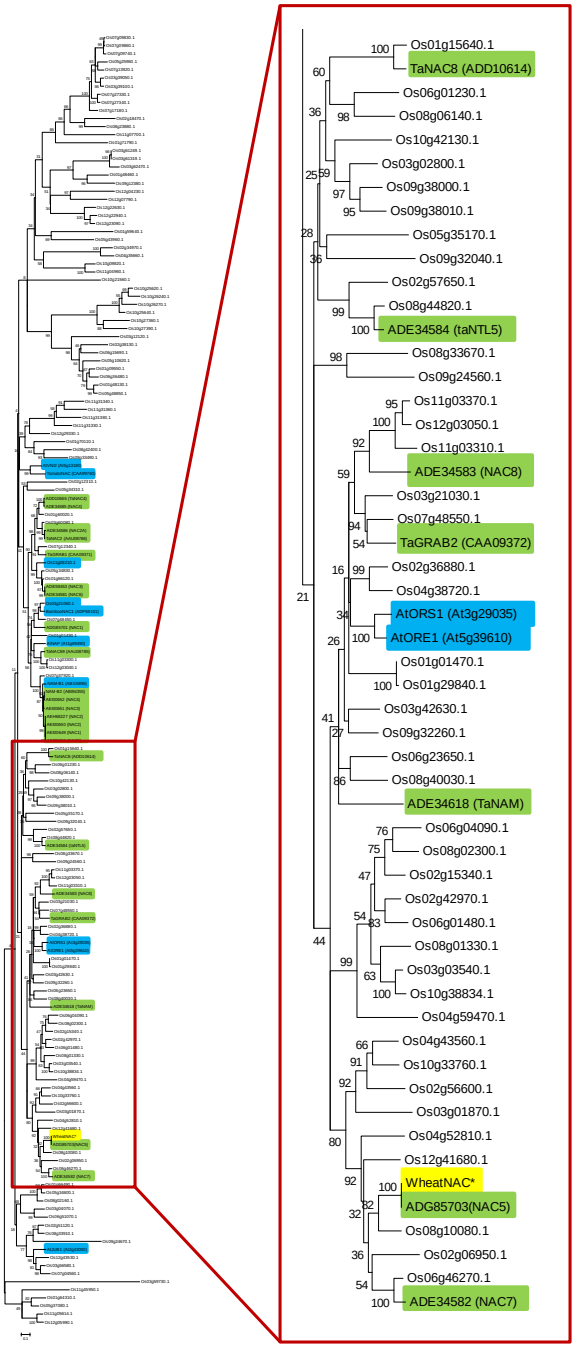

Figure 5.2: Phylogenetic analysis of the wheat NAC protein (yellow*), senescence-associated NAC proteins from all plant species (blue), other known wheat NAC protein sequences (green), and all remaining known rice NAC proteins (white). Amino acids within the NAC domains were aligned in MEGA5 using the ClustalW algorithm (Larkin et al., 2007). The phylogenetic tree was constructed using the Neighbor-Joining method (Tamura et al., 2011). Bootstrap values of 1000 replicates are indicated at each node.

5.3 EXPRESSION OF THE NAC GENE IN WHEAT TISSUES

In studies of field-grown wheat it was established that expression of the NAC gene decreased with senescence of leaf two (Chapter 3). An experiment was set up to test whether the NAC gene is expressed in tissues other than leaves (Figure 5.3). Roots were harvested at booting, flowers were dissected at 7 days post-anthesis when grain has just become visible, while all other tissues were harvested at anthesis. Expression was measured by semi-quantitative RT-PCR (Section 2.2.1 – 2.2.3).

Expression of the NAC gene was highest in the second leaf, third leaf and leaf sheath, which are the organs that will have been starting to senesce at the time of sampling. Expression was lower in the flag leaf and stem, while NAC expression was barely or not detectable in the glume and lemna, grain, rachis and roots.

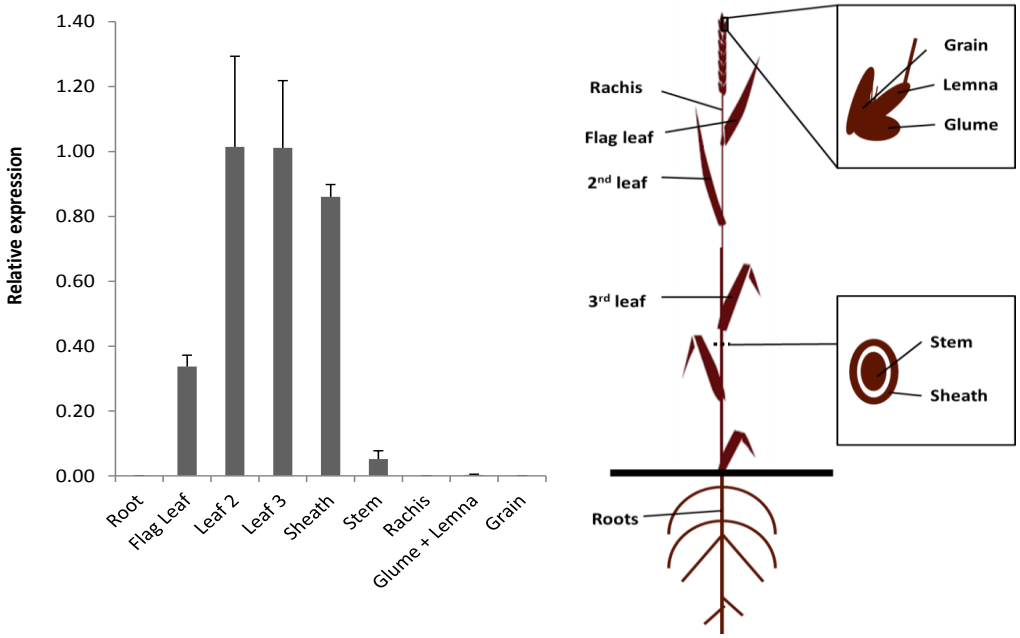

Figure 5.3: Expression of the NAC gene in wheat tissues. Glume, lemna and grain were harvested seven days post-anthesis, roots at booting, the other tissues at anthesis. Data are means + SE of three replicate plants.

5.4 OVEREXPRESSION OF THE NAC GENE IN WHEAT

5.4.1 Creation of NAC-Overexpressing Wheat

Expression of the NAC transcription factor was found to be correlated with senescence of the second leaf of wheat (Chapter 3). This correlation in itself is not evidence for an actual role of this gene in leaf senescence. To get a better idea of the role of this NAC gene in leaf senescence, or in any other aspect of wheat development, a transgenics approach was employed to manipulate NAC gene expression. Since expression of the NAC gene decreased during senescence, it was anticipated overexpression of the NAC gene may delay leaf senescence if it has a regulatory role in leaf senescence.

Two overexpression constructs containing different promoters were used (Figure 5.4): one containing the rice tungro bacilliform virus (RTBV) promoter (Bhattacharyya-Pakrasi et al., 1993), which has strong expression in wheat leaves (Rothamsted Cereal Transformation Group, unpublished), and another containing the rice *actin1* promoter which is considered to be constitutively expressed in all tissues (Zhang et al., 1991).

The two constructs were used to transform the wheat cultivar Cadenza. Eight independent pRTBV-NAC (R1-R8) and two independent pActin-NAC plants (A1 and A2) were generated. Offspring from each were grown (T1 generation), screened by PCR (Sections 2.2.4 and 2.2.5) for transgenic individuals and the seed of three separate transgenic plants was collected. Seeds of one of these plants (T2 generation) per line were grown and screened by PCR. Four of these plants were used for the further studies.

The copy number was determined for a selection of the lines (Dr Peter Buchner (Rothamsted Research) and IDna Genetics Ltd.). Line pActin-NAC 1 appeared to have one copy inserted (homozygous lines have two). pRTBV-NAC lines 2, 3, 5, 6 and 8 had between 3 and 15 copies for hemizygous lines. Many are suspected to have multiple insertions.

a

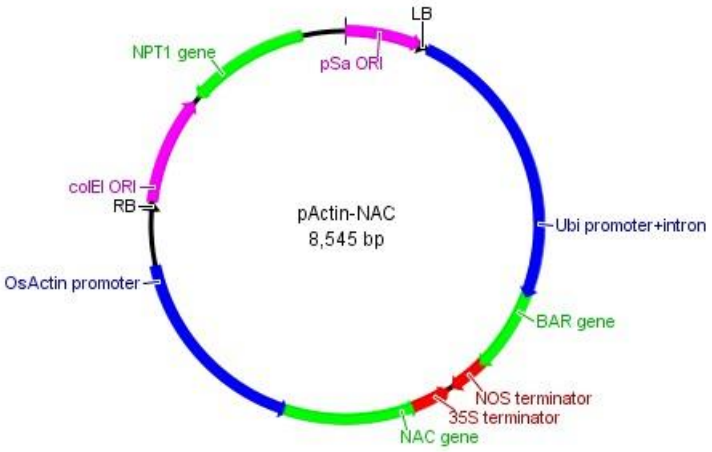

b

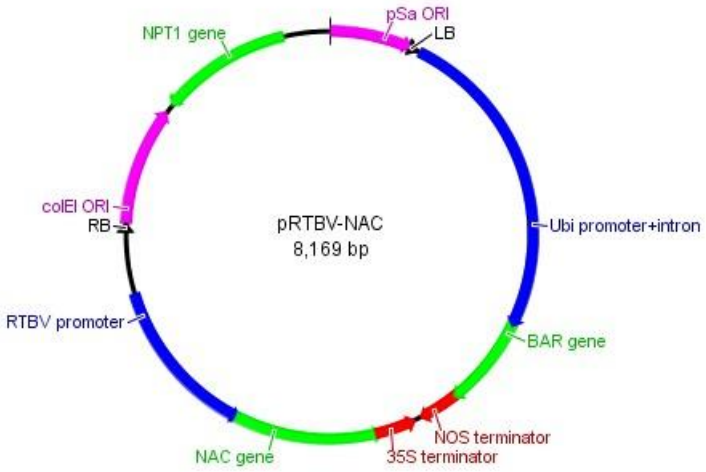

Figure 5.4: Plasmids for NAC overexpression under the control of rice actin (a) and RTBV (b) promoters. Apart from the promoters the two constructs are identical. The plasmids contain a broad host range origin of replication (ORI) for use in *Agrobacterium tumefaciens* (pSA) and an ORI for *Escherichia coli* (colEI) and the *NPT1* kanamycin-resistance gene for selection of bacteria. The part between the left and right borders (LB and RB) is meant for insertion into the plant genome. Apart from the promoter-NAC-35S-terminator sequence this includes a BAR gene (phosphinothricin resistance) under control of an ubiquitin promoter to allow for plant selection. Genes in green, promoters in blue, terminators in red and ORI in pink. Constructs made by Dr Peter Buchner (Rothamsted Research).

5.4.2 Morphology and Development

To determine if overexpression of the NAC gene affects development, the timing of four key developmental stages of the main shoot was compared: completion of flag leaf emergence (Zadoks Growth Stage 39), transition of booting to heading (GS49), start of anthesis (GS61), and physiological maturity (GS89). Highly significant differences were found between lines for all four growth stages (all $P<0.001$).

The first three growth stages all gave a similar picture. The flag leaf of line pRTBV-NAC 8 (R8) emerged significantly earlier than that of all other lines except R2, while lines R1, R5 and R6 reached this growth stage significantly later than both transformation control (C) and wild-type (WT) (Figure 5.5). R8 also reached the heading stage significantly earlier than C and WT, whilst R5 and R6 reached this stage significantly later (Figure 5.5). R8 was still earlier in anthesis than WT and C but this difference was not significant, while R1, R5 and R6 flowered significantly later than C and WT (Figure 5.5). At all three stages line R2 was early, but never significantly differed from both C and WT. The difference between early and late lines was between six to eight days.

At physiological maturity differences between lines were smaller, at a maximum of five days (Figure 5.5). Line R2 still reached maturity before the control lines (not significant). Line R6 reached this stage significantly later than C and WT. But while line R8 had reached the other stages early, it reached physiological maturity significantly later than all other lines. Therefore R8 had a longer post-anthesis canopy longevity than the other lines.

To examine whether the differences in development were similar for the tillers or just the main shoot, the start of anthesis was assessed for the first three tillers (Figure 5.6). Differences in anthesis date of the first two tillers were smaller and not significant. The anthesis dates of the third tiller were highly significantly different ($P<0.001$) between lines, and the anthesis date of

the third tiller of plants carrying the pRTBV-NAC construct was significantly later overall as well (P<0.05). The third tiller of R1 flowered significantly later than both C and WT, whilst R8 reached anthesis significantly later than all lines including R1. So while the main shoot of R8 flowered early, the third tiller was flowering very late, displaying a wide spread in flowering dates of the ears within one plant.

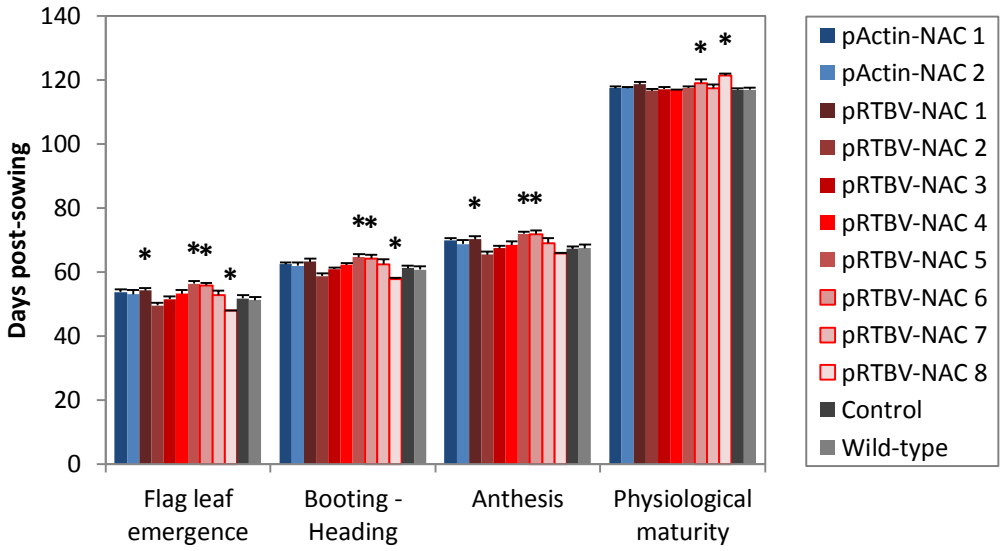

Figure 5.5: Development of the main shoot of NAC-overexpressing wheat. Development was assessed by measuring the time (days post-sowing) required to reach a certain growth stage. Flag leaf emergence (GS39), transition booting to heading (GS49), start anthesis (GS61), physiological maturity (GS89). * significantly different from both control and wild-type (P<0.05). Data are means + SE of four replicate plants.

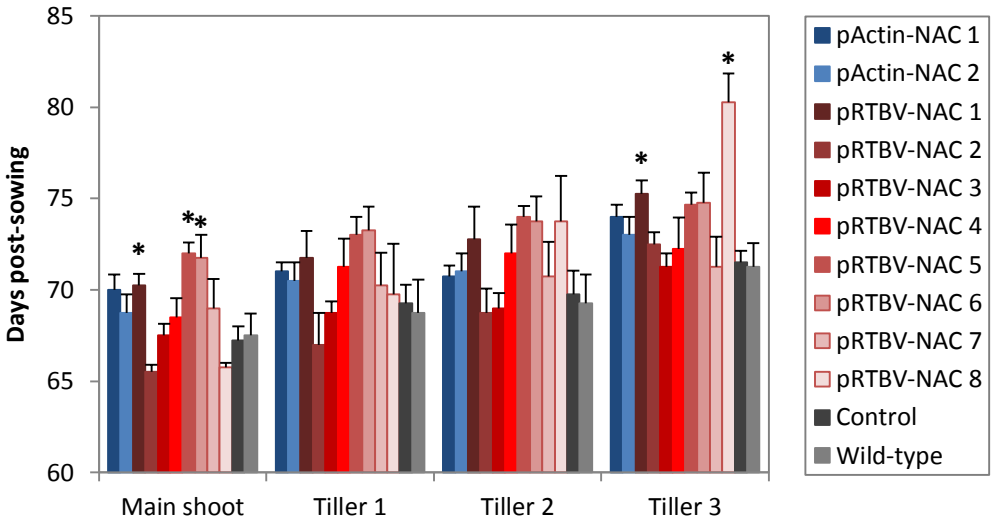

Figure 5.6: Time (post-sowing) in which the main shoot and first three tillers of NAC-overexpressing wheat reached anthesis (GS61). * significantly different from both control and wild-type ($P<0.05$). Data are means + SE of four replicate plants.

Apart from the timing of development, line R8 was untypical in a number of other traits. R8 was more than 20 cm shorter than the other lines (Figure 5.7), and this was the case for the main shoot and the tillers ($P<0.001$). In addition, around anthesis the number of tillers seemed lower (data not shown), although the final number of tillers at maturity reached a number comparable to wild-type (Figure 5.8.a; no significant differences between lines) because the tillers developed later (Figure 5.6). The number of culm leaves on the main shoot, which should correspond to the number of internodes, was also significantly lower in comparison to all the other lines (Figure 5.8.b; $P<0.001$).

Overall, the plants carrying the pRTBV-NAC construct had significantly shorter shoots and tillers than non-transgenic plants (Figure 5.7).

Since the NAC gene is thought to be involved in leaf senescence, it is important to establish whether leaf morphology is affected. Therefore the

leaf size was assessed by measuring length (Figure 5.9.a) and width (Figure 5.9.b) of the top three leaves of the main shoot. When comparing the leaf lengths, only flag leaves differed significantly between lines ($P<0.05$) but not constructs. R5 is the only line with significantly shorter flag leaves than C and WT, while no line had significantly longer flag leaves. R5 also had shorter second and third leaves, and all its leaves were the narrowest measured, but these differences were not significant. The widths of all top three leaves differed significantly between lines ($P<0.01$) but not constructs. The top two leaves of R8 were significantly wider than those of all lines (flag leaf) or at least the control lines C and WT (leaf 2). R4 had significantly wider second leaves than C and WT, whilst R7 had significantly wider second and third leaves.

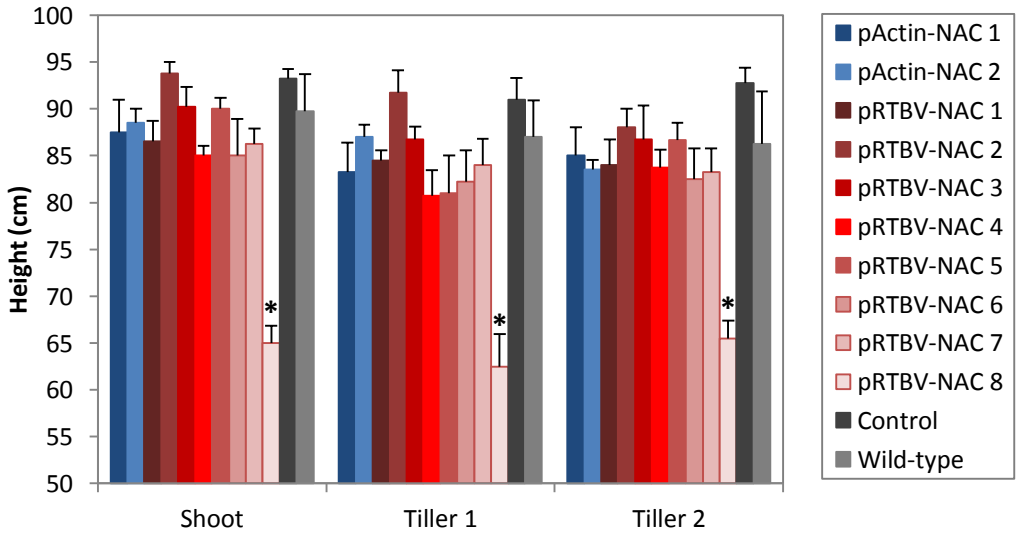

Figure 5.7: The height of the main shoot and the first two tillers of NAC-overexpressing wheat. * significantly different from both control and wild-type ($P<0.05$). Data are means + SE of four replicate plants.

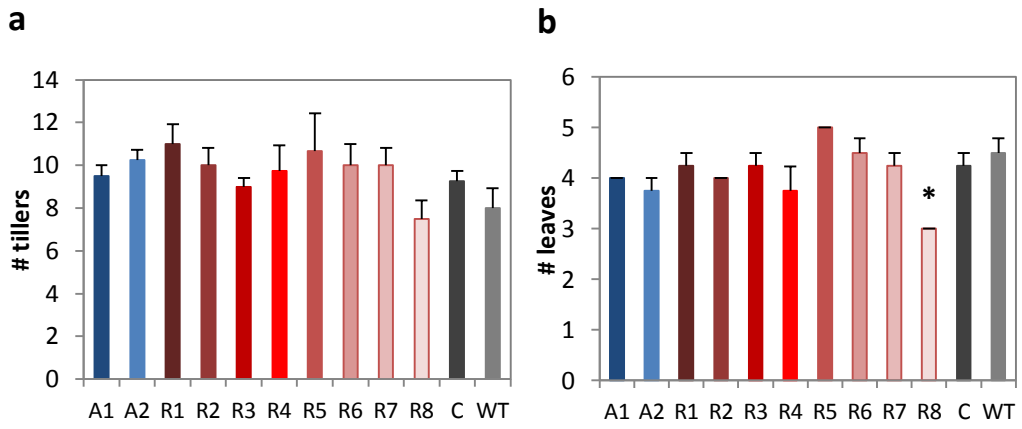

Figure 5.8: The number of tillers (including the main shoot) at physiological maturity (a) and the number of leaves on the main shoot (b) of NAC-overexpressing wheat. The number of culm leaves on the main shoot should be equivalent to the number of internodes. A1-2 = pActin-NAC lines 1 and 2 (blue), R1-8 = pRTBV-NAC lines 1-8 (red), C = transformation control line and WT = Cadenza wild-type (grey). * significantly different from both control and wild-type (P<0.05). Data are means + SE of four replicate plants.

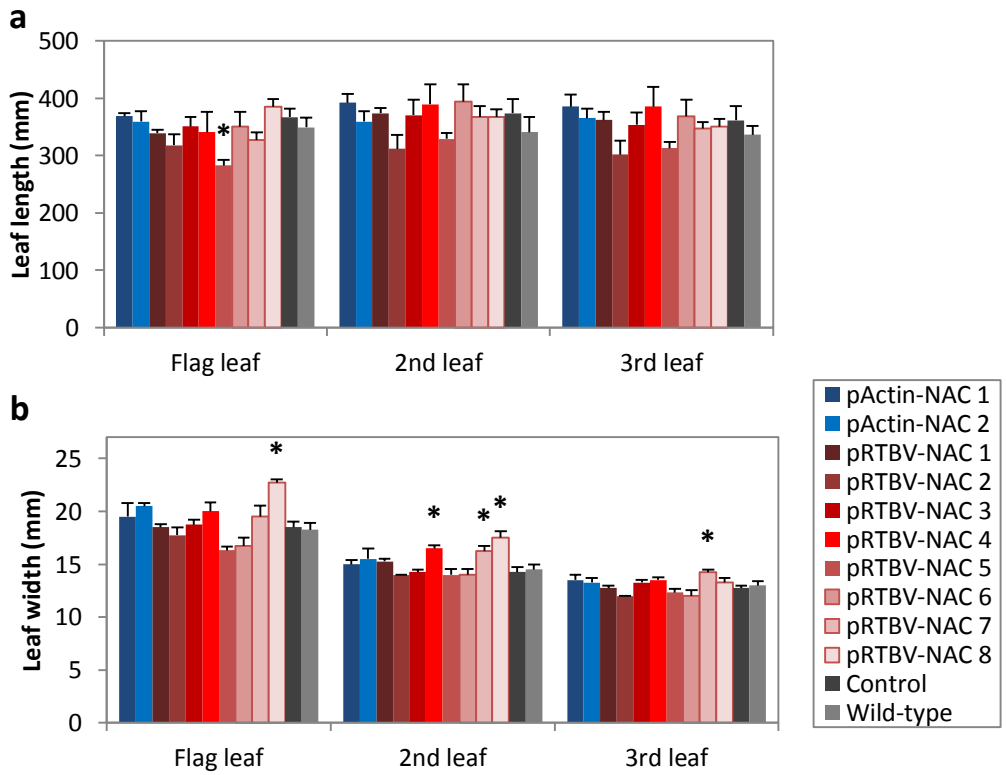

Figure 5.9: Length (a) and width (b) of the first three leaves of the main shoot of NAC-overexpressing wheat. * significantly different from both control and wild-type (P<0.05). Data are means + SE of four replicate plants.

5.4.3 Leaf Senescence

To assess post-anthesis leaf senescence, the relative chlorophyll content (SPAD) and quantum yield (QY = F_V'/F_M') of the top three leaves of the main shoot were measured weekly from anthesis until 49 days post-anthesis (Figures 5.10, 5.11 and 5.12). At this point the leaves of all but one line had completely senesced.

The wild-type and bombardment control lines showed similar senescence patterns, indicating that the transformation process itself did not affect senescence. When comparing the pActin-NAC lines with the two control lines, there was no difference in senescence. Most of the pRTBV-NAC lines showed a delayed onset or lower rate of senescence of the top three leaves compared to the control lines.

The sequential senescence of wheat was easily visible. In the wild-type Cadenza the third leaf started to rapidly senesce at 21 days post-anthesis (Figure 5.10), the second leaf one week later at 28 dpa (Figure 5.11), and the flag leaf one week after that at 35 dpa (Figure 5.12). The differences in senescence appeared greater in the second and third leaf compared to the flag leaf. In addition, SPAD measurements started to decrease about a week before QY.

There were significant interactions between construct, line and time in both SPAD and QY of the third leaf (Figure 5.10; $P<0.001$), indicating that genotype influenced the timing and rate of senescence. pRTBV-NAC plants had higher overall SPAD and QY values than pActin-NAC and control plants. SPAD values were higher between 14 and 28 dpa, while QY was higher between 21 and 35 dpa. At 14 dpa pRTBV-NAC lines 2, 3, 5, 6 and 8 all had a significantly higher SPAD than C and WT, but there were no differences in QY. At 21 dpa the same lines except R3 maintained the difference in SPAD, whilst R2 and R8 had a higher QY. At 28 dpa R8 had a higher SPAD and R6 a higher QY. At 35 dpa R8

had both a higher SPAD and QY than the control lines, whilst at 42 dpa R8 still had a higher QY.

For the second leaf there was a highly significant construct x line x time interaction for relative chlorophyll content ($P<0.001$), but QY only differed significantly between the constructs (pRTBV > pActin and control), not between the separate lines. Relative chlorophyll content of the second leaf of all but one pRTBV-NAC lines was maintained at a higher level for longer to some extent than the control lines (Figure 5.11.a). Again the greenness of R8 declined slowly, maintaining higher chlorophyll for weeks longer than all the other lines, and its SPAD was significantly higher than the control lines between 21 and 42 dpa. R8 also maintained some photosystem II capacity (Figure 5.11.b). Line R5 stood out with significantly higher SPAD values between 7 and 28 dpa, thus having a later onset of senescence, after which it plummeted to zero within a week.

There were fewer differences in flag leaf senescence between the lines. R8 was the only line that had a significantly higher photosystem II efficiency in flag leaves than the control lines (Figure 5.12.b; $P<0.05$). There were no significant differences in relative chlorophyll content for the flag leaves, but line R8 was again the line with the slowest rate of senescence, maintaining relative chlorophyll content the longest (Figure 5.12.a).

In summary, most of the pRTBV-NAC lines showed a delayed onset and / or lower rate of senescence of the top three leaves compared to the control lines. R8 had the slowest rate of senescence for all three leaves, whilst R2 and R5 displayed a late onset of senescence for the third and second leaf respectively.

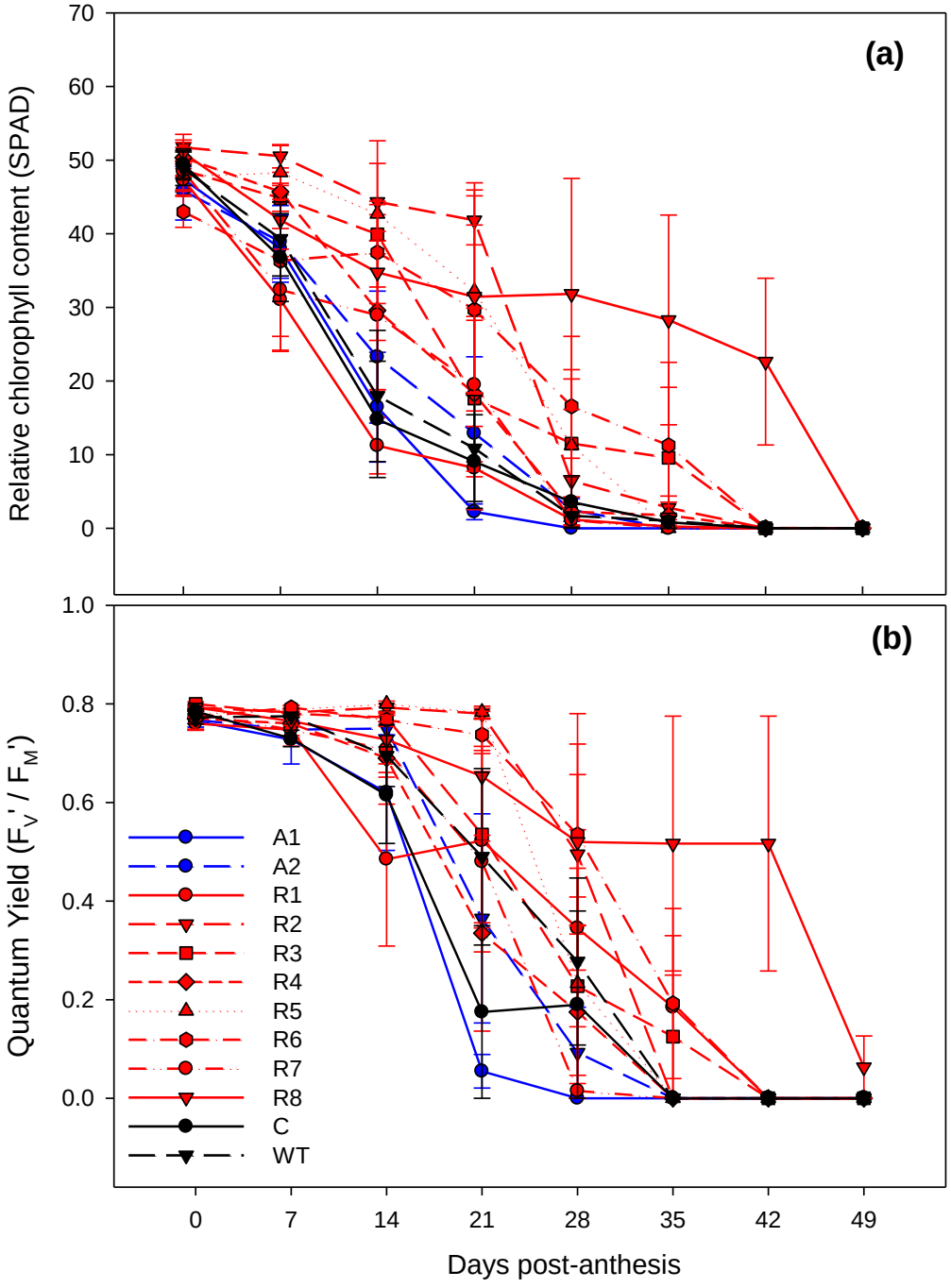

Figure 5.10: Progression of post-anthesis senescence of the third leaf of the main shoot of NAC-overexpressing wheat. (a) Relative chlorophyll content as determined with a SPAD meter. LSD = 14.85. **(b)** Quantum yield (F_V'/F_M'), which is a measure of Photosystem II efficiency. LSD = 0.246. A1-2 = pActin-NAC lines 1 and 2 (blue), R1-8 = pRTBV-NAC lines 1-8 (red), C = transformation control line and WT = Cadenza wild-type (black). Data are means ± SE of four replicate plants.

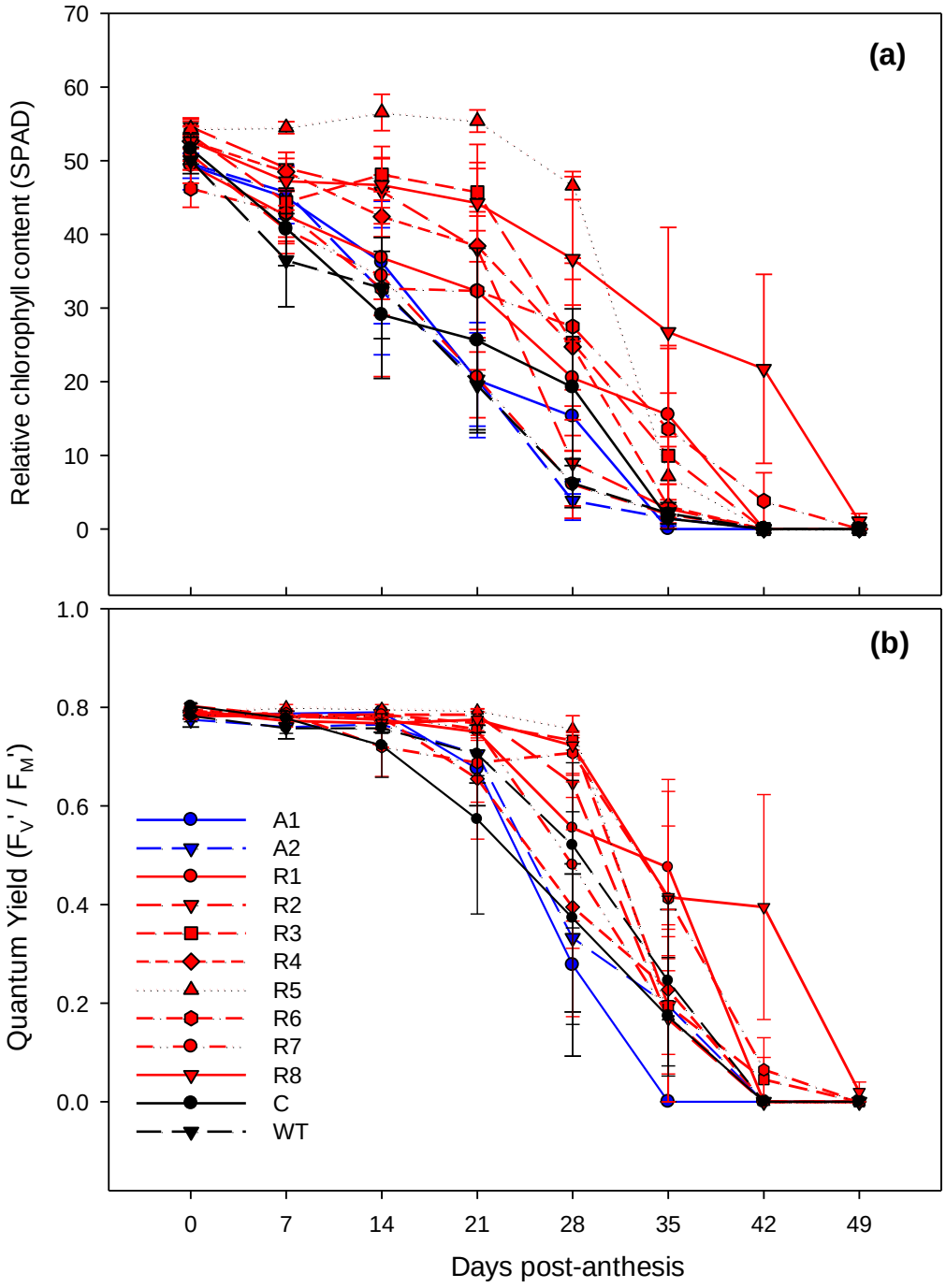

Figure 5.11: Progression of post-anthesis senescence of the second leaf of the main shoot of NAC-overexpressing wheat. (a) Relative chlorophyll content as determined with a SPAD meter. LSD = 15.66. **(b)** Quantum yield (F_V'/F_M'), which is a measure of Photosystem II efficiency. LSD = 0.230. A1-2 = pActin-NAC lines 1 and 2 (blue), R1-8 = pRTBV-NAC lines 1-8 (red), C = transformation control line and WT = Cadenza wild-type (black). Data are means ± SE of four replicate plants.

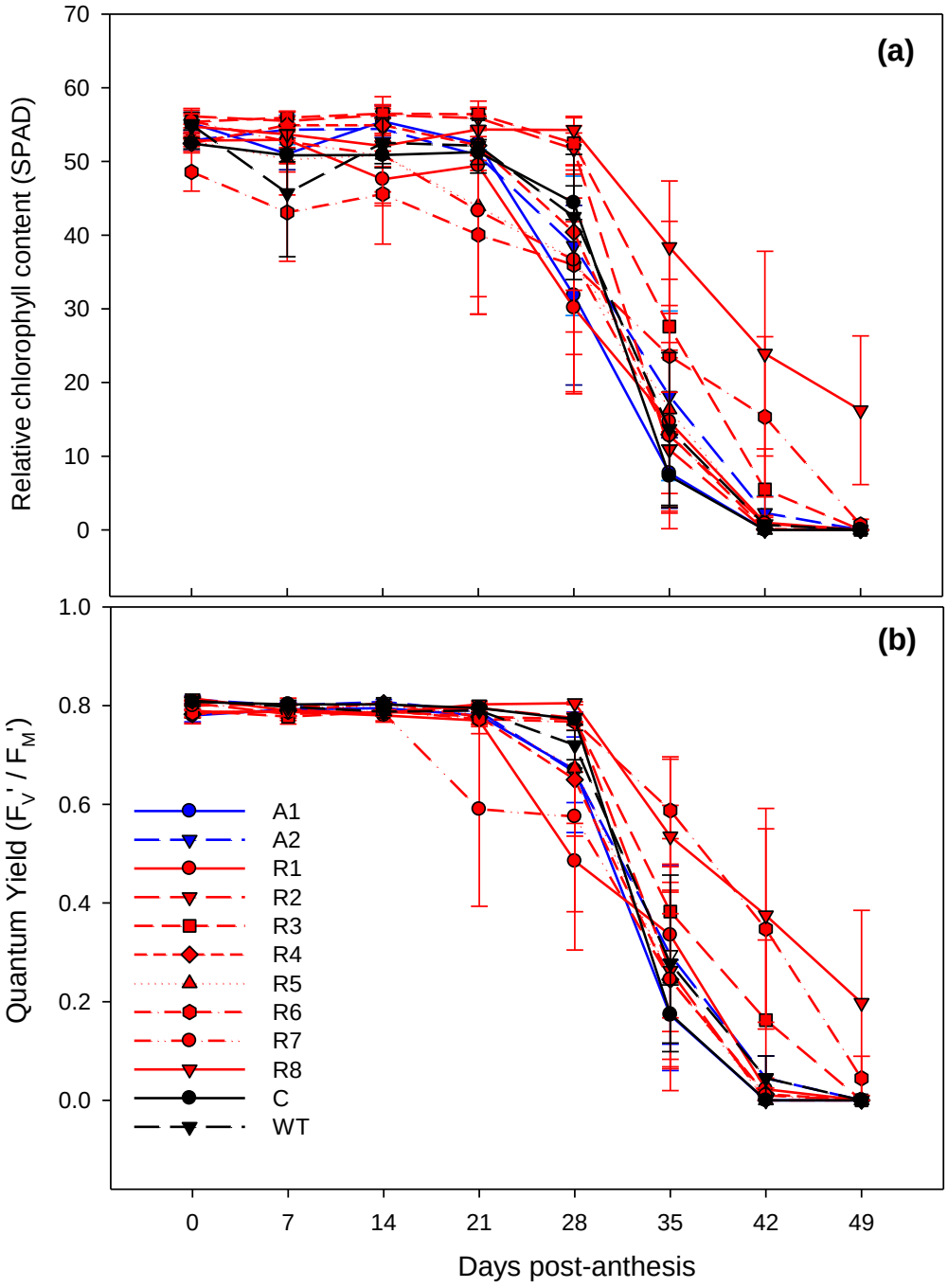

Figure 5.12: Progression of post-anthesis senescence of the flag leaf of the main shoot of NAC-overexpressing wheat. (a) Relative chlorophyll content as determined with a SPAD meter. LSD = 16.07. **(b)** Quantum yield (F_V'/F_M'), which is a measure of Photosystem II efficiency. LSD = 0.217. A1-2 = pActin-NAC lines 1 and 2 (blue), R1-8 = pRTBV-NAC lines 1-8 (red), C = transformation control line and WT = Cadenza wild-type (black). Data are means ± SE of four replicate plants.

5.4.4 Grain Yield

To see whether the differences in development and senescence resulted in differences in grain yield, total seed from all plants was collected and weighed. There was no significant difference in grain yield per plant between the constructs, but line R8 had a significantly lower grain yield than all the other lines (Figure 5.13.a). Since R8 had the lowest tiller number (Figure 5.8.a), the grain yield per ear was determined to see whether tiller number was a determining factor for grain yield. This turned out not to be the case, since grain yield per ear of R8 was significantly lower than that of both C and WT as well (Figure 5.13.b). R1, which is the line with the highest tiller number, turned out to have a significantly lower grain yield per ear than C and WT.

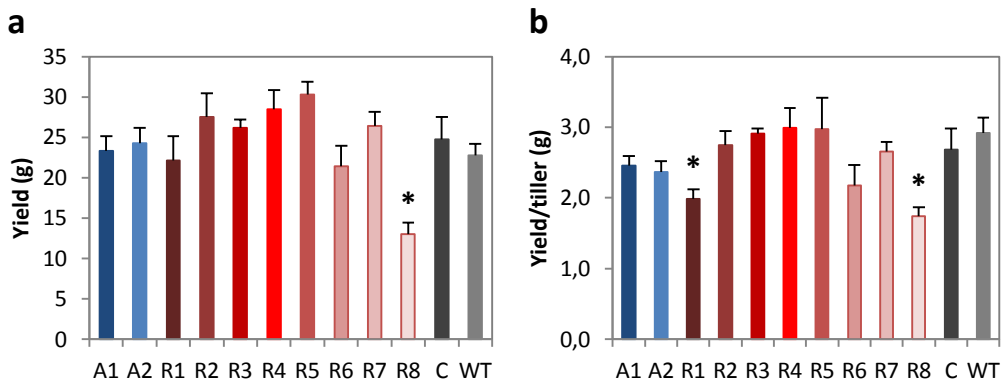

Figure 5.13: Grain yield per plant (a) and per ear (b) of NAC-overexpressing wheat. A1-2 = pActin-NAC lines 1 and 2 (blue), R1-8 = pRTBV-NAC lines 1-8 (red), C = transformation control line and WT = Cadenza wild-type (black). * significantly different from both C and WT ($P<0.05$). Data are means + SE of four replicate plants.

5.5 GENE EXPRESSION, BIOMASS AND GRAIN NITROGEN

5.5.1 Experimental Design

A second experiment was set up to measure the expression of the NAC gene during senescence, biomass differences and grain nitrogen concentration and content of a selection of the NAC-overexpressing lines. The lines included were the line with the greenest second leaf pRTBV-NAC 5 (R5), the line with the longest green duration of the second leaf pRTBV-NAC 8 (R8), an average stay-green line pRTBV-NAC 4 (R4), a line with the actin promoter pActin-NAC 1 (A1) and the transformation control line (C) as the line of reference.

5.5.2 Leaf Senescence

Before the gene expression and biomass distribution could be assessed, the behaviour of the lines compared to the previous experiment was evaluated. Since senescence is related to anthesis date, the anthesis date was determined first (Figure 5.14). As in the first experiment, R5 had a significantly later anthesis date than the control line ($P<0.05$). However, in contrast to the first experiment, A1 also reached anthesis later than C.

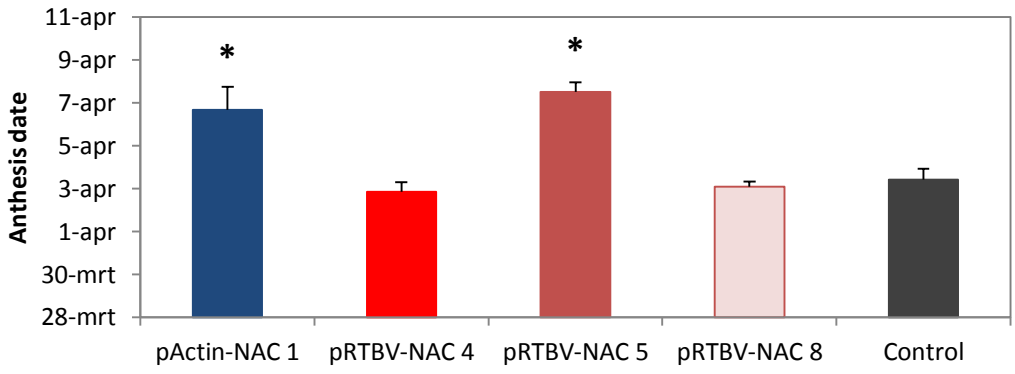

Figure 5.14: Anthesis date (in 2012) of a selection of NAC-overexpressing lines of wheat in the glasshouse. * significantly different from the control line ($P<0.05$). Data are means + SE of three replicate plants.

Senescence of the top three leaves of the main shoot was measured at four time points (Figure 5.15). Since senescence differed between the replicate blocks, the time points were taken per block at matching senescence states of the plants. All four transgenic lines had significantly greener flag leaves than the control line ($P<0.01$). R5 had significantly greener second and third leaves than the other lines. This is mainly explained by the limited senescence of R5 leaves, confirming the stay-green phenotype of R5 that was observed in the previous experiment (Figures 5.10, 5.11 and 5.12). As previously found, R4 displayed a stay-green phenotype in this experiment. In contrast to the previous experiment, A1 now displayed a stay-green phenotype. Unexpectedly, line R8, which stayed the greenest for longer in the first experiment, now showed a similar senescence pattern to the control line.

5.5.3 Gene Expression

The second leaves of the main shoots were sampled for gene expression analysis. However, since the main goal of the experiment was to measure NAC expression during senescence, leaves that were fully senesced were not sampled, but a leaf from another tiller was taken instead. The most-senesced leaves did not contain enough RNA for gene expression analysis. This is why the greenness of the leaves used for gene expression studies (Figure 5.16) does not fully match that of the senescence of the second leaf of the main shoot (Figure 5.15.b).

To check if senescence at the molecular level matches senescence as measured with a SPAD meter, expression of the marker genes *RBCS* and *SAG12* was determined by semi-quantitative RT-PCR. As expected, *RBCS* expression decreased during senescence (Figure 5.17.a), and correlated significantly with greenness (Figure 5.17.b; $P<0.01$). *SAG12* showed the opposite pattern with an increase in expression in senescing less-green leaves (Figure 5.18). For both marker genes the expression changed least in R5, validating its stay-green phenotype.

Total expression of the NAC gene (endogenous and transgenic) was very low in the control line (Figure 5.19.a). The difference with the transgenic lines was about ten-fold. Overall, total NAC expression was correlated with greenness (Figure 5.20.a; $P<0.001$), but this was mainly driven by expression of line R4, which showed a strong increase in expression in time (Figure 5.19.a). In all lines endogenous NAC expression decreased in time (Figure 5.19.b), and positively correlated with senescence (Figure 5.20.b; $P<0.01$). Expression of the transgenic NAC gene was absent in line C, while it increased in lines A1, R4 and R5 (Figure 5.19.c). There was a significant relationship with leaf greenness (Figure 5.20.c; $P<0.001$), following the same pattern as total NAC expression (Figure 5.20.a).

Overall, total NAC expression correlated significantly with transgenic NAC expression ($P<0.001$) but not with endogenous NAC expression (Figure 5.21), indicating the transgenic approach raised NAC expression in leaves throughout the whole senescence period.

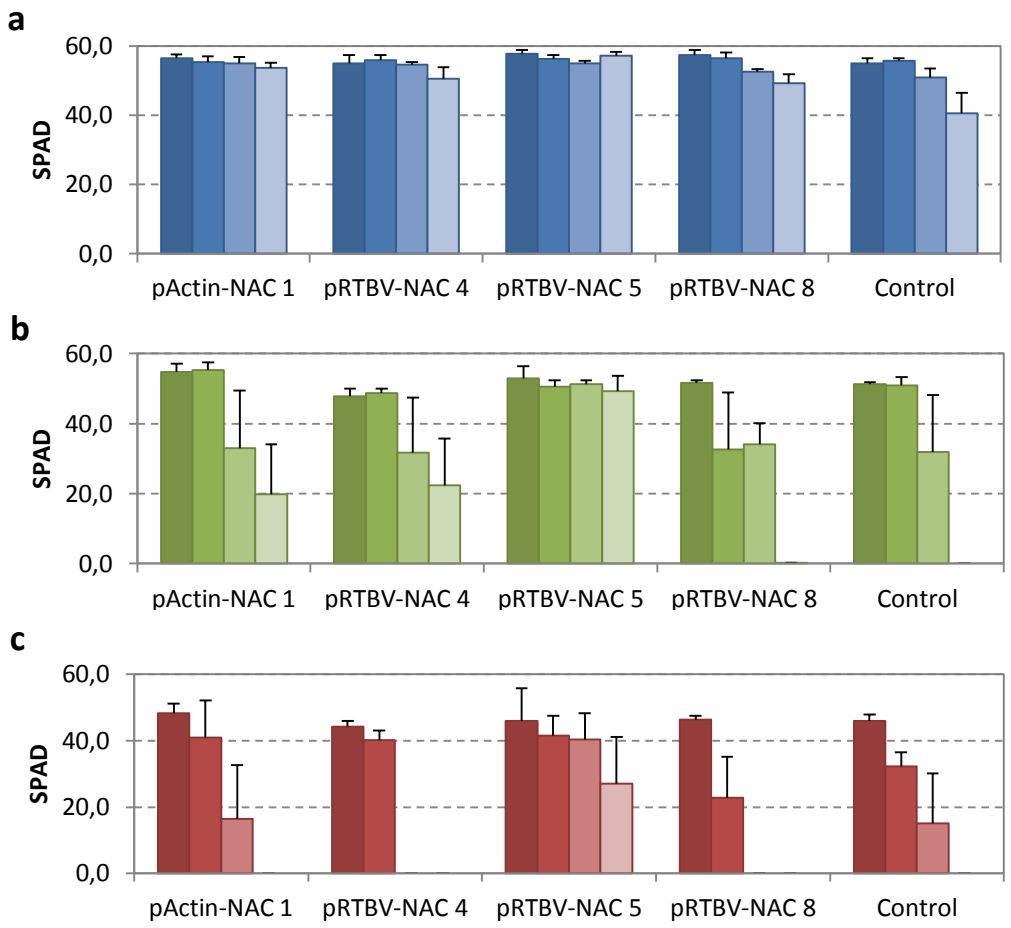

Figure 5.15: Senescence of the flag leaf (a), second leaf (b) and third leaf (c) of the main shoot of a selection of NAC-overexpressing lines of wheat as determined with a SPAD meter. Measurements were done at four time points starting at anthesis and ending when control second leaves were fully senesced. Data are means + SE of three replicate plants.

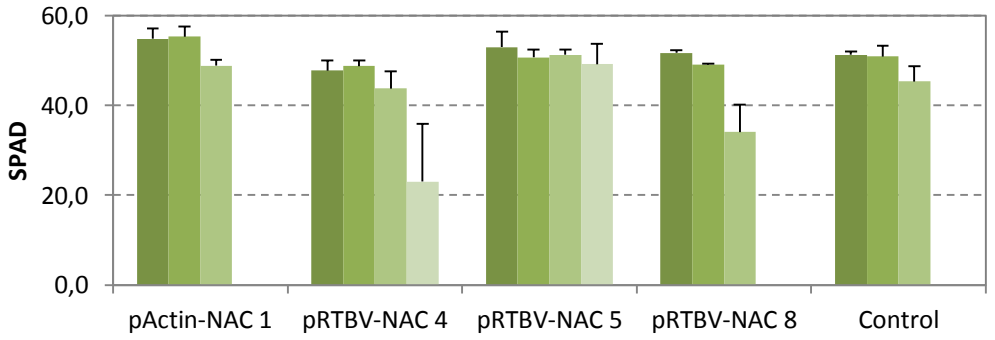

Figure 5.16: Senescence status of the second leaves of a selection of NAC-overexpressing lines of wheat that were actually used for gene expression analysis. Data are means + SE of three replicate plants.

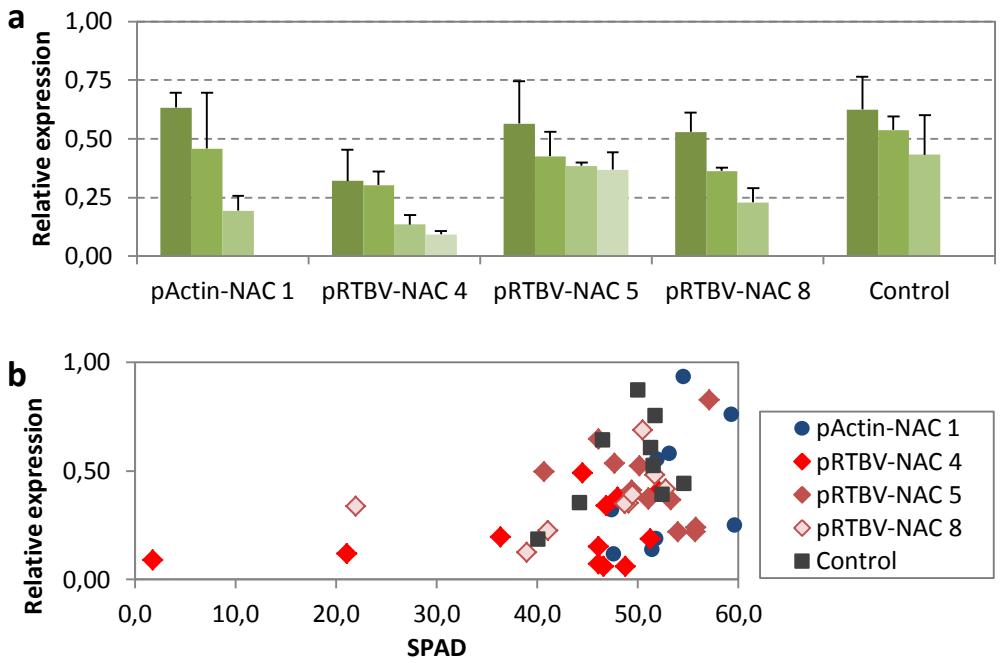

Figure 5.17: Relative *RBCS* expression during senescence of the second leaf (a) and the relation of *RBCS* expression with greenness (b) of a selection of NAC-overexpressing lines of wheat. (a) Data are means + SE of three replicate plants. (b) Data points represent individual plants.

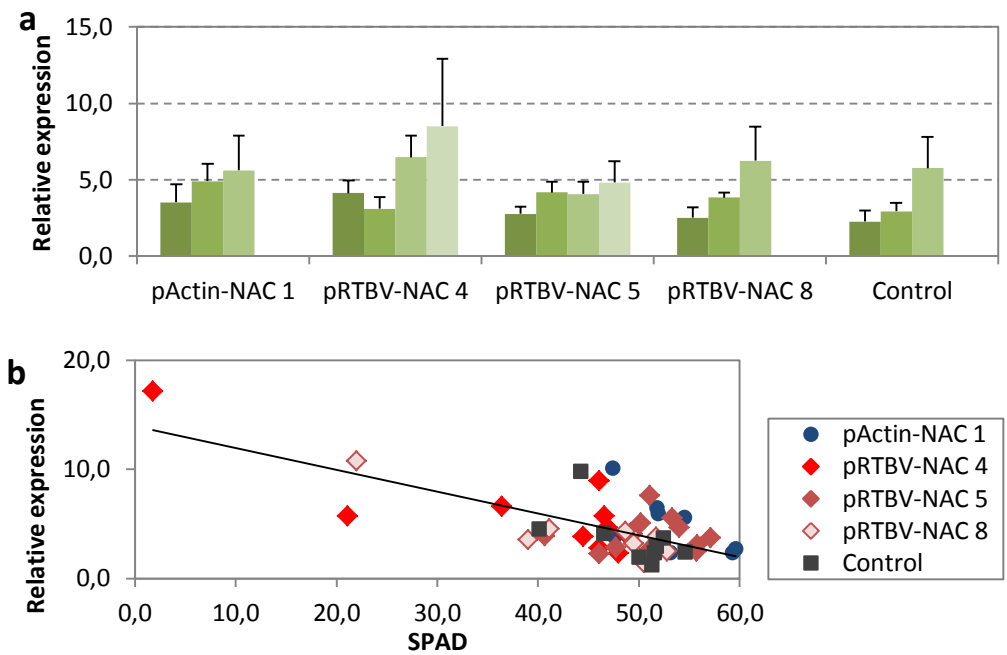

Figure 5.18: Relative *SAG12* expression during senescence of the second leaf (a) and the relation of *SAG12* expression with greenness (b) of a selection of NAC-overexpressing lines of wheat. (a) Data are means + SE of three replicate plants. (b) Data points represent individual plants. y = -0.2003x + 13.975; R^2 = 0.4811; P < 0.001.

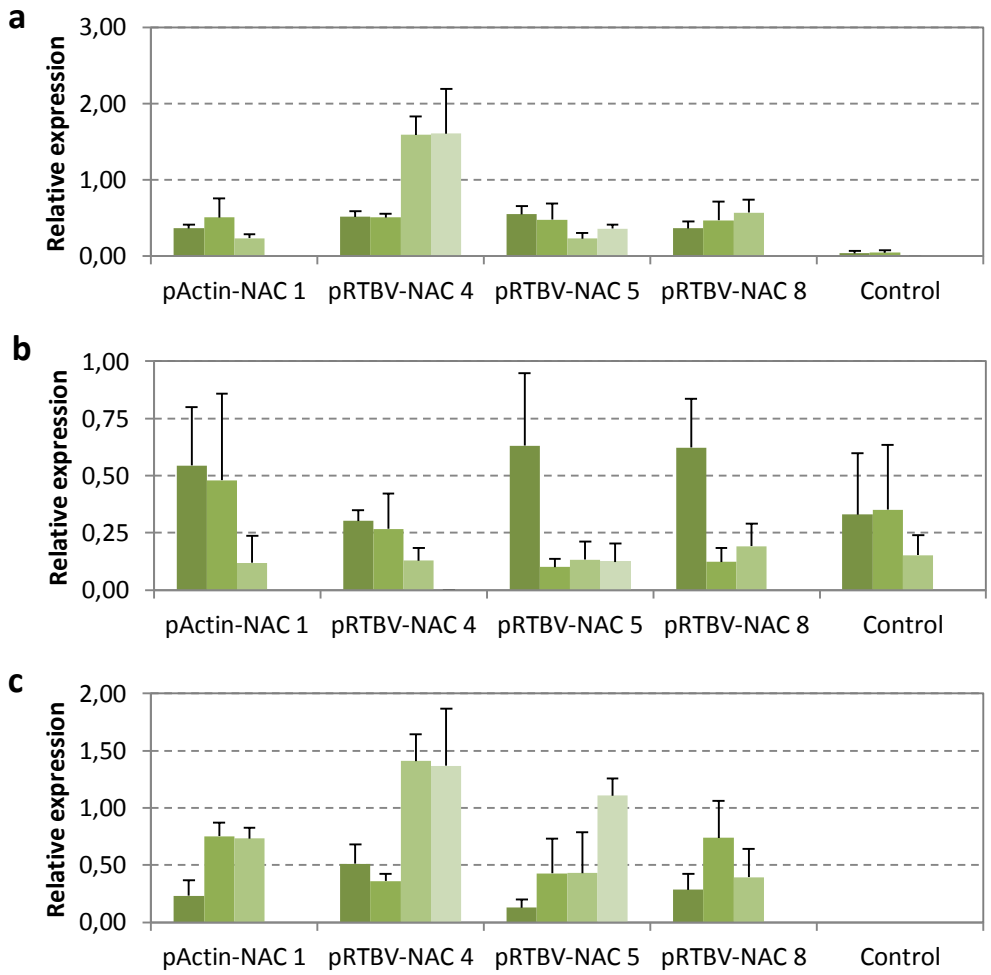

Figure 5.19: Relative total expression of the NAC gene (a), and expression of the endogenous NAC gene (b) and the transgenic NAC gene (c) during senescence of a selection of NAC-overexpressing lines of wheat. Data are means + SE of three replicate plants.

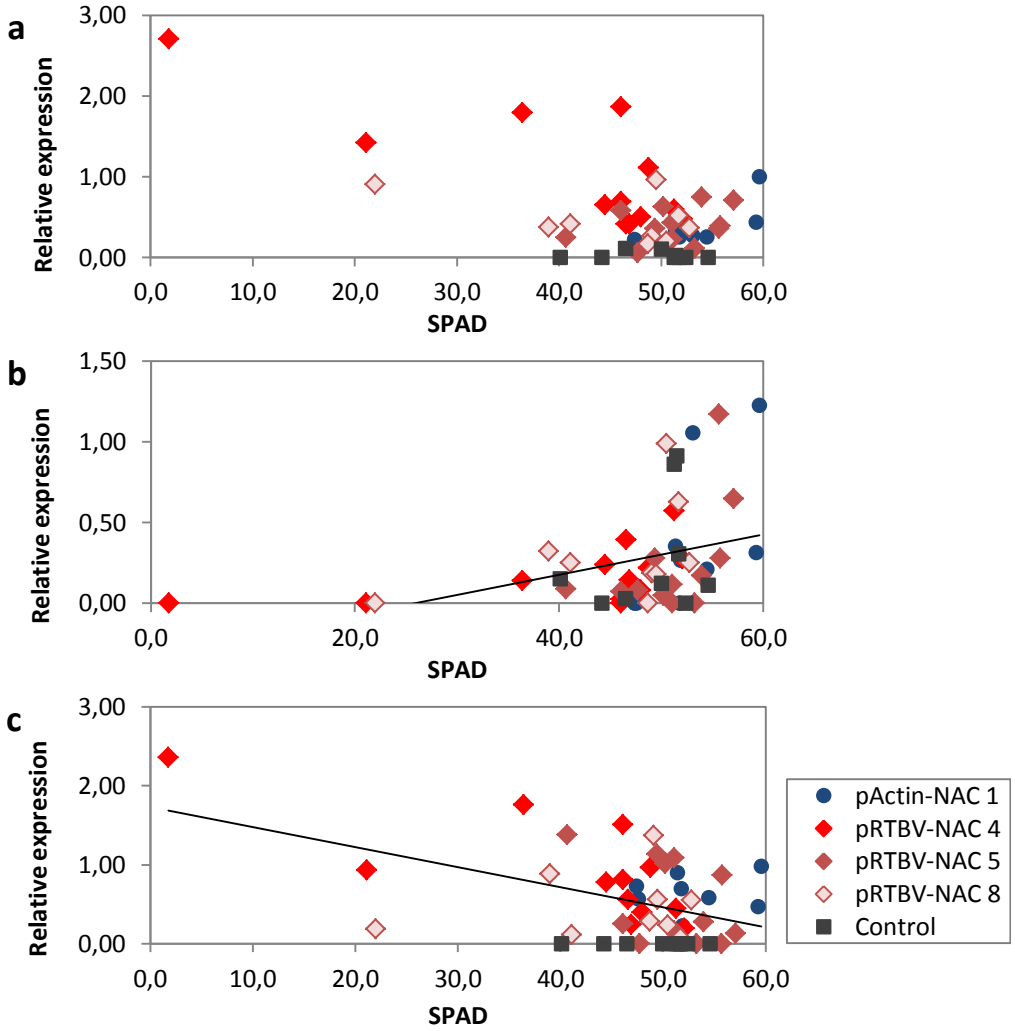

Figure 5.20: Relation of greenness with relative total expression of the NAC gene (a), expression of the endogenous NAC gene (b) and expression of the transgenic NAC gene (c) during senescence of a selection of NAC-overexpressing lines of wheat. Data points represent individual plants. (a) n.s., (b) $y = 0.0125x - 0.3237$; $R^2 = 0.1400$; $P = 0.0068$ and (c) $y = -0.0255x + 1.735$; $R^2 = 0.2170$; $P = 0.0006$.

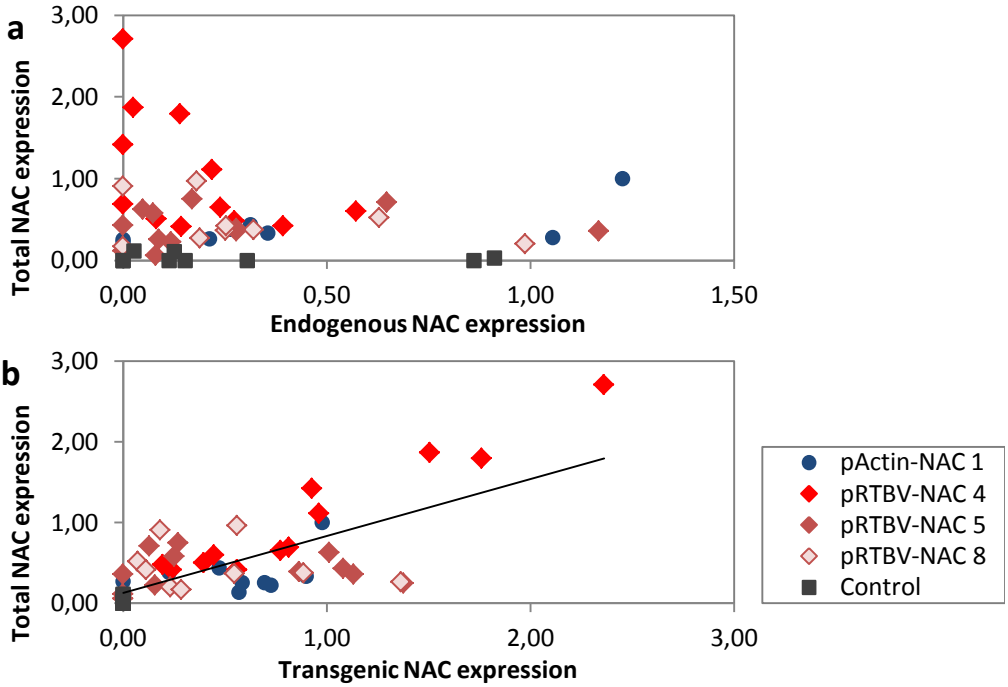

Figure 5.21: Relation between expression of the endogenous NAC gene and relative total NAC expression (a), and between expression of the transgenic NAC gene and total NAC expression (b) during senescence of a selection of NAC-overexpressing lines of wheat. Data points represent individual plants. (a) n.s. and (b) $y = 0.7063x - 0.1264$; $R^2 = 0.5128$; $P < 0.001$.

5.5.4 Biomass Accumulation and Grain Yield

Total biomass increased significantly between anthesis and maturity (Figure 5.22; $P<0.05$), indicating photosynthesis was still taking place. There was no significant interaction between line and time. Overall, R8 had a significantly lower biomass than most of the lines, which since the number of tillers did not differ (Figure 5.8.a), must be explained by its reduced height (Figure 5.7). Surprisingly, control line C had a relatively low biomass at anthesis and the highest biomass at maturity, suggesting it had the highest photosynthetic production during the grain-filling period.

There were no significant differences between the lines in grain and straw yields and the harvest index, but patterns can be observed (Figure 5.23). The control line had the highest straw and chaff yield and an average grain yield, resulting in the lowest harvest index. In contrast, stay-green line R5 had the highest grain yield and average straw yield, resulting in the highest harvest index. R8, A1 and R4 had near identical harvest indexes that were between C and R5.

5.5.5 Grain Nitrogen Concentration and Content

Grain nitrogen concentrations differed significantly between the lines ($P<0.01$). R8 had a significantly higher nitrogen concentration than C, while the other lines had intermediate grain nitrogen concentrations (Figure 5.24.a). Total grain nitrogen content did not differ significantly between the lines. R5 had the highest grain N content (Figure 5.24.b), because it had the highest grain yield (Figure 5.23.a). Despite the low grain yield of R8 (Figure 5.23.a), its high grain N concentration resulted in the second highest N content (Figure 5.24). Over the whole experiment, grain N concentration correlated significantly with grain yield ($P<0.001$). However, at similar grain yields as control plants, the transgenic plants reached higher grain N concentrations (Figure 5.25; compare dashed and solid lines). The differences were greater at lower grain yields.

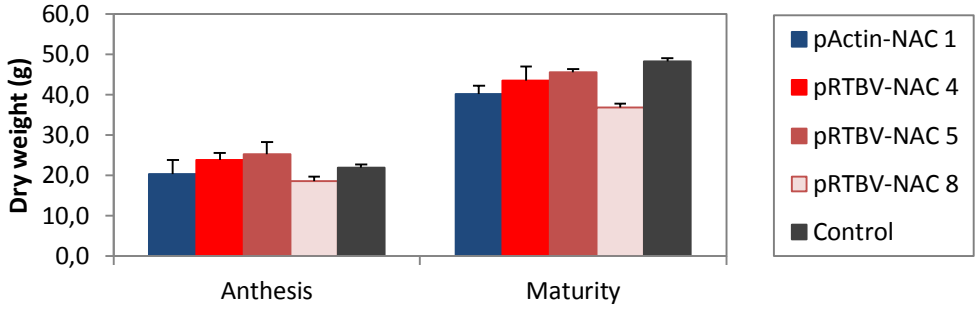

Figure 5.22: Aboveground biomass per plant at anthesis and maturity of a selection of NAC-overexpressing lines of wheat. Data are means + SE of four replicate plants at anthesis (GS61) and nine replicate plants at maturity (GS92).

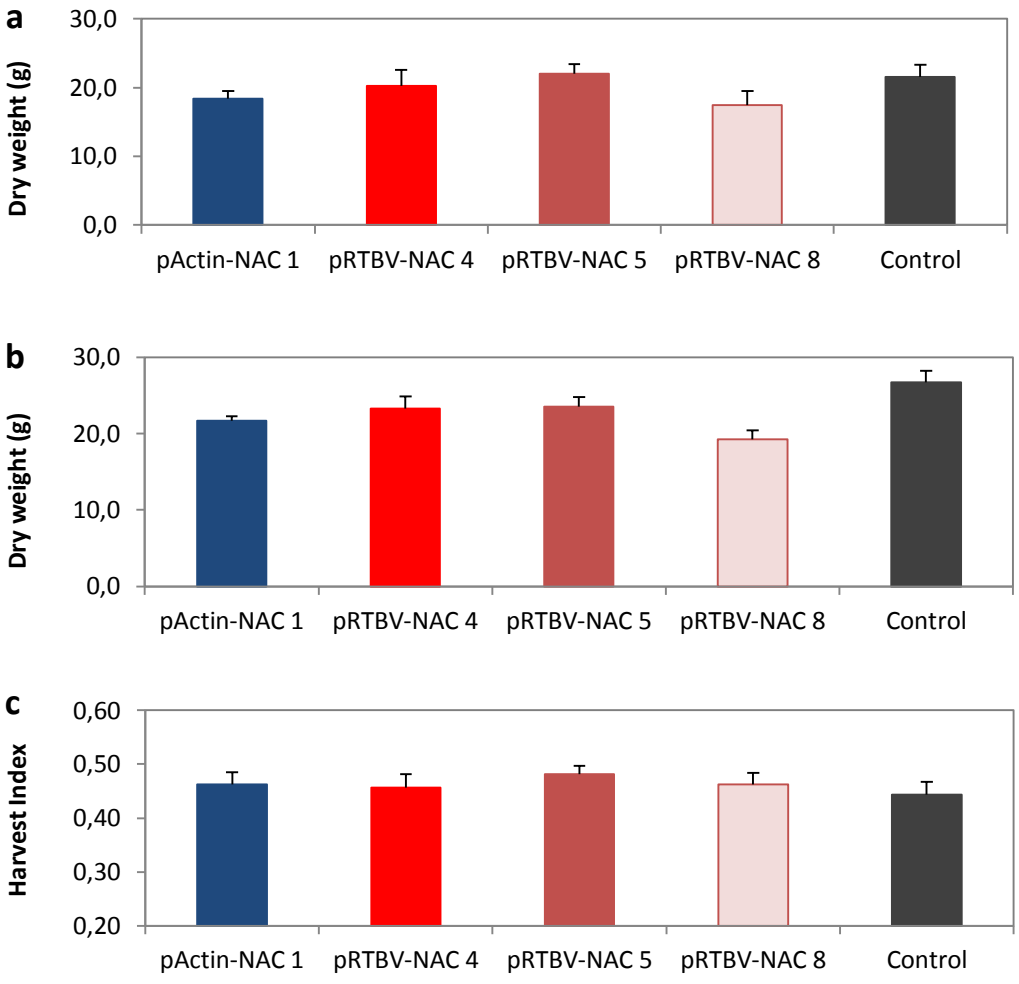

Figure 5.23: Grain yield per plant (a), straw and chaff yield per plant (b) and harvest index (c) of a selection of NAC-overexpressing lines of harvest-ready wheat. Data are means + SE of nine replicate plants.

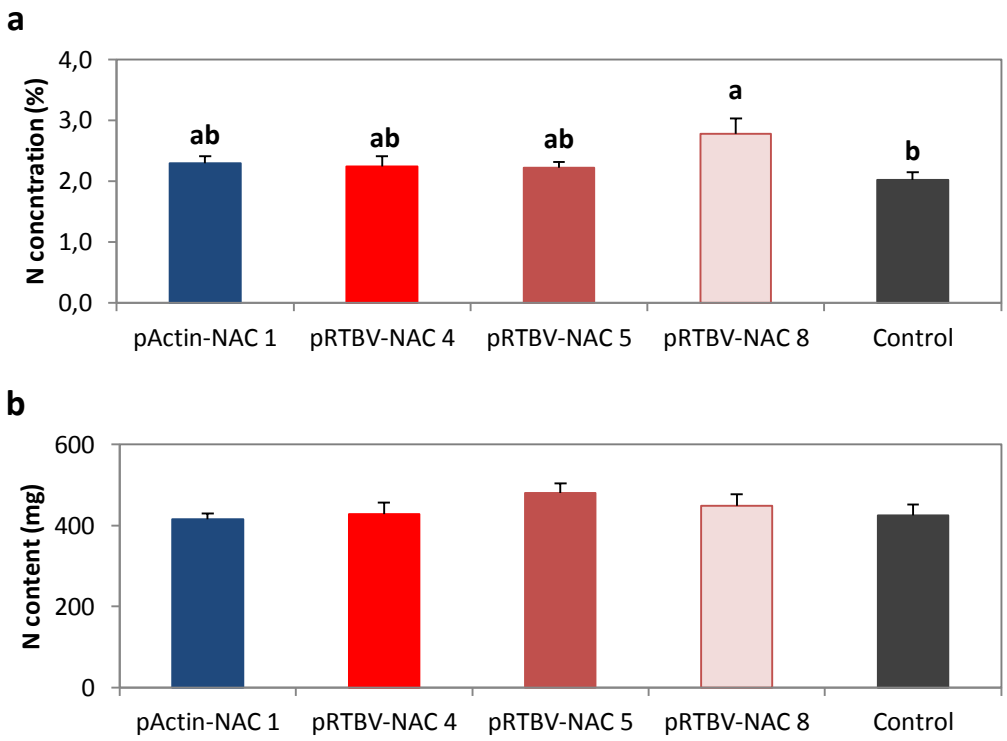

Figure 5.24: Grain nitrogen concentration (a) and total grain nitrogen content (b) of a selection of NAC-overexpressing lines of harvest-ready wheat. Data are means + SE of nine replicate plants. Letters indicate significant differences at the 0.05 level as determined by using the LSD.

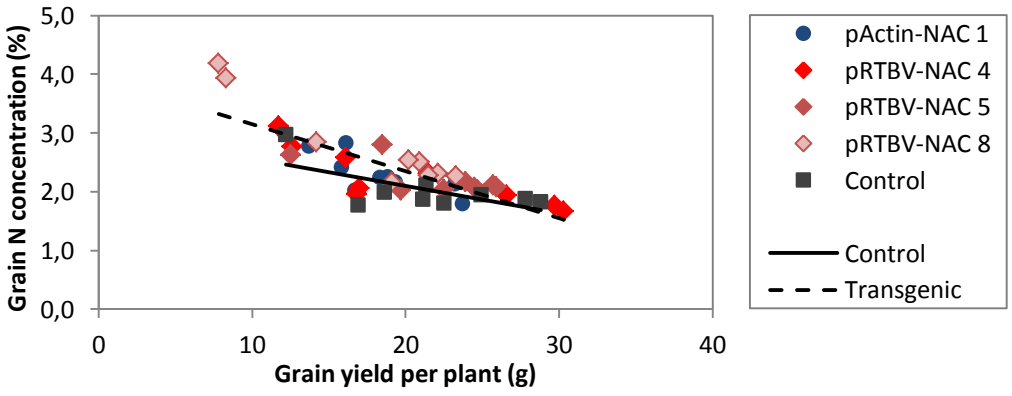

Figure 5.25: Relationship between grain yield per plant (GY) and grain nitrogen concentration (GNC) of a control line (solid line) and of a selection of transgenic NAC-overexpressing lines of wheat (dashed line). Each data point represents one plant. Control: $y = -0.0467x + 3.0323$; $R^2 = 0.4389$; $P < 0.05$. Transgenic: $y = -0.0802x + 3.9532$; $R^2 = 0.6662$; $P < 0.001$.

5.6 DISCUSSION AND CONCLUSIONS

The expression of the endogenous wheat NAC gene decreased with senescence (Chapter 3 and Figure 5.19.b), indicating the gene is a potential negative regulator of leaf senescence. NAC genes that are negative regulators of senescence seem to be quite rare: so far only the *JUB1* gene has been unequivocally identified as a regulator of senescence (Wu et al., 2012). Apart from this example, a wheat gene showing strong homology with rice *NAC2* was identified in a transcriptome study comparing *GPC*-RNAi with wild-type wheat during senescence (Cantu et al., 2011), but its function has not been determined.

NAC overexpression under the RTBV promoter resulted in delayed leaf senescence, whilst overexpression under the actin promoter did not alter leaf senescence in most cases (Figures 5.10, 5.11, 5.12 and 5.15). In the most detailed experiment, line R8 was the only line that maintained a higher chlorophyll content and / or photosystem II capacity than wild-type and control in all three top leaves (Figures 5.10, 5.11 and 5.12). Line R5 had especially green second leaves, while R5, R2, R3 R6 and R7 all had significantly higher chlorophyll content in the third leaf at some point during senescence. In another experiment, the top three leaves of R5 clearly stayed the greenest, while R4 and A1 also maintained greener than C (Figure 5.15). R8 performed similar to wild-type in the second experiment (Figure 5.15), while in the initial detailed experiment it was the line that clearly stayed the greenest for longest (Figures 5.10, 5.11 and 5.12).

The differences between the two experiments can partly be explained by environmental conditions, even in the relative constant conditions of the glasshouse. In the second experiment the plants experienced an unexpected hot and sunny week in March about one week after anthesis, inducing rapid senescence. In the first experiment senescence progressed more gradually,

less influenced by fluctuations in temperature. The senescence data from the first experiment are therefore probably more reliable.

Grain yields and aboveground biomass were not significantly different between NAC-overexpressing and control lines (Figures 5.13, 5.22 and 5.23.a), although the most stable stay-green line R5 had the highest grain yield and seemed to have a relatively high harvest index (Figure 5.23.c). Surprisingly, the control line had the biggest post-anthesis biomass gain, suggesting that the stay-green lines did not have a higher post-anthesis photosynthetic production. These results confirm the hypothesis that grain yield is generally not source-limited, as has been found before for wheat, including stay-green varieties (Borrás et al., 2004; Gong et al., 2005).

Grain nitrogen concentration and content were higher for the four examined NAC-overexpressing lines than for the control plants (Figure 5.24). Transgenic plants reached higher grain N concentrations at similar grain yields, especially when grain yield was relatively low (Figure 5.25). Line R8 had the highest grain N concentration but the lowest grain yield, so its high N concentration was probably caused by less carbon dilution, although this cannot be known for certain without information about the grain number. Line R5 had the highest grain N content, which was due to its relatively high grain yield. Since control plants had the highest straw biomass (Figure 5.23.b), it can be speculated they invested relatively more nitrogen in the vegetative parts and less into the grain. However, nitrogen concentration and content data for the whole plant are required to be able to discriminate between a lower nitrogen harvest index and a lower N uptake.

Line R8 was dissimilar from the other lines in development and morphology: short in stature, initially few but late developing tillers, and fewer and wider leaves (Figures 5.5, 5.6, 5.7, 5.8, 5.9 and 5.13). In the first experiment R8 coupled an early developing main shoot with late maturation (Figure 5.5), and therefore had greater post-anthesis longevity. In the second experiment it

reacted very strongly to a short peak in temperature, inducing fast senescence, suggesting it did not well tolerate stress conditions. Expression levels of the transgene did not seem much different from that of the other transgenic lines. It could be that the transgene was inserted into a gene or an active genomic region, affecting function or expression of other genes.

For the expression results it is important to remember that no gene expression data are available for the last time point for three of the lines. Expression in later stages of senescence is therefore difficult to compare. Line R4 had the highest NAC expression but not the strongest stay-green phenotype. This indicates that the level of overexpression was not directly correlated with the stay-green phenotype, but that expression probably had to be above a certain threshold. Transgenic NAC expression increased across the senescence time course, suggesting that the RTBV and actin promoters were more active in later stages of leaf development, or alternatively, that the transgenic RNA was not degraded very efficiently.

The observation that NAC overexpression under the actin promoter did not usually result in a phenotype is remarkable. The actin promoter is constitutively expressed (Zhang et al., 1991) and therefore should be expressed in leaves too, so it is not obvious why there was no effect. The RTBV promoter is supposed to be more strongly expressed in wheat leaves than the actin promoter (Rothamsted Cereal Transformation Group, unpublished), although this has not been confirmed throughout leaf development. Alternatively, the timing of expression in the leaves could be different. It is also possible that expression in other plant organs under the actin promoter interferes with the effect of the expression in leaf tissues.

Apart from the changes in leaf senescence, the overexpression lines did not show any other consistent change in phenotype. Therefore it is likely the function of the NAC gene is primarily in the regulation of leaf senescence. Expression analysis has shown the closest rice gene, Os08g10080, is

differentially expressed in response to infection with the rice tungro spherical virus (Nuruzzaman et al., 2010) and mild drought stress (Nuruzzaman et al., 2012). This could indicate a function in stress responses, although the opposite expression pattern for different stresses contradicts this. Since orthologous NAC transcription factors in wheat and rice have been shown to have diverse functions (Distelfeld et al., 2012), the rice expression does not necessarily have relevance for the wheat gene. However, since many genes involved in senescence are also involved in stress responses, the response of the wheat NAC gene to different stressors would be an obvious topic for further investigation.

The greenness of leaves is a measure of leaf nitrogen content (Richardson et al., 2002). In agreement with this, the stay-green trait was found to be positively correlated to nitrogen use efficiency (Gaju et al., 2011). Therefore the response of the NAC-overexpressing lines to differences in nitrogen nutrition would be of interest.

It has been hypothesised that maintenance of N uptake during grain-filling is determined by the carbon supply to the roots and that this would result in a stay-green phenotype by less N remobilisation from the leaves (Rajcan and Tollenaar, 1999b). Furthermore, higher than expected grain N concentrations as found for the NAC-overexpressing lines (Figure 5.25) have been shown to be mainly determined by N uptake (Bogard et al., 2010). Therefore it would be interesting to know whether there are differences in N uptake between the lines, both pre- and post-anthesis, and whether such differences could be explained by differences in root biomass or morphology.

In summary, a NAC1-type NAC transcription factor with decreasing expression in leaf senescence of wheat has been identified. Overexpression of this NAC gene in wheat resulted in delayed leaf senescence and increased grain nitrogen concentrations, but had no significant effects on shoot biomass or grain yield.

6. FUNCTIONAL STUDY OF A SENESCENCE-ASSOCIATED WRKY TRANSCRIPTION FACTOR IN WHEAT

6.1 INTRODUCTION

Members of the WRKY transcription factor superfamily have been shown to be involved in many physiological and developmental processes, such as hormone signalling, abiotic stress and disease responses, wounding, embryogenesis, cell maturation in roots, seed coat and trichome development, seed germination, and biosynthesis of anthocyanin, starch and sesquiterpene (Ülker and Somssich, 2004; Xie et al., 2005). Several senescence-associated WRKY genes have been described in Arabidopsis (Besseau et al., 2012; Hinderhofer and Zentgraf, 2001; Robatzek and Somssich, 2001; Ülker et al., 2007; Zhou et al., 2011b) and rice (Jing et al., 2009; Ricachenevsky et al., 2010). In wheat four WRKY genes were up-regulated in senescing leaves (Wu et al., 2008a), but these genes were not functionally analysed.

A transcriptomics study of six winter wheat varieties grown at multiple levels of nitrogen (Hawkesford and Howarth, 2010) resulted in a list of candidate genes that might be involved in leaf senescence and nitrogen remobilisation during grain-filling (Howarth et al, unpublished). To corroborate the expression patterns of several of these genes, their expression was evaluated during senescence of wheat cultivar Hereward and two Avalon x Cadenza doubled haploid lines grown under different nitrogen levels in the field in multiple years (Chapter 3) and in wild-type and a fast-senescing mutant lines of wheat cultivar Paragon grown at two N levels (Section 4.4.7). The increasing expression of this WRKY transcription factor during senescence in all tested leaf materials suggested this gene could be a positive regulator of

leaf senescence in wheat. The role of this WRKY transcription factor in senescence was studied in more detail.

The aims of the experiments reported in this chapter were:

1. To establish the possible identity of the WRKY gene by analysing its sequence and phylogeny.
2. To analyse the effects of RNAi knockdown of the WRKY gene on morphology, development, senescence and grain yield of wheat.
3. To determine in which plant tissues the WRKY gene is expressed.

6.2 SEQUENCE AND PHYLOGENETIC ANALYSES

WRKY transcription factors are defined by the presence of one or two WRKY domains: the conserved amino acid sequence WRKYGQK plus a unique zinc-finger-like motif structure of the form $CX_{4–5}CX_{22–23}HXH$ (Eulgem et al., 2000).

Since attempts to obtain the full coding sequence of the WRKY gene by PCR were not successful (data not shown), only the C-terminal part of the gene was available for evaluation. This fragment of the wheat WRKY gene does actually not contain the nucleotides coding for the four tell-tale WRKY amino acids, but its identity as a WRKY transcription factor is revealed by the presence of the second part of the WRKY domain at the start of the sequence: the zinc-finger motif unique to WRKY transcription factors (Figure 6.1).

To determine the relationship with previously described WRKY genes, a phylogenetic tree of WRKY protein sequences was constructed (Figure 6.2). This tree encompasses all senescence-related WRKY genes in all other plant species (Arabidopsis, rice, and wheat), all rice (cv. Japonica) WRKY proteins, and all described wheat WRKY proteins so far. The WRKY gene displayed most resemblance to the rice genes Os02g47060 *(OsWRKY66)* and Os04g50920 *(OsWRKY37)*. Neither gene has been characterised in detail.

a. DNA sequence of the wheat WRKY gene (fragment)

TTCCCCATACCCAAGAGGGTACTACAGATGCAGTAGCTCCAAGGGGTGCCCTGCACGGAAGCAA
GTGGAGCGCAGCCGGACGGACCCCAACATGCTGGTCATCACCTACACCTCGGAGCACAACCACC
CCGTGGCCGACGCAGCGCAACGTGCTCGCCGGCTCCACTCGGTCCCACTACGCGAAGAACAGCAG
CAACACAGATGCAGCTTCGTCCAAGAACAGCAAGAACTCCTCGCGCAACCAGCACAAGCCAGTC
GTCAAGGCAGAATCAAAGGACCAATCCGCCGCCACCCCGGCCGCGACGAGCACGACCACCACG
GCGACCACAAGCACCGGCAACAACACACCTCCGATGGCTGTGAAAGAGGAGGCAGAAATGGAG
AGAAGGATAGGCGGTGATACTACAGCAACGGTGGGTTATTACAGTGACCATCTCCTGCAGCAGA
TGTTCAGCCAGAGCTACAGGCCGATGATGCCCGAGGAGGCCGGCGGCTATCACCACCAGGACG
ACTTCTTCGCCGACCTCACTGAGCTGGACTCCGACCCTGTCAGCCTCATCTTCTCCACGGAGTACA
TGGAGGCCAGACCTGGCAAGGAGAAGGCAGCAGCCAAGGACGACGTGGATTCATTATTCATGA
TGGACTGGGCGCCCGCTAGTGCTGCTGTTACTACTTCTGCAGGGAGCGCGCTTGAGCAAGGGG
ACATGGGTTTA**TGA***gttttgacgtcaattagttaccttaaaacataccaggcttgcaccatcgatgcatgtgcaaatg*
cgaacaccacatttgaggacatttagatataggcttgaaataaccttgatgataacaggagcaagaaaaggaaagtat
gggttttccccctctctctttactctttatattagttattacacactgcgtgctccttcctgatgttattgagtatggtttgttgaa
gatgatctagtatatagtac

b. Protein sequence of the wheat WRKY gene (fragment)

SPYPRGYYRCSSSKGCPARKQVERSRTDPNMLVITYTSEHNHPWPTQRNVLAGSTRSHYAKNSSNT
DAASSKNSKNSSRNQHKPVVKAESKDQSAATPAATSTTTTATTSTGNNTPPMAVKEEAEMERRIGG
DTTATVGYYSDHLLQQMFSQSYRPMMPEEAGGYHHQDDFFADLTELDSDPVSLIFSTEYMEARPGK
EKAAAKDDVDSLFMMDWAPASAAVTTSAGSALEQGDMGL

Figure 6.1: Sequence analysis of the wheat WRKY gene. (a) The DNA sequence and **(b)** the translated protein sequence. The (incomplete) WRKY domain is highlighted in yellow with the zinc-finger domain underlined and the fragment used for RNAi in green. Coding nucleotides are capitalised, the stop coding in **bold**, and the nucleotides in the 3'-untranslated region are in lower case *italics*.

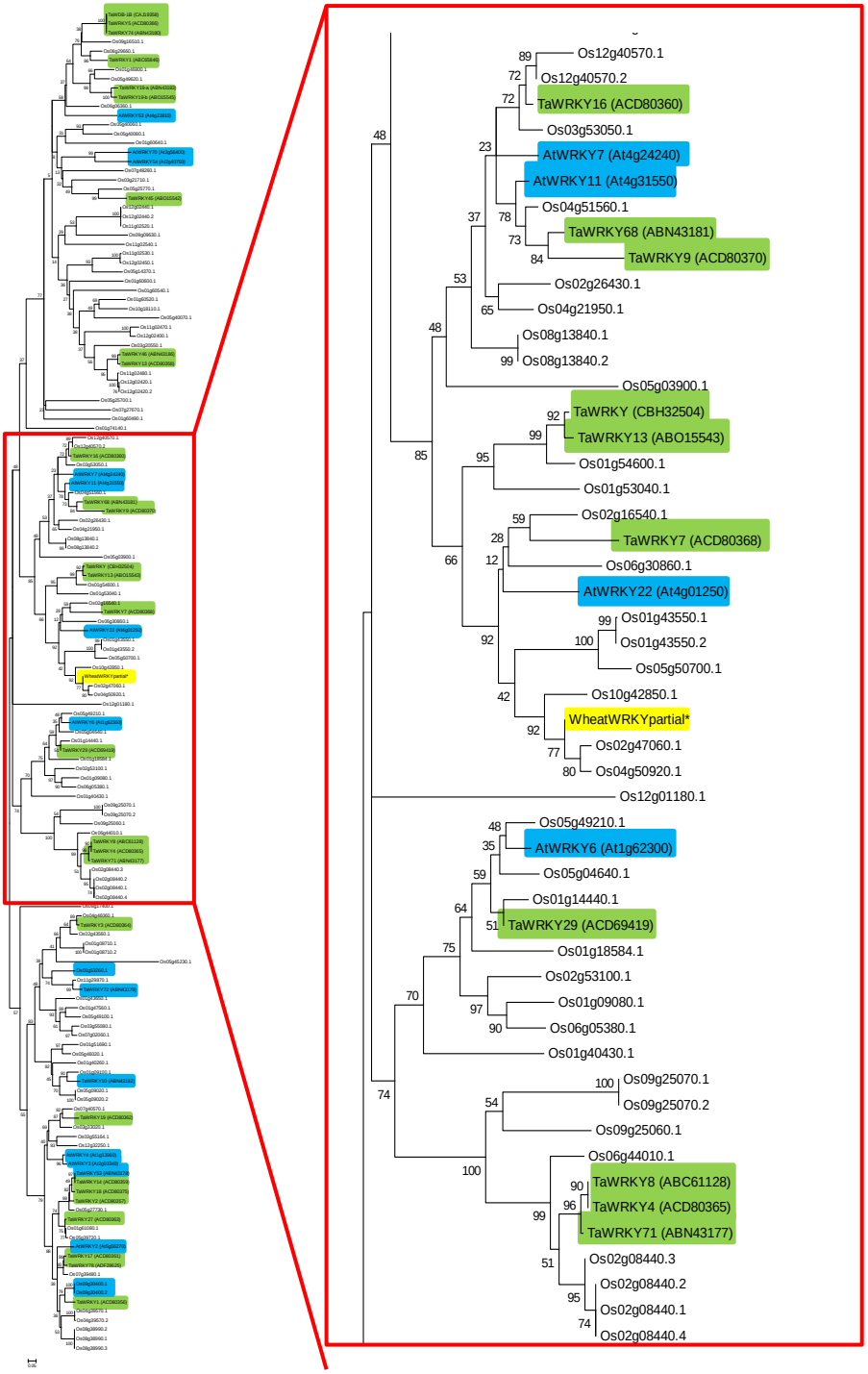

Figure 6.2: Phylogenetic analysis of the wheat WRKY protein fragment (yellow*), senescence-associated WRKY proteins from all plant species (blue), other known wheat WRKY protein sequences (green), and all remaining known rice WRKY proteins (white). Amino acids within the WRKY domains were aligned in MEGA5 using the ClustalW algorithm (Larkin et al., 2007). The phylogenetic tree was constructed using the Neighbor-Joining method (Tamura et al., 2011). Bootstrap values of 1000 replicates are indicated at each node.

6.3 RNAi-KNOCKDOWN OF THE WRKY GENE IN WHEAT

6.3.1 Creation of WRKY-RNAi-Knockdown Wheat

Expression of the WRKY transcription factor was found to be correlated with senescence of the second leaf of wheat (Chapter 3). This correlation in itself is not evidence for an actual role of this gene in leaf senescence. To get a better idea of the role of this WRKY gene in leaf senescence, or in any other aspect of wheat development, a transgenics approach was employed to manipulate WRKY gene expression. Since expression of the WRKY gene increased during senescence, it was anticipated that knockdown of the WRKY gene may delay leaf senescence if it has a regulatory role in leaf senescence.

Two RNAi-constructs containing different promoters were used (Figure 6.3): one containing the rice tungro bacilliform virus (RTBV) promoter which has strong expression in wheat leaves (Rothamsted Cereal Transformation Group, unpublished), and another containing the rice *actin1* promoter which is considered to be constitutively expressed in all tissues (Zhang et al., 1991).

The two constructs were used to transform the wheat cultivar Cadenza. Eleven independent pRTBV-WRKY-RNAi (R1-R11) and seven independent pActin-WRKY-RNAi plants (A1-A7) were generated. A4 did not provide enough seed to use further. Offspring from all other lines was grown (T1 generation), screened by PCR (Sections 2.2.4 and 2.2.5) for transgenic individuals and the seed of three separate transgenic plants per line was collected. Seeds of one of these plants (T2 generation) per line were grown and screened by PCR. Four of these plants were used for the further studies.

a

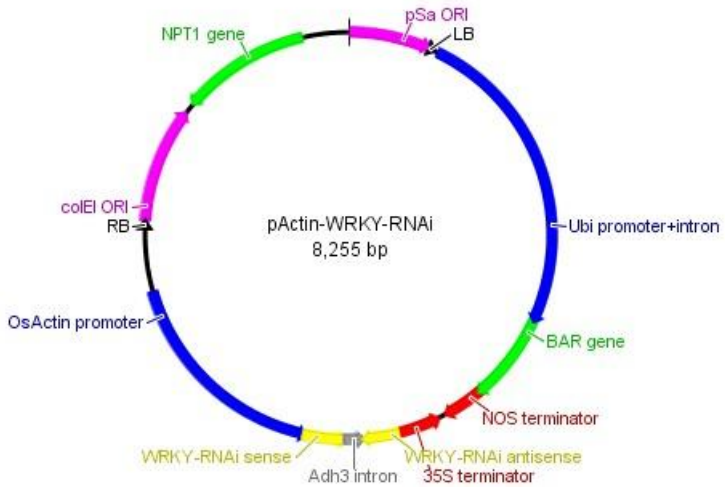

b

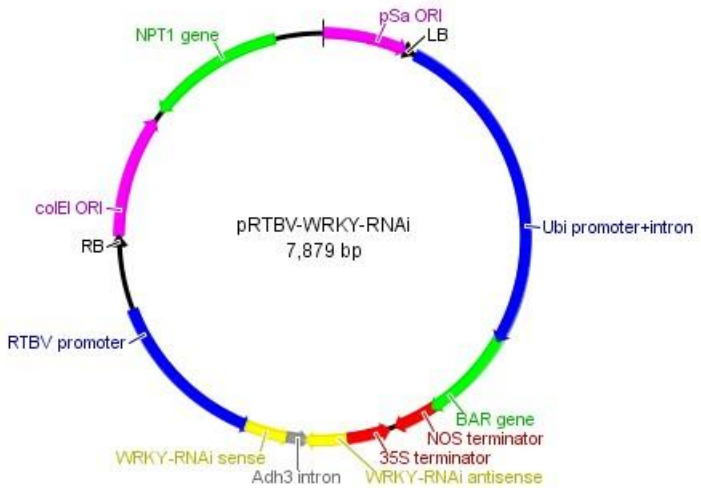

Figure 6.3: Plasmids for WRKY knockdown via RNAi under the control of rice actin (a) and RTBV (b) promoters. Apart from the promoters the two constructs are identical. The plasmids contain a broad host range origin of replication (ORI) for use in *Agrobacterium tumefaciens* (pSA) and an ORI for *Escherichia coli* (colEI) and the *NPT1* kanamycin-resistance gene for selection of bacteria. The part between the left and right borders (LB and RB) is meant for insertion into the plant genome. Apart from the promoter-WRKY-RNAi-35S-terminator sequence this includes a BAR gene (phosphinothricin resistance) under control of an ubiquitin promoter to allow for plant selection. Genes in green, RNAi fragment in yellow with the intron in grey, promoters in blue, terminators in red and ORI in pink. Constructs made by Dr Peter Buchner (Rothamsted Research).

6.3.2 Morphology and Development

To determine if knockdown of the WRKY gene affected development, the timing of four key developmental stages of the main shoot was compared: completion of flag leaf emergence (Zadoks Growth Stage 39), transition of booting to heading (GS49), start of anthesis (GS61), and physiological maturity (GS89). The anthesis date of the first three tillers and the time in which the whole plant (all tillers) reached physiological maturity also was recorded.

Overall, wild-type and transformation control plants reached the flag leaf emergence stage significantly earlier than plants carrying a WRKY-RNAi-construct (Figure 6.4; $P<0.05$). In addition, the heading and anthesis stages were reached significantly earlier by the control lines (Figure 6.4; $P<0.001$). Plants carrying the pRTBV-WRKY-RNAi construct reached the heading stage significantly later than those with the pActin-WRKY-RNAi construct (Figure 6.4; $P<0.001$). There were no differences between plants with or without RNAi-construct for time to physiological maturity.

Highly significant differences between the individual lines were found for all developmental stages. pRTBV-WRKY-RNAi lines 4, 6 and 9 had their flag leaves fully emerged significantly later than both the control lines C and WT (Figure 6.4; $P<0.001$). The same three lines plus R2 and R11 reached heading significantly later than C and WT (Figure 6.4; $P<0.001$). Lines R6, R9, R11 and pActin-WRKY-RNAi line 2 reached the anthesis stage significantly later than the control lines (Figure 6.4; $P<0.001$). There were significant differences between the lines in the time in which the main shoot reached physiological maturity ($P<0.01$), but none of the transgenic lines differed significantly from both C and WT (Figure 6.4). However, for physiological maturity of the whole plant lines A7 and R6 were maturing significantly later than both transformation control and wild-type (Figure 6.5; $P<0.001$). This was probably caused by later development of the tillers, since the first three tillers of A7

and R6 arrived at anthesis significantly later than C and WT (Figure 6.6; $P<0.001$).

The WRKY-RNAi transgenics plants differed morphologically from the control lines in several ways. Overall, WRKY-knockdown plants were significantly taller than the control plants (Figure 6.7; $P<0.001$). Additionally, the transgenic lines had a significantly higher number of tillers (Figure 6.8.a; $P<0.001$). On average the transgenic lines had between eight and eleven seed-producing tillers (including the main shoot), while the control lines had only six. The number of culm leaves on the main shoot, which should be equivalent to the number of internodes, did not differ (Figure 6.8.b), so the differences in height were not caused by a different number of internodes.

Since this WRKY gene is believed to be involved in leaf senescence, it is important to establish whether leaf morphology is affected. Therefore the leaf size was assessed by measuring length and width of the top three leaves of the main shoot (Figure 6.9). Although individual lines did not have significantly different leaf lengths, pActin-WRKY-RNAi plants overall had significantly longer first and second leaves than control plants (Figure 6.9.a; $P<0.05$). Some lines had significantly wider or thinner leaves than the control plants (Figure 6.9.b), but overall the transgenic plants did not differ significantly from control plants. However, pActin-WRKY-RNAi plants had significantly wider first and second leaves than pRTBV-WRKY-RNAi plants ($P<0.001$ and $P<0.05$ respectively).

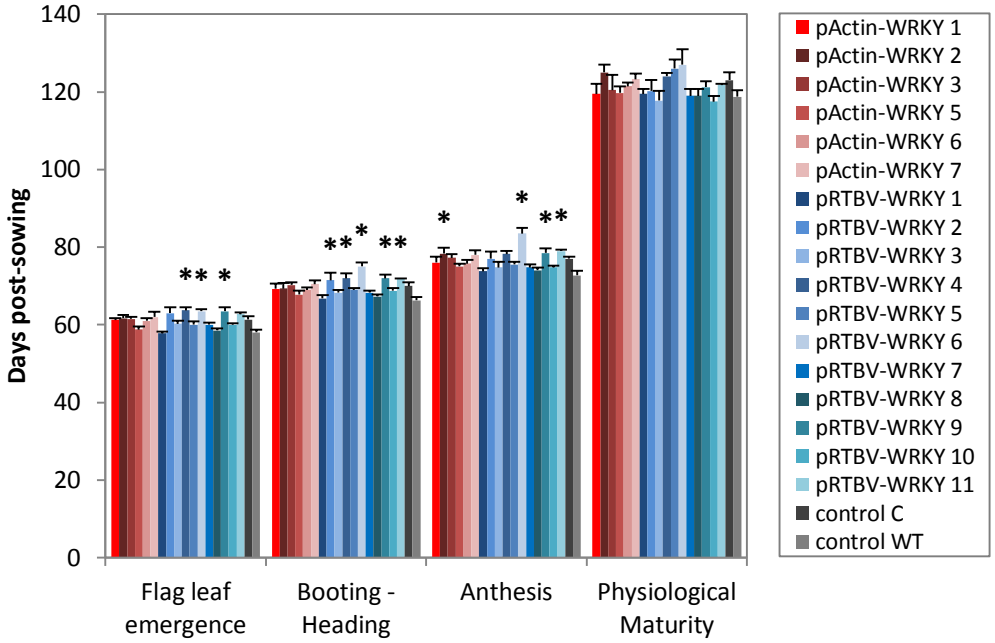

Figure 6.4: Development of the main shoot of WRKY-RNAi wheat. Development was assessed by measuring the time (days post-sowing) required to reach a certain growth stage. Flag leaf emergence (GS39), transition booting to heading (GS49), start anthesis (GS61), physiological maturity (GS89). * significantly different from both transformation control and wild-type (P<0.05). Data are means + SE of four replicate plants.

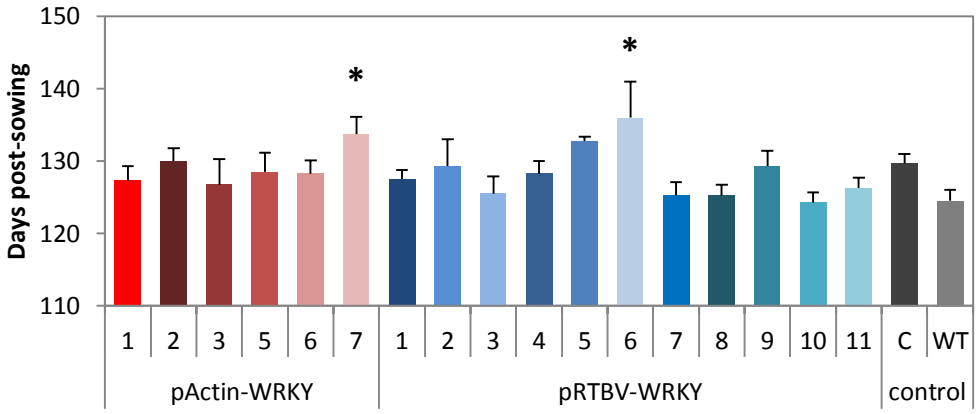

Figure 6.5: Time (days post-sowing) in which the whole plant of WRKY-RNAi wheat reached physiological maturity (GS89). * significantly different from both transformation control and wild-type (P<0.05). Data are means + SE of four replicate plants.

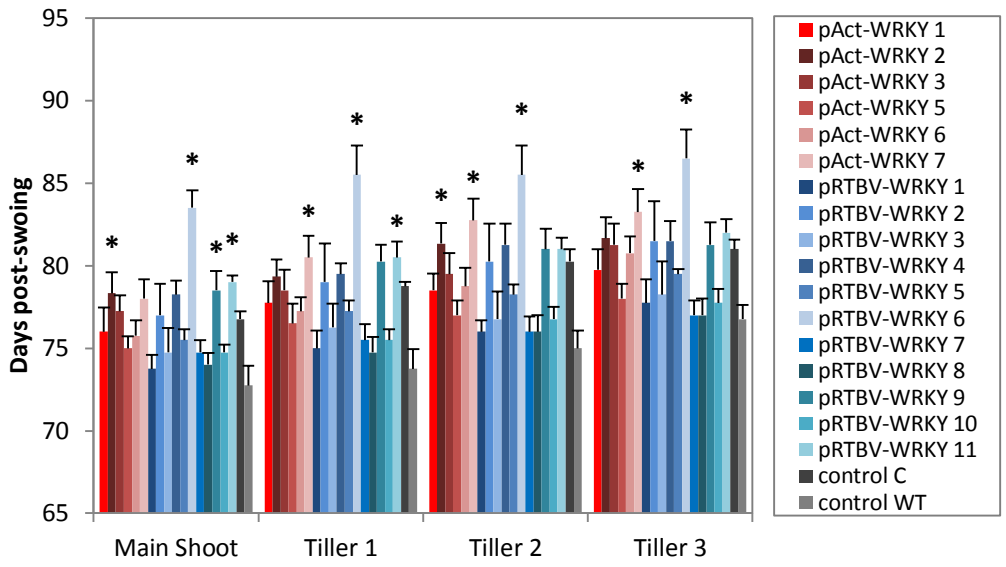

Figure 6.6: Time (days post-sowing) in which the main shoot and first three tillers of WRKY-RNAi wheat reached anthesis (GS61). * significantly different from both transformation control and wild-type (P<0.05). Data are means + SE of four replicate plants.

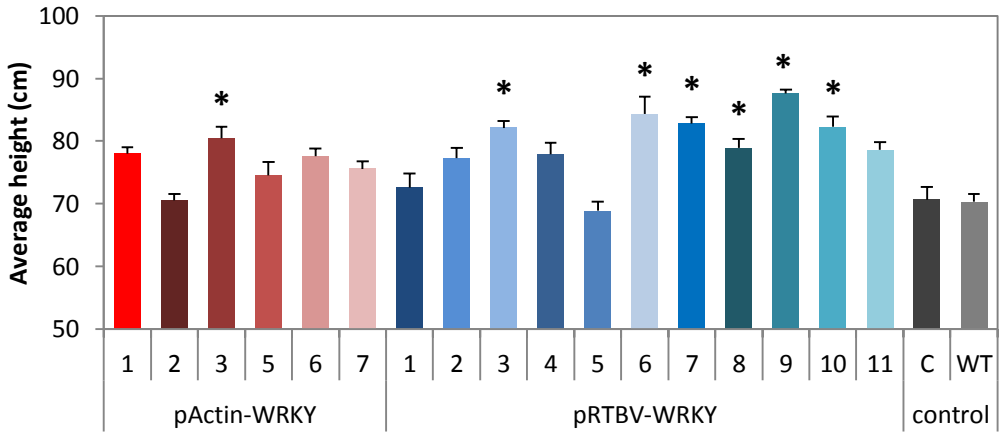

Figure 6.7: Average height of the main shoot and first three tillers of WRKY-RNAi wheat. * significantly different from both transformation control and wild-type (P<0.05). Data are means + SE of four replicate plants.

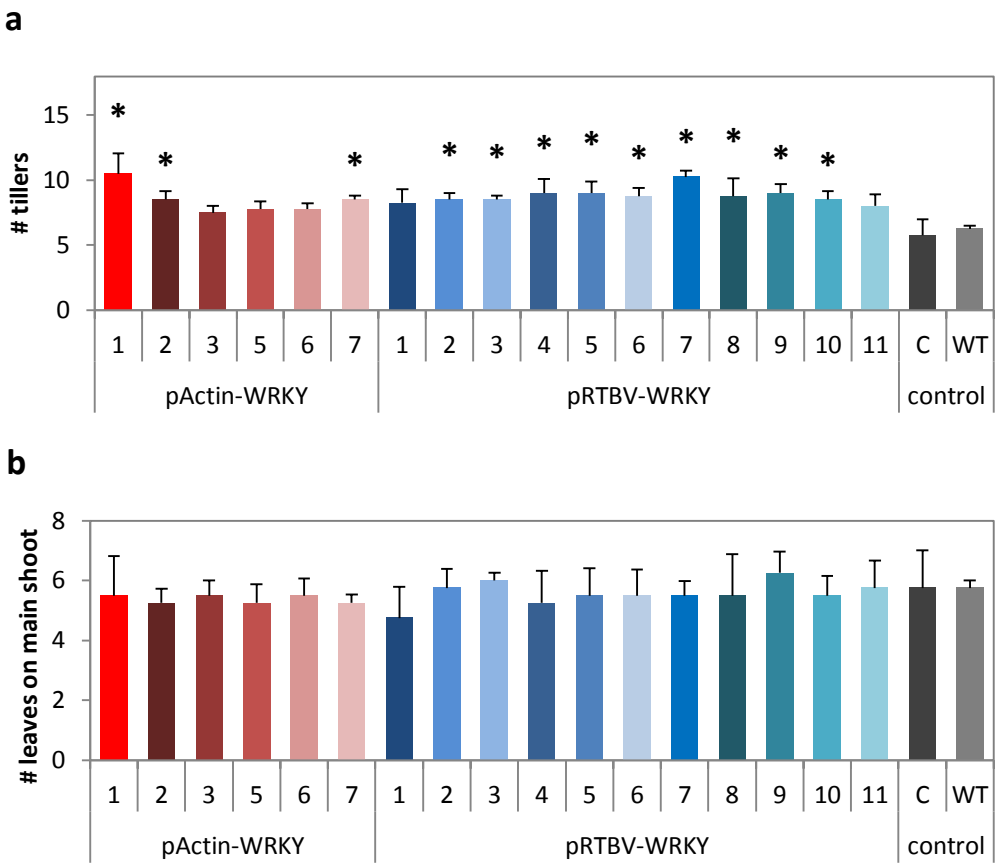

Figure 6.8: The number of tillers (including main shoot) per plant at physiological maturity (a) and the number of leaves on the main shoot (b) of WRKY-RNAi wheat. * significantly different from both transformation control and wild-type (P<0.05). Data are means + SE of four replicate plants.

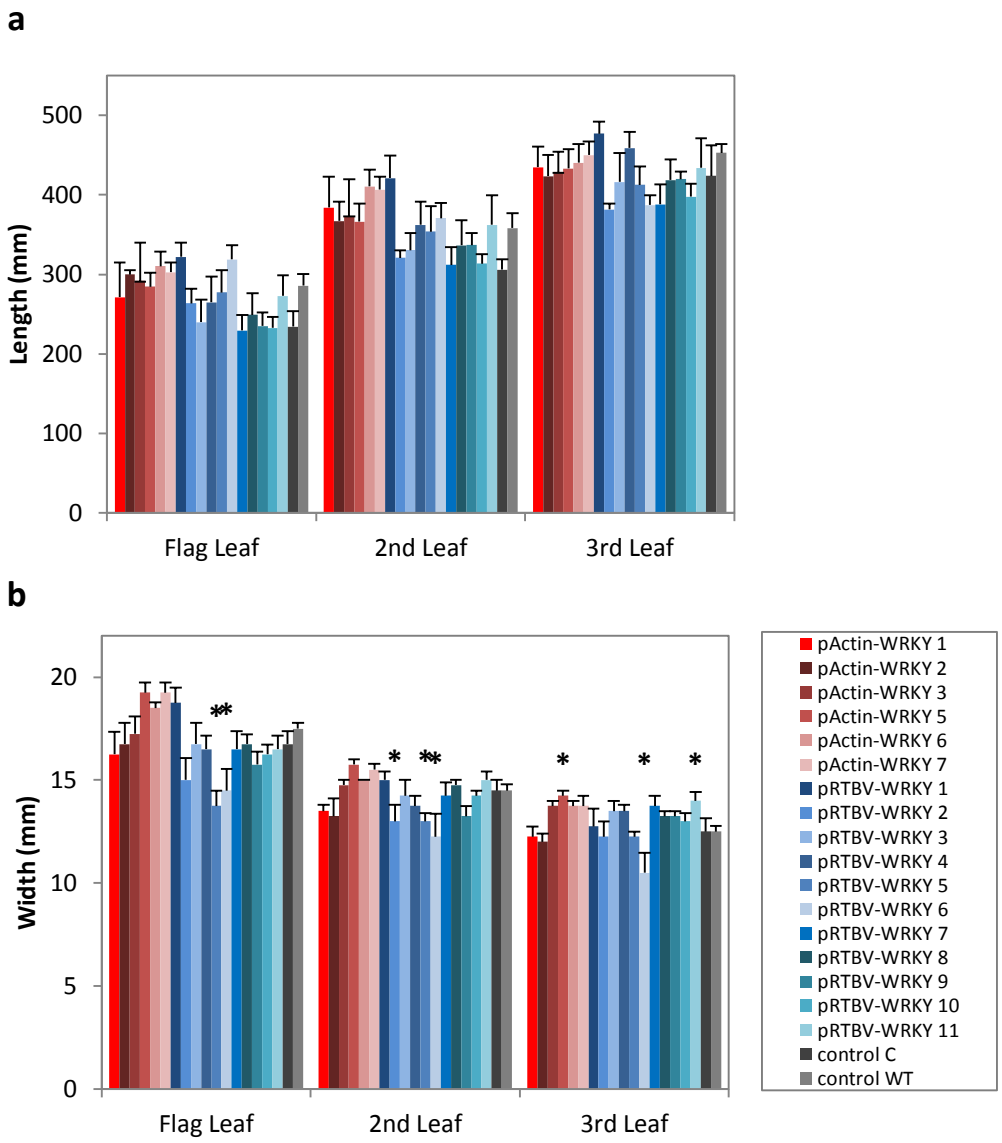

Figure 6.9: Length (a) and width (b) of the first three leaves of the main shoot of WRKY-RNAi wheat. * significantly different from both control and wild-type (P<0.05). Data are means + SE of four replicate plants.

6.3.3 Leaf Senescence

Leaf senescence was evaluated for the top three leaves of the main shoot from anthesis until at 42 days post-anthesis when all leaves had senesced. Relative chlorophyll content (SPAD) was measured to assess the changes in greenness of the leaves (Figures 6.10, 6.12 and 6.14), and the photosystem II efficiency was assessed by measuring chlorophyll fluorescence (quantum yield (QY) = F_V'/F_M') to examine whether the leaves still had the ability to photosynthesize (Figures 6.11, 6.13 and 6.15).

On average, flag leaves of transgenic plants first significantly decreased in greenness between 21 and 28 dpa, whilst control plants did not lose greenness until 28 dpa (Figure 6.10; $P<0.001$). At 28 dpa lines A1, R6, R9 and R11 were significantly less green than both control lines, and at 35 dpa R6 and R11 were completely senesced ($P<0.01$). Control lines C and WT had significantly higher quantum yield than R6 and R9 at 28 dpa and R6 and R11 at 35 dpa (Figure 6.11; $P<0.05$). However, at 35 dpa both SPAD and QY values of C and WT differed significantly from each other, indicating there was a lot of natural variation in the exact time of onset and / or the rate of senescence of the flag leaf.

Transgenic plants lost greenness of the second leaf significantly earlier than control plants: at 21 dpa they were significantly less green than at 7 dpa, whilst control plants first significantly lost greenness between 21 and 28 dpa (Figure 6.12; $P<0.05$). There were no significant differences in timing or rate of the decrease in quantum yield (Figure 6.13). As for the flag leaf, the onset of senescence of the second leaf was the earliest in lines A1, R6, R9 and R11 (Figures 6.12 and 6.13).

There was substantial variation in onset and rate of senescence of the third leaf (Figures 6.14 and 6.15), but overall the third leaf of WRKY-RNAi plants was significantly less green than that of non-transgenic plants throughout senescence ($P<0.01$).

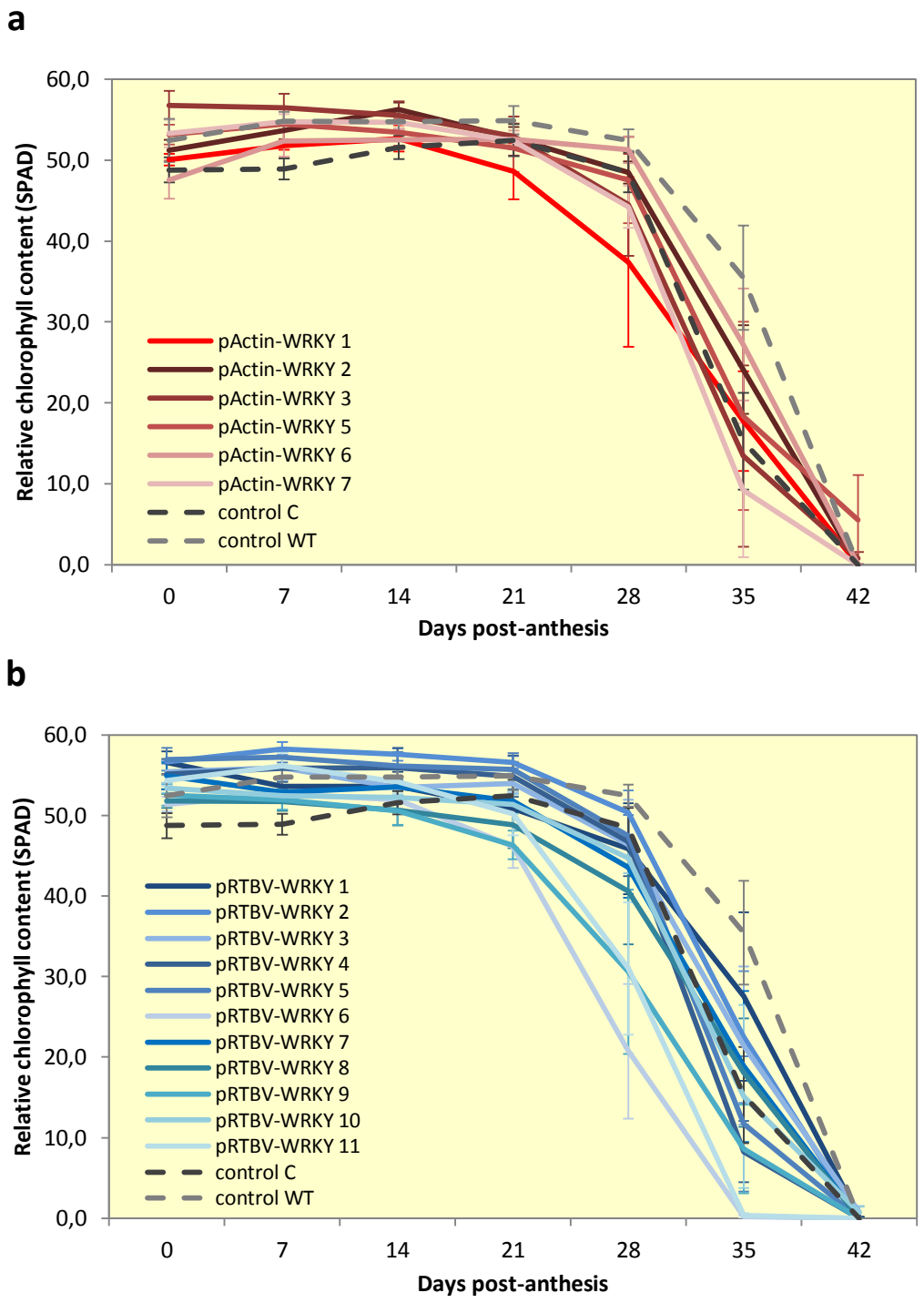

Figure 6.10: Relative chlorophyll content (SPAD) during post-anthesis senescence of the flag leaf of the main shoot of pActin-WRKY-RNAi (a) and pRTBV-WRKY-RNAi (b) wheat. LSD = 10.79. Data are means ± SE of four replicate plants. Data for pActin-WRKY-RNAi and pRTBV-WRKY-RNAi plants are shown in two separate graphs for clarity, but statistical analysis was performed encompassing both WRKY-RNAi-constructs.

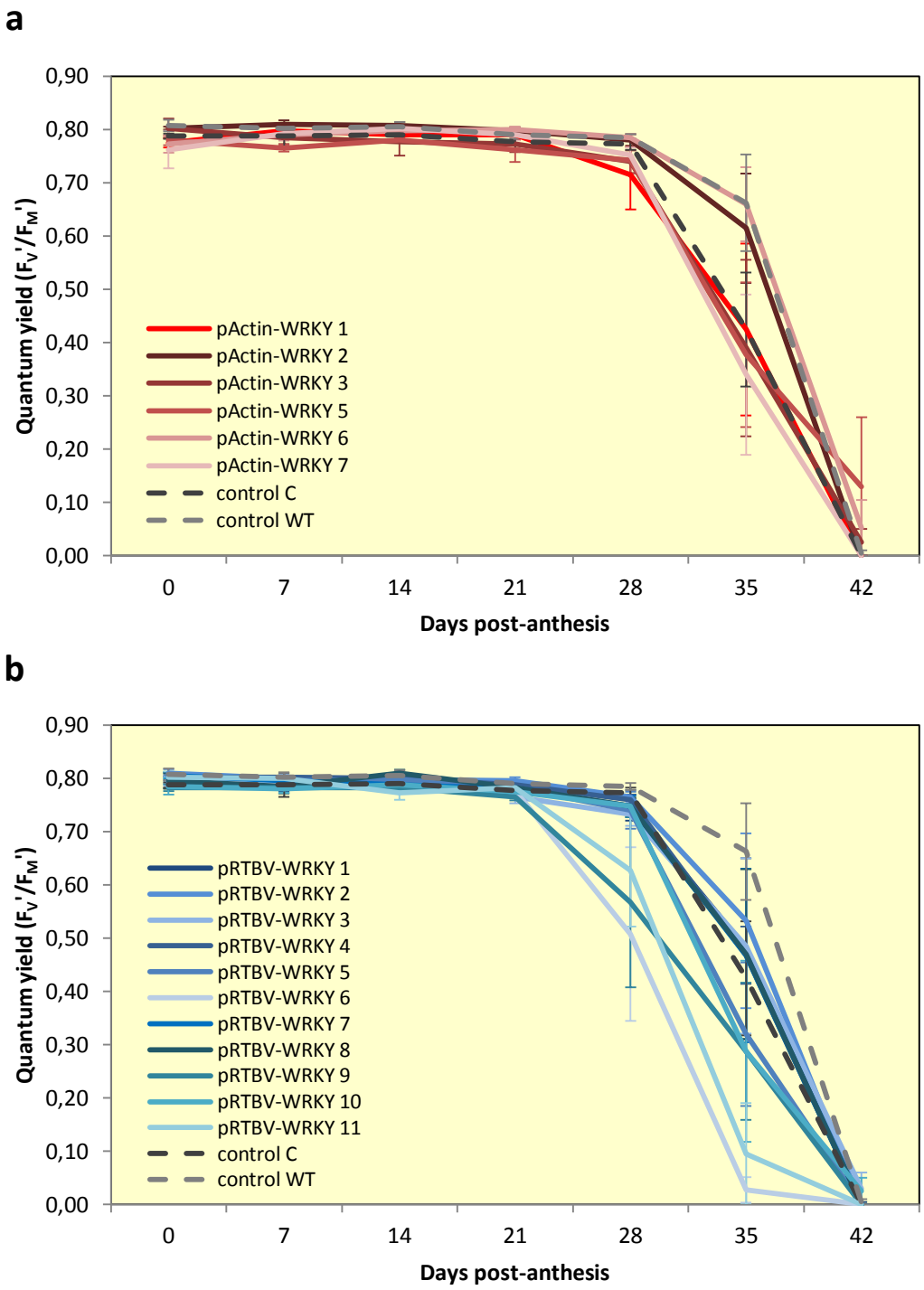

Figure 6.11: Photosystem II efficiency (quantum yield) during post-anthesis senescence of the flag leaf of the main shoot of pActin-WRKY-RNAi (a) and pRTBV-WRKY-RNAi (b) wheat. LSD = 0.161. Data are means ± SE of four replicate plants. Data for pActin-WRKY-RNAi and pRTBV-WRKY-RNAi plants are shown in two separate graphs for clarity, but statistical analysis was performed encompassing both WRKY-RNAi-constructs.

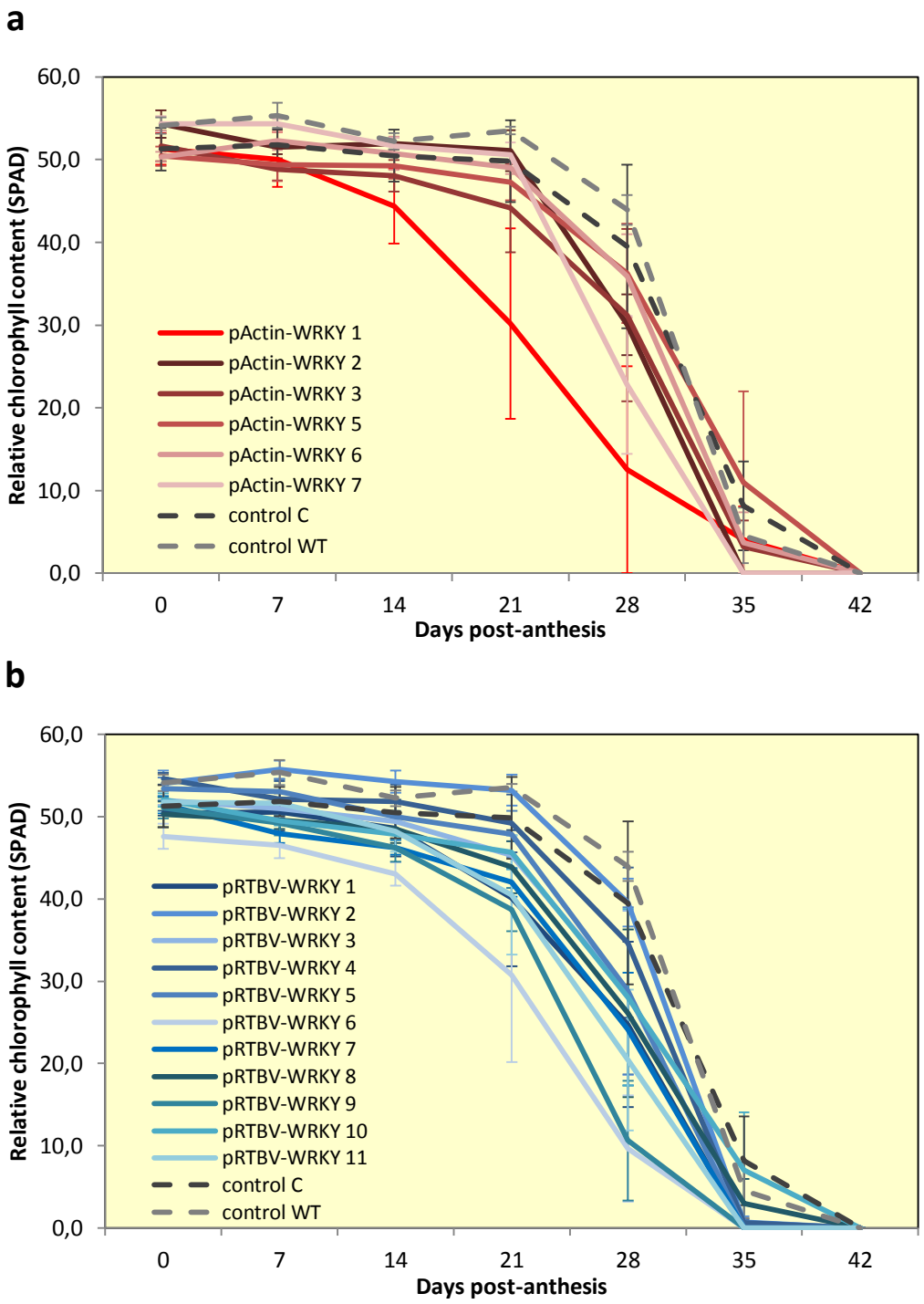

Figure 6.12: Relative chlorophyll content (SPAD) during post-anthesis senescence of the second leaf of the main shoot of pActin-WRKY-RNAi (a) and pRTBV-WRKY-RNAi (b) wheat. LSD = 12.41. Data are means ± SE of four replicate plants. Data for pActin-WRKY-RNAi and pRTBV-WRKY-RNAi plants are shown in two separate graphs for clarity, but statistical analysis was performed encompassing both WRKY-RNAi-constructs.

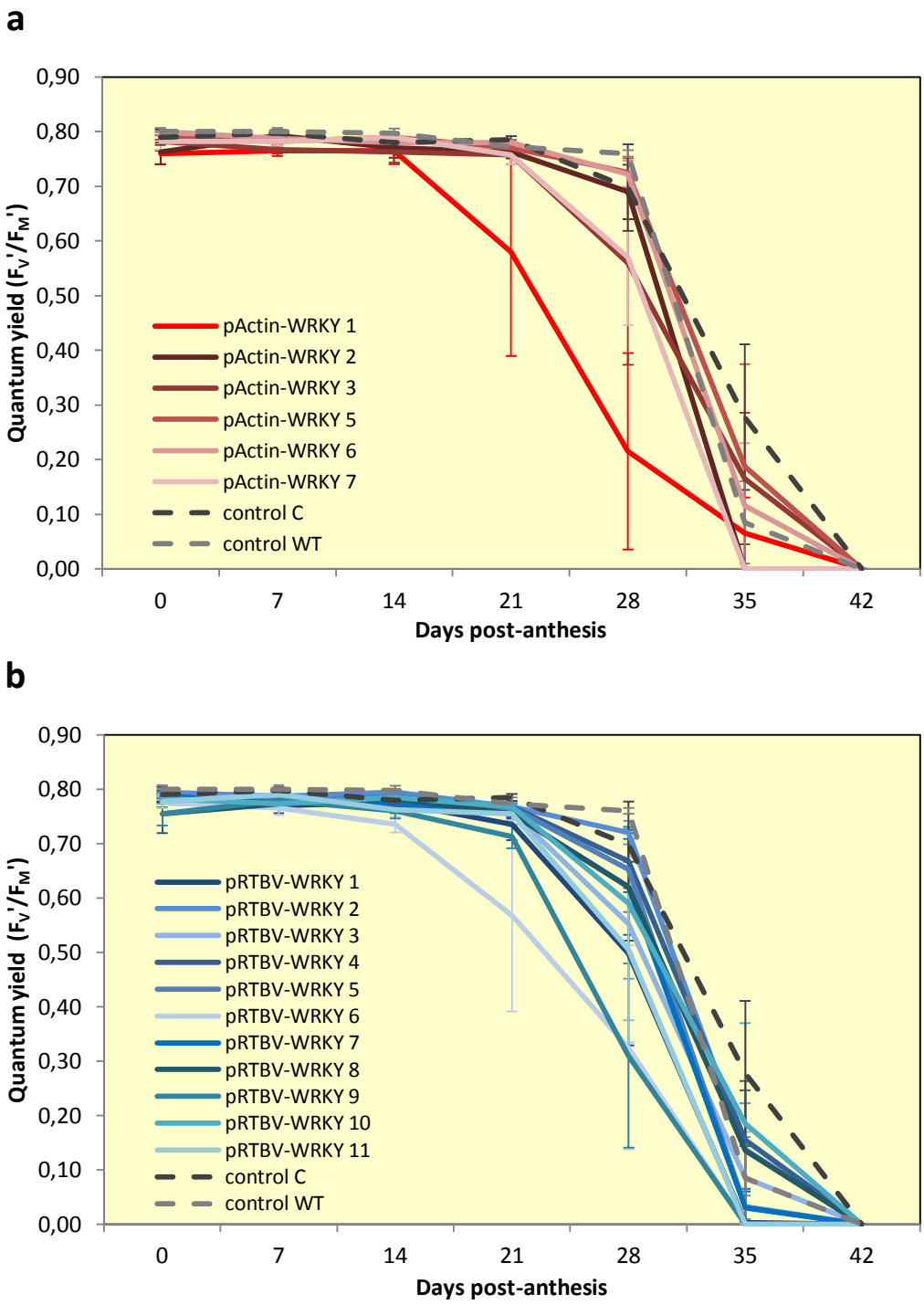

Figure 6.13: Photosystem II efficiency (quantum yield) during post-anthesis senescence of the second leaf of the main shoot of pActin-WRKY-RNAi (a) and pRTBV-WRKY-RNAi (b) wheat. LSD = 0.191. Data are means ± SE of four replicate plants. Data for pActin-WRKY-RNAi and pRTBV-WRKY-RNAi plants are shown in two separate graphs for clarity, but statistical analysis was performed encompassing both WRKY-RNAi-constructs.

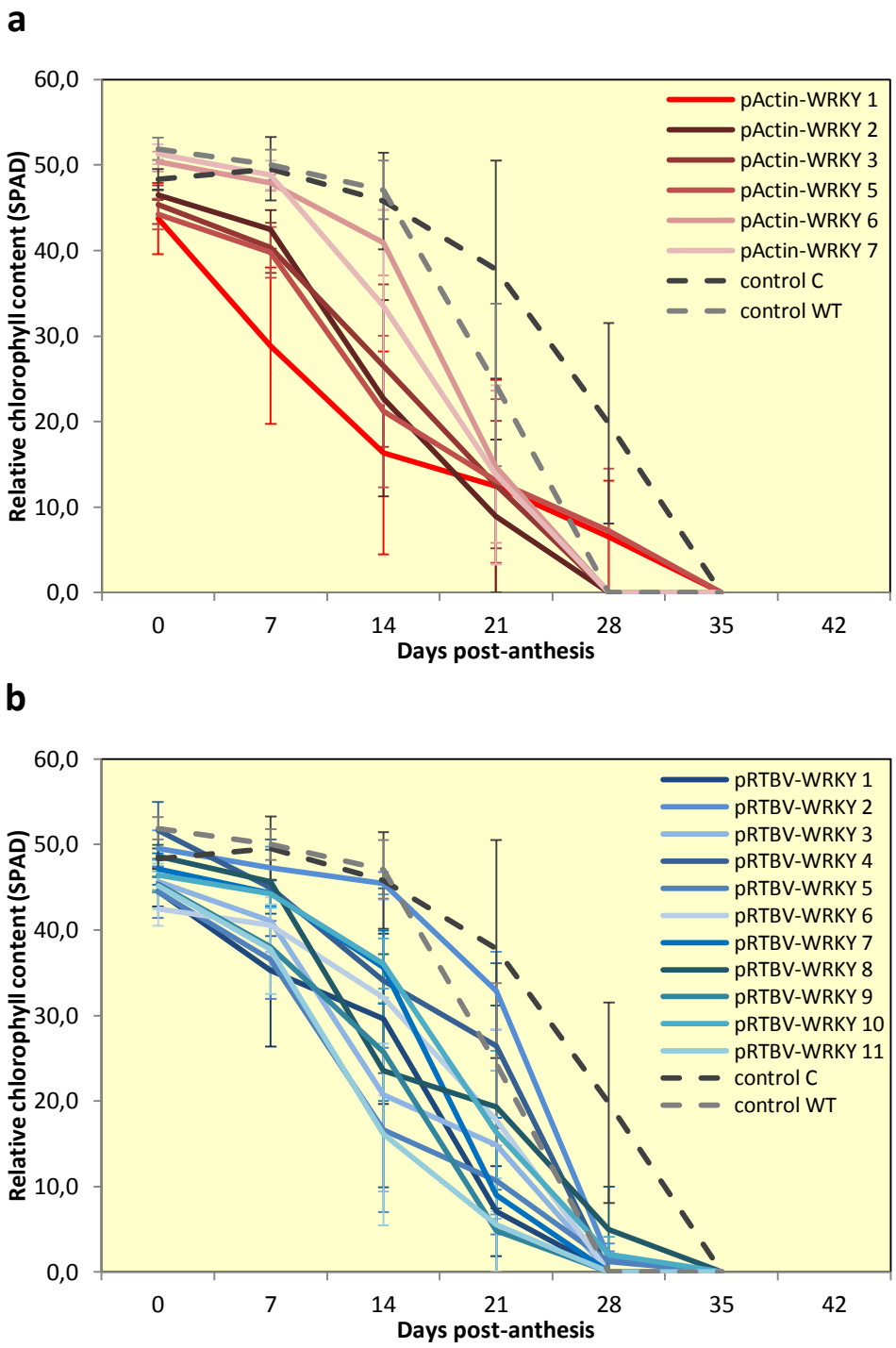

Figure 6.14: Relative chlorophyll content (SPAD) during post-anthesis senescence of the third leaf of the main shoot of pActin-WRKY-RNAi (a) and pRTBV-WRKY-RNAi (b) wheat. LSD = 17.49. Data are means ± SE of four replicate plants. Data for pActin-WRKY-RNAi and pRTBV-WRKY-RNAi plants are shown in two separate graphs for clarity, but statistical analysis was performed encompassing both WRKY-RNAi-constructs.

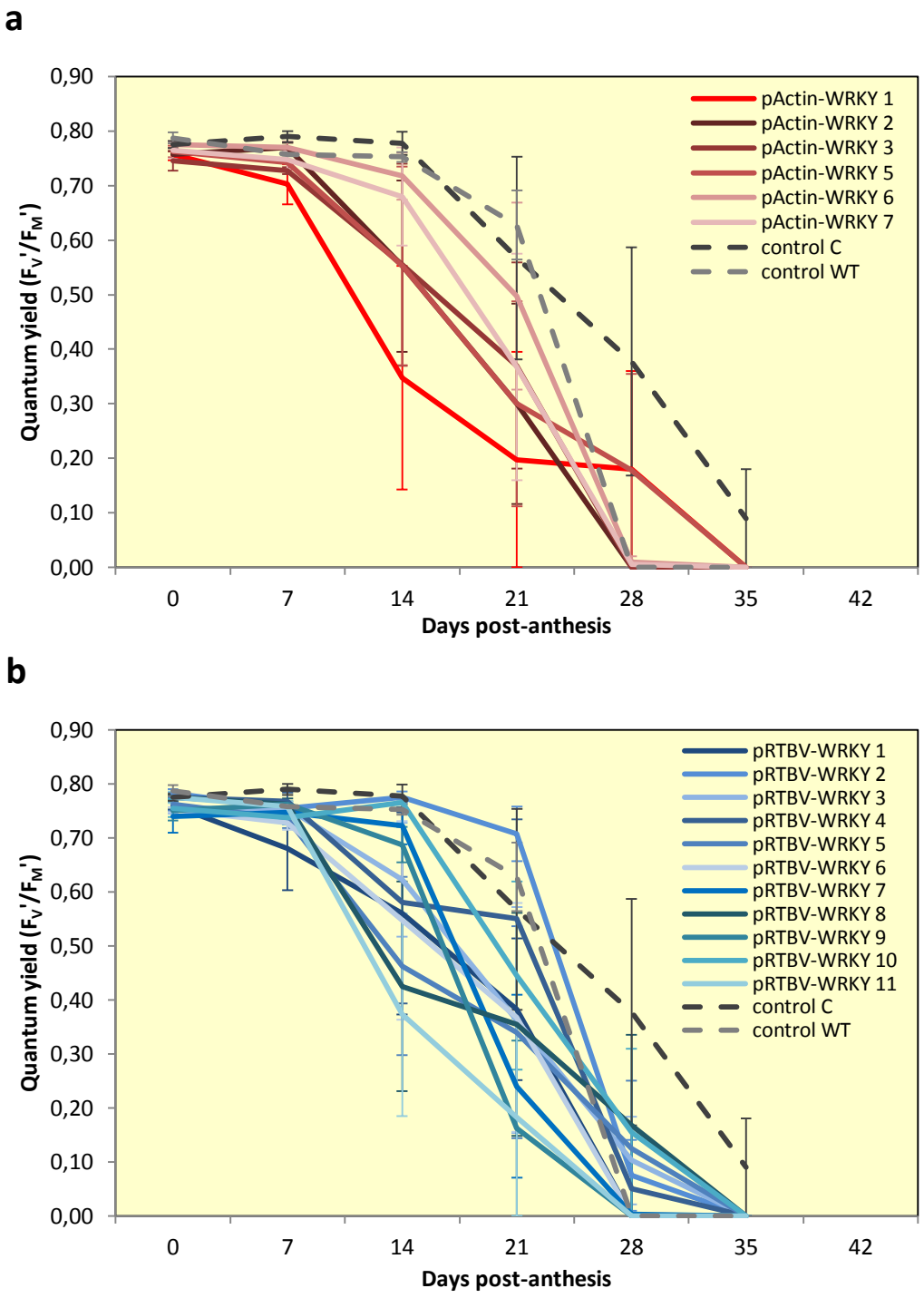

Figure 6.15: Photosystem II efficiency (quantum yield) during post-anthesis senescence of the third leaf of the main shoot of pActin-WRKY-RNAi (a) and pRTBV-WRKY-RNAi (b) wheat. LSD = 0.307. Data are means ± SE of four replicate plants. Data for pActin-WRKY-RNAi and pRTBV-WRKY-RNAi plants are shown in two separate graphs for clarity, but statistical analysis was performed encompassing both WRKY-RNAi-constructs.

6.3.4 Grain Yield

Even though only two transgenic lines had significantly higher grain yields than the transformation control and wild-type lines (Figure 6.16.a; $P<0.05$), overall total grain yield per plant of WRKY-RNAi plants was significantly higher than that of the reference plants ($P<0.01$). The average difference was thirty per cent. Grain yield per ear was not significantly different between transgenic and non-transgenic lines (Figure 6.16.b), line R6 being the only exception. Grain yield per plant correlated significantly with tiller number ($R^2 = 0.4754$; $P<0.001$), indicating the differences in total grain yield between the lines could be due to differences in tiller number (Figure 6.8.a).

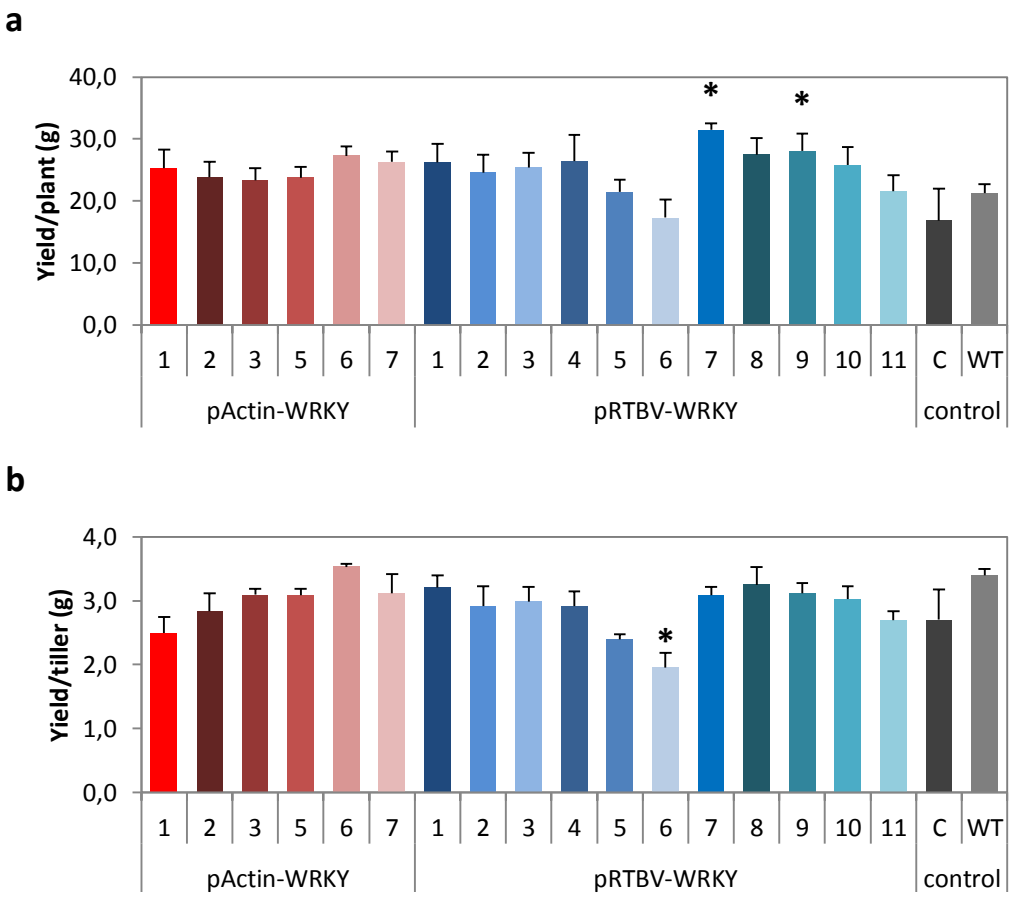

Figure 6.16: Grain yield per plant (a) and per ear (b) of WRKY-RNAi wheat. * significantly different from both transformation control and wild-type ($P<0.05$). Data are means + SE of four replicate plants.

6.3.5 Gene Expression

For gene expression analysis, the second leaves of the first three tillers were harvested at green leaf stage (7 days post-anthesis), early senescence (21 dpa) and advanced senescence (28 dpa). Five lines were examined: two pActin-WRKY-RNAi lines, A3 and A7; two pRTBV-WRKY-RNAi lines, R9 and R10, and wild-type.

The two pActin-WRKY-RNAi and the two pRTBV-WRKY-RNAi lines were chosen for differences in onset and rate of leaf senescence (Figure 6.17). However, many of the senescing leaves did not contain enough RNA for expression analysis, so few leaves in an advanced stage of senescence were available. Therefore in addition to the expression patterns in time, regression analysis between expression and leaf greenness was performed (Figures 6.18, 6.19 and 6.20).

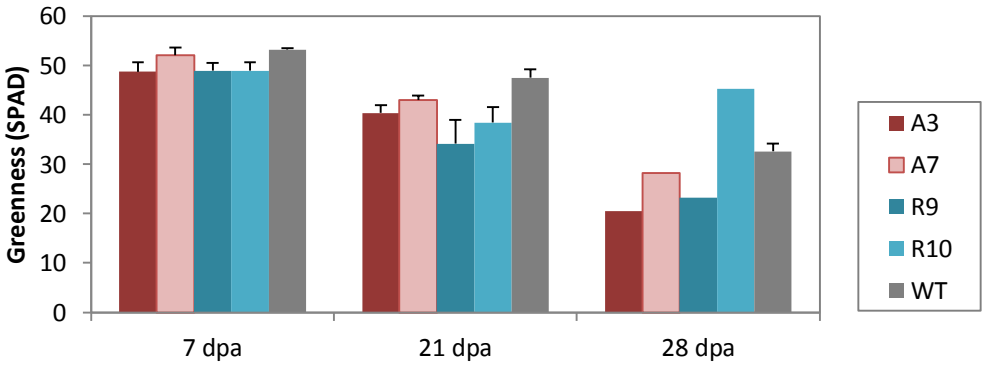

Figure 6.17: Senescence status of the second leaves of a selection of WRKY-RNAi lines of wheat that were used for gene expression analysis. A3 and A7 = pActin-WRKY lines 3 and 7 (red), R9 and R10 = pRTBV-WRKY lines 9 and 10 (blue), WT = wild-type (grey). Data are means + SE of one to four replicate plants, the number depending on whether the leaves still contained RNA.

Generally, expression of the marker gene *RBCS* (Figure 6.18.a) followed the same pattern as senescence (Figure 6.17) and therefore showed a significantly positive relationship with leaf greenness (Figure 6.18.b; P<0.001). Line A7 was an exception: expression of *RBCS* was often lower than expected based on leaf greenness, which is indicated by the data points away from the regression line (Figure 6.18.b).

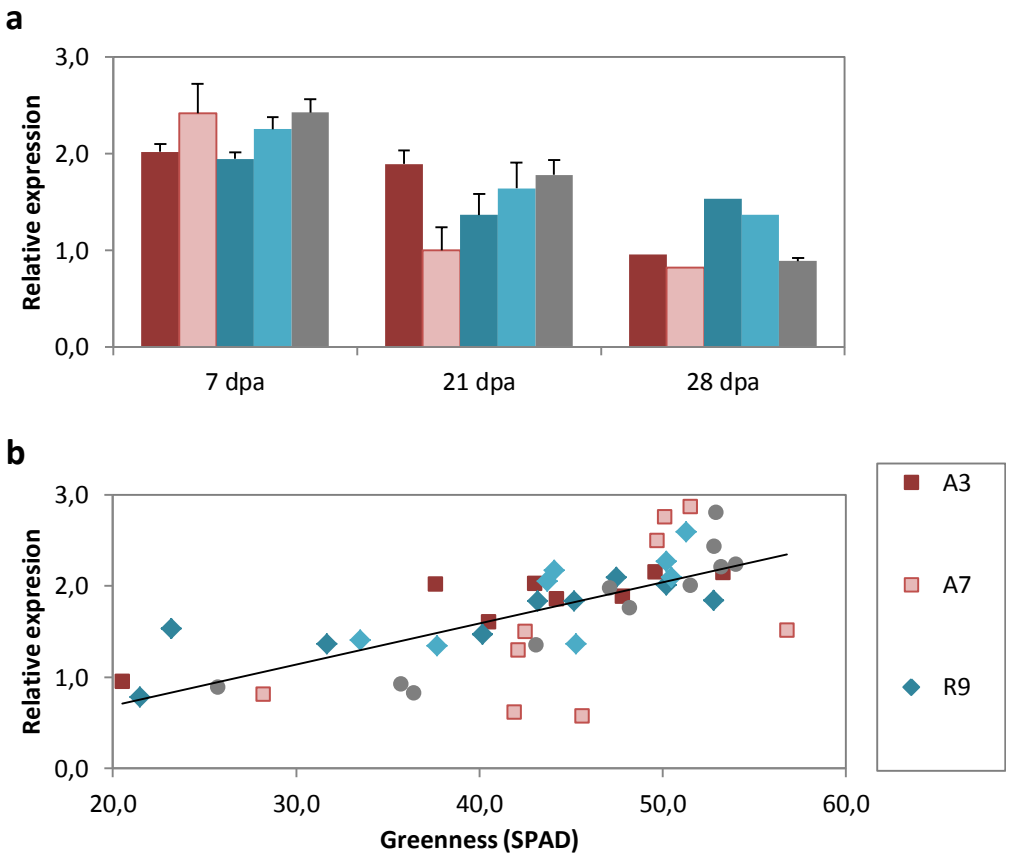

Figure 6.18: Relative *RBCS* expression during senescence of the second leaf (a), and the relation between relative *RBCS* expression and greenness (b) of a selection of WRKY-RNAi lines of wheat. A3 and A7 = pActin-WRKY lines 3 and 7 (red), R9 and R10 = pRTBV-WRKY lines 9 and 10 (blue), WT = wild-type (grey). (a) Data are means + SE of one to four replicate plants, the number depending on whether the leaves still contained RNA. (b) Data points represent individual leaves. $y = 0.045x - 0.2093$; $R^2 = 0.4779$; $P < 0.001$.

Expression of *SAG12* followed exactly the opposite pattern. *SAG12* expression increased during senescence (Figure 6.19.a) and therefore showed a significant negative relationship with leaf greenness (Figure 6.19.b; P<0.001). The same leaves of line A7 showed a higher expression than one would expect (Figure 6.19.b). So expression of the marker genes *RBCS* and *SAG12* would lead to the conclusion that senescence of these leaves is progressed further than the SPAD measurements would suggest.

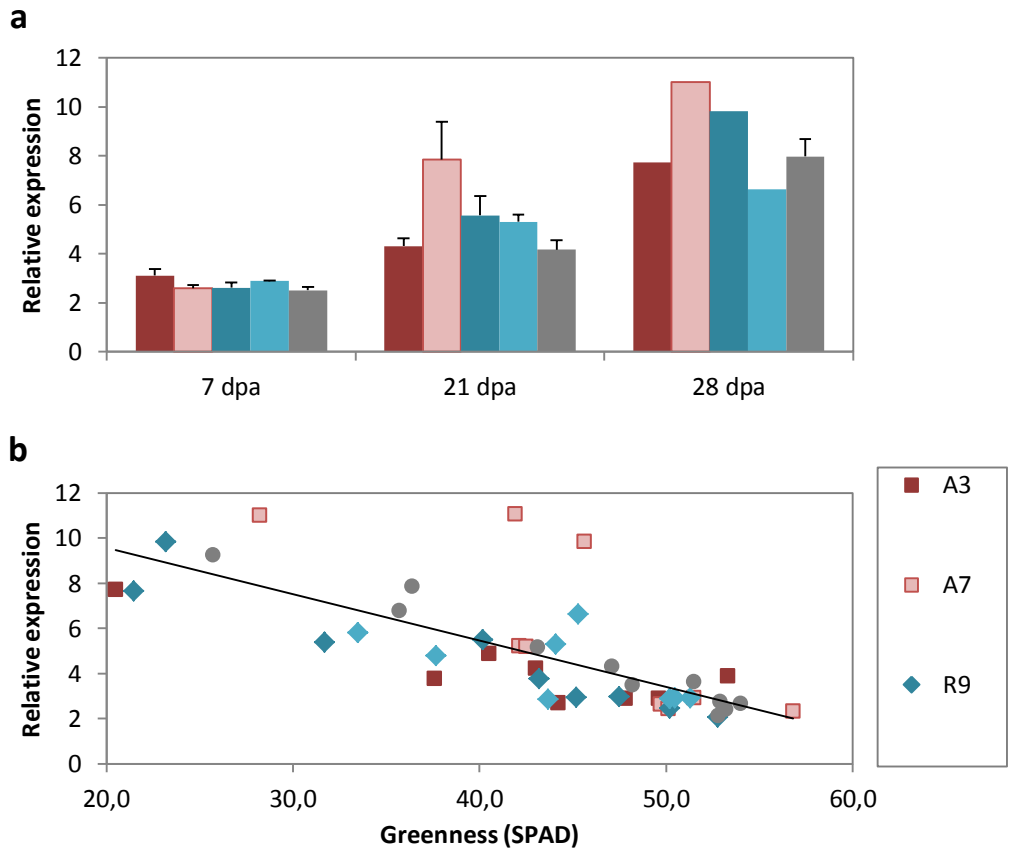

Figure 6.19: Relative *SAG12* expression during senescence of the second leaf (a), and the relation between relative *SAG12* expression and greenness (b) of a selection of WRKY-RNAi lines of wheat. A3 and A7 = pActin-WRKY lines 3 and 7 (red), R9 and R10 = pRTBV-WRKY lines 9 and 10 (blue), WT = wild-type (grey). (a) Data are means + SE of one to four replicate plants, the number depending on whether the leaves still contained RNA. (b) Data points represent individual leaves. y = -0.2059x + 13.698; R^2 = 0.5618; P < 0.001.

Expression of the WRKY transcription factor increased during leaf senescence in all lines (6.20.a), and correlated well with greenness (6.20.b). Line A7 showed anomalously high expression. There was no sign of a reduction in WRKY expression due to RNAi in the transgenic lines; in fact WRKY expression seems to have been the lowest in wild-type plants (Figure 6.20). This result was confirmed with a second set of PCR primers (data not shown).

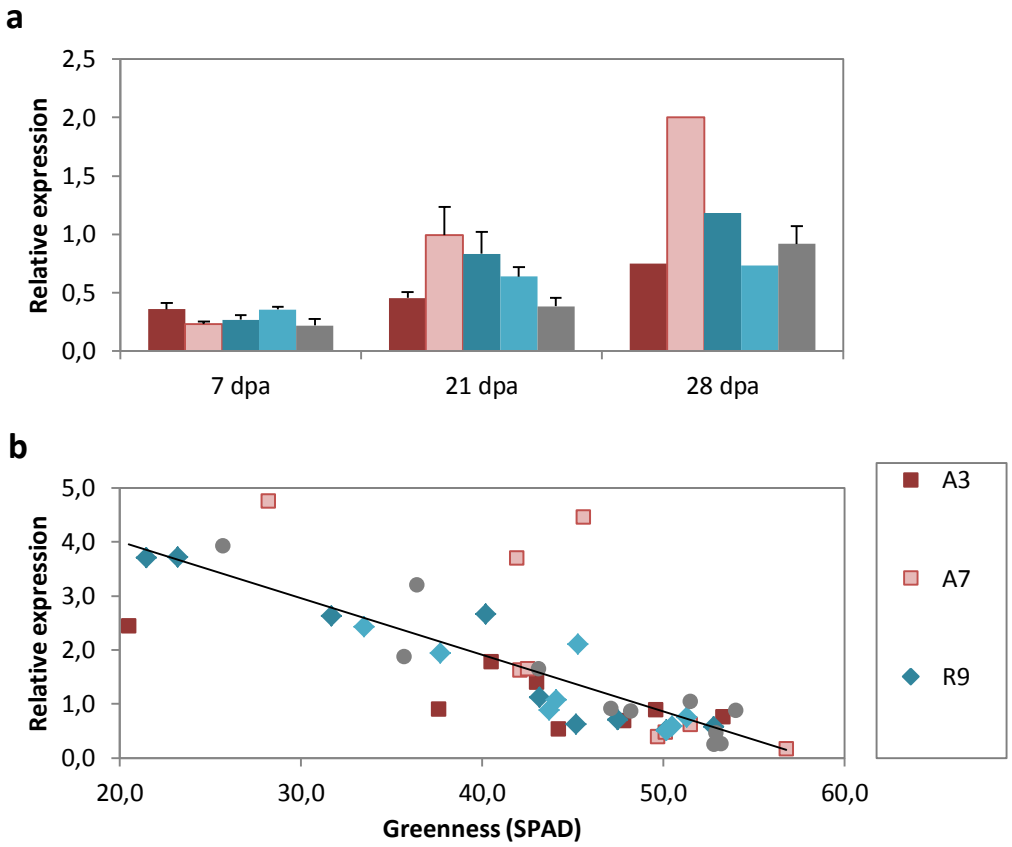

Figure 6.20: Relative WRKY expression during senescence of the second leaf (a), and the relation between relative WRKY expression and greenness (b) of a selection of WRKY-RNAi lines of wheat. A3 and A7 = pActin-WRKY lines 3 and 7 (red), R9 and R10 = pRTBV-WRKY lines 9 and 10 (blue), WT = wild-type (grey). (a) Data are means + SE of one to four replicate plants, the number depending on whether the leaves still contained RNA. (b) Data points represent individual leaves. $y = -0.1048x + 6.1006$; $R^2 = 0.6028$; $P < 0.001$.

A PCR analysis specifically amplifying the RNAi-fragment indicated expression only in the A7 leaf samples (Figure 6.21), suggesting either a low RNA stability or folding of the RNA prevented the amplification of the RNAi-fragment by PCR in most lines. However, it proved there was good expression of the RNAi-fragment in line A7. Expression of the WRKY gene in leaves of A7 during senescence was higher than in any other line (Figure 6.20.a). This result indicates that the presence of the WRKY-RNAi-fragment did not reduce expression of the WRKY gene in this line, but potentially even lead to an increase.

Figure 6.21: RT-PCR evaluating expression of the RNAi fragment in senescing leaves of WRKY-RNAi plants. The different samples of the same line at one time point originate from different plants (biological replicates). The ladder is the GeneRuler 100bp DNA ladder (Fermentas).

6.4 EXPRESSION OF THE WRKY GENE IN WHEAT TISSUES

Since effects of expression of the WRKY-RNAi construct were not limited to leaf senescence, but delayed pre-anthesis development and increased plant height and tiller number (Figures 6.4, 6.7 and 6.8.a), it is likely the wheat WRKY gene does not solely have a role in leaf senescence. Therefore an experiment was set up to test whether the WRKY gene is expressed in tissues other than leaf two (Figure 6.22).

The WRKY gene was expressed in all tested tissues apart from the grain (Figure 6.22). Expression was highest in roots, although there was great variation. Expression was also high in the rachis and leaf sheath. The WRKY gene showed higher expression in flag leaves than in leaf two and three, while these lower leaves will senesce before the top leaf. These results suggest the WRKY gene almost certainly does not solely have a role in leaf senescence.

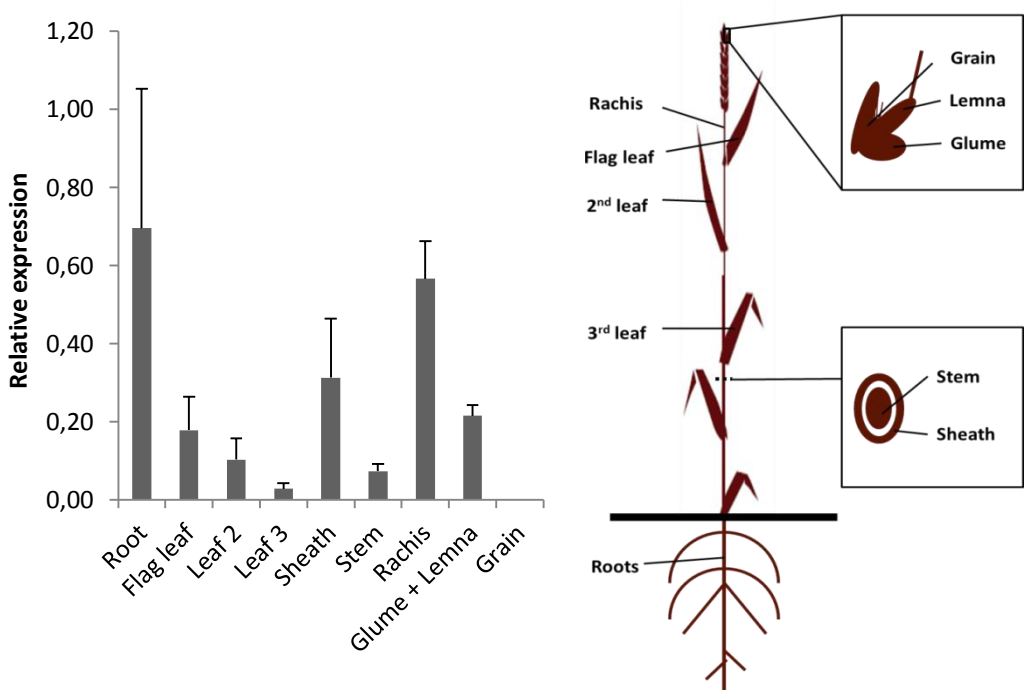

Figure 6.22: Expression of the WRKY gene in wheat tissues. Glume, lemna and grain were harvested seven days post-anthesis, roots at booting, the other tissues at anthesis. Data are means + SE of three replicate samples.

6.5 DISCUSSION AND CONCLUSIONS

Expression of a WRKY transcription factor was shown to increase during leaf senescence in wheat (Chapter 3), indicating this gene might be a positive regulator of senescence. This conclusion matched with the observation that all senescence-regulating WRKY transcription factors described at present are positive regulators of senescence (Besseau et al., 2012; Hinderhofer and Zentgraf, 2001; Jing et al., 2009; Ricachenevsky et al., 2010; Robatzek and Somssich, 2001; Ülker et al., 2007; Zhou et al., 2011b).

Unexpectedly, the WRKY-RNAi plants did not show reduced levels of the WRKY messenger RNA (mRNA) during senescence; in fact it was higher (Figure 6.20). However, the consistent phenotype of the transgenic lines demonstrated that WRKY gene function must have been affected. There is, however, no certainty that only the target WRKY gene was affected. The risk of knocking down other WRKY genes was reduced by not targeting the WRKY-domain itself (Figure 6.1), but nevertheless the RNAi-process could have modified the expression of more than one gene.

Even when only the target WRKY gene was knocked down, there are still multiple possible ways in which RNAi could have had an effect without noticeably altering WRKY expression. An auto-regulation mechanism has been described for *WRKY53* in Arabidopsis (Miao et al., 2004), so it is conceivable that the initial decrease in WRKY expression mediated by RNAi induced higher endogenous WRKY expression. Furthermore, translational repression has been reported for RNAi in plants (Brodersen et al., 2008), so RNAi cannot only lead to degradation of mRNA but can also prevent gene function by inhibiting the translation of the mRNA. To confirm WRKY gene function is actually reduced in the RNAi plants, protein levels will have to be measured. Another route to confirm the WRKY function would be to test the result of overexpression of the WRKY gene.

RNAi-knockdown of the WRKY transcription factor in wheat did not result in delayed leaf senescence as hypothesised, but instead in accelerated senescence, at least of the top three leaves (Figures 6.10 – 6.15). Plant height, the number of productive tillers and grain yield were all increased significantly (Figures 6.7, 6.8.a and 6.16.a). It is in fact possible that the increased tiller number is an indirect cause of the accelerated senescence phenotype of the transgenic wheat. If the plants were limited in certain nutrients, especially nitrogen, increased plant height and tiller number would result in lower nutrient concentrations throughout the plant, resulting in premature senescence since there were less surplus nutrients available for grain-filling. Additionally, as suggested by the higher grain yield, the increased tiller number was likely to be accompanied by a higher grain number, thus raising grain sink demand for nutrients such as nitrogen. Since the trials were carried out in pots meant for normal-sized plants, it is possible that nutrition limitation occurred. Furthermore, if this was the case, it would imply that by supplying ample fertiliser grain yield could be raised even further than the thirty per cent found in this study (Figure 6.16.a). However, experiments with controlled levels of nutrients are necessary to confirm these hypotheses.

WRKY-RNAi expression under control of the actin and the RTBV promoters resulted in the same phenotype. The RTBV promoter had been selected because of its good expression in leaves, but it is hard to see how knockdown of a gene in leaves can affect plant height or tiller number. However, all that has been determined so far is that the RTBV promoter gives expression in leaves, immature floral tissues and endosperm of wheat but not in roots, pollen or the axis of immature zygotic embryo (Rothamsted Cereal Transformation Group, unpublished). So it is possible the RTBV promoter is expressed in other tissues, for instance the stem. Alternatively, it is possible that an RNAi-derived silencing signal was transported throughout the plant via the phloem (Voinnet et al., 1998). This is particularly an option since RTBV-expression in rice leaves was found to be specifically high in the phloem (Bhattacharyya-Pakrasi et al., 1993).

Phylogenetic analysis (Figure 6.2) showed the genes most resembling the wheat gene are rice *OsWRKY37* (Os04g50920) and *OsWRKY66* (Os02g47060). These two genes have not been functionally analysed, so a function in leaf senescence cannot be excluded. Transcription analysis showed that *OsWRKY66* was not expressed in either young or mature leaves (Ramamoorthy et al., 2008), suggesting this closely related rice gene is not involved in the regulation of senescence. However, the same study also showed completely different expression patterns for closely-related WRKY genes in rice (Ramamoorthy et al., 2008), indicating it is difficult to assign a function to a WRKY gene based on homology. Nevertheless, the expression of the WRKY gene in various plant tissues (Figure 6.22), markedly the roots, and the diverse effects of RNAi on wheat morphology, indicate it is implausible the wheat WRKY gene is involved exclusively in leaf senescence.

In summary, a WRKY transcription factor has been identified that showed increasing expression during leaf senescence in wheat. Introduction of a WRKY-RNAi construct in wheat did not result in a reduction of WRKY mRNA levels, but brought about accelerated leaf senescence and significantly increased plant height, the number of fertile tillers and grain yield.

7. GENERAL DISCUSSION

7.1 BACKGROUND

In the past fifty years there has been a substantial growth in food production, allowing for a fall in the proportion of hungry people despite the doubling of the global population (Godfray et al., 2010). However, agricultural production must increase further to feed an ever-growing global population. Additionally, increasingly biofuel crops are grown to raise energy production and relieve climate change, increasing competition for land. Therefore a growth in crop production is required and will have to come from increasing crop yields per unit area.

Since the introduction of semi-dwarfing genes in the green revolution, wheat productivity has been raised by increasing genetic yield potential, resistance to diseases, and adaptation to abiotic stresses (Reynolds et al., 2009), as well as improved agronomic practices such as the supply of optimal levels of nitrogen (N) fertilisers (Kant et al., 2011). However, N fertiliser is the main cost factor of agriculture and can damage the environment by leaching and subsequent eutrophication and ecosystem damage, as well as emissions of gaseous forms of N such as nitrous oxide which are potent greenhouse gasses (Carpenter et al., 1998; Crutzen et al., 2008; Good et al., 2004). Therefore it would be highly beneficial to breed crops that use nitrogen more efficiently; thus have a higher yield per unit N input.

Possible routes to achieve both higher nitrogen use efficiency (NUE) and crop yield would be to increase total photosynthetic production during a plant's lifespan, particularly during grain-filling, by increasing photosynthetic rate, photosynthetic leaf area, or duration of photosynthesis. To date, increases in grain yield of wheat have been achieved by increasing green leaf area duration, mostly by control of foliar diseases, but without increasing the rate

of photosynthesis or the total shoot biomass (Richards, 2000). Therefore extending the duration of photosynthesis is considered to be the easiest way to raise total photosynthesis, aboveground biomass and grain yield.

Apart from controlling foliar diseases, an increase in the duration of photosynthesis can be achieved by lengthening the growing seasons by postponing the anthesis date, or by extending the period of post-anthesis photosynthesis either by bringing forward the anthesis date or by delaying leaf senescence during grain-filling. Changes in anthesis date could be precarious, however, since a delay in anthesis increases the chance wheat will be exposed to heat stress during flowering and drought during grain-filling, especially now hot and dry weather episodes are expected to become more common in Europe because of climate change (Semenov and Shewry, 2011), whilst bringing forward the anthesis date will increase the chance of frost damage (Fuller et al., 2007). Therefore delaying the onset and / or rate of canopy senescence is probably the most promising way to increase the duration of photosynthesis, and accordingly, total photosynthetic production.

Delayed senescence phenotypes in which greenness and photosynthesis are maintained for longer compared to a reference phenotype are termed “functional stay-green” (Thomas and Howarth, 2000). The central hypothesis underpinning the work described in this thesis is that functionally stay-green wheat phenotypes can be identified and used to increase grain yield and NUE in wheat. Analysis of functional stay-green wheat phenotypes also could provide fundamental knowledge about the relationships between leaf senescence, nitrogen remobilisation, grain yield and grain nitrogen concentration and content. Furthermore, enhanced knowledge of the genetic regulation of the stay-green trait could result in the identification of novel genes to be deployed in wheat breeding programmes.

7.2 THE EFFECTS OF THE STAY-GREEN TRAIT ON GRAIN YIELD AND NITROGEN CONTENT

The recycling of nutrients, specifically nitrogen, to developing tissues such as the grain is considered to be the main function of leaf senescence. Generally, greenness and total protein content of leaves during senescence are well correlated, except for non-functional stay-green mutants (Thomas et al., 2002). Differences in leaf senescence should therefore correspond to differences in nitrogen remobilisation from the leaf. However, if senescence is merely delayed or taking place at a slower rate but is eventually completed, so total N remobilisation is not restricted, one would expect that final total grain nitrogen content will be conserved. This appears to have been the case for most experiments described in this thesis. Despite displaying differences in senescence, the Avalon x Cadenza doubled haploid lines AC82 and AC127 described in Chapter 3 had similar total grain nitrogen content at all N fertiliser regimes in two growing seasons. In contrast, the stay-green and fast-senescing mutant lines of wheat identified in Section 4.3 generally had lower total grain nitrogen contents than wild-type. However, in the nitrogen nutrition experiment (Section 4.4), some of the same lines, FS2 and SG3, had similar total grain N contents as WT at both low and high N supply. Stay-green mutant line SG3 even had a higher total grain N content than fast-senescing mutant line FS2 and wild-type at high N, but this was not because of differences in leaf senescence, but due to a higher grain yield driven by a higher tiller number while grain N concentrations were unchanged. Finally, the NAC-overexpressing lines of wheat characterised in Chapter 5, which displayed a stay-green phenotype, had similar grain N contents as a control line. These results indicate that total nitrogen remobilisation from the leaves during grain-filling was not affected by delayed leaf senescence. This contradicts previous reports, which showed that higher N remobilisation was associated with an earlier onset and faster rate of leaf senescence in sorghum (Borrell and Hammer, 2000) and high N utilisation efficiency was associated with earlier onset of senescence in wheat at low N supply (Gaju et al., 2011).

Four NAC-overexpressing lines of wheat had higher grain N concentrations than the control line, also when grain yields were similar. In addition, both the fast-senescing and the stay-green mutants had higher grain N concentrations than wild-type. Grain nitrogen concentration of SG3 was higher than that of wild-type at all N levels, also when grain yields were equivalent. These results indicate that nitrogen was not limiting grain growth and development, challenging the general assumption that grain N content is source-limited (Martre et al., 2003).

In contrast to the studies showing that the stay-green trait in wheat increased final shoot biomass and / or grain yield (Chen et al., 2011a; Chen et al., 2010; Christopher et al., 2008; Gong et al., 2005; Luo et al., 2006; Spano et al., 2003), the stay-green phenotypes described in this thesis did not have higher aboveground biomass or grain yields than the reference phenotypes. Of the mutant lines, stay-green line SG3 had the highest post-anthesis biomass production and the lowest carbon (C) remobilisation at all N levels. However, SG3 had lower shoot biomass at maturity, lower or similar grain yields as WT in all experiments, and the harvest indexes were comparable. Stay-green doubled haploid line AC82 had similar grain yields as faster-senescing AC127. AC82 had a higher harvest index than AC127, but this was because of a lower straw biomass (and thus a lower total aboveground biomass). The NAC-overexpressing lines did not differ from the control lines in final aboveground biomass, grain yield or harvest index. However, the control line had a relatively low biomass at anthesis and the highest biomass at maturity, indicating it had a higher post-anthesis level of photosynthesis than the stay-green NAC-overexpressing lines. So even though in most cases the post-anthesis photosynthetic production of the stay-green phenotypes was higher, final aboveground biomass and grain yields were not. These results indicate that no additional photo-assimilates were remobilised from the canopy to the grain. This has been described previously for a stay-green wheat phenotype (Gong et al., 2005). One possible explanation is that wheat is not source-

limited, as concluded by Borrás et al. (2004), and that the plants therefore had no capacity to exploit extra carbon for grain-filling.

The stay-green trait in wheat has been reported to be advantageous under abiotic stress conditions such as low N supply (Gaju et al., 2011), and heat and drought (Christopher et al., 2008; Naruoka et al., 2012). At low N, WT and FS2 had a reduced nitrogen harvest index (NHI) compared to high N, while SG3 maintained its NHI at low N. Additionally, grain yield of SG3 was higher than WT at low N in the field (Derkx et al., 2012). These results reinforce the hypothesis that stay-green phenotypes could be better adapted to stress conditions such as low N availability.

Since plant nitrogen status has been shown to be an important determinant of onset and progression of leaf senescence (Schildhauer et al., 2008; van Oosterom et al., 2010), it is possible that the mutations of the stay-green and fast-senescing mutants affected N status, and that the different leaf senescence phenotypes were indirect consequences. Likewise, the premature senescence of the WRKY-RNAi plants characterised in Chapter 6 could have been due to nutrient deficiency, most likely nitrogen, since the increased tiller number must have increased the nutritional requirements and the plants were grown in pots intended for “normal-sized” plants.

In summary, the stay-green phenotypes studied in this thesis had similar or reduced grain yields compared to the reference phenotypes, probably because carbon remobilisation was limited. Nitrogen remobilisation was unaffected; therefore grain N concentrations were higher but total grain N content unchanged. This is essentially the opposite of what had been predicted. However, since post-anthesis biomass production was found to be higher in most stay-green phenotypes and N remobilisation was unaffected, there is potential for yield improvement if carbon remobilisation can be enhanced. Furthermore, stay-green phenotypes might be useful to increase yield potential under adverse environmental conditions.

7.3 PROSPECTS FOR FUTURE RESEARCH AND WHEAT IMPROVEMENT

7.3.1 NAC-Overexpressing and WRKY-RNAi-Knockdown Wheat

Overexpression of the NAC transcription factor resulted in a stay-green phenotype as hypothesised, but grain yield was not increased. However, RNAi-knockdown of the WRKY transcription factor had unexpected results: leaf senescence was accelerated instead of delayed, the plants were taller and they had more fertile tillers. To get a better idea of the exact functions of the WRKY and NAC genes, it would be of interest to identify the genes regulated by these transcription factors, for instance by a transcriptome study of the transgenic plants compared to the wild-type using microarrays or RNA-sequencing. Another approach would be to identify the promoter region to which the NAC and WRKY genes bind, and the genes containing this promoter, by bioinformatics. A chromatin immunoprecipitation (ChIP) based method would be possible as well, but for this the NAC and WRKY proteins would have to be purified.

Even though the RTBV promoter was used to manipulate gene expression in leaves, its expression pattern in leaves throughout development has not been established. In rice the expression of the RTBV promoter was predominantly localised to the phloem, although there was also lower expression in the mesophyll parenchyma (Bhattacharyya-Pakrasi et al., 1993). The NAC-overexpressing experiment showed that under control of the RTBV promoter NAC expression increased during leaf senescence (Figure 5.19), but RTBV expression has not been established in expanding leaves. Additionally, since the WRKY-RNAi plants had increased plant height and tiller number, the RTBV promoter might be expressed in other tissues such as the stem or the meristems which form the leaves and tillers. Clarification of where and when the RTBV promoter is expressed is thus indispensable to properly understand the phenotypes of the transgenic plants.

Although RNAi-knockdown of the WRKY transcription factor did not result in the anticipated stay-green phenotype, it increased the plant height and the number of productive tillers, resulting in a thirty per cent increase in grain yield. The increased tiller number would obviously be a very interesting trait for wheat breeding. Since most tillers were producing seed, the WRKY-mediated tillering-trait might also be useful for improving tillering-economy; thus reducing the number of wasteful unproductive tillers and thereby improving the harvest index. On the other hand, the increased height would make the plants more vulnerable to lodging when grown in the field. It should therefore be investigated whether the effects on height and tillering are inseparable or whether they can be disconnected. Furthermore, since yield differences in the glasshouse do not always translate into higher yields in the field (see for instance SG3 described in Chapter 4 and Derkx et al. (2012)), field trials under a range of conditions are required to validate the high-yielding phenotype.

Whether transgenic studies of wheat will have an immediate impact on wheat breeding in general is debatable. The global area of genetically modified (GM) crops, mainly maize, cotton and soybean, has been increasing by 8% a year and reached 160 million hectares in 2011, representing a monetary value of $13.3 billion (James, 2011). However, GM technology has aroused a lot of suspicion, particularly in Europe, resulting in an extensive regulatory framework in the European Union. It is certainly possible first to identify candidate genes by transgenic approaches, then identify plants carrying mutations in this gene by TILLING (Targeting Induced Local Lesions in Genomes), and subsequently include these plants in conventional breeding programmes. This would, however, be rather time-consuming. Alternatively, European attitudes to GM may perhaps change in the future, as feeding an increasing global population with a growing taste for meat, and simultaneously growing enough crops for biofuels to satisfy the growing demand for energy, all in a sustainable manner while there is less land available for agriculture, might turn out to be progressively more problematic.

7.3.2 Stay-Green Mutants

For the stay-green and fast-senescing mutant lines of wheat, biomass and nitrogen partitioning were examined for the main shoot. However, root size and activity were largely ignored. Root size could be relevant because (a) larger roots systems with increased root length density (root length per unit soil volume) should be able to take up more water and nutrients from the soil, and (b) the roots could be hidden stores of both nitrogen and carbon. This could particularly be important under drought stress. Increased root biomass (carbon allocation) has been suggested to be the reason for higher water and nitrogen uptake in stay-green phenotypes of sorghum, wheat and maize (Borrell and Hammer, 2000; Christopher et al., 2008; Rajcan and Tollenaar, 1999b). The importance of post-anthesis N uptake was also established in the nitrogen nutrition experiment, which showed that grain N content of all three lines was more dependent on post-anthesis N uptake than on N remobilisation, especially at low N (Figure 4.30). Naruoka et al. (2012) estimated root biomass by measuring xylem exudate and found that it was positively correlated with stay-green of the flag leaf and grain weight and diameter under hot and dry conditions. Measuring root biomass at anthesis and maturity could be useful to assess total and post-anthesis C and N uptake of the whole plant.

The stay-green mutants and transgenic lines described in this thesis were assessed in the glasshouse, where temperature, water, nutrients and pests and diseases were controlled to a greater level than is possible in the field. Despite evidence that stay-green phenotypes have higher water use efficiency (Christopher et al., 2008; Górny and Garczyński, 2002) and NUE at low N supply (Gaju et al., 2011), and are more resistant to spot blotch (Joshi et al., 2007), only in the instance of the comparison of FS2, SG3 and wild-type the effects of one of these factors, nitrogen nutrition, was investigated. Environmental effects may become even more important in the future because of climate change: Lobell and Field (2007) estimated that recent climate trends already have suppressed global wheat yields by 19 Mt per year

since the 1980s. It is thus important to dissect the interactions between the stay-green trait and appropriate external factors such as heat, drought, nitrogen supply and foliar diseases, to allow for a proper assessment of the usefulness of the stay-green trait for breeding wheat varieties more resistant to abiotic stress and diseases.

If the stay-green trait of SG3 would be deemed to be worth introgressing into new wheat varieties, identification of the relevant mutated genes would be required. The stay-green and fast-senescing plants were fifth- or sixth-generation descendants of EMS mutants. The mutations have never been identified at the genetic or molecular level, making marker-assisted breeding impossible at this time. Furthermore, since the mutations were induced by the EMS procedure, their phenotypes might depend on more than one mutation. So these mutations cannot be employed for wheat breeding at this stage, although the Paragon mutants themselves could be grown.

In theory, a delay in leaf senescence would increase grain yields but lower grain N concentrations because the total N content would be unaffected, thereby increasing NUE. Therefore the experiments described in this thesis were originally thought to benefit mainly wheat cultivation for biofuels, animal feed, and brewing and distilling, purposes for which relatively high carbon and low protein contents are required. However, the stay-green wheat phenotypes described in this thesis were found to have higher grain N concentrations and similar or lower grain yields, suggesting that the grain of these stay-green phenotypes could actually be suitable for bread-making, for which a high grain protein content is essential. However, this would change if both the grain yields and NUE of the stay-green phenotypes could be improved as intended.

7.4 CONCLUSION

In this thesis several stay-green phenotypes of wheat were identified: Avalon x Cadenza doubled haploid line AC82, EMS mutants SG1, SG2 and SG3, and transgenic wheat overexpressing a senescence-associated NAC transcription factor. These stay-green phenotypes had similar or reduced grain yields compared to the reference phenotypes, probably because carbon remobilisation was limited. Nitrogen remobilisation was unaffected; therefore grain N concentrations were higher but total grain N content unchanged. These results conflict with the original hypothesis that stay-green phenotypes would have higher yields and lower grain N concentrations.

Contrary to what had been anticipated, RNAi-knockdown of a senescence-associated WRKY transcription factor accelerated leaf senescence, possibly because of nutrient deficiency. It also resulted in an increased plant height, the number of ear-bearing tillers at maturity and grain yield.

These results show that the relationships between senescence, nitrogen remobilisation and grain yield, N concentration and N content are complex and not easily manipulated. Further studies ought to further elucidate the genetic and physiological bases of the stay-green and high-tillering phenotypes, whether the phenotypes are comparable in the glasshouse and in the field, and under which environmental conditions the stay-green trait is most beneficial. The high-tillering phenotype of the WRKY-RNAi plants should increase grain yield, and there is also potential for yield improvement of the stay-green phenotypes if carbon remobilisation can be enhanced. Furthermore, the stay-green trait has been associated with improved tolerance to abiotic stress and foliar diseases. The phenotypes and genes identified in this thesis could provide a valuable contribution to wheat improvement, particularly as wheat-farming under sub-optimal conditions may well become more important in the future because of climate change.

BIBLIOGRAPHY

ABREU ME and MUNNÉ-BOSCH S (2009). Salicylic acid deficiency in *NahG* transgenic lines and *sid2* mutants increases seed yield in the annual plant *Arabidopsis thaliana*. *Journal of Experimental Botany* **60**: 1261-1271.

AGÜERA E, CABELLO P and DE LA HABA P (2010). Induction of leaf senescence by low nitrogen nutrition in sunflower (*Helianthus annuus*) plants. *Physiologia Plantarum* **138**: 256-267.

ANDERSSON A, KESKITALO J, SJÖDIN A, BHALERAO R, STERKY F, WISSEL K, TANDRE K, ASPEBORG H, MOYLE R, OHMIYA Y, BRUNNER A, GUSTAFSSON P, KARLSSON J, LUNDEBERG J, NILSSON O, SANDBERG G, STRAUSS S, SUNDBERG B, UHLEN M, JANSSON S and NILSSON P (2004). A transcriptional timetable of autumn senescence. *Genome Biology* **5**: R24.

ARMSTEAD I, DONNISON I, AUBRY S, HARPER J, HÖRTENSTEINER S, JAMES C, MANI J, MOFFET M, OUGHAM H, ROBERTS L, THOMAS A, WEEDEN N, THOMAS H and KING I (2007). Cross-species identification of Mendel's *I* locus. *Science* **315**: 73-73.

AY N, CLAUSS K, BARTH O and HUMBECK K (2008). Identification and characterization of novel senescence-associated genes from barley (*Hordeum vulgare*) primary leaves. *Plant Biology* **10**: 121-135.

AY N, IRMLER K, FISCHER A, UHLEMANN R, REUTER G and HUMBECK K (2009). Epigenetic programming via histone methylation at *WRKY53* controls leaf senescence in *Arabidopsis thaliana*. *Plant Journal* **58**: 333-346.

BALAZADEH S, KWASNIEWSKI M, CALDANA C, MEHRNIA M, ZANOR MI, XUE GP and MUELLER-ROEBER B (2011). ORS1, an H_2O_2-responsive NAC transcription factor, controls senescence in *Arabidopsis thaliana*. *Molecular Plant* **4**: 346-360.

BALAZADEH S, RIAÑO-PACHÓN DM and MUELLER-ROEBER B (2008). Transcription factors regulating leaf senescence in *Arabidopsis thaliana*. *Plant Biology* **10**: 63-75.

BALAZADEH S, SIDDIQUI H, ALLU AD, MATALLANA-RAMIREZ LP, CALDANA C, MEHRNIA M, ZANOR MI, KÖHLER B and MUELLER-ROEBER B (2010). A gene regulatory network controlled by the NAC transcription factor ANAC092/AtNAC2/ORE1 during salt-promoted senescence. *Plant Journal* **62**: 250-264.

BANCAL P (2009). Decorrelating source and sink determinism of nitrogen remobilization during grain filling in wheat. *Annals of Botany* **103**: 1315-1324.

BARBOTTIN A, LECOMTE C, BOUCHARD C and JEUFFROY MH (2005). Nitrogen remobilization during grain filling in wheat: Genotypic and environmental effects. *Crop Science* **45**: 1141-1150.

BARRY CS (2009). The stay-green revolution: Recent progress in deciphering the mechanisms of chlorophyll degradation in higher plants. *Plant Science* **176**: 325-333.

BARRY CS, MCQUINN RP, CHUNG MY, BESUDEN A and GIOVANNONI JJ (2008). Amino acid substitutions in homologs of the STAY-GREEN protein are responsible for the green-flesh and chlorophyll retainer mutations of tomato and pepper. *Plant Physiology* **147**: 179-187.

BERRI S, ABBRUSCATO P, FAIVRE-RAMPANT O, BRASILEIRO ACM, FUMASONI I, SATOH K, KIKUCHI S, MIZZI L, MORANDINI P, PÉ ME and PIFFANELLI P (2009). Characterization of *WRKY* co-regulatory networks in rice and Arabidopsis. *BMC Plant Biology* **9**: 120.

BESSEAU S, LI J and PALVA ET (2012). WRKY54 and WRKY70 co-operate as negative regulators of leaf senescence in *Arabidopsis thaliana*. *Journal of Experimental Botany* **63**: 2667-79.

BHATTACHARYYA-PAKRASI M, PENG J, ELMER JS, LACO G, SHEN P, KANIEWSKA MB, KONONOWICZ H, WEN F, HODGES TK and BEACHY RN (1993). Specificity of a promoter from the rice tungro bacilliform virus for expression in phloem tissues. *Plant Journal* **4**: 71-79.

BI YM, KANT S, CLARK J, GIDDA S, MING F, XU JY, ROCHON A, SHELP BJ, HAO LX, ZHAO R, MULLEN RT, ZHU T and ROTHSTEIN SJ (2009). Increased nitrogen-use efficiency in transgenic rice plants over-expressing a nitrogen-responsive early nodulin gene identified from rice expression profiling. *Plant Cell and Environment* **32**: 1749-1760.

BLAKE NK, LANNING SP, MARTIN JM, SHERMAN JD and TALBERT LE (2007). Relationship of flag leaf characteristics to economically important traits in two spring wheat crosses. *Crop Science* **47**: 491-496.

BOGARD M, ALLARD V, BRANCOURT-HULMEL M, HEUMEZ E, MACHET JM, JEUFFROY MH, GATE P, MARTRE P and LE GOUIS J (2010). Deviation from the grain protein concentration-grain yield negative relationship is highly correlated to post-anthesis N uptake in winter wheat. *Journal of Experimental Botany* **61**: 4303-4312.

BOGARD M, JOURDAN M, ALLARD V, MARTRE P, PERRETANT MR, RAVEL C, HEUMEZ E, ORFORD S, SNAPE J, GRIFFITHS S, GAJU O, FOULKES J and LE GOUIS J (2011). Anthesis date mainly explained correlations between post-anthesis leaf senescence, grain yield, and grain protein concentration in a winter wheat population segregating for flowering time QTLs. *Journal of Experimental Botany* **62**: 3621-3636.

BORRÁS L, SLAFER GA and OTEGUI ME (2004). Seed dry weight response to source-sink manipulations in wheat, maize and soybean: a quantitative reappraisal. *Field Crops Research* **86**: 131-146.

BORRELL AK and HAMMER GL (2000). Nitrogen dynamics and the physiological basis of stay-green in sorghum. *Crop Science* **40**: 1295-1307.

BREEZE E, HARRISON E, MCHATTIE S, HUGHES L, HICKMAN R, HILL C, KIDDLE S, KIM YS, PENFOLD CA, JENKINS D, ZHANG CJ, MORRIS K, JENNER C, JACKSON S, THOMAS B, TABRETT A, LEGAIE R, MOORE JD, WILD DL, OTT S, RAND D, BEYNON J, DENBY K, MEAD A and BUCHANAN-WOLLASTON V (2011). High-resolution temporal profiling of transcripts during *Arabidopsis* leaf senescence reveals a distinct chronology of processes and regulation. *Plant Cell* **23**: 873-894.

BREMNER JM (1997). Sources of nitrous oxide in soils. *Nutrient Cycling in Agroecosystems* **49**: 7-16.

BRODERSEN P, SAKVARELIDZE-ACHARD L, BRUUN-RASMUSSEN M, DUNOYER P, YAMAMOTO YY, SIEBURTH L and VOINNET O (2008). Widespread translational inhibition by plant miRNAs and siRNAs. *Science* **320**: 1185-1190.

BUCHANAN-WOLLASTON V, PAGE T, HARRISON E, BREEZE E, LIM PO, NAM HG, LIN JF, WU SH, SWIDZINSKI J, ISHIZAKI K and LEAVER CJ (2005). Comparative transcriptome analysis reveals significant differences in gene expression and signalling pathways between developmental and dark/starvation-induced senescence in Arabidopsis. *Plant Journal* **42**: 567-585.

CANTU D, PEARCE SP, DISTELFELD A, CHRISTIANSEN MW, UAUY C, AKHUNOV E, FAHIMA T and DUBCOVSKY J (2011). Effect of the down-regulation of the high *Grain Protein Content (GPC)* genes on the wheat transcriptome during monocarpic senescence. *BMC Genomics* **12**.

CARPENTER SR, CARACO NF, CORRELL DL, HOWARTH RW, SHARPLEY AN and SMITH VH (1998). Nonpoint pollution of surface waters with phosphorus and nitrogen. *Ecological Applications* **8**: 559-568.

CHARDON F, BARTHÉLÉMY J, DANIEL-VEDELE F and MASCLAUX-DAUBRESSE C (2010). Natural variation of nitrate uptake and nitrogen use efficiency in *Arabidopsis thaliana* cultivated with limiting and ample nitrogen supply. *Journal of Experimental Botany* **61**: 2293-2302.

CHEN CC, HAN GQ, HE HQ and WESTCOTT M (2011a). Yield, protein, and remobilization of water soluble carbohydrate and nitrogen of three spring wheat cultivars as influenced by nitrogen input. *Agronomy Journal* **103**: 786-795.

CHEN JB, LIANG Y, HU XY, WANG XX, TAN FQ, ZHANG HQ, REN ZL and LUO PG (2010). Physiological characterization of 'stay green' wheat cultivars during the grain filling stage under field growing conditions. *Acta Physiologiae Plantarum* **32**: 875-882.

CHEN YX, QIU K, KUAI BK and DING YL (2011b). Identification of an NAP-like transcription factor BeNAC1 regulating leaf senescence in bamboo (*Bambusa emeiensis* 'Viridiflavus'). *Physiologia Plantarum* **142**: 361-371.

CHRISTOPHER JT, MANSCHADI AM, HAMMER GL and BORRELL AK (2008). Developmental and physiological traits associated with high yield and stay-green phenotype in wheat. *Australian Journal of Agricultural Research* **59**: 354-364.

CLIFTON-BROWN JC, LEWANDOWSKI I, BANGERTH F and JONES MB (2002). Comparative responses to water stress in stay-green, rapid- and slow senescing genotypes of the biomass crop, Miscanthus. *New Phytologist* **154**: 335-345.

CRUTZEN PJ, MOSIER AR, SMITH KA and WINIWARTER W (2008). N_2O release from agro-biofuel production negates global warming reduction by replacing fossil fuels. *Atmospheric Chemistry and Physics* **8**: 389-395.

DE LA VEGA AJ, CANTORE MA, SPOSARO MM, TRÁPANI N, LÓPEZ PEREIRA M and HALL AJ (2011). Canopy stay-green and yield in non-stressed sunflower. *Field Crops Research* **121**: 175-185.

DERKX AP, FOULKES MJ and HAWKESFORD MJ (2010). Variation in leaf senescence, nitrogen remobilisation and harvest index in two lines of wheat. *Aspects of Applied Biology* **105**: 233-237.

DERKX AP, ORFORD S, GRIFFITHS S, FOULKES MJ and HAWKESFORD MJ (2012). Identification of differentially senescing mutants of wheat and impacts on yield, biomass and nitrogen partitioning. *Journal of Integrative Plant Biology* **54**: 555-566.

DIAZ C, LEMAÎTRE T, CHRIST A, AZZOPARDI M, KATO Y, SATO F, MOROT-GAUDRY JF, LE DILY F and MASCLAUX-DAUBRESSE C (2008). Nitrogen recycling and remobilization are differentially controlled by leaf senescence and development stage in Arabidopsis under low nitrogen nutrition. *Plant Physiology* **147**: 1437-1449.

DING L, WANG KJ, JIANG GM, BISWAS DK, XU H, LI LF and LI YH (2005). Effects of nitrogen deficiency on photosynthetic traits of maize hybrids released in different years. *Annals of Botany* **96**: 925-930.

DISTELFELD A, PEARCE SP, AVNI R, SCHERER B, UAUY C, PISTON F, SLADE A, ZHAO RR and DUBCOVSKY J (2012). Divergent functions of orthologous NAC transcription factors in wheat and rice. *Plant Molecular Biology* **78**: 515-524.

DONNISON IS, GAY AP, THOMAS H, EDWARDS KJ, EDWARDS D, JAMES CL, THOMAS AM and OUGHAM HJ (2007). Modification of nitrogen remobilization, grain fill and leaf senescence in maize (*Zea mays*) by transposon insertional mutagenesis in a protease gene. *New Phytologist* **173**: 481-494.

DUMAS JBA (1831). Procédès de l'analyse organique. *Annales de Chimie et de Physique* **2**: 198–213.

ECHARTE L, ROTHSTEIN S and TOLLENAAR M (2008). The response of leaf photosynthesis and dry matter accumulation to nitrogen supply in an older and a newer maize hybrid. *Crop Science* **48**: 656-665.

ELLIS CM, NAGPAL P, YOUNG JC, HAGEN G, GUILFOYLE TJ and REED JW (2005). A*UXIN RESPONSE FACTOR1* and *AUXIN RESPONSE FACTOR2* regulate senescence and floral organ abscission in *Arabidopsis thaliana*. *Development* **132**: 4563-4574.

ERLEY GSA, WIJAYA KA, ULAS A, BECKER H, WIESLER F and HORST WJ (2007). Leaf senescence and N uptake parameters as selection traits for nitrogen efficiency of oilseed rape cultivars. *Physiologia Plantarum* **130**: 519-531.

ESPINDULA LF, MINELLA E and DELATORRE CA (2009). Low-P tolerance mechanisms and differential gene expression in contrasting wheat genotypes. *Pesquisa Agropecuaria Brasileira* **44**: 1100-1105.

EULGEM T, RUSHTON PJ, ROBATZEK S and SOMSSICH IE (2000). The WRKY superfamily of plant transcription factors. *Trends in Plant Science* **5**: 199-206.

FANG YJ, YOU J, XIE KB, XIE WB and XIONG LZ (2008). Systematic sequence analysis and identification of tissue-specific or stress-responsive genes of NAC transcription factor family in rice. *Molecular Genetics and Genomics* **280**: 547-563.

FAO (2010). *http://faostat.fao.org/site/291/default.aspx* [Online]. Food and Agriculture Organization of the United Nations Statistical Databases (FAOSTAT).

FITTER DW, MARTIN DJ, COPLEY MJ, SCOTLAND RW and LANGDALE JA (2002). *GLK* gene pairs regulate chloroplast development in diverse plant species. *Plant Journal* **31**: 713-727.

FU J and LEE B (2008). Changes in photosynthetic characteristics during grain filling of a functional stay-green rice SNU-SG1 and its F1 hybrids. *Journal of Crop Science and Biotechnology* **11**: 75-82.

FULLER MP, FULLER AM, KANIOURAS S, CHRISTOPHERS J and FREDERICKS T (2007). The freezing characteristics of wheat at ear emergence. *European Journal of Agronomy* **26**: 435-441.

GAJU O, ALLARD V, MARTRE P, SNAPE JW, HEUMEZ E, LE GOUIS J, MOREAU D, BOGARD M, GRIFFITHS S, ORFORD S, HUBBART S and FOULKES MJ (2011). Identification of traits to improve the nitrogen-use efficiency of wheat genotypes. *Field Crops Research* **123**: 139-152.

GAN SS and AMASINO RM (1995). Inhibition of leaf senescence by autoregulated production of cytokinin. *Science* **270**: 1986-1988.

GODFRAY HCJ, BEDDINGTON JR, CRUTE IR, HADDAD L, LAWRENCE D, MUIR JF, PRETTY J, ROBINSON S, THOMAS SM and TOULMIN C (2010). Food security: The challenge of feeding 9 billion people. *Science* **327**: 812-818.

GONG YH, ZHANG J, GAO JF, LU JY and WANG JR (2005). Slow export of photoassimilate from stay-green leaves during late grain-filling stage in hybrid winter wheat (*Triticum aestivum* L.). *Journal of Agronomy and Crop Science* **191**: 292-299.

GOOD AG, JOHNSON SJ, DE PAUW M, CARROLL RT and SAVIDOV N (2007). Engineering nitrogen use efficiency with alanine aminotransferase. *Canadian Journal of Botany-Revue Canadienne De Botanique* **85**: 252-262.

GOOD AG, SHRAWAT AK and MUENCH DG (2004). Can less yield more? Is reducing nutrient input into the environment compatible with maintaining crop production? *Trends in Plant Science* **9**: 597-605.

GÓRNY AG and GARCZYŃSKI S (2002). Genotypic and nutrition-dependent variation in water use efficiency and photosynthetic activity of leaves in winter wheat (*Triticum aestivum* L.). *Journal of Applied Genetics* **43**: 145-160.

GREGERSEN PL and HOLM PB (2007). Transcriptome analysis of senescence in the flag leaf of wheat (*Triticum aestivum* L.). *Plant Biotechnology Journal* **5**: 192-206.

GREGERSEN PL, HOLM PB and KRUPINSKA K (2008). Leaf senescence and nutrient remobilisation in barley and wheat. *Plant Biology* **10**: 37-49.

GUIBOILEAU A, YOSHIMOTO K, SOULAY F, BATAILLÉ MP, AVICE JC and MASCLAUX-DAUBRESSE C (2012). Autophagy machinery controls nitrogen remobilization at the whole-plant level under both limiting and ample nitrate conditions in Arabidopsis. *New Phytologist* **194**: 732-740.

GUO Y, CAI Z and GAN S (2004). Transcriptome of Arabidopsis leaf senescence. *Plant Cell and Environment* **27**: 521-549.

GUO YF and GAN SS (2006). AtNAP, a NAC family transcription factor, has an important role in leaf senescence. *Plant Journal* **46**: 601-612.

GUO YF and GAN SS (2012). Convergence and divergence in gene expression profiles induced by leaf senescence and 27 senescence-promoting hormonal, pathological and environmental stress treatments. *Plant Cell and Environment* **35**: 644-655.

GUTIÉRREZ RA, STOKES TL, THUM K, XU X, OBERTELLO M, KATARI MS, TANURDZIC M, DEAN A, NERO DC, MCCLUNG CR and CORUZZI GM (2008). Systems approach identifies an organic nitrogen-responsive gene network that is regulated by the master clock control gene CCA1. *Proceedings of the National Academy of Sciences of the United States of America* **105**: 4939-4944.

HAJOUJ T, MICHELIS R and GEPSTEIN S (2000). Cloning and characterization of a receptor-like protein kinase gene associated with senescence. *Plant Physiology* **124**: 1305-1314.

HAO YJ, SONG QX, CHEN HW, ZOU HF, WEI W, KANG XS, MA BA, ZHANG WK, ZHANG JS and CHEN SY (2010). Plant NAC-type transcription factor proteins contain a NARD domain for repression of transcriptional activation. *Planta* **232**: 1033-1043.

HAUCK B, GAY AP, MACDUFF J, GRIFFITHS CM and THOMAS H (1997). Leaf senescence in a non-yellowing mutant of *Festuca pratensis*: implications of the stay-green mutation for photosynthesis, growth and nitrogen nutrition. *Plant Cell and Environment* **20**: 1007-1018.

HAWKESFORD MJ and HOWARTH JR (2010). Transcriptional profiling approaches for studying nitrogen use efficiency. *In:* FOYER C H and ZHANG H (eds.) *Nitrogen metabolism in plants in the post-genomic era.* Wiley-Blackwell.

HENSEL LL, GRBIĆ V, BAUMGARTEN DA and BLEECKER AB (1993). Developmental and age-related processes that influence the longevity and senescence of photosynthetic tissues in Arabidopsis. *Plant Cell* **5**: 553-564.

HINDERHOFER K and ZENTGRAF U (2001). Identification of a transcription factor specifically expressed at the onset of leaf senescence. *Planta* **213**: 469-473.

HIREL B, LE GOUIS J, NEY B and GALLAIS A (2007). The challenge of improving nitrogen use efficiency in crop plants: towards a more central role for genetic variability and quantitative genetics within integrated approaches. *Journal of Experimental Botany* **58**: 2369-2387.

HOISINGTON D, KHAIRALLAH M, REEVES T, RIBAUT JV, SKOVMAND B, TABA S and WARBURTON M (1999). Plant genetic resources: What can they contribute toward increased crop productivity? *Proceedings of the National Academy of Sciences of the United States of America* **96**: 5937-5943.

HÖRTENSTEINER S and FELLER U (2002). Nitrogen metabolism and remobilization during senescence. *Journal of Experimental Botany* **53**: 927-937.

HÖRTENSTEINER S and KRÄUTLER B (2011). Chlorophyll breakdown in higher plants. *Biochimica Et Biophysica Acta-Bioenergetics* **1807**: 977-988.

HUMBECK K, QUAST S and KRUPINSKA K (1996). Functional and molecular changes in the photosynthetic apparatus during senescence of flag leaves from field-grown barley plants. *Plant Cell and Environment* **19**: 337-344.

ISHIDA H, YOSHIMOTO K, IZUMI M, REISEN D, YANO Y, MAKINO A, OHSUMI Y, HANSON MR and MAE T (2008). Mobilization of rubisco and stroma-localized fluorescent proteins of chloroplasts to the vacuole by an ATG gene-dependent autophagic process. *Plant Physiology* **148**: 142-155.

JAMES C (2011). Global status of commercialized biotech/GM crops in 2011. ISAAA **43**(16): Ithaca, NY, USA.

JING HC, STURRE MJG, HILLE J and DIJKWEL PP (2002). *Arabidopsis onset of leaf death* mutants identify a regulatory pathway controlling leaf senescence. *Plant Journal* **32**: 51-63.

JING S, ZHOU X, SONG Y and YU D (2009). Heterologous expression of *OsWRKY23* gene enhances pathogen defense and dark-induced leaf senescence in *Arabidopsis*. *Plant Growth Regulation* **58**: 181-190.

JORDI W, SCHAPENDONK A, DAVELAAR E, STOOPEN GM, POT CS, DE VISSER R, VAN RHIJN JA, GAN S and AMASINO RM (2000). Increased cytokinin levels in transgenic P_{SAG12}-*IPT* tobacco plants have large direct and indirect effects on leaf senescence, photosynthesis and N partitioning. *Plant Cell and Environment* **23**: 279-289.

JOSHI AK, KUMARI M, SINGH VP, REDDY CM, KUMAR S, RANE J and CHAND R (2007). Stay green trait: variation, inheritance and its association with spot blotch resistance in spring wheat (*Triticum aestivum* L.). *Euphytica* **153**: 59-71.

JUKANTI AK, HEIDLEBAUGH NM, PARROTT DL, FISCHER IA, MCINNERNEY K and FISCHER AM (2008). Comparative transcriptome profiling of near-isogenic barley (*Hordeum vulgare*) lines differing in the allelic state of a major grain protein content locus identifies genes with possible roles in leaf senescence and nitrogen reallocation. *New Phytologist* **177**: 333-349.

KADE M, BARNEIX AJ, OLMOS S and DUBCOVSKY J (2005). Nitrogen uptake and remobilization in tetraploid 'Langdon' durum wheat and a recombinant substitution line with the high grain protein gene *Gpc-B1*. *Plant Breeding* **124**: 343-349.

KANG S, SEO M, MOON J, YUN H, LEE Y, KIM S, HWANG Y, LEE S and CHOUNG M (2010). Introduction of stay green mutant for the development of black seed coat and green cotyledon soybean variety. *Korean Journal of Crop Science / Hanguk Jakmul Hakhoe Chi* **55**: 187-194.

KANT S, BI YM and ROTHSTEIN SJ (2011). Understanding plant response to nitrogen limitation for the improvement of crop nitrogen use efficiency. *Journal of Experimental Botany* **62**: 1499-1509.

KICHEY T, HIREL B, HEUMEZ E, DUBOIS F and LE GOUIS J (2007). In winter wheat (*Triticum aestivum* L.), post-anthesis nitrogen uptake and remobilisation to the grain correlates with agronomic traits and nitrogen physiological markers. *Field Crops Research* **102**: 22-32.

KIM JH, WOO HR, KIM J, LIM PO, LEE IC, CHOI SH, HWANG D and NAM HG (2009). Trifurcate feed-forward regulation of age-dependent cell death involving *miR164* in *Arabidopsis*. *Science* **323**: 1053-1057.

KIM JI, MURPHY AS, BAEK D, LEE SW, YUN DJ, BRESSAN RA and NARASIMHAN ML (2011). *YUCCA6* over-expression demonstrates auxin function in delaying leaf senescence in *Arabidopsis thaliana*. *Journal of Experimental Botany* **62**: 3981-3992.

KONG ZS, LI MN, YANG WQ, XU WY and XUE YB (2006). A novel nuclear-localized CCCH-type zinc finger protein, OsDOS, is involved in delaying leaf senescence in rice. *Plant Physiology* **141**: 1376-1388.

KURAI T, WAKAYAMA M, ABIKO T, YANAGISAWA S, AOKI N and OHSUGI R (2011). Introduction of the ZmDof1 gene into rice enhances carbon and nitrogen assimilation under low-nitrogen conditions. *Plant Biotechnology Journal* **9**: 826-837.

LACERENZA JA, PARROTT DL and FISCHER AM (2010). A major grain protein content locus on barley (*Hordeum vulgare* L.) chromosome 6 influences flowering time and sequential leaf senescence. *Journal of Experimental Botany* **61**: 3137-3149.

LARKIN MA, BLACKSHIELDS G, BROWN NP, CHENNA R, MCGETTIGAN PA, MCWILLIAM H, VALENTIN F, WALLACE IM, WILM A, LOPEZ R, THOMPSON JD, GIBSON TJ and HIGGINS DG (2007). Clustal W and clustal X version 2.0. *Bioinformatics* **23**: 2947-2948.

LEE IC, HONG SW, WHANG SS, LIM PO, NAM HG and KOO JC (2011). Age-dependent action of an ABA-inducible receptor kinase, RPK1, as a positive regulator of senescence in Arabidopsis leaves. *Plant and Cell Physiology* **52**: 651-662.

LEE S, SEO PJ, LEE HJ and PARK CM (2012). A NAC transcription factor NTL4 promotes reactive oxygen species production during drought-induced leaf senescence in Arabidopsis. *Plant Journal* **70**: 831-844.

LI H, LIN F, WANG G, JING R, ZHENG Q, LI B and LI Z (2012). Quantitative trait loci mapping of dark-induced senescence in winter wheat (*Triticum aestivum*). *Journal of Integrative Plant Biology* **54**: 33-44.

LI Z, GAO Q, LIU Y, HE C, ZHANG X and ZHANG J (2011). Overexpression of transcription factor *ZmPTF1* improves low phosphate tolerance of maize by regulating carbon metabolism and root growth. *Planta* **233**: 1129-1143.

LIM PO, KIM HJ and NAM HG (2007). Leaf senescence. *Annual Review of Plant Biology* **58**: 115-136.

LIN JF and WU SH (2004). Molecular events in senescing *Arabidopsis* leaves. *Plant Journal* **39**: 612-628.

LIN LL, SHI QH, WANG HS, QIN AG and YU XC (2011). Over-expression of tomato GDP-mannose pyrophosphorylase (GMPase) in potato increases ascorbate content and delays plant senescence. *Agricultural Sciences in China* **10**: 534-543.

LIN R, DING Z, LI L and KUANG T (2001). A rapid and efficient DNA minipreparation suitable for screening transgenic plants. *Plant Molecular Biology Reporter* **19**: 379.

LIU L, ZHOU Y, ZHOU G, YE RJ, ZHAO L, LI XH and LIN YJ (2008). Identification of early senescence-associated genes in rice flag leaves. *Plant Molecular Biology* **67**: 37-55.

LOBELL DB and FIELD CB (2007). Global scale climate - crop yield relationships and the impacts of recent warming. *Environmental Research Letters* **2**: No. 014002.

LUO PG, REN ZL, WU XH, ZHANG HY, ZHANG HQ and FENG JA (2006). Structural and biochemical mechanism responsible for the stay-green phenotype in common wheat. *Chinese Science Bulletin* **51**: 2595-2603.

LUQUEZ VM and GUIAMÉT JJ (2001). Effects of the 'stay green' genotype *GGd1d1d2d2* on leaf gas exchange, dry matter accumulation and seed yield in soybean (*Glycine max* L. Merr.). *Annals of Botany* **87**: 313-318.

LUQUEZ VM and GUIAMÉT JJ (2002). The stay green mutations *d1* and *d2* increase water stress susceptibility in soybeans. *Journal of Experimental Botany* **53**: 1421-1428.

MA W, SMIGEL A, WALKER RK, MOEDER W, YOSHIOKA K and BERKOWITZ GA (2010). Leaf senescence signaling: The Ca^{2+}-conducting Arabidopsis Cyclic Nucleotide Gated Channel2 acts through nitric oxide to repress senescence programming. *Plant Physiology* **154**: 733-743.

MANGELSEN E, KILIAN J, BERENDZEN KW, KOLUKISAOGLU UH, HARTER K, JANSSON C and WANKE D (2008). Phylogenetic and comparative gene expression analysis of barley (*Hordeum vulgare*) WRKY transcription factor family reveals putatively retained functions between monocots and dicots. *BMC Genomics* **9**.

MARTIN A, BELASTEGUI-MACADAM X, QUILLERÉ I, FLORIOT M, VALADIER MH, POMMEL B, ANDRIEU B, DONNISON I and HIREL B (2005). Nitrogen management and senescence in two maize hybrids differing in the persistence of leaf greenness: agronomic, physiological and molecular aspects. *New Phytologist* **167**: 483-492.

MARTINEZ DE, COSTA ML, GOMEZ FM, OTEGUI MS and GUIAMÉT JJ (2008). 'Senescence-associated vacuoles' are involved in the degradation of chloroplast proteins in tobacco leaves. *Plant Journal* **56**: 196-206.

MARTRE P, PORTER JR, JAMIESON PD and TRIBOÏ E (2003). Modeling grain nitrogen accumulation and protein composition to understand the sink/source regulations of nitrogen remobilization for wheat. *Plant Physiology* **133**: 1959-1967.

MASCLAUX-DAUBRESSE C, REISDORF-CREN M and ORSEL M (2008). Leaf nitrogen remobilisation for plant development and grain filling. *Plant Biology* **10**: 23-36.

MAXWELL K and JOHNSON GN (2000). Chlorophyll fluorescence - a practical guide. *Journal of Experimental Botany* **51**: 659-668.

MI GH, TANG L, ZHANG FS and ZHANG JH (2000). Is nitrogen uptake after anthesis in wheat regulated by sink size? *Field Crops Research* **68**: 183-190.

MIAO Y, LAUN T, ZIMMERMANN P and ZENTGRAF U (2004). Targets of the WRKY53 transcription factor and its role during leaf senescence in *Arabidopsis*. *Plant Molecular Biology* **55**: 853-867.

MIAO Y and ZENTGRAF U (2007). The antagonist function of *Arabidopsis* WRKY53 and ESR/ESP in leaf senescence is modulated by the jasmonic and salicylic acid equilibrium. *Plant Cell* **19**: 819-830.

MIAO Y and ZENTGRAF U (2010). A HECT E3 ubiquitin ligase negatively regulates Arabidopsis leaf senescence through degradation of the transcription factor WRKY53. *Plant Journal* **63**: 179-188.

MISHINA TE, LAMB C and ZEIER J (2007). Expression of a nitric oxide degrading enzyme induces a senescence programme in *Arabidopsis*. *Plant Cell and Environment* **30**: 39-52.

NARUOKA Y, SHERMAN JD, LANNING SP, BLAKE NK, MARTIN JM and TALBERT LE (2012). Genetic analysis of green leaf duration in spring wheat. *Crop Science* **52**: 99-109.

NIU Y-H and GUO F-Q (2012). Nitric oxide regulates dark-induced leaf senescence through *EIN2* in Arabidopsis. *Journal of Integrative Plant Biology* **54**: 516-25.

NOH YS and AMASINO RM (1999). Identification of a promoter region responsible for the senescence-specific expression of SAG12. *Plant Molecular Biology* **41**: 181-194.

NURUZZAMAN M, MANIMEKALAI R, SHARONI AM, SATOH K, KONDOH H, OOKA H and KIKUCHI S (2010). Genome-wide analysis of NAC transcription factor family in rice. *Gene* **465**: 30-44.

NURUZZAMAN M, SHARONI AM, SATOH K, MOUMENI A, VENUPRASAD R, SERRAJ R, KUMAR A, LEUNG H, ATTIA K and KIKUCHI S (2012). Comprehensive gene expression analysis of the *NAC* gene family under normal growth conditions, hormone treatment, and drought stress conditions in rice using near-isogenic lines (NILs) generated from crossing Aday Selection (drought tolerant) and IR64. *Molecular Genetics and Genomics* **287**: 389-410.

OKA M, SHIMODA Y, SATO N, INOUE J, YAMAZAKI T, SHIMOMURA N and FUJIYAMA H (2012). Abscisic acid substantially inhibits senescence of cucumber plants (*Cucumis sativus*) grown under low nitrogen conditions. *Journal of Plant Physiology* **169**: 789-796.

OLSEN AN, ERNST HA, LO LEGGIO L and SKRIVER K (2005). NAC transcription factors: structurally distinct, functionally diverse. *Trends in Plant Science* **10**: 79-87.

OOKA H, SATOH K, DOI K, NAGATA T, OTOMO Y, MURAKAMI K, MATSUBARA K, OSATO N, KAWAI J, CARNINCI P, HAYASHIZAKI Y, SUZUKI K, KOJIMA K, TAKAHARA Y, YAMAMOTO K and KIKUCHI S (2003). Comprehensive analysis of NAC family genes in *Oryza sativa* and *Arabidopsis thaliana*. *DNA Research* **10**: 239-247.

OSAKI M (1995). Comparison of productivity between tropical and temperate maize.1. Leaf senescence and productivity in relation to nitrogen nutrition. *Soil Science and Plant Nutrition* **41**: 439-450.

OTEGUI MS, NOH YS, MARTINEZ DE, VILA PETROFF MG, ANDREW STAEHELIN L, AMASINO RM and GUIAMÉT JJ (2005). Senescence-associated vacuoles with intense proteolytic activity develop in leaves of Arabidopsis and soybean. *Plant Journal* **41**: 831-844.

PASK AJD, SYLVESTER-BRADLEY R, JAMIESON PD and FOULKES MJ (2012). Quantifying how winter wheat crops accumulate and use nitrogen reserves during growth. *Field Crops Research* **126**: 104-118.

PAYNE RW, MURRAY DA, HARDING SA, BAIRD DB and SOUTAR DM (2009). *GenStat for Windows (12th Edition) Introduction*, VSN International, Hemel Hempstead.

PENG MS, HANNAM C, GU HL, BI YM and ROTHSTEIN SJ (2007). A mutation in *NLA*, which encodes a RING-type ubiquitin ligase, disrupts the adaptability of *Arabidopsis* to nitrogen limitation. *Plant Journal* **50**: 320-337.

POURTAU N, JENNINGS R, PELZER E, PALLAS J and WINGLER A (2006). Effect of sugar-induced senescence on gene expression and implications for the regulation of senescence in *Arabidopsis*. *Planta* **224**: 556-568.

PRINS A, VAN HEERDEN PDR, OLMOS E, KUNERT KJ and FOYER CH (2008). Cysteine proteinases regulate chloroplast protein content and composition in tobacco leaves: a model for dynamic interactions with ribulose-1,5-bisphosphate carboxylase/oxygenase (Rubisco) vesicular bodies. *Journal of Experimental Botany* **59**: 1935-1950.

PROIETTI S, BERTINI L, VAN DER ENT S, LEON-REYES A, PIETERSE CMJ, TUCCI M, CAPORALE C and CARUSO C (2011). Cross activity of orthologous WRKY transcription factors in wheat and *Arabidopsis*. *Journal of Experimental Botany* **62**: 1975-1990.

QUICK WP, SCHURR U, SCHEIBE R, SCHULZE ED, RODERMEL SR, BOGORAD L and STITT M (1991). Decreased ribulose-1,5-biphosphate carboxylase-oxygenase in transgenic tobacco transformed with antisense rbcS. Impact on photosynthesis in ambient growth-conditions. *Planta* **183**: 542-554.

QUIRINO BF, NOH YS, HIMELBLAU E and AMASINO RM (2000). Molecular aspects of leaf senescence. *Trends in Plant Science* **5**: 278-282.

RAAB S, DRECHSEL G, ZAREPOUR M, HARTUNG W, KOSHIBA T, BITTNER F and HOTH S (2009). Identification of a novel E3 ubiquitin ligase that is required for suppression of premature senescence in Arabidopsis. *Plant Journal* **59**: 39-51.

RAJCAN I and TOLLENAAR M (1999a). Source: sink ratio and leaf senescence in maize: I. Dry matter accumulation and partitioning during grain filling. *Field Crops Research* **60**: 245-253.

RAJCAN I and TOLLENAAR M (1999b). Source: sink ratio and leaf senescence in maize: II. Nitrogen metabolism during grain filling. *Field Crops Research* **60**: 255-265.

RAMAMOORTHY R, JIANG SY, KUMAR N, VENKATESH PN and RAMACHANDRAN S (2008). A comprehensive transcriptional profiling of the *WRKY* gene family in rice under various abiotic and phytohormone treatments. *Plant and Cell Physiology* **49**: 865-879.

RAMPINO P, SPANO G, PATALEO S, MITA G, NAPIER JA, DI FONZO N, SHEWRY PR and PERROTTA C (2006). Molecular analysis of a durum wheat 'stay green' mutant: Expression pattern of photosynthesis-related genes. *Journal of Cereal Science* **43**: 160-168.

REYNOLDS M, FOULKES MJ, SLAFER GA, BERRY P, PARRY MAJ, SNAPE JW and ANGUS WJ (2009). Raising yield potential in wheat. *Journal of Experimental Botany* **60**: 1899-1918.

RICACHENEVSKY FK, SPEROTTO RA, MENGUER PK and FETT JP (2010). Identification of Fe-excess-induced genes in rice shoots reveals a WRKY transcription factor responsive to Fe, drought and senescence. *Molecular Biology Reports* **37**: 3735-3745.

RICHARDS RA (2000). Selectable traits to increase crop photosynthesis and yield of grain crops. *Journal of Experimental Botany* **51**: 447-458.

RICHARDSON AD, DUIGAN SP and BERLYN GP (2002). An evaluation of noninvasive methods to estimate foliar chlorophyll content. *New Phytologist* **153**: 185-194.

RIEFLER M, NOVAK O, STRNAD M and SCHMULLING T (2006). *Arabidopsis* cytokinin receptor mutants reveal functions in shoot growth, leaf senescence, seed size, germination, root development, and cytokinin metabolism. *Plant Cell* **18**: 40-54.

RIVERO RM, KOJIMA M, GEPSTEIN A, SAKAKIBARA H, MITTLER R, GEPSTEIN S and BLUMWALD E (2007). Delayed leaf senescence induces extreme drought tolerance in a flowering plant. *Proceedings of the National Academy of Sciences of the United States of America* **104**: 19631-19636.

ROBATZEK S and SOMSSICH IE (2001). A new member of the Arabidopsis WRKY transcription factor family, *At*WRKY6, is associated with both senescence- and defence-related processes. *Plant Journal* **28**: 123-133.

ROBATZEK S and SOMSSICH IE (2002). Targets of AtWRKY6 regulation during plant senescence and pathogen defense. *Genes & Development* **16**: 1139-1149.

ROBERTS IN, CAPUTO C, CRIADO MV and FUNK C (2012). Senescence-associated proteases in plants. *Physiologia Plantarum* **145**: 130-139.

ROBERTS IN, CAPUTO C, KADE M, CRIADO MV and BARNEIX AJ (2011). Subtilisin-like serine proteases involved in N remobilization during grain filling in wheat. *Acta Physiologiae Plantarum* **33**: 1997-2001.

SAKURABA Y, SCHELBERT S, PARK SY, HAN SH, LEE BD, ANDRÈS CB, KESSLER F, HÖRTENSTEINER S and PAEK NC (2012). STAY-GREEN and chlorophyll catabolic enzymes interact at light-harvesting complex II for chlorophyll detoxification during leaf senescence in *Arabidopsis*. *Plant Cell* **24**: 507-518.

SANDAÑA PA, HARCHA CI and CALDERINI DF (2009). Sensitivity of yield and grain nitrogen concentration of wheat, lupin and pea to source reduction during grain filling. A comparative survey under high yielding conditions. *Field Crops Research* **114**: 233-243.

SANFORD JC (1988). The biolistic process. *Trends in Biotechnology* **6**: 299-302.

SATO Y, MORITA R, KATSUMA S, NISHIMURA M, TANAKA A and KUSABA M (2009). Two short-chain dehydrogenase/reductases, NON-YELLOW COLORING 1 and NYC1-LIKE, are required for chlorophyll *b* and light-harvesting complex II degradation during senescence in rice. *Plant Journal* **57**: 120-131.

SCHILDHAUER J, WIEDEMUTH K and HUMBECK K (2008). Supply of nitrogen can reverse senescence processes and affect expression of genes coding for plastidic glutamine synthetase and lysine-ketoglutarate reductase/saccharopine dehydrogenase. *Plant Biology* **10**: 76-84.

SEMENOV MA and SHEWRY PR (2011). Modelling predicts that heat stress, not drought, will increase vulnerability of wheat in Europe. *Scientific Reports* **1**: no. 66.

SHAN XY, WANG JX, CHUA LL, JIANG DA, PENG W and XIE DX (2011). The role of Arabidopsis rubisco activase in jasmonate-induced leaf senescence *Plant Physiology* **155**: 751-764.

SHRAWAT AK, CARROLL RT, DEPAUW M, TAYLOR GJ and GOOD AG (2008). Genetic engineering of improved nitrogen use efficiency in rice by the tissue-specific expression of *alanine aminotransferase*. *Plant Biotechnology Journal* **6**: 722-732.

SILVA SA, CARVALHO FIFD, CAETANO VDR, OLIVEIRA ACD, COIMBRA JLMD, VASCONCELLOS NJSD and LORENCETTI C (2000). Genetic basis of stay-green trait in bread wheat. *Journal of New Seeds* **2**: 55-68.

SINCLAIR TR, PURCELL LC and SNELLER CH (2004). Crop transformation and the challenge to increase yield potential. *Trends in Plant Science* **9**: 70-75.

SMYKOWSKI A, ZIMMERMANN P and ZENTGRAF U (2010). G-box binding factor1 reduces *CATALASE2* expression and regulates the onset of leaf senescence in Arabidopsis. *Plant Physiology* **153**: 1321-1331.

SPANO G, DI FONZO N, PERROTTA C, PLATANI C, RONGA G, LAWLOR DW, NAPIER JA and SHEWRY PR (2003). Physiological characterization of 'stay green' mutants in durum wheat. *Journal of Experimental Botany* **54**: 1415-1420.

SPARKS CA and JONES HD (2009). Biolistics transformation of wheat. *Methods in Molecular Biology* **478**: 71-92.

SPEROTTO RA, RICACHENEVSKY FK, DUARTE GL, BOFF T, LOPES KL, SPERB ER, GRUSAK MA and FETT JP (2009). Identification of up-regulated genes in flag leaves during rice grain filling and characterization of *Os*NAC5, a new ABA-dependent transcription factor. *Planta* **230**: 985-1002.

SRIVALLI B and KHANNA-CHOPRA R (2004). The developing reproductive 'sink' induces oxidative stress to mediate nitrogen mobilization during monocarpic senescence in wheat. *Biochemical and Biophysical Research Communications* **325**: 198-202.

SUBEDI KD and MA BL (2005). Nitrogen uptake and partitioning in stay-green and leafy maize hybrids. *Crop Science* **45**: 740-747.

SÝKOROVÁ B, KUREŠOVÁ G, DASKALOVA S, TRČKOVÁ M, HOYEROVÁ K, RAIMANOVÁ I, MOTYKA V, TRÁVNÍČKOVÁ A, ELLIOTT MC and KAMÍNEK M (2008). Senescence-induced ectopic expression of the *A. tumefaciens ipt* gene in wheat delays leaf senescence, increases cytokinin content, nitrate influx, and nitrate reductase activity, but does not affect grain yield. *Journal of Experimental Botany* **59**: 377-387.

TAMURA K, PETERSON D, PETERSON N, STECHER G, NEI M and KUMAR S (2011). MEGA5: Molecular Evolutionary Genetics Analysis using maximum likelihood, evolutionary distance, and maximum parsimony methods. *Molecular Biology and Evolution* **28**: 2731-2739.

TAYLOR L, NUNES-NESI A, PARSLEY K, LEISS A, LEACH G, COATES S, WINGLER A, FERNIE AR and HIBBERD JM (2010). Cytosolic pyruvate,orthophosphate dikinase functions in nitrogen remobilization during leaf senescence and limits individual seed growth and nitrogen content. *Plant Journal* **62**: 641-652.

THOENEN M, HERRMANN B and FELLER U (2007). Senescence in wheat leaves: is a cysteine endopeptidase involved in the degradation of the large subunit of Rubisco? *Acta Physiologiae Plantarum* **29**: 339-350.

THOMAS H and HOWARTH CJ (2000). Five ways to stay green. *Journal of Experimental Botany* **51**: 329-337.

THOMAS H, OUGHAM H, CANTER P and DONNISON I (2002). What stay-green mutants tell us about nitrogen remobilization in leaf senescence. *Journal of Experimental Botany* **53**: 801-808.

TILMAN D, SOCOLOW R, FOLEY JA, HILL J, LARSON E, LYND L, PACALA S, REILLY J, SEARCHINGER T, SOMERVILLE C and WILLIAMS R (2009). Beneficial biofuels - the food, energy, and environment trilemma. *Science* **325**: 270-271.

UAUY C, BREVIS JC and DUBCOVSKY J (2006a). The high grain protein content gene *Gpc-B1* accelerates senescence and has pleiotropic effects on protein content in wheat. *Journal of Experimental Botany* **57**: 2785-2794.

UAUY C, DISTELFELD A, FAHIMA T, BLECHL A and DUBCOVSKY J (2006b). A NAC gene regulating senescence improves grain protein, zinc, and iron content in wheat. *Science* **314**: 1298-1301.

ÜLKER B, MUKHTAR MS and SOMSSICH IE (2007). The WRKY70 transcription factor of *Arabidopsis* influences both the plant senescence and defense signaling pathways. *Planta* **226**: 125-137.

ÜLKER B and SOMSSICH IE (2004). WRKY transcription factors: from DNA binding towards biological function. *Current Opinion in Plant Biology* **7**: 491-498.

VAN DER GRAAFF E, SCHWACKE R, SCHNEIDER A, DESIMONE M, FLÜGGE UI and KUNZE R (2006). Transcription analysis of Arabidopsis membrane transporters and hormone pathways during developmental and induced leaf senescence. *Plant Physiology* **141**: 776-792.

VAN OOSTEROM EJ, CHAPMAN SC, BORRELL AK, BROAD IJ and HAMMER GL (2010). Functional dynamics of the nitrogen balance of sorghum. II. Grain filling period. *Field Crops Research* **115**: 29-38.

VERMA V, FOULKES MJ, WORLAND AJ, SYLVESTER-BRADLEY R, CALIGARI PDS and SNAPE JW (2004). Mapping quantitative trait loci for flag leaf senescence as a yield determinant in winter wheat under optimal and drought-stressed environments. *Euphytica* **135**: 255-263.

VERWOERD TC, DEKKER BMM and HOEKEMA A (1989). A small-scale procedure for the rapid isolation of plant RNAs. *Nucleic Acids Research* **17**: 2362-2362.

VIJAYALAKSHMI K, FRITZ AK, PAULSEN GM, BAI GH, PANDRAVADA S and GILL BS (2010). Modeling and mapping QTL for senescence-related traits in winter wheat under high temperature. *Molecular Breeding* **26**: 163-175.

VOINNET O, VAIN P, ANGELL S and BAULCOMBE DC (1998). Systemic spread of sequence-specific transgene RNA degradation in plants is initiated by localized introduction of ectopic promoterless DNA. *Cell* **95**: 177-187.

WADA S, ISHIDA H, IZUMI M, YOSHIMOTO K, OHSUMI Y, MAE T and MAKINO A (2009). Autophagy plays a role in chloroplast degradation during senescence in individually darkened leaves. *Plant Physiology* **149**: 885-893.

WAGSTAFF C, YANG TJW, STEAD AD, BUCHANAN-WOLLASTON V and ROBERTS JA (2009). A molecular and structural characterization of senescing Arabidopsis siliques and comparison of transcriptional profiles with senescing petals and leaves. *Plant Journal* **57**: 690-705.

WANG H, MCCAIG TN, DEPAUW RM and CLARKE JM (2008). Flag leaf physiological traits in two high-yielding Canada Western Red Spring wheat cultivars. *Canadian Journal of Plant Science* **88**: 35-42.

WATERS BM, UAUY C, DUBCOVSKY J and GRUSAK MA (2009a). Wheat (*Triticum aestivum*) NAM proteins regulate the translocation of iron, zinc, and nitrogen compounds from vegetative tissues to grain. *Journal of Experimental Botany* **60**: 4263-74.

WATERS MT, WANG P, KORKARIC M, CAPPER RG, SAUNDERS NJ and LANGDALE JA (2009b). GLK transcription factors coordinate expression of the photosynthetic apparatus in *Arabidopsis*. *Plant Cell* **21**: 1109-1128.

WEAVER LM, GAN SS, QUIRINO B and AMASINO RM (1998). A comparison of the expression patterns of several senescence-associated genes in response to stress and hormone treatment. *Plant Molecular Biology* **37**: 455-469.

WINGLER A, MARÈS M and POURTAU N (2004). Spatial patterns and metabolic regulation of photosynthetic parameters during leaf senescence. *New Phytologist* **161**: 781-789.

WINGLER A, PURDY SJ, EDWARDS SA, CHARDON F and MASCLAUX-DAUBRESSE C (2010). QTL analysis for sugar-regulated leaf senescence supports flowering-dependent and -independent senescence pathways. *New Phytologist* **185**: 420-433.

WITTENBACH VA (1979). Ribulose biphosphate carboxylase and proteolytic activity in wheat leaves from anthesis through senescence. *Plant Physiology* **64**: 884-887.

WOO HR, CHUNG KM, PARK JH, OH SA, AHN T, HONG SH, JANG SK and NAM HG (2001). ORE9, an F-box protein that regulates leaf senescence in Arabidopsis. *Plant Cell* **13**: 1779-1790.

WU AH, ALLU AD, GARAPATI P, SIDDIQUI H, DORTAY H, ZANOR MI, ASENSI-FABADO MA, MUNNÉ-BOSCH S, ANTONIO C, TOHGE T, FERNIE AR, KAUFMANN K, XUE GP, MUELLER-ROEBER B and BALAZADEH S (2012). *JUNGBRUNNEN1*, a reactive oxygen species-responsive NAC transcription factor, regulates longevity in *Arabidopsis*. *Plant Cell* **24**: 482-506.

WU HL, NI ZF, YAO YY, GUO GG and SUN QX (2008a). Cloning and expression profiles of 15 genes encoding WRKY transcription factor in wheat (*Triticum aestivem* L.). *Progress in Natural Science* **18**: 697-705.

WU K, ZHANG L, ZHOU C, YU CW and CHAIKAM V (2008b). HDA6 is required for jasmonate response, senescence and flowering in *Arabidopsis*. *Journal of Experimental Botany* **59**: 225-234.

XIE Z, ZHANG ZL, ZOU XL, HUANG J, RUAS P, THOMPSON D and SHEN QJ (2005). Annotations and functional analyses of the rice *WRKY* gene superfamily reveal positive and negative regulators of abscisic acid signaling in aleurone cells. *Plant Physiology* **137**: 176-189.

XU F, MENG T, LI P, YU Y, CUI Y, WANG Y, GONG Q and WANG NN (2011). A soybean dual-specificity kinase, GmSARK, and its Arabidopsis homolog, AtSARK, regulate leaf senescence through synergistic actions of auxin and ethylene. *Plant Physiology* **157**: 2131-53.

XU H, WANG XC and CHEN J (2010). Overexpression of the *Rap2.4f* transcriptional factor in *Arabidopsis* promotes leaf senescence. *Science China-Life Sciences* **53**: 1221-1226.

YAN H, SAIKA H, MAEKAWA M, TAKAMURE I, TSUTSUMI N, KYOZUKA J and NAKAZONO M (2007). Rice tillering dwarf mutant *dwarf3* has increased leaf longevity during darkness-induced senescence or hydrogen peroxide-induced cell death. *Genes & Genetic Systems* **82**: 361-366.

YANAGISAWA S, AKIYAMA A, KISAKA H, UCHIMIYA H and MIWA T (2004). Metabolic engineering with Dof1 transcription factor in plants: Improved nitrogen assimilation and growth under low-nitrogen conditions. *Proceedings of the National Academy of Sciences of the United States of America* **101**: 7833-7838.

YANG SD, SEO PJ, YOON HK and PARK CM (2011). The *Arabidopsis* NAC transcription factor VNI2 integrates abscisic acid signals into leaf senescence via the *COR/RD* genes. *Plant Cell* **23**: 2155-2168.

YANG XT, PANG XQ, XU LY, FANG RQ, HUANG XM, GUAN PJ, LU WJ and ZHANG ZQ (2009). Accumulation of soluble sugars in peel at high temperature leads to stay-green ripe banana fruit. *Journal of Experimental Botany* **60**: 4051-4062.

YI KK, WU ZC, ZHOU J, DU LM, GUO LB, WU YR and WU P (2005). *OsPTF1*, a novel transcription factor involved in tolerance to phosphate starvation in rice. *Plant Physiology* **138**: 2087-2096.

YOO SC, CHO SH, ZHANG H, PAIK HC, LEE CH, LI J, YOO JH, LEE BW, KOH HJ, SEO HS and PAEK NC (2007). Quantitative trait loci associated with functional stay-green SNU-SG1 in rice. *Molecules and Cells* **24**: 83-94.

YOON HK, KIM SG, KIM SY and PARK CM (2008). Regulation of leaf senescence by NTL9-mediated osmotic stress signaling in *Arabidopsis*. *Molecules and Cells* **25**: 438-445.

YOSHIDA S, ITO M, CALLIS J, NISHIDA I and WATANABE A (2002a). A delayed leaf senescence mutant is defective in arginyl-tRNA : protein arginyltransferase, a component of the N-end rule pathway in *Arabidopsis*. *Plant Journal* **32**: 129-137.

YOSHIDA S, ITO M, NISHIDA I and WATANABE A (2002b). Identification of a novel gene *HYS1/CPR5* that has a repressive role in the induction of leaf senescence and pathogen-defence responses in *Arabidopsis thaliana*. *Plant Journal* **29**: 427-437.

ZADOKS JC, CHANG TT and KONZAK CF (1974). Decimal code for growth stages of cereals. *Weed Research* **14**: 415-421.

ZAPATA JM, GUÉRA A, ESTEBAN-CARRASCO A, MARTIN M and SABATER B (2005). Chloroplasts regulate leaf senescence: delayed senescence in transgenic *ndhF*-defective tobacco. *Cell Death and Differentiation* **12**: 1277-1284.

ZENTGRAF U, LAUN T and MIAO Y (2010). The complex regulation of *WRKY53* during leaf senescence of *Arabidopsis thaliana*. *European Journal of Cell Biology* **89**: 133-137.

ZHANG WG, MCELROY D and WU R (1991). Analysis of rice Act1 5' region activity in transgenic rice plants. *Plant Cell* **3**: 1155-1165.

ZHANG X, JU HW, CHUNG MS, HUANG P, AHN SJ and KIM CS (2011). The R-R-type MYB-like transcription factor, AtMYBL, is involved in promoting leaf senescence and modulates an abiotic stress response in Arabidopsis. *Plant and Cell Physiology* **52**: 138-148.

ZHOU CE, HAN L, PISLARIU C, NAKASHIMA J, FU CX, JIANG QZ, QUAN L, BLANCAFLOR EB, TANG YH, BOUTON JH, UDVARDI M, XIA GM and WANG ZY (2011a). From model to crop: Functional analysis of a STAY-GREEN gene in the model legume *Medicago truncatula* and effective use of the gene for Alfalfa improvement. *Plant Physiology* **157**: 1483-1496.

ZHOU CJ, CAI ZH, GUO YF and GAN SS (2009). An Arabidopsis mitogen-activated protein kinase cascade, MKK9-MPK6, plays a role in leaf senescence. *Plant Physiology* **150**: 167-177.

ZHOU X, JIANG YJ and YU DQ (2011b). WRKY22 transcription factor mediates dark-induced leaf senescence in *Arabidopsis*. *Molecules and Cells* **31**: 303-313.